
Dépôt Institutionnel de l'Université libre de Bruxelles /
Université libre de Bruxelles Institutional Repository
Thèse de doctorat/ PhD Thesis

Citation APA:

Richardson, J. (2013). *Topology optimization of truss-like structures, from theory to practice* (Unpublished doctoral dissertation). Université libre de Bruxelles, Ecole polytechnique de Bruxelles – Constructions, Bruxelles.

Disponible à / Available at permalink : <https://dipot.ulb.ac.be/dspace/bitstream/2013/209534/4/e6b62b49-ab30-44d2-bbb0-4402ef7ae198.txt>

(English version below)

Cette thèse de doctorat a été numérisée par l'Université libre de Bruxelles. L'auteur qui s'opposerait à sa mise en ligne dans DI-fusion est invité à prendre contact avec l'Université (di-fusion@ulb.be).

Dans le cas où une version électronique native de la thèse existe, l'Université ne peut garantir que la présente version numérisée soit identique à la version électronique native, ni qu'elle soit la version officielle définitive de la thèse.

DI-fusion, le Dépôt Institutionnel de l'Université libre de Bruxelles, recueille la production scientifique de l'Université, mise à disposition en libre accès autant que possible. Les œuvres accessibles dans DI-fusion sont protégées par la législation belge relative aux droits d'auteur et aux droits voisins. Toute personne peut, sans avoir à demander l'autorisation de l'auteur ou de l'ayant-droit, à des fins d'usage privé ou à des fins d'illustration de l'enseignement ou de recherche scientifique, dans la mesure justifiée par le but non lucratif poursuivi, lire, télécharger ou reproduire sur papier ou sur tout autre support, les articles ou des fragments d'autres œuvres, disponibles dans DI-fusion, pour autant que :

- Le nom des auteurs, le titre et la référence bibliographique complète soient cités;
- L'identifiant unique attribué aux métadonnées dans DI-fusion (permalink) soit indiqué;
- Le contenu ne soit pas modifié.

L'œuvre ne peut être stockée dans une autre base de données dans le but d'y donner accès ; l'identifiant unique (permalink) indiqué ci-dessus doit toujours être utilisé pour donner accès à l'œuvre. Toute autre utilisation non mentionnée ci-dessus nécessite l'autorisation de l'auteur de l'œuvre ou de l'ayant droit.

----- English Version -----

This Ph.D. thesis has been digitized by Université libre de Bruxelles. The author who would disagree on its online availability in DI-fusion is invited to contact the University (di-fusion@ulb.be).

If a native electronic version of the thesis exists, the University can guarantee neither that the present digitized version is identical to the native electronic version, nor that it is the definitive official version of the thesis.

DI-fusion is the Institutional Repository of Université libre de Bruxelles; it collects the research output of the University, available on open access as much as possible. The works included in DI-fusion are protected by the Belgian legislation relating to authors' rights and neighbouring rights. Any user may, without prior permission from the authors or copyright owners, for private usage or for educational or scientific research purposes, to the extent justified by the non-profit activity, read, download or reproduce on paper or on any other media, the articles or fragments of other works, available in DI-fusion, provided:

- The authors, title and full bibliographic details are credited in any copy;
- The unique identifier (permalink) for the original metadata page in DI-fusion is indicated;
- The content is not changed in any way.

It is not permitted to store the work in another database in order to provide access to it; the unique identifier (permalink) indicated above must always be used to provide access to the work. Any other use not mentioned above requires the authors' or copyright owners' permission.

Topology Optimization of Truss-like Structures: from Theory to Practice

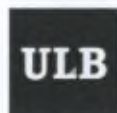
Thesis submitted in fulfillment of the requirements for the award of the degree of
DOCTOR IN ENGINEERING SCIENCES by

James Norman Richardson

21 November 2013

Advisors:

Prof. Rajan Filomeno Coelho (ULB)
Prof. Sigrid Adriaenssens (VUB)



Brussels School of Engineering
Department of Building,
Architecture and Town planning



Vrije
Universiteit
Brussel

Faculty of Engineering
Department of Mechanics
of Materials and Constructions

*Not to remain stuck to a person—every person is a prison, also a nook.
Not to remain stuck to a fatherland—not even if it suffers most and
needs help most—it is less difficult to sever one's heart from a
victorious fatherland. Not to remain stuck to some pity—not even for
higher men into whose rare torture and helplessness some accident
allowed us to look.*

F.W. NIETZSCHE
Beyond Good and Evil, Part 2, par. 41

Members of the PhD jury

Prof. Hugues Bersini	Université libre de Bruxelles
Prof. James K. Guest	Johns Hopkins University
Prof. Thierry J. Massart	Université libre de Bruxelles
Prof. Sigrid Adriaenssens	Vrije Universiteit Brussel, Princeton University
Prof. Philippe Bouillard	Université libre de Bruxelles
Prof. Rajan Filomeno Coelho	Université libre de Bruxelles
Prof. Catherine Knopf-Lenoir	Université de Technologie de Compiègne
Prof. Rik Pintelon	Vrije Universiteit Brussel
Prof. Tine Tysmans	Vrije Universiteit Brussel

Acknowledgements

My deepest thanks to my exceptional thesis advisors Prof. Rajan Filomeno Coelho and Prof. Sigrid Adriaenssens. It goes without saying that without them this PhD would not have been possible. I am eternally grateful for their tireless efforts, patience, guidance, knowledge and help. Prof. Philippe Bouillard was also very instrumental in allowing me to pursue this research and providing guidance and help, especially at the critical early stages of the PhD. I would also like to thank Prof. Patrick De Wilde for some very early inspiration and interest in the topic of structural optimization. My colleagues at the ULB, the VUB and Princeton Universities were the source of many interesting discussions about this and other topics. I thank the members of the jury for their invaluable insights and contributions to the final manuscript.

Thanks to my parents Beverley Stone and Marshall Richardson for supporting my decisions throughout the process of this PhD, and my studies in general. Finally thanks to my brothers Victor, Norman, Marshall and Louis. I also owe a debt of gratitude to my close friends Fabien Cadet De Fontenay, Sean McVeigh, Shawn Swainland, Steven Kremers, and Gregory Tate.

Financial support by the Fonds de la Recherche Scientifique (FNRS) is gratefully acknowledged.

Contents

1	Introduction	15
1.1	Context of the research	16
1.1.1	Historical framing	16
1.1.2	Structural topology optimization in context	16
1.2	Thesis objectives and overview	19
	Bibliography	22
2	Algorithm performance in discrete topology optimization	25
2.1	Introduction	26
2.2	KSR approach	28
2.2.1	Parameterization of the structures	28
2.2.2	Hypotheses	28
2.2.3	Optimization framework	28
2.3	Single-objective topology optimization	34
2.3.1	Problem formulation	34
2.3.2	Examples	35
2.4	Multiobjective topology optimization	40
2.4.1	Problem formulation	40
2.4.2	Examples	40
2.4.3	Cantilevered 3D structure: topology and sizing optimization	44
2.5	Conclusions and future prospects	48
	Bibliography	48
3	Grid shell topology optimization	51
3.1	Introduction	52
3.2	Problem statement	54
3.3	Approach	54
3.4	Two-phase approach to the preliminary design of single layer grid shells	58
3.4.1	Form-finding of grid shells	58
3.4.2	Grid configuration optimization of grid shells	58
3.5	Validation of the two-phase methodology: preliminary design of $24m \times 24m$ grid shells	61
3.5.1	Description of the case studies	61
3.5.2	Computation and convergence	61
3.5.3	Designs resulting from the two-phase form-finding and optimization procedure for the $24m \times 24m$ grid shells	62
3.6	Conclusions and Future Prospects	66
	Bibliography	67

4	Discrete optimization applied to façade bracing	71
4.1	Introduction	72
4.2	Description of façade structural system	73
4.3	Façade bracing problem definition	75
4.4	Approach: Multiobjective Topology Optimization using GA's	76
4.4.1	Multiobjective structural optimization	76
4.4.2	Pareto optimality	76
4.4.3	Multiobjective Genetic Algorithm	76
4.5	Calculation procedure and parameters	78
4.6	Results: a catalogue of optimal solutions	79
4.7	Conclusions and further work	82
	Bibliography	82
5	Symmetry considerations in discrete optimization	85
5.1	Introduction	86
5.2	Scope and definitions	87
5.2.1	General definitions	87
5.2.2	Group theory and group representation	87
5.3	Search space and symmetric subset	88
5.4	Objective functions and constraints	89
5.4.1	Mass objective function	89
5.4.2	Compliance objective function	89
5.5	Convex combination: existence of solutions	89
5.5.1	Convex combination and variable mapping	90
5.5.2	Convex combination with discrete variables	90
5.6	Examples	91
5.6.1	20 bar 2D truss	92
5.6.2	9 bar truss	95
5.6.3	24 bar 3D truss	96
5.7	Conclusions and discussion	99
	Bibliography	100
6	Structural optimization under uncertainty	103
6.1	Introduction	104
6.2	Modelling of uncertainties for continuum and truss-like structures	105
6.3	Introducing uncertainties for robust topology optimization	106
6.3.1	Deterministic continuum topology optimization with the SIMP method	106
6.3.2	Principle of the spectral stochastic finite element method	107
6.3.3	Stochastic finite element method for uncertainty propagation in topology optimization	107
6.4	Computational examples	108
6.4.1	2D Continuum cantilever	108
6.4.2	3D Continuum bridge	110
6.4.3	2D truss problem	112
6.5	Conclusions	114
	Bibliography	115
7	Truss optimization with discrete design variables under uncertainty	117
7.1	Introduction	118
7.2	Uncertainty quantification and optimization approach	119
7.2.1	Material uncertainties	119
7.2.2	Loading uncertainties	121
7.2.3	Spectral Stochastic Finite Element Method	121

7.2.4	Objectives and constraints	121
7.3	Multiobjective approach	122
7.4	Examples	123
7.4.1	Robustness topology optimization for compliance minimization as a multiob- jective problem	123
7.4.2	Optimization of a truss-like structure for minimum mass and deflection	124
7.5	Conclusions and further work	126
	Bibliography	126
8	Conclusions and further work	129
8.1	Main findings of the research	130
8.1.1	Improving genetic-based topology optimization by incorporating kinematic sta- bility considerations	130
8.1.2	Optimization methods applied to grid shell and façade bracing design	130
8.1.3	Accounting for random uncertainty in structural optimization	131
8.2	Suggested further work	131
	Bibliography	133
	Appendices	135
A	Derivation of robust compliance objective sensitivities	137
	Bibliography	140
B	Overview of solution algorithms in structural optimization	141
B.1	Overview of gradient-based optimization algorithms in topology optimization	142
B.2	Overview of gradient-free optimization algorithms in topology optimization	142
	Bibliography	143
	148
	160

List of Figures

1.3	An example of a continuous (left) and discrete (right) function space	17
1.1	Categorization of type of optimization of discrete and continuum structures. Six types of problems can be distinguished	18
1.2	Discrete vs. continuous design variables, for truss and continuum structures	18
1.4	Overview of the various publications making up the Ph.D.	21
2.1	Numerous truss structures at the New Galveston Causeway Railroad Lift Bridge. Image courtesy of Patrick Feller	25
2.2	The backplane support structure for NASA's James Webb Space Telescope in Magna, Utah. Image courtesy of NASA	25
2.3	Typical parameter representation	28
2.4	Analogy between VEGA (top) and KSR (bottom)	29
2.5	2D procedure 1	30
2.6	3D procedure 1	30
2.7	2D procedure 2	31
2.8	Average effect of composition of initial population on final solution for 54-bar multiobjective problem	31
2.9	Average effect of size of stable initial population on final solution for 54-bar multiobjective problem	31
2.10	Modified genetic algorithm	32
2.11	Chromosome repair checks (a) and (b)	33
2.12	Repair procedure algorithm	34
2.13	Proportion of stable structures in the search space	34
2.14	10 bar truss ground structure	35
2.15	10 bar problem: Optimized truss structure	36
2.16	10 bar 2D problem: convergence of KSR algorithm	36
2.17	10 bar 2D problem: Comparison of average objective function values (first 70 generations)	37
2.18	14 bar truss ground structure	37
2.19	Solution to the 14 bar sizing and topology optimization	37
2.20	25 bar 3D problem	38
2.21	25 bar 3D problem topology after optimization	39
2.22	14 bar 2D truss: Pareto optimal topologies	41
2.23	14 bar 2D truss: Best solution convergence relative to reference solution	42
2.24	54 bar cantilever truss ground structure	42
2.25	54 bar MOGA: Pareto fronts	43
2.26	54 bar MOGA initial population: Procedure 1, Procedure 2 and randomly seeded individuals	44
2.27	3D cantilevered structure: nodal positions	46
2.28	3D cantilevered structure: loading	46
2.29	3D cantilevered structure: ground structure	46
2.30	3D cantilevered structure: Pareto front	47

3.1	An architectural rendering of grid shell canopy structures	51
3.2	Grid shell roof structure by Buro Happold at the British Museum, London, UK. Image courtesy of Travis Simon	51
3.3	A configuration of three grids of varying orientation with common nodes	53
3.4	A two-phase approach: (i) A dynamic relaxation procedure with kinetic damping provides the grid shell global form input for (ii) the optimization loop consisting of a genetic algorithm optimizer coupled to a finite element analysis	55
3.5	Chromosome representation of a 4 node structure. Entries in the chromosome correspond to shape variables (coordinates of nodes) and topology variables (existence or non-existence of elements)	55
3.6	Cross sections of single layer and non-single layer grid shell systems	56
3.7	An example of how kinematically stable grid shell designs in the initial population can be generated. The figure represents a segment of a symmetric grid shell with two planes of mirror symmetry, one in the $x-z$ and one in the $y-z$ plane. (1) A stable core structure is first produced. (2, 3) Groups of elements are added onto the stable core to incorporate other nodes. (4) Once all nodes are connected the procedure is stopped. Repeating this topology according to the symmetry of the structure generally leads to a kinematically stable grid shell	57
3.8	Algorithm for DR with kinetic damping used in Phase 1 of the two-phase method . . .	59
3.9	Nodal shape variable interpolation: for a given set of original nodal positions (0), an imaginary surface is defined through these points (1). For a change in nodal coordinate Δx , the z coordinate is found on the surface (2)	59
3.10	The nodes connecting structural elements (solid black lines), are projected onto a horizontal surface (grey dashed lines). The Voronoi polygons are calculated based on this projection and the relative area sizes translated to vertical point loads on the nodes . . .	60
3.11	A general framework of the GA used in Phase 2 of the coupled method	61
3.12	The $24m \times 24m$ grid shell initial connectivities	62
3.13	The three grid shell forms obtained after Phase 1, the form-finding. These topologies represent the ground structures for Phase 2	63
3.14	Several methods for controlling the form of the free edges used in form-finding techniques	64
3.16	Changes in the optimal topology and nodal positions with increasing evenly distributed loading	65
3.15	The three grid shells obtained after Phase 2, the grid configuration optimization	66
4.1	Bracing of the façade of a tall building, New York NY, USA. Image courtesy of Lionel Ponce	71
4.2	National Museum of African American History and Culture, Washington DC, USA. The façade for the museum is braced with cable X-bracing. Image courtesy of Adjeye Associates	71
4.3	Hanging façade system	74
4.4	Façade structure wind loading principle	74
4.5	Isometry detail of corner of hanging façade system	75
4.6	Simplified models of the four façades: the grey shaded areas represent zones where no bracing can be located. The bracing in the West façade (under the grey zone) are compulsory design elements	75
4.7	Basic algorithm scheme: a multiobjective Genetic Algorithm is coupled to a Finite Element Analysis (FEA) program	76
4.9	MOGA used in the façade bracing topology optimization. Several biologically inspired processes are used to optimize a population of structures. The binary string manipulation is demonstrated next to each operation	77
4.10	The relationship between chromosome and the bracing topology	77
4.8	An illustration of the principals of non-dominance and Pareto front	78

4.11	Deflected shape in plane	79
4.12	Combined Pareto fronts: configuration grouping	80
4.13	Hypothetical design evaluation based on changes in design requirements	80
5.1	Various types of symmetry are present in the design of the Biosphere by Buckminster Fuller, Montreal, Canada. Image courtesy of Simon Bonaventure	85
5.2	A tiling pattern with five-fold rotational symmetry	85
5.3	A 6 bar 2D truss design. The dashed line indicates a possible connection between nodes 1 and 2. This connection forms part of the problem ground structure, but is absent in this specific design	87
5.4	Sets and subsets of the variable space	88
5.5	Symmetric structure variable vector reduction: an illustration	89
5.6	20 bar 2D problem ground structure. Nodes are labelled with numbers, while the bar numbering is circled	92
5.8	20 bar 2D truss problem: minimum objective function values, both mass and compliance ($V \leq 0.4$)	93
5.7	20 bar 2D truss problem: symmetric and asymmetric structure mass objective functions	94
5.9	20 bar 2D truss problem: minimum mass stable, symmetric structure	95
5.10	9 bar 3D structure	95
5.11	9 bar 3D structure plan view and numbering	95
5.12	Probability of symmetry resulting through convex combination of asymmetric optimal solutions for the 9 bar truss	96
5.15	24 bar 3D structure: least mass solutions	97
5.13	24 bar 3D structure ground structure	98
5.14	24 bar 3D structure ground structure plan view	98
5.16	24 bar 3D structure: lowest compliance energy solutions	98
5.17	24 bar 3D truss: contribution of terms to probability of symmetry resulting through convex combination of asymmetric optimal solutions	99
5.18	24 bar 3D truss: probability of symmetry resulting through convex combination of asymmetric optimal solutions	99
6.1	Truss topology optimization problems with deterministic and variable loading	103
6.2	The Millennium Bridge over the River Liffey, Dublin, Ireland. Image courtesy of William Murphy	103
6.3	Truss element-level 1D random fields	106
6.4	2D cantilever problem. Problem set up and deterministic solution	109
6.5	2D cantilever problem. Plot of the objective function values for various values of α and $f(\mathbf{x})$	110
6.7	3D bridge problem. Resulting topologies for various values of the standard deviation σ and the correlation length l	111
6.6	3D bridge problem. Problem set up and deterministic solution	112
6.9	2D truss problem probabilistic solutions	113
6.8	2D truss problem: Problem set up and deterministic solution	114
6.10	Values of the objective function for various parameters	115
7.1	Test samples from a series of tension tests to determine the characteristics of the yield stress of a material	117
7.2	A truss pedestrian bridge at the Devos Hospital in Grand Rapids, MI, USA, undergoing construction. The loading of the bridge throughout its lifetime is subject to a large amount of random variation. Image courtesy of John Eisenschenk	117
7.3	Schematic representation of the uncertainties on the material stiffness and loading magnitude and direction	120
7.5	Solutions to the robust compliance problem in mean and standard deviation space	123

7.4	2D cantilever truss-like ground structure	123
7.6	Pareto front of the solutions to the mass and compliance minimization multiobjective problems	125

List of Tables

2.3	10 bar 2D truss: Comparison of results	36
2.1	Geometric and material parameters	36
2.2	10-bar 2D single objective problem: GA parameters	36
2.4	14 bar 2D truss: Comparison of results	38
2.5	25 bar 3D truss: Loading	38
2.6	25 bar 3D truss: Comparison of results	39
2.7	25 bar 3D truss: Topology and cross-section areas obtained	39
2.8	14 bar 2D truss multiobjective problem: GA parameters	40
2.9	14 bar 2D truss: Comparison of algorithm performance	42
2.10	54 bar 2D truss: Geometric and material parameters	42
2.11	54 bar 2D truss: GA parameters	42
2.13	54 bar 2D truss: Effect of composition of initial population	43
2.12	54 bar 2D truss: Comparison of performance of algorithms	44
2.14	Material parameters and maximum deflection	45
2.15	3D cantilevered structure: truss nodal positions (m)	45
2.16	3D Cantilevered structure: GA parameters	45
3.1	GA parameters for the $24m \times 24m$ grid shells	62
3.2	Comparison of grid shells after Phase 1 and Phase 2 of the two-phase method. The values in the table represent the constraint values of the grid shells before Phase 2 . . .	65
4.1	Genetic algorithm parameters. * indicates built in DAKOTA methods	79
4.2	Several solutions in the 'catalogue'	81
6.1	2D cantilever problem. Resulting topologies for various values of the standard deviation σ and the factor α	109
6.2	Comparison of SSFEM and Monte Carlo results for compliance statistics for the 2D cantilever problem	110

Chapter 1

Introduction

1.1 Context of the research

1.1.1 Historical framing

Structural optimization has emerged as a prominent field of academic study in recent decades. While the practice is often most associated with modern computational techniques and hardware, it can be argued that the concept has been latent within almost all engineering endeavours and advances throughout history. Any act of engineering requires, in the first instance, the solution of a physical problem, however this solution is almost never unique. Decision making is therefore unavoidable, implying the valuation of distinct solutions, based on criteria (or objectives). For the longest period of the history of engineering, trial and error, accumulated knowledge and deductive reasoning assisted the designer in this decision making process. Quite separately from engineering practice, formal recognition of the mathematical concept of optimization arose from the work of Leibniz, Newton, Cauchy and others in the latter quarter of the previous millennium [1]. While the methods developed by these pioneers opened up great possibilities for structural designers and engineers, they were not fully embraced at the time. One reason for this was certainly the lack of computational technology to solve the complex optimization problems posed by structural engineering. However, another barrier can be found in the way civil engineering as a discipline has developed, forced to rely on trial and error for achieving advances, often with dire consequences. Furthermore there is a perception amongst practising civil engineers that optimization implies *fragility*, a misunderstanding that has arisen from the culture of safety factors and conservative approximate solutions.

In the past structural optimization theory has largely focussed on gradient-based algorithms which are well suited for mathematically well-defined problems such as compliance minimization of continuum structures. This type of problem is congruent to the needs of the aerospace, automotive and mechanical engineering industries, where the greatest advances have been achieved. Secondly, but not unrelated, the definition of cost is quite problematic to quantify and not the only objective of importance. A lack of access to high performance computational hardware within the civil engineering industry has undoubtedly also been a

limiting factor.

In recent years attempts have been made to address these problems in the civil engineering community. Increased performance of small-scale computers, the introduction of gradient-free algorithms and the increased awareness of the impact structural engineering can have on the environment, have all been important to the rising interest in practical implementation of optimization in civil engineering. Yet this requires research which specifically addresses the needs of the civil engineering community. A thorough understanding of the problems faced by civil engineers and the objectives they wish to achieve is invaluable for the task of introducing optimization into the field of practice.

1.1.2 Structural topology optimization in context

The formalized subject of structural optimization became intensively researched in the latter half of the 20th century, largely due to developments in numerical techniques and efficient and powerful computational hardware and the needs of the aerospace and automotive industry. This coincided largely with the development of numerical analysis methods, most prominently the Finite Element Method (FEM) [1].

Simply stated, the aim of structural optimization is to find the layout of structural material with specified properties that provides optimal structural performance, while satisfying a number of requirements of the problem [18]. In mathematical terms this can be stated as follows:

$$\begin{aligned} & \min_{\mathbf{x}} \mathbf{f}(\mathbf{x}) \\ & \text{subject to: } \begin{cases} \mathbf{g}(\mathbf{x}) \leq 0 \\ \mathbf{h}(\mathbf{x}) = 0 \end{cases} \quad \mathbf{x} \in \mathbf{X} \end{aligned}$$

where \mathbf{f} is a vector of functions known as *objective functions*, \mathbf{x} is a vector of variables, called the *design variables*, \mathbf{g} and \mathbf{h} are respectively *inequality* and *equality constraints*, and \mathbf{X} is the design space. In structural optimization a distinction is made between optimization of truss-like structures (trusses, braced frames, etc.) and continuum structures (such as plates or shells), both of which can easily be analysed using FEM models. FEM also lends itself well to parametrization in terms of various design variables required for structural optimization. A parametrization is the process

of defining the parameters to accurately characterize a model mathematically. The parametrization of the problem to be solved will define the space within which the search will be carried out. In order to characterize selection choices accurately this implies the correct classification of parameters (or variables). Furthermore an effective parametrization implies a minimal modelling in terms of the combinatorial possibilities of the chosen variables, while maintaining a rich enough dimensionality to enable effective use of an optimization routine. Broadly speaking in engineering applications parameters are either continuous or discrete. A third type, categorical parameters can be seen as a subtype of discrete parameters¹. The type of structural optimization can be categorized in terms of the structural property to be optimized, either sizing, shape or topology²:

1. Sizing optimization considers the cross sectional dimensions as design variables.
2. Shape optimization considers the geometrical variables related to the shape of the structure. The topology remains constant.
3. Topology optimization involves defining the optimal distribution of material, often from a given initial distribution, called 'ground structure' [5] in truss problems, or a bulk of material in continuum structures.

Figure 1.1 summarizes these distinctions, showing some of the types of problems which can be considered. Specifically shape [12] and sizing [8] optimization have received much attention and are relatively mature areas of research. These aspects tend to present fewer challenges with regard to computational cost [19] than topology optimization. The concepts of sizing and shape optimization are also much more evident and intuitive than topology. Topology as a concept has its roots in geometry, yet has been generalized as a very useful concept in various fields of mathematics. Geometric topology (as we use it in terms of structural topology optimization) can be most easily defined as: the study of the properties of geometric figures or solids that are not changed by homeomorphisms, such as stretching or bending [2]. Simply

¹The reader is referred to [7] in which some of the specific issues associated with categorical variables are discussed.

²Other nomenclature exists in the literature, often the result of combinations of these three subdivisions. An example of this is *layout optimization*: concurrent sizing, shape and topology optimization.

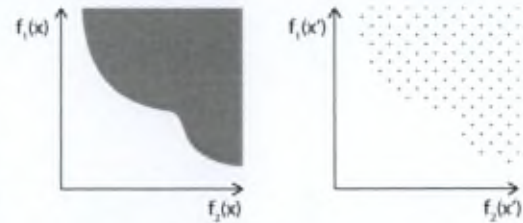


Figure 1.3: An example of a continuous (left) and discrete (right) function space

put, in terms of the structures discussed above, the connectivity of the bar elements in truss structures, and the number of voids in continuum structures. Continuum topology optimization has been extensively developed since the seminal work by Bendsoe and Kikuchi [6], however over the past three decades the problem of truss topology optimization has also received some attention [9]. Furthermore, problems can either be deterministic (only the mean values of the structural parameters are considered) or probabilistic (the variations on the loading, geometric, and material parameters are also included in the problem formulation).

Consider figure 1.2 where these distinctions are made for topology design variables. Truss structures with continuous cross section area sizes can have any real value for the area of their cross section, between specified bounds. A discrete version of this function may include only a few possible cross section values, including 1 and 0. A visual interpretation of two function spaces with objective functions f_1 and f_2 , respectively in continuous variables \mathbf{x} and discrete variables \mathbf{x}' is given in figure 1.3. Continuum structures with continuous density function at any point in the bulk may lead to smooth, organic forms. An example of discrete parameters in a continuum is the existence or non-existence of a perforation, or a perforation of a limited number of possible sizes.

As discussed previously, the essence of optimization is decision making. Decision making requires information about the possible choices and how to compare them. The comparison occurs by means of an ordering or ranking, a quantitative comparison. Herein lies the difficulty with optimization: the number of choices is typically too vast to be able to compare exhaustively. To solve this conundrum, the designer uses optimization techniques. A summary of some of the commonly used opti-

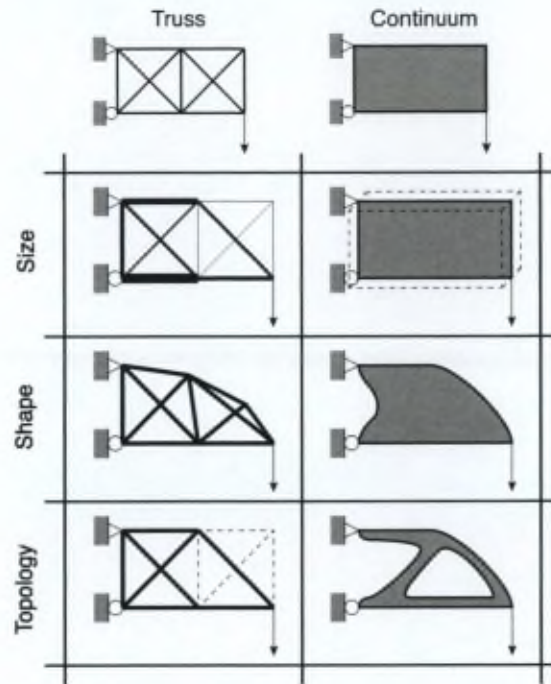


Figure 1.1: Categorization of type of optimization of discrete and continuum structures. Six types of problems can be distinguished

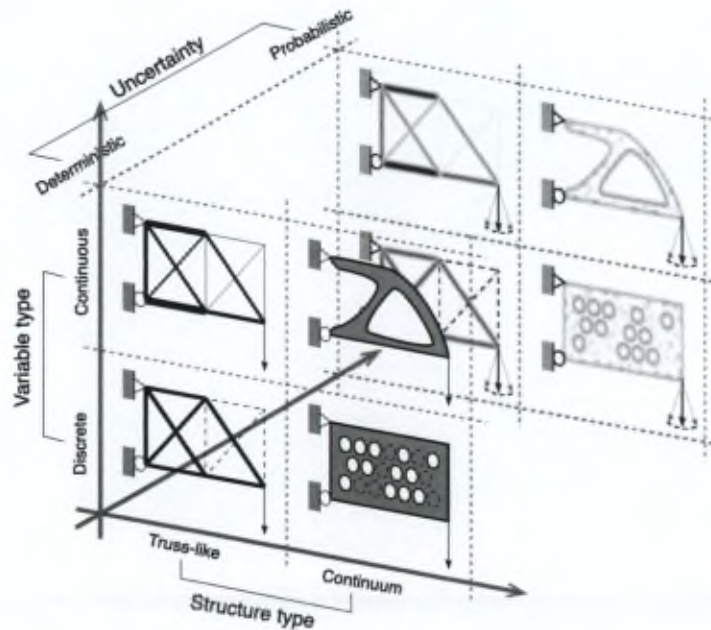


Figure 1.2: Discrete vs. continuous design variables, for truss and continuum structures

mization techniques is given in appendix B.

1.2 Thesis objectives and overview

The goal of this thesis is the development of theoretical methods targeting the implementation of topology optimization in structural engineering applications. The work is aimed mainly at truss-like structures in civil engineering applications, however several of the developments are general enough to encompass continuum structures and other areas of engineering research too. As mentioned, topology optimization has its roots in the aerospace and (to a lesser extent) automotive industries. The immediate, reproducible need to save mass or maximize stiffness has led to the use of optimization methods on components such as plates and bulk materials. This type of optimization requires continuum methods, where the structural domain discretization is not critical to the problem definition. In civil engineering, however, structures are typically assemblies of many standardized components, such as bars, where the largest gains can be made during the preliminary design of the overall structure [11].

The term truss-like is used loosely to describe structures consisting of elements which are distinguishable from one another and usually linear (meaning that one dimension is much greater than the other(s)). These structures include classical trusses, frame structures, braced frames, grid shells, spatial structures, and truss-like continua. This as opposed to plate-like or massive structures. Experience suggests that truss-like structures make up the majority of structural engineering applications. Given the recent interest in industry [11] for structural optimization applied to civil engineering structures, several pertinent challenges have become apparent:

1. Discrete variable optimization, generally necessary for truss problems in civil engineering, tends to be *computationally very expensive*,
2. the gap between *industrial applications* in civil engineering and *optimization research* is quite large, meaning that the developed methods are currently not fully embraced in practice, and
3. industrial applications demand *robust and reliable solutions* to the real-world problems they are faced with in order to be taken seriously by the civil engineering profession for

practical applications.

In order to address some of these issues, the research carried out in this thesis has followed several paths in the form of research papers. The research papers are included as chapters in the thesis manuscript. An overview of the papers making up the chapters of this manuscript, and their relation to one another, is given in figure 1.4. This thesis aims to address the above points as follows:

- The absence of function gradient information at points in the design space has led to the development of gradient-free methods (such as population-based methods with randomly generated initial populations). One of the main drawbacks of this class of optimization method is the need to sample many possible solutions. When discrete variables representing presence and absence of elements are used in structural topology optimization, many randomly selected sample solutions will be mechanisms and therefore provide no information to the heuristic algorithm. This leads to very large computational cost and often failure of the algorithm, especially for large scale (read practical) structures. Challenge 1 is addressed in chapter 2, where a novel method is developed for improving the performance of topology optimization problems in truss structures with discrete design variables, using so-called Kinematic Stability Repair (KSR) [13].
- Many practical problems in civil engineering require discrete existence/absence (1/0) variables such as those discussed above. Two typical examples of this are bracing systems and steel grid shell structures. The elements of these structures are almost always selected from standardized fabricated sections. Only a limited number of section sizes are available, so, for practical purposes, an accurate description of the problem requires discrete variables. Challenge 2 is addressed in chapters 3 and 4, where important industrial applications are investigated. In chapter 3 a novel method is developed for topology optimization of grid shells whose global shape has been determined by form-finding [15]. Chapter 4 illustrates a novel technique for façade bracing optimization [16]. In this application a multiobjective approach was used to give the designers freedom to make changes within the optimal set, as the design advanced at various stages of the design process. The two publications arising from this research are shown in figure 1.4 (upper center).
- The application of these two methods to practical engineering problems, however, inspired a theoretical development which has wide-reaching implications for discrete optimization: the pitfalls of symmetry reduction [14] (figure 1.4 upper right). As already alluded to, optimization techniques in fact amount to means of search space evaluation of varying efficiency. One of the most general means of increasing efficiency of this process is reduction of the search space size. In a discrete sense this is formally termed *cardinality reduction*. A very popular and seemingly self-evident (yet deceptively problematic) method of cardinality reduction is the use of geometric symmetry reduction in structures [3, 4, 10]. This idea has its origins in structural analysis and has been shown to be valid for continuous variable problems [17]. However, as demonstrated in chapter 5, is not valid for discrete variable problems. This issue is formally explained in chapter 5. Despite intuition to the contrary, for symmetric problems, asymmetric solutions may be *more* optimal than their symmetric counterparts. Ideally, this insight could influence the role of asymmetry in structural design.
- In order for designs to be implemented in real-world applications, it is necessary to recognize some of the fundamental problems arising from idealization of structural models. In reality many uncertainties exist on geometry, loading and material properties in structural systems. This has an effect on the safety (reliability) and performance (robustness) of the non-ideal, realized structure compared to the deterministic model. Fortunately these uncertainties can themselves be modelled mathematically and taken into account in the optimization process to ensure reliable and robust solutions to the optimization problem. Challenge 3 is addressed in chapters 6 and 7. The first of these chapters introduces a general robust topology optimization

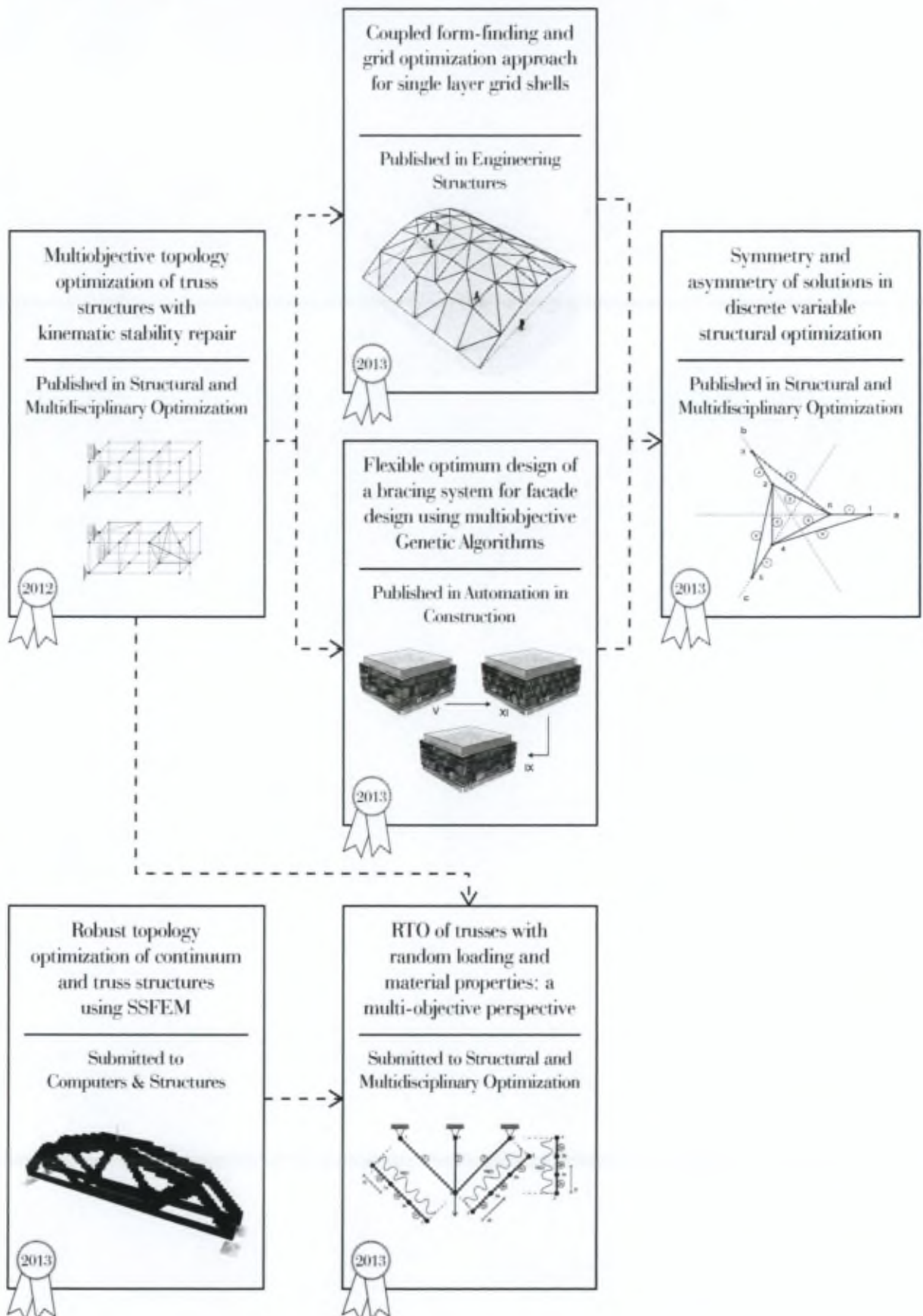


Figure 1.4: Overview of the various publications making up the Ph.D.

framework for both continuum and truss-like structures, developing a novel analysis technique for truss structures under material uncertainties. Chapter 7 extends this framework to discrete variable, multiobjective optimization problems of truss structures, taking uncertainties on the material stiffness and the loading into account. Two papers corresponding to the two chapters were submitted to the journal *Computers and Structures and Structural and Multidisciplinary Optimization* (figure 1.4 lower left).

Finally, a concluding chapter (Chapter 8) summarizes the main findings of the research. A number of appendices are included at the end of the manuscript, clarifying several issues.

Bibliography

- [1] *Topics in Applied Mechanics*, chapter Structural Optimization History and State-of-the-art, pages 339–345. Kluwer Academic Publishers, 1993.
- [2] The american heritage dictionary of the english language, fourth edition, 2003.
- [3] I.A. Azid, A.S.K. Kwan, and K.N. Seetharamu. An evolutionary approach for layout optimization of a three-dimensional truss. *Structural and Multidisciplinary Optimization*, 24(4):333–337, 2002.
- [4] Y. Bai, E. Klerk, D. Pasechnik, and R. Sotirov. Exploiting group symmetry in truss topology optimization. *Optimization and Engineering*, 10(3):331–349, 2008.
- [5] M. Beckers and C. Fleury. A primal-dual approach in truss topology optimization. *Computers & Structures*, 64(1-4):77–88, 1997.
- [6] M.P. Bendsøe and N. Kikuchi. Generating optimal topologies in structural design using a homogenization method. *Computer Methods in Applied Mechanics and Engineering*, 71(2):197–224, 1988.
- [7] R. Filomeno Coelho. Metamodels for mixed variables based on moving least squares. *Optimization and Engineering*, pages 1–19, 2013.
- [8] L. Gil and A. Andreu. Shape and cross-section optimisation of a truss structure. *Computers & Structures*, 79(7):681–689, 2001.
- [9] P. Hajela and E. Lee. Genetic algorithms in truss topological optimization. *International Journal of Solids and Structures*, 32(22):3341–3357, 1995.
- [10] A.C.C. Lemonge, H. J.C. Barbosa, L.G. da Fonseca, and A.L.G.A. Coutinho. A genetic algorithm for topology optimization of dome structures. In H. Rodrigues, J. Herskovits, C.M. Soares, J.M. Guedes, J. Folgado, A. Araújo, F. Moleiro, J.P. Kuzhichalil, J.A. Madeira, and Z. Dimitrovová, editors, *Proceedings of the 2nd International Conference on Engineering Optimization EngOpt 2010, Lisbon, Portugal*, 2010.
- [11] C. Luebke and K. Shea. Cdo: Computational design + optimization in building practice. *The Arup Journal*, 3:17–21, 2005.
- [12] P. Pedersen. Optimal joint positions for space trusses. *Journal of the Structural Division*, 99(12):2459–2476, 1973.
- [13] J.N. Richardson, S. Adriaenssens, Ph. Bouillard, and R. Filomeno Coelho. Multiobjective topology optimization of truss structures with kinematic stability repair. *Structural and Multidisciplinary Optimization*, 46:513–532, 2012.
- [14] J.N. Richardson, S. Adriaenssens, Ph. Bouillard, and R. Filomeno Coelho. Symmetry and asymmetry of solutions in discrete variable structural optimization. *Struct. Multidiscip. Optim.*, 47(5):631–643, May 2013.
- [15] J.N. Richardson, S. Adriaenssens, R. Filomeno Coelho, and Ph. Bouillard. Coupled form-finding and grid optimization approach for single layer grid shells. *Engineering Structures*, 52(0):230 – 239, 2013.
- [16] J.N. Richardson, G. Nordenson, R. Laberrenne, R. Filomeno Coelho, and S. Adriaenssens. Flexible optimum design of a bracing system for façade design using multiobjective genetic algorithms. *Automation in Construction*, 32(0):80 – 87, 2013.

- [17] G.I.N. Rozvany. On symmetry and non-uniqueness in exact topology optimization. *Structural and Multidisciplinary Optimization*, pages 1–21, 2010.
- [18] C.C. Swan and S.F. Rahmatalla. Strategies for Computational Efficiency in Continuum Structural Topology Optimization. *Advances in Engineering Structures, Mechanics & Construction*, pages 673–683, 2006.
- [19] D. Šešok and R. Belevicius. Global optimization of trusses with a modified genetic algorithm. *Journal of Civil Engineering and Management*, 14(3):147–154, 2008.

Chapter 2

Algorithm performance in discrete topology optimization

Truss-like structures are exceedingly common in engineering applications (for example those in figures 2.1 and 2.2). Design optimization of these structures can lead to significant improvement of structural performance and material savings. Discrete variable topology optimization of truss-like structures poses a number of distinctive challenges for optimization algorithms. One very pertinent issue relates to the computational efficiency of the algorithms, particularly for large-scale problems. We are especially interested in large-scale structural problems, since these are the kind most commonly encountered in industrial applications where structural optimization could have the greatest impact. The inability to solve these problems with a reasonable computation expense is a barrier to the use of current optimization methods. To address this, the following paper presents a method for targeting an aspect of discrete topology optimization of truss structures, namely the problem of kinematic instability in randomly generated truss topologies. It is shown in the paper that using this approach, the genetic algorithm used can be significantly improved in terms of performance.



Figure 2.1: Numerous truss structures at the New Galveston Causeway Railroad Lift Bridge. Image courtesy of Patrick Feller



Figure 2.2: The backplane support structure for NASA's James Webb Space Telescope in Magna, Utah. Image courtesy of NASA

Multiobjective topology optimization of truss structures with kinematic stability repair¹

Abstract

This paper addresses single and multiobjective topology optimization of truss-like structures using genetic algorithms (GA's). In order to improve the performance of the GA's (despite the presence of binary topology variables) a novel approach based on kinematic stability repair (KSR) is proposed. The methodology consists of two parts, namely the creation of a number of kinematically stable individuals in the initial population (IP) and a chromosome repair procedure. The proposed method is developed for both 2D and 3D structures and is shown to produce (in the single-objective case) results which are better than, or equal to, those found in the literature, while significantly increasing the rate of convergence of the algorithm. In the multiobjective case, the proposed modifications produce superior results compared to the unmodified GA. Finally the algorithm is successfully applied to a cantilevered 3D structure.

2.1 Introduction

Optimization of discrete structures, such as trusses, grid shells and frames, is of great importance in structural engineering. While shape and sizing [14] optimization have received much attention and are relatively mature areas of research, several challenges still face researchers in the field of discrete topology optimization:

1. The topology variables considered are discrete, meaning that traditional gradient-based optimization techniques are not directly applicable.
2. In general multiple objectives may be of interest to the designer [7]. Multiobjective topology optimization increases the complexity of the problem.

3. Optimization techniques developed to deal with discrete variable problems tend to have poor computational performance as pointed out by [32]. Large scale structures, with a large number of variables, such as those typically encountered in civil engineering problems, further magnify this problem.
4. Practical design and construction constraints further exacerbate the difficulties.

The presence of discrete or mixed variables in optimization problems has led to the successful development of optimization techniques such as stochastic search methods, of which genetic algorithms (GA) [15, 17, 22, 25] have become particularly popular. Population based stochastic methods, such as GA's, are also well suited to multiobjective problems [26], since a number of individuals may be considered at any given time. This aspect is consistent with the notion of Pareto optimality in which a number of non-dominated (i.e. 'best compromise') solutions make up an optimal set (the Pareto optimal set). Much success has been achieved in the combination of multiobjective optimization with GA's in other fields of structural optimization [5]. However, relatively few papers [2, 24, 33, 36] on multiobjective topology optimization of truss structures are found in the literature.

The Multiobjective Genetic Algorithm used as a basis for the proposed method was introduced by Fonseca and Fleming [13]. The use of a well established algorithm such as this allows for the effects of modifications to the algorithm to become clear. Nevertheless, in truss topology optimization, GA's tend to have poor computational performance in terms of CPU time [32].

One of the main focuses of current research is improving the cost and efficiency of the GA in discrete topology optimization by reducing the large number of unnecessary calculations. Two approaches exist in this context, namely avoiding duplicate calculations [32] and avoiding calculation of non-feasible solutions [8, 18, 22]. The fea-

¹J.N. Richardson, S. Adriaenssens, Ph. Bouillard, and R. Filomeno Coelho. Multiobjective topology optimization of truss structures with kinematic stability repair. *Structural and Multidisciplinary Optimization*, 46:513–532, 2012

sible solutions make up the feasible solution set Ω of the search space S which is defined by the constraints on the problem. Much research has been conducted on other issues relating to the constraints of the discrete topology optimization problem [30, 31], but the kinematic stability of trusses has been largely overlooked. In discrete design problems, definition of Ω appears to have been almost completely neglected, particularly in engineering applications [35]. Several constraints typically characterize Ω in structural topology optimization (although this list is by no means exhaustive):

1. Stress constraints in the structure.
2. Constraints on local stability of structural elements (such as buckling of elements).
3. Constraints on the stiffness of the structure (or relating to the overall deflection of the structure).
4. Constraints on the natural frequencies of the structure [38].
5. The condition of kinematic stability of the structure is particularly relevant to discrete topology optimization.

The kinematic stability of a discrete structure is intimately linked to the topology variables. While virtually all other constraints are present in sizing and shape optimization, the kinematic stability is exclusively of interest in topology optimization. In general, academic research focuses on very simple, small scale structures in which the problem of kinematic stability remains manageable. However, most civil engineering applications deal with large scale problems with numerous degrees of freedom. The smaller the relative size of the kinematically stable subset $\Omega_{ks} \subseteq S$ with respect to S , the less likely the population is to contain a significant number of kinematically stable structures. Simply identifying unstable structures does not solve this problem.

The relative number of kinematically stable solutions evaluated by genetic algorithms have in the past been increased in three ways. Firstly stable solutions can be introduced as the seed for the initial population. Hajela & Lee [17] propose a strategy composed of two successive optimization procedures, first generating a population

of kinematically stable structures, ignoring structural response constraints. These least weight stable topologies form the basis for a topology optimization and member resizing optimization stage, where a lethargization technique is used to eliminate unstable topologies. The second method involves targeting the constraints of the solution by identifying unstable solutions directly. Approaches to dealing with constraints in evolutionary algorithms are summarized in [6]. In most previous studies a check on the kinematic stability of the structure is performed, followed by penalization of the fitness of unstable structures [32]. [8] suggest first penalizing individuals which do not satisfy the Chebyshev-Grübler-Kutzbach criterion², then penalizing individuals with non-positive definite stiffness matrices.

Though these approaches seem to provide adequate results for small scale problems, they do not address the problem of scale inherent to the size of Ω_{ks} . As the number of variables increases (for the same boundary conditions), the relative size of Ω_{ks} decreases dramatically. For larger problems, penalization may not be effective at all. This problem has been demonstrated by [22] who adopted a third approach whereby only stable topologies are produced by the GA using a novel genome coding method. However, this approach can limit the search space too much in large structures.

Based on these considerations the approach proposed in this paper, topology optimization with kinematic stability repair (or KSR), suggests two adaptations of the genetic algorithm specifically developed for truss topology optimization. Firstly, individuals with guaranteed kinematic stability are introduced into the initial population. Negligible computational effort is required for this initial step and a 'good' starting point for the algorithm is produced. Secondly, a chromosome repair operation is introduced which modifies a class of kinematically unstable structures produced by the other genetic operations. Chromosome repair in this context refers to mechanisms which alter the chromosome after cross-over and mutation in order to attempt to ensure the integrity of the structure. Repair algorithms have been used with success on problems with discrete design variables in other fields of optimization [11], and in continuum multiobjective topology optimization with GA's [23].

² $DOF = dn - m - n_s$, where d is the dimension, n is the number of nodes, m the number of bar members and n_s the number of degrees of freedom constrained by the supports. It should be verified that DOF is not positive.

Some research has been conducted on the possibility of improving the performance of GA's in truss topology optimization using a genotype refinement technique [39], however these studies focus on the stress constraint.

Starting from these considerations, the paper is organized as follows: after a description of the KSR approach (§ 2.2), a number of examples illustrate single-objective (§ 2.3) and multiobjective applications of the method (§ 2.4), followed by concluding remarks and future prospects (§ 2.5).

2.2 KSR approach

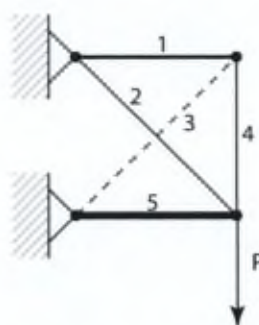
2.2.1 Parameterization of the structures

A fixed length vector (or chromosome) is used to represent the design variables (fig. 2.3): separate binary topology variables are concatenated to sizing variables (where relevant) in the chromosome representation. The discrete topology variables are mapped to 2-tuples of positive integers representing the coordinate numbering of the end nodes of the bar elements. These tuples are in turn mapped to tuples of coordinates in Euclidean \mathbb{R}^2 or \mathbb{R}^3 space depending on the problem dimension. The ground structure allows for the first mapping, while the problem space (the nodal positions) allows for the second. The ground structure approach was chosen as it is the most common in the literature and allows us to more easily compare our results to the benchmark problems, taking only the effects of our modifications into account.

2.2.2 Hypotheses

The following hypotheses are assumed:

1. The structures are made up of linear bar elements, subject only to axial forces.
2. The elements and connections of the trusses are devoid of imperfections such as eccentricities.
3. The materials under consideration are linear elastic.
4. The connections between the bars are perfectly frictionless, pinned joints.
5. The masses of the joints and members are neglected.



1	1	0	1	1	2	1	0	1	3
---	---	---	---	---	---	---	---	---	---

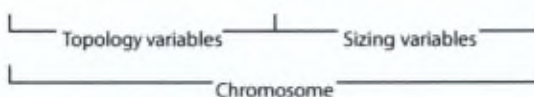


Figure 2.3: Typical parameter representation

6. Uncertainties (on the material properties, the loading, etc.) are not taken into account.

In future investigations several of these assumptions could be relaxed, however these are enforced here for simplicity.

2.2.3 Optimization framework

The KSR method employs a genetic algorithm optimization loop coupled to a finite element analysis which generates the necessary responses. For this investigation the finite element code FEAP [37] was used. The design domain comprises a set of nodes with fixed spatial coordinates, a set of supports and a set of loads. The ground structure defines the upper bound of the topological search space [9]. Introducing knowledge of the structures into the GA through a stable initial population and kinematic stability repair takes the conflicting nature of the objective functions in multiobjective optimization into account (see § 2.2.3).

Initial population

In multiobjective structural optimization most studies available in the literature consider two conflicting objectives. Therefore, a strategy is proposed in which two additional procedures are used to generate the initial population for the GA search procedure. When the general effect of a particular type of configuration of elements on the objective

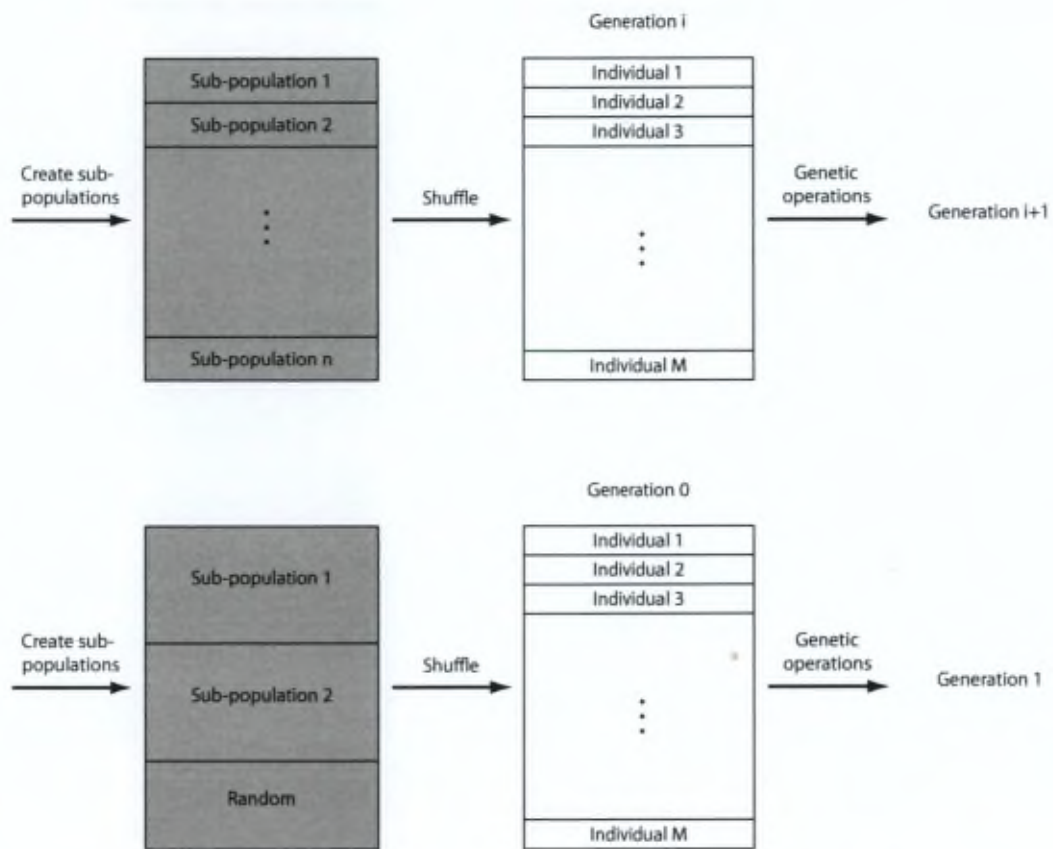


Figure 2.4: Analogy between VEGA (top) and KSR (bottom)

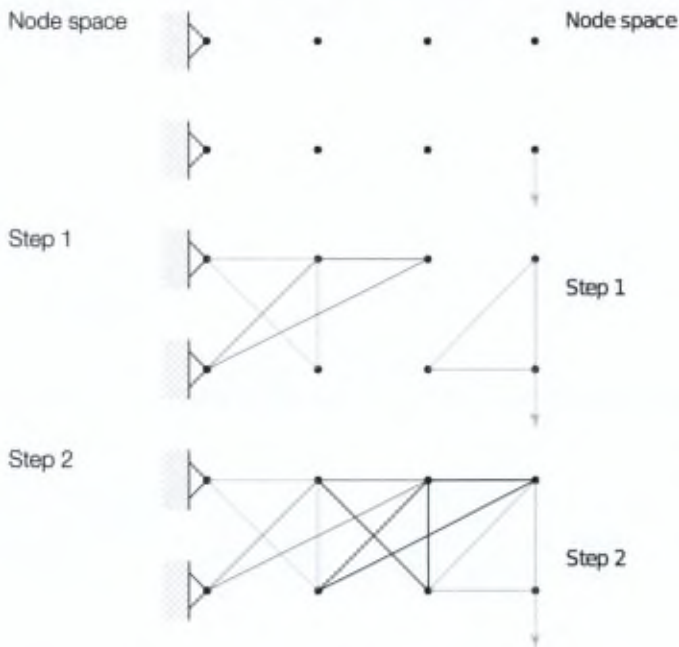


Figure 2.5: 2D procedure 1

functions is known, procedures may be devised which tend to generate these types of structures as members of the initial population. In this investigation, the procedures are intuitively developed, but a more rigorous approach is conceivable, (for example) through criterion selection. In the VEGA algorithm [34] a criterion selection technique is used to create sub-populations corresponding to separate objectives performances. These populations are then combined to create the entire population (fig. 2.4).

Two procedures are used in the multiobjective examples. The first produces individuals with large natural frequencies or greater stiffness (procedure 1); the second individuals with low masses (procedure 2). Procedure 1 uses a triangulation (for 2D problems) or tetrahedron (for 3D problems) meshing of a region of the space defined by the nodes. The loaded nodes and support nodes are given special precedence and loosely define the area to be meshed. In the 2D case, a triangle is generated for each support node or loaded node (fig. 2.5). Thereafter, the gaps between these triangles are bridged by consecutive triangular structures. The procedure in the 3D case is equivalent, using tetrahedron (fig. 2.6).

Procedure 2 employs a similar approach to that found in [22]. A stable triangular or tetrahedral *kernel* is produced randomly in the design domain.

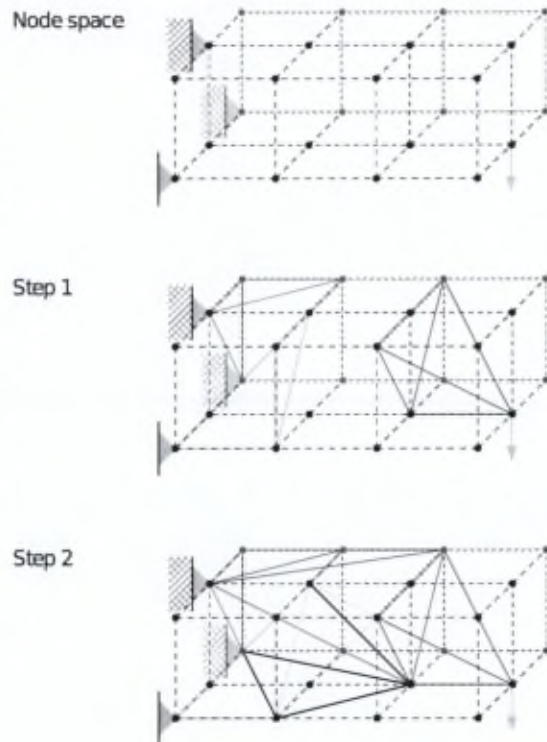


Figure 2.6: 3D procedure 1

Thereafter, the structure is grown around this kernel by adding two (in the 2D case) respectively three elements (in the 3D case) attached to nodes already in the structure, sharing a common node. This process is continued, encouraging inclusion of nodes in the direction of unconnected loaded or supported nodes, until all of these nodes form part of the connected structure. Figure 2.7 illustrates this procedure for a very simple truss problem in two dimensions. The degree to which these two methods produce different results depends on the problem configuration (nodal positions, number of boundary constrained nodes, density of the ground structure, etc.). In addition to the kinematically stable individuals, a certain proportion of the initial population is randomly seeded to encourage diversity. In the VEGA approach the various sub-populations have the same size. Similarly, the kinematically stable sub-populations have roughly the same size.

In multiobjective optimization, a number of measures, called 'metrics', can be used to quantify the performance of a set of solutions. For example, the generational distance metric (I_{GD}) (see [41] for details and other metrics) measures the normalized

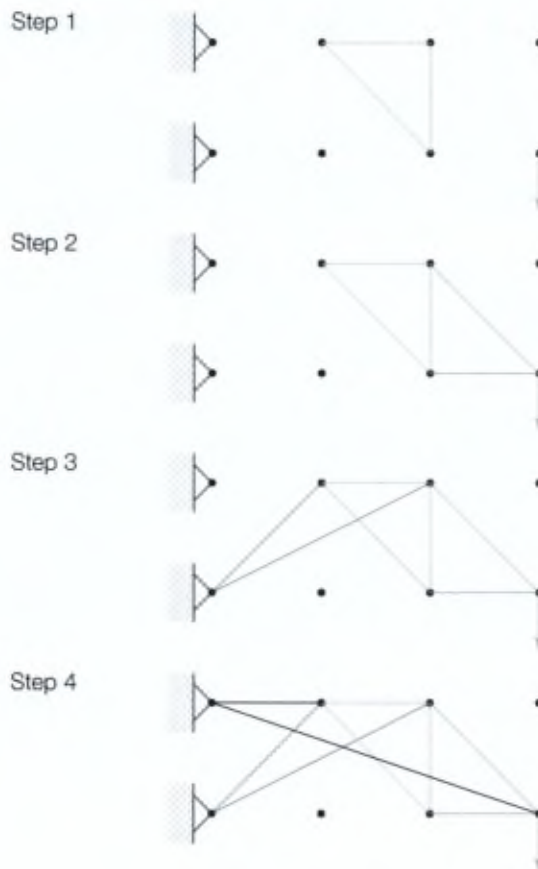


Figure 2.7: 2D procedure 2

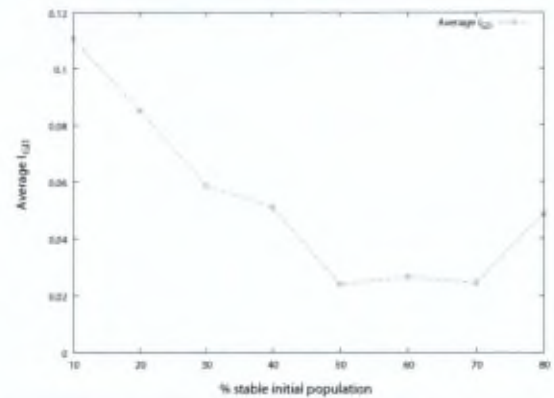


Figure 2.8: Average effect of composition of initial population on final solution for 54-bar multiobjective problem

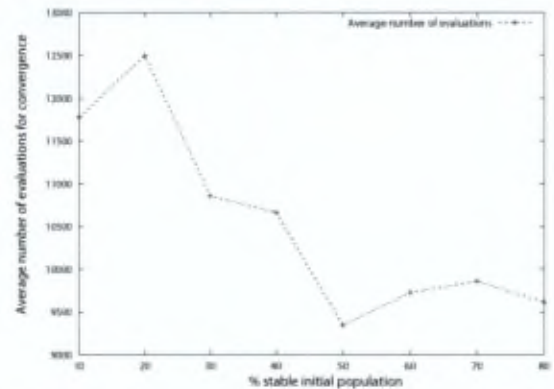


Figure 2.9: Average effect of size of stable initial population on final solution for 54-bar multiobjective problem

distance between two Pareto fronts. We use IGD here to evaluate the performance of Pareto fronts relative to the Pareto optimal solution. $IGD = 0$ signifies a convergence to the reference Pareto optimal solution. The results of a study of the size and composition of the initial population for the 54 bar example discussed in section 2.4.2 can be seen in figures 2.8 and 2.9. Note that both the minimum number of function evaluations required, and the average accuracy of the calculations coincide with a stable initial population of 50 to 80%.

Chromosome repair

The first requirement for the repair procedure is the identification of kinematic instability. Identification of unstable structures can be done in several of ways:

- Checking the positive definiteness of the structure's stiffness matrix \mathbf{K} . If \mathbf{K} is positive-definite, the truss is kinematically stable. This requires the assembly of the stiffness matrix and generally a numerical procedure to determine the condition of positive definiteness.
- Checking for satisfaction of the Chebyshev-Grübler-Kutzbach criterion, a necessary, yet not sufficient criterion for the kinematic stability. Instabilities cannot be identified directly, since the position within the structure and the nature of the instability is unknown, making this check unsuitable for repair operations.
- Checks on the connectivity of specific nodes. This can provide an indication of instabilities, yet is also a necessary but not sufficient set of criteria. Not all mechanisms can be identified in this way. A check of the positive-definiteness of \mathbf{K} is still necessary.
- The Singular Value Decomposition of the equilibrium matrix [28] provides detailed information about instabilities within the structure. This procedure can be computationally very expensive and does not necessarily indicate how a repair may take place.

The third approach is adopted here, since it provides specific structural information on how a repair to the structure can be carried out. The analysis of the stiffness matrix is carried out by default during the finite element analysis, and so a check on the instability of the structure is readily available in the event of instabilities which are not detected using the proposed approach. Two types of checks are made and repairs carried out prior to the stiffness matrix assembly (fig. 2.10). These checks identify several causes of kinematic instability and structurally undesirable configurations directly and allow for easy rectification of the detected problems:

1. The connectivity check identifies the nodes which are insufficiently connected to the rest of the structure³. The following should be checked:

- (a) The connection of the loaded and support nodes. These nodes should be connected to the structure by at least one element.

³This does not include unconnected nodes.

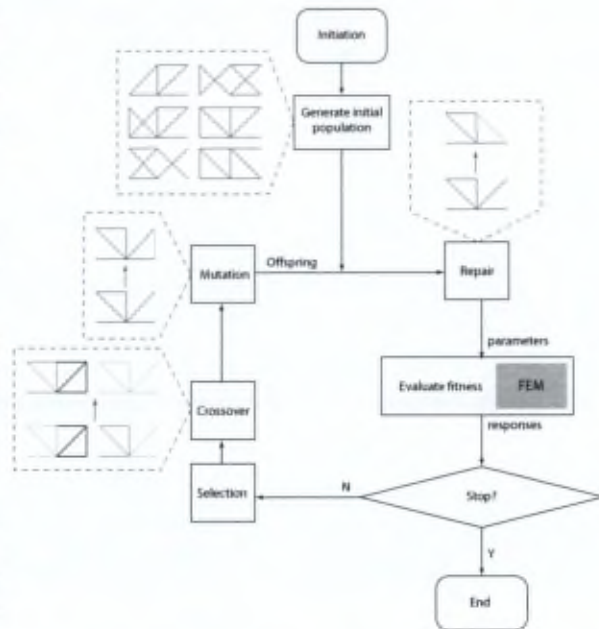


Figure 2.10: Modified genetic algorithm

- (b) Nodes connected to the structure by only one element (2D) or either one or two elements (3D). Isolated elements, connecting two nodes, but disconnected from the structure.

2. In the 2D case the linear independence check identifies all nodes connected to two elements. If the three nodes concerned are not linearly independent, the common node is identified for repair. In the 3D case the planar check identifies nodes which are connected to 3 elements only. If the 4 nodes are planar, the common node is identified for repair.

The connectivity check (fig. 2.11(a))⁴ examines the connectivity vector of tuples. If, for node i , ($i = 1 \dots n_e$), $0 \leq n_i \leq d$ a repair is carried out. Here n_e is the total number of nodes and d is the number of dimension in the problem. The linear/planar independence check (fig. 2.11(b)) analyses the connectivity of the structure and the geometric relationships between the nodes connected to common elements. Two types of operations are performed on the chromosomes in order to potentially move the structure into Ω_{ks} :

1. Addition of elements.

⁴Note that the structures conform to the Chebyshev-Grübler-Kutzbach criterion.

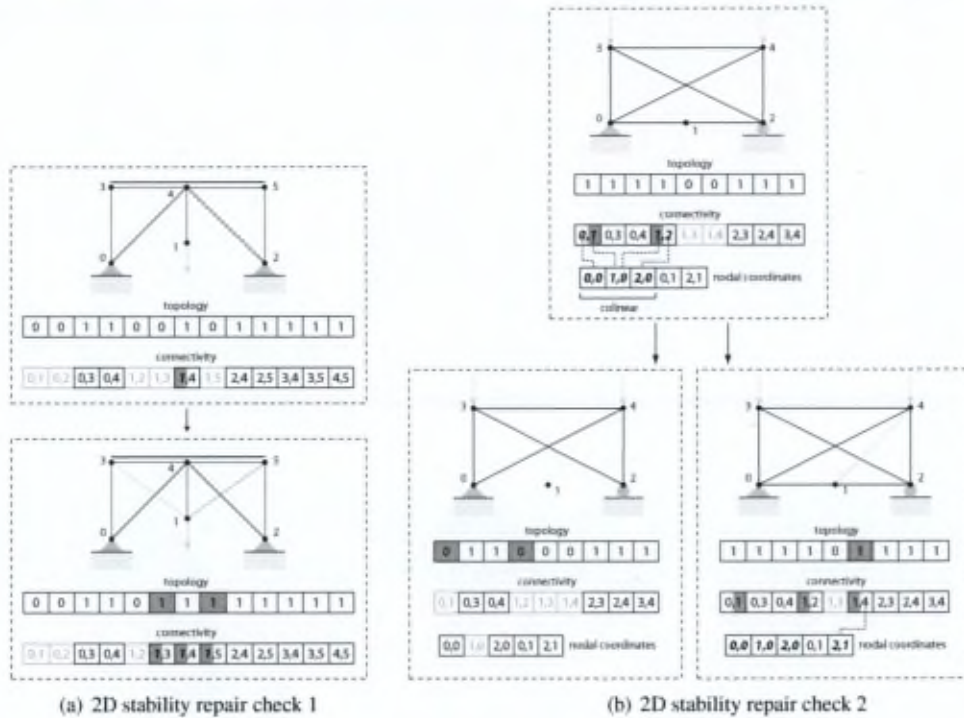


Figure 2.11: Chromosome repair checks (a) and (b)

2. Elimination of unnecessary elements.

Combinations of these operations are carried out until the structure is suitably stable from the point of view of this constraint check. The number of elements added or removed is chosen with a probability decided by the user⁵. The repair algorithm is shown in figure 2.12. Experience shows the type of kinematic instabilities identified by these checks are by far the most common, given the stable initial population generation and the use of crossover and mutation genetic operators preceding the repair operation. In fact, when repeating the trials carried out by [22], we found (fig. 2.13) that all instabilities (for this type of structure) could be repaired using the repair procedure described above. The repair algorithm, in a sense, decreases the size of the search space and therefore the size of the problem. The use of both addition and elimination of elements aids in preservation of diversity and preventing convergence towards a single solution [7], sometimes called genetic drift [4]. Fur-

thermore, local repair operations do not significantly alter the chromosomes of the individuals. Large scale repairing could negate the stochastic nature of the genetic algorithm through systematic repair of large swathes of the chromosome.

⁵During collinear/planar repair, it is ensured that the number of elements removed does not lead to the node connected to one or two elements, respectively in 2D and 3D problems. This is to avoid connectivity violations, while technically satisfying the collinear/planar check.

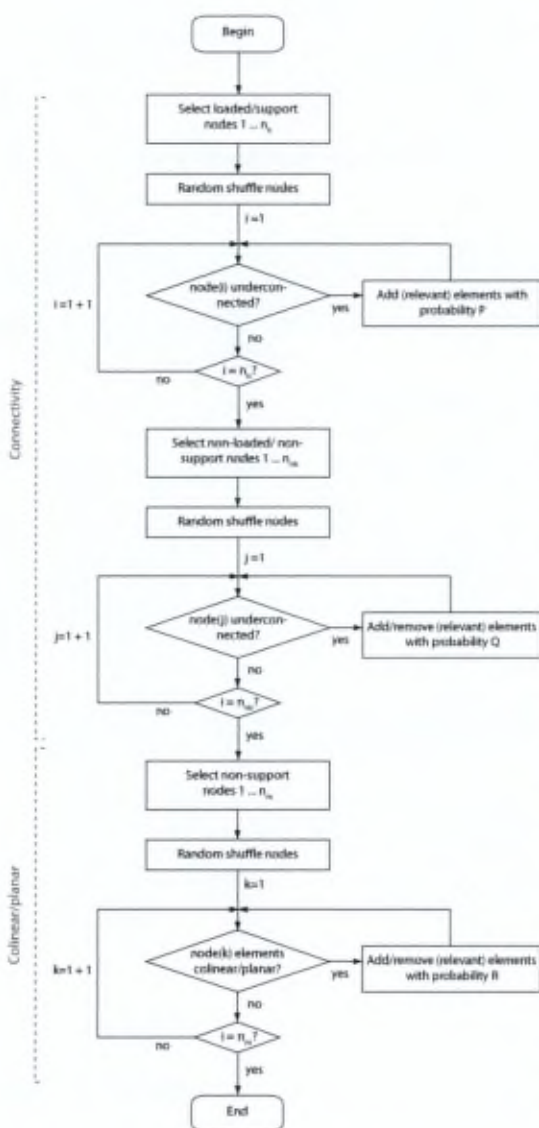


Figure 2.12: Repair procedure algorithm

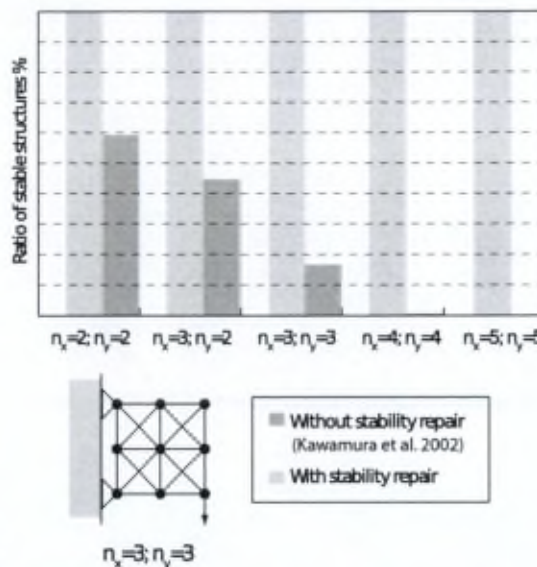


Figure 2.13: Proportion of stable structures in the search space

2.3 Single-objective topology optimization

The KSR approach suggested in the preceding sections is implemented in a number of test problems. The methodology has been developed for multi-objective problems, however we use a number of well-known single-objective problems to test the efficacy of the proposed modifications to the GA.

2.3.1 Problem formulation

A review of the literature reveals the minimization of the mass of a structure (2.1) to be one of the most commonly studied objective functions. Four constraints are considered, namely the maximum stress in the elements (2.2), local stability of the individual elements (2.3), the maximum deflection of the structure (2.4) and kinematic stability. Since we cannot be certain that all possible types of instability can be detected and repaired structures still deemed to be kinematically unstable (after repair operations are carried out if any) are penalized, similarly to the method suggested in [8]. The problem is explicitly formulated as follows:

$$f = \min_{t_i, A_i} \left\{ W = \sum_{i=1}^M \rho_i t_i A_i l_i \right\} \quad (2.1)$$

subject to:

1. Stress constraints⁶:

$$\frac{t_i |\sigma_i|}{\sigma_i^{\max}} \leq 1 \quad (2.2)$$

2. Buckling constraints:

$$\frac{t_i \sigma_i}{-\sigma_i^{cr}} \leq 1 \quad (2.3)$$

where $\sigma_i^{cr} = \frac{-\pi^2 E_i I_i}{A_i l_i^2}$ and all cross-sections are circular.

3. Vertical deflection constraint:

$$\frac{\delta_z}{\delta_z^{\max}} \leq 1 \quad (2.4)$$

where $\delta_z = \max(\mathbf{d}_z) = \max((\mathbf{K}^{-1}\mathbf{f})_z)$

where M is the number of bar elements, $i = 1 \dots M$, W is the mass of the structure, ρ_i the density of material for element i , $t_i \in \{0, 1\}$ the topological variable for element i , A_i the cross-section area of element i , l_i the length of the bar element i , σ_i the stress in element i , E_i the elastic modulus of material i , and I_i the area moment of inertia of element i .

2.3.2 Examples

Three benchmark problems commonly found in the literature are discussed in this section. For these calculations the DAKOTA [10] platform was used, with the single-objective method as the basis for the optimization scheme. For all single objective problems, the iterative procedure is stopped when the best (feasible) fitness values of the population do not improve significantly over 10 generations, or the limit value of the number of function evaluation or iterations has been reached. The built-in DAKOTA 'multi-point binary crossover' and 'merit function fitness type', with a 'favor feasible' replacement scheme were used. Furthermore, constraint penalization and an 'offset normal' mutation type were used. Further information on these genetic operators can be found in the reference above. In all examples the number of function evaluations refers to the number of calls to the FE model. In practice the computational effort required to produce the initial population is negligible compared to the total computational cost. In

⁶Note that the problem of singular topologies is eliminated through the presence of the topology variable

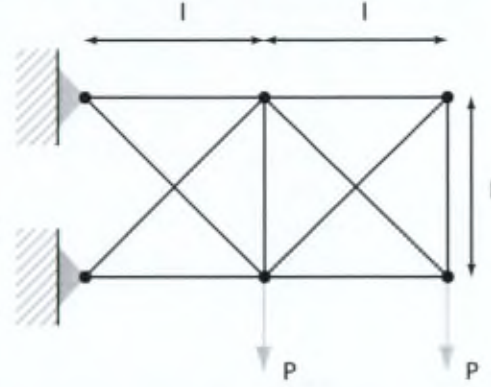


Figure 2.14: 10 bar truss ground structure

the examples discrete sizing variables were considered. 10 runs of each problem were made, each with a different initial population.

10 bar 2D truss: sizing and topology optimization

A comparison is made between a single-objective GA with kinematically stable initial population (here referred to simply as SOGA) and the results obtained by Deb & Gulati [8], as well as the results of Hajela et al. [18]. Next these results are compared to the results of the single-objective KSR algorithm. In this example, the sizing and the topology of the structure are optimized concurrently. The constraints on the problem do not include the buckling constraint (2.3), in order to conform to the same problem statement as the reference works.

Parameters: The ground structure is shown in figure 2.14. The geometric and material parameters used are found in table 2.1, while the genetic algorithm parameters are summarized in table 2.2:

Results: The optimal topology for this problem is well known (fig. 2.15). The SOGA with a randomly seeded initial population did not converge within a reasonable time (270 iterations). The SOGA with a kinematically stable initial population did, however, converge after an average of 215 generations. The results of the best solutions of the 10 runs are shown in table 2.3. The SOGA with kinematically stable initial population outperforms the results found in [18], having a

Table 2.3: 10 bar 2D truss: Comparison of results

Element	[8] A [m ²]	[18] A [m ²]	SOGA A [m ²]	KSR A [m ²]
0	0.019355	0.01806	0.019355	0.019355
1	0.01548	0.01548	0.01548	0.01548
2	0.0103	0.0103	0.009677	0.0103
3	0.00387	0.00387	0.00387	0.00387
4	0.0129	0.01355	0.012258	0.0129
5	0.01355	0.0142	0.01484	0.01355
Best mass [kg]	2228.44	2241.97	2235.2	2228.44

Table 2.1: Geometric and material parameters

Parameter	Value
l	9.144 m
P	448.2 kN
A	{6.4516E-4, 1.935E-2} m ² in increments of 6.4516E-4 m ²
E	6.895 × 10 ¹⁰ Pa
ρ	2768 kg.m ⁻³
σ _i ^{max}	1.724 × 10 ⁸ Pa
δ _c ^{max}	0.0508 m

Table 2.2: 10-bar 2D single objective problem: GA parameters

Parameter	Value
Population_size	220
Stable_proportion of IP	60%
Cross-over_rate	0.9
Mutation_rate	0.1

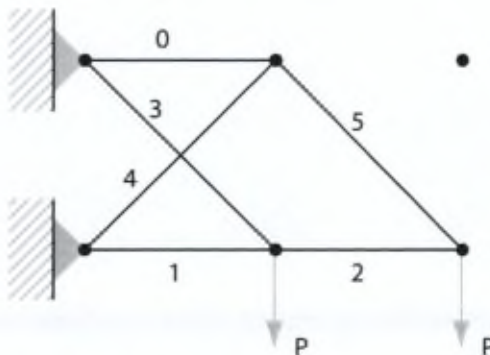


Figure 2.15: 10 bar problem: Optimized truss structure

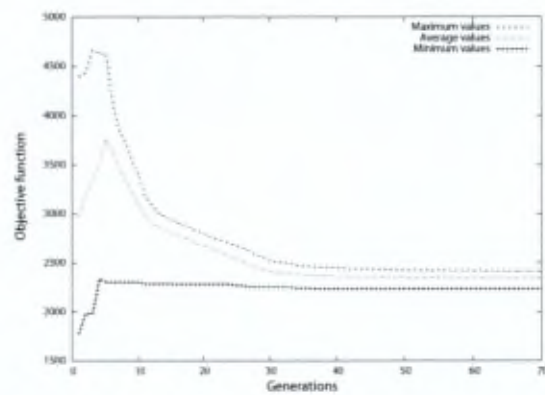


Figure 2.16: 10 bar 2D problem: convergence of KSR algorithm

marginally smaller mass by about 0.3 %. However, it fails to match or surpass the results in [8] who used a real-coded GA in which individuals are penalized after the kinematic stability has been evaluated.

The KSR algorithm converges on average after only 89 generations, and finds (in the majority of cases) the same solution as that found by Deb & Gulati. In figure 2.16, the maximum, minimum and average values (including non-feasible solutions) of the objective functions are shown for successive generations of the best performing solution which converges after 70 generations. In figure 2.17, the average function values of the best performing SOGA and KSR runs are shown for the first 70 generations. During the initial generations many non-feasible solutions with low mass are retained, leading to lower average masses. A process of penalization gradually increases the number of feasible solutions in the SOGA population until a peak is reached at which time the average

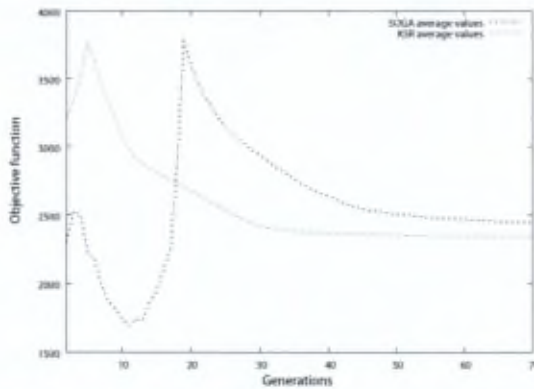


Figure 2.17: 10 bar 2D problem: Comparison of average objective function values (first 70 generations)

masses decrease once more. This is far less pronounced in the KSR population, with the peak being reached very early on. Theoretically, the two algorithms have very similar initial populations. The repair procedure greatly reduces the amount of structures penalized for being unfeasible. This example demonstrates the advantages of the KSR approach over the traditional penalization approach.

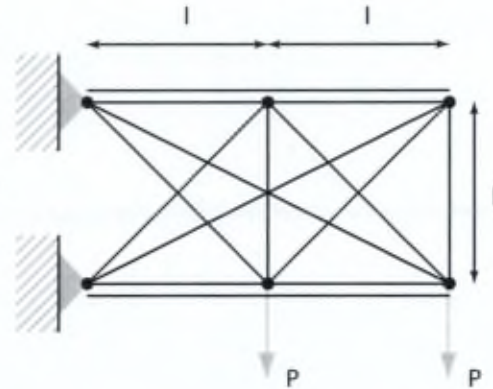


Figure 2.18: 14 bar truss ground structure

14 bar 2D truss: sizing and topology optimization

In this example a 2D 14 bar truss with the same parameters as the previous example is investigated. The ground structure is shown⁷ in figure 2.18.

Results: For this problem the same topology found in the previous problem (fig. 2.15) has been found using a multistage algorithm [17] in the literature. However using the KSR algorithm (and even the SOGA with stable initial population) a different topology is found (fig. 2.19). A comparison of the (stress and displacement constrained) problem solutions is shown in table 2.4. Note that the mass objective function of this truss optimization (in all cases) is smaller than in the previous example. This is due to the larger search space made possible by a greater number of variables. The KSR algorithm finds a smaller mass than found by Hajela & Lee, by about 4 %. The KSR algorithm

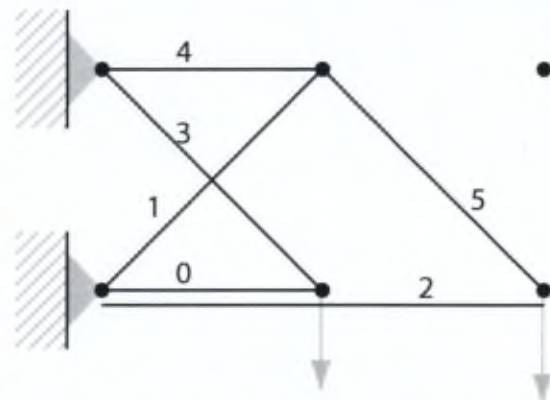


Figure 2.19: Solution to the 14 bar sizing and topology optimization

⁷ In the figures one of the two overlapping members is drawn below or above the other to avoid confusion. These members are connected to the nodes above or below them at the end points only.

Table 2.4: 14 bar 2D truss: Comparison of results

	[17]	SOGA	KSR
Average generations for stable topology	14	8	2
Mass [kg]	2241.97	2190.18	2153.56

also finds a lower mass than the SOGA with stable initial population.

25 bar 3D truss: sizing and topology optimization

In this example a benchmark 3D structure is optimized (fig. 2.20). Both sizing and topology variables are considered. The results are compared to [21], in which an initial population of good candidates is produced, followed by the systematic reduction of the search space.

Parameters: The member cross-section areas are selected from the discrete set {1.255, 2.142, 3.348, 4.065, 4.632, 6.542, 7.742, 9.032, 10.839, 12.671, 14.581, 21.483, 34.839, 44.516, 52.903, 60.258, 65.226}. The Young's modulus for the material used is $E = 68.97 \times 10^9 \text{ N.m}^{-2}$ and density of the material is $\rho = 27126.4 \text{ N.m}^{-3}$. Two load cases are considered (table 2.5). The buckling data and variable definition can be found in [21]. The maximum deflection of the structure is set at $\delta_{\max} = 8.89 \text{ mm}$. In this case only chromosome repair is implemented in the modified GA. A population size of 50 was chosen, however no stable initial population is created to show the improvement achieved by KSR only.

Results: The solution obtained is shown in figure 2.21 and the cross-section areas in table 2.7. This solutions are both identical to that found in the reference work, finding the same mass, however with slightly improved performance (table 2.6).

In this example it can be seen that kinematic stability repair has a positive effect on the efficiency of the algorithm. 81.25% of the possible topologies are found to be unstable. This structure only has 8 independent topology variables. In practice, one topology variable can be eliminated since it is always necessary for the stability

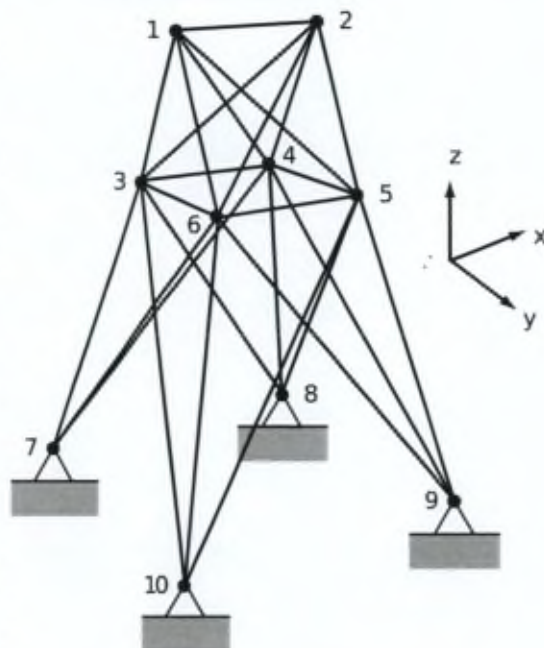


Figure 2.20: 25 bar 3D problem

Table 2.5: 25 bar 3D truss: Loading

Loading case	Node	F_x (kN)	F_y (kN)	F_z (kN)
1	1	4.45	44.5	-22.25
1	2	0	44.5	-22.25
1	3	2.225	0	0
1	6	2.225	0	0
2	1	0	89	-22.25
2	2	0	-89	-22.25

Table 2.6: 25 bar 3D truss: Comparison of results

	[21]	SOGA	KSR
Generations	100	82	64
Weight [N]	2517.24	2517.24	2517.24

Table 2.7: 25 bar 3D truss: Topology and cross-section areas obtained

Cross section	1	2	3	4	5	6	7	8
Area (cm^2)	-	10.839	21.483	-	-	6.542	12.671	14.581

of the structure. Problems such as this are of little interest as they present few challenges to current topology optimization algorithms. However this problem illustrates the efficacy of the method even on small scale 3D problems, where symmetry has been taken into account. The key to implementing the repair procedure is the appropriate parameterization of the structure so that stability and instability can be identified correctly.

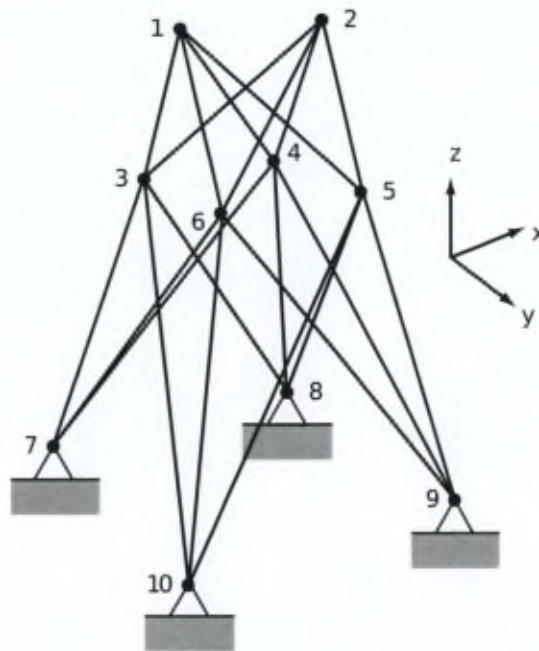


Figure 2.21: 25 bar 3D problem topology after optimization

Conclusions

In the above examples – using the KSR algorithm – the optimal topology is found, and begins to dominate the population, after only a few generations. The remaining iterations are necessary mainly to refine the sizing of the bars. The sizing optimization is not the focus of this investigation, however to be able to compare results it has been introduced. The algorithm remains valid and advantageous with this adjustment. It is clear that the multistage approach is not always beneficial. Unmodified, randomly seeded GA's may require particularly large convergence times compared to the modified KSR GA. The stable initial population improves the performance of the GA significantly. The advantages of the algorithm are expected to be greater in larger problems. The repair approach outperforms the penalization techniques used in the reference works which do not explicitly take structural knowledge into account. If, as in most studies, the kinematic stability is taken to be a binary condition, it is not possible to meaningfully penalize kinematically unstable solutions as a function of the degree to which the constraint has been violated.

2.4 Multiobjective topology optimization

2.4.1 Problem formulation

The multiobjective problems in this section make use of the objective function and constraints in § 2.3.1. In addition the dynamical objective function and the maximum deflection objective function are introduced:

$$f_2 = \min_{t_i, A_i} \{ -(\omega_{n,0})^2 \} \quad (2.5)$$

$$f_3 = \min_{t_i, A_i} \left\{ \delta_z = \max(\mathbf{d}_z) = \max \left((\mathbf{K}^{-1} \mathbf{f})_z \right) \right\} \quad (2.6)$$

where $\omega_{n,0}$ is the smallest (first) natural frequency of the structure. The response of a structure to excitation depends largely on the first few natural frequencies [40]. In the literature dynamic aspects of the structure have been handled as constraints for discrete structures [16, 20, 38], or explicitly as an objective function for continuum topology optimization [19, 27]. Here we wish to maximize the smallest (first) natural frequency of the structure.

2.4.2 Examples

Three problems are discussed in this section. For these calculations the DAKOTA Multiobjective Genetic Algorithm (MOGA) was used. This method performs Pareto optimization using a metric tracker to evaluate the convergence of the algorithm. This tracker evaluates three metrics associated with consecutive Pareto fronts and is described in detail in [10]. This method has much in common with the aforementioned SOGA method implemented by DAKOTA. Therefore, the modifications to the SOGA and the MOGA algorithms were not significantly different. The algorithm is judged to have converged once the value of the metric tracker does not change significantly for 10 generations. The built-in DAKOTA multi-point binary crossover and domination count fitness type, with a 'below limit' (with a value of 6) replacement scheme were used. Furthermore, constraint penalization and an 'offset normal' mutation type were used.

14 bar 2D truss: topology optimization

The 14 bar truss example with only topology variables is used to demonstrate the effectiveness

Table 2.8: 14 bar 2D truss multiobjective problem: GA parameters

Parameter	Value
Population_size:	100
Stable_proportion of IP	60%
Crossover_rate:	0.8
mutation_rate:	0.2
Cross-section:	0.01419352 m^2

of this algorithm on small-scale examples. The ground structure and geometry (with the exception of the cross-section which is constant in this problem) are identical to that in figure 2.18. The KSR algorithm is tested against the MOGA algorithm with a stable initial population.

Parameters: The objective functions considered are the total mass (2.1) of the structure and the maximum vertical nodal displacement (2.6). The structure is subject to constraints on the stresses in the elements (2.2) only, while only topology variables are considered. The genetic algorithm parameters for both algorithms are summarized in table 2.8.

Results: A comparison of the two algorithms performances is shown in table 2.9. The Pareto optimal set can be seen in figure 2.22. Clearly there are advantages in terms of computational performance to the modified algorithm. The KSR algorithm converges on average several times faster than the MOGA. In figure 2.23 the generational distance metric, relative to the Pareto optimal solution, for successive generations of the best solutions out of the 10 MOGA and KSR runs is shown. Clearly the KSR algorithm is advantageous in terms of convergence. It is worth noting that on average, for this problem 3 of the solutions in the Pareto optimal set were found in the initial population using procedures 1 and 2. While this is a relatively large proportion, it is expected that the likelihood of finding these optimal solutions simply by generating an initial population will decrease as the problem becomes larger.

54 bar 2D truss: topology optimization

The KSR algorithm is specifically aimed at large scale problems with binary topology variables. The 54 bar cantilever problem discussed in this

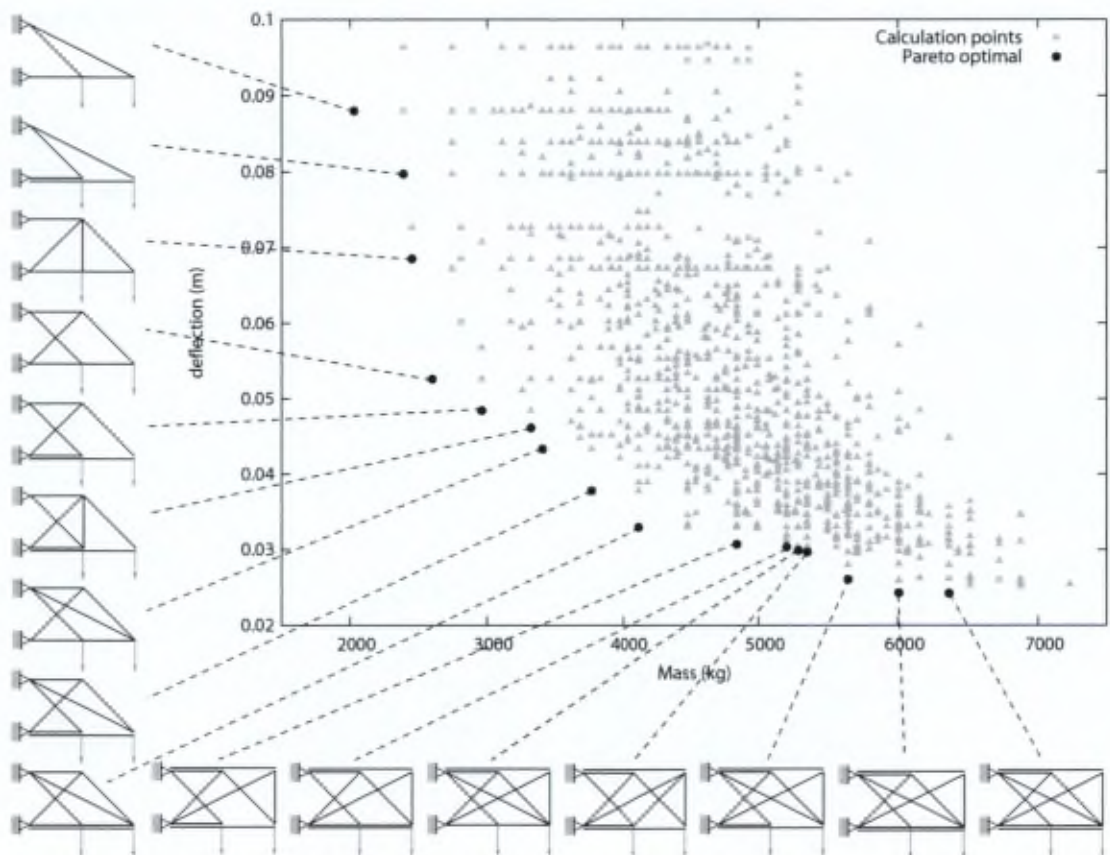


Figure 2.22: 14 bar 2D truss: Pareto optimal topologies

Table 2.9: 14 bar 2D truss: Comparison of algorithm performance

Algorithm:	MOGA	KSR
Average generations for convergence	126	47
Average I_{GD}	0.0173	0.0036
Average Pareto set size	14.4	15.6

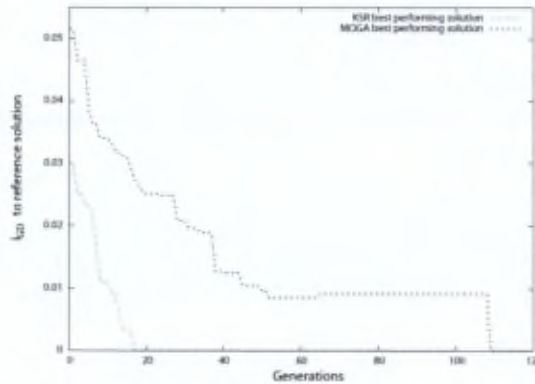


Figure 2.23: 14 bar 2D truss: Best solution convergence relative to reference solution

section is of this type. The objective functions in this problem are the mass and first natural frequency of the structure $\omega_{n,0}$, expressed in equation (2.5) and the constraints include the stress constraint on the members (2.2), the buckling of the members (2.3) and the deflection constraint (2.4).

Parameters: The ground structure is shown in figure 2.24. The two nodes on the left of the structure are restrained in both vertical and horizontal direction. Four cases are considered. In the first three cases symmetry considerations are not implemented to reduce the size of the problem, which consists of a length 54 vector of discrete binary design variables. A study of the 29 variable symmetric problem was also made to show the effects of forcing symmetry. The geometric and material parameters characterizing the problem can be found in table 2.10 and the GA parameters in table 2.11. The nominal cross-section area is chosen as $A_{nom} = 2 \times 10^{-3} \text{ m}^2$.

Results: The Pareto fronts of the best performing MOGA with stable initial population, the symmetric problem and the multiobjective KSR algorithm can be seen in figure 2.25. Solution of the symmetric problem relied on the MOGA with

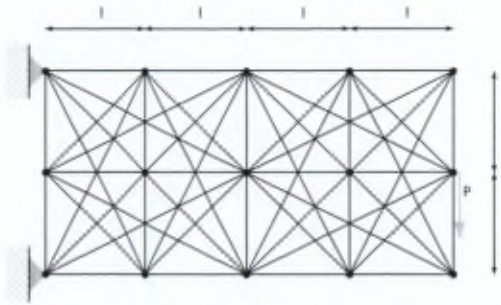


Figure 2.24: 54 bar cantilever truss ground structure

Table 2.10: 54 bar 2D truss: Geometric and material parameters

Parameter	Value
l	1 m
P	100 kN
E	$6.9 \times 10^{10} \text{ Pa}$
ρ	2768 kg.m^{-3}
σ_i^{\max}	$1.724 \times 10^8 \text{ Pa}$

Table 2.11: 54 bar 2D truss: GA parameters

Parameter	Value
Population_size	400
Cross-over_rate	0.8
Mutation_rate	0.5
Stable_proportion	0.7

a stable initial population. The generational distance between the MOGA and KSR Pareto fronts is found to be $I_{GD} = 0.0707$. The MOGA algorithm, for all but one of the runs, reached the maximum number of iterations (500) before satisfying the convergence criterion. The topologies in the Pareto optimal sets are also shown in figure 2.25. Note the asymmetry in the topologies where no symmetry was forced, and their superiority to the symmetric solutions. While the problem is geometrically symmetrical, the presence of the buckling constraint introduces asymmetry, namely the absence of the constraint in tension elements. It is also noted that the buckling constraint is active in all of the above topologies. Furthermore, the use of discrete design variables can have the effect of producing asymmetric topologies even in symmetrical problems [1]. The generational distance between the KSR and symmetric Pareto fronts is

Table 2.13: 54 bar 2D truss: Effect of composition of initial population

	70% Procedure 1	70% Procedure 1	35% Procedure 1, 35% Procedure 2
Ave. evaluations for convergence	11596	10034	9861
Average I_{GD}	0.0415	0.06725	0.024375

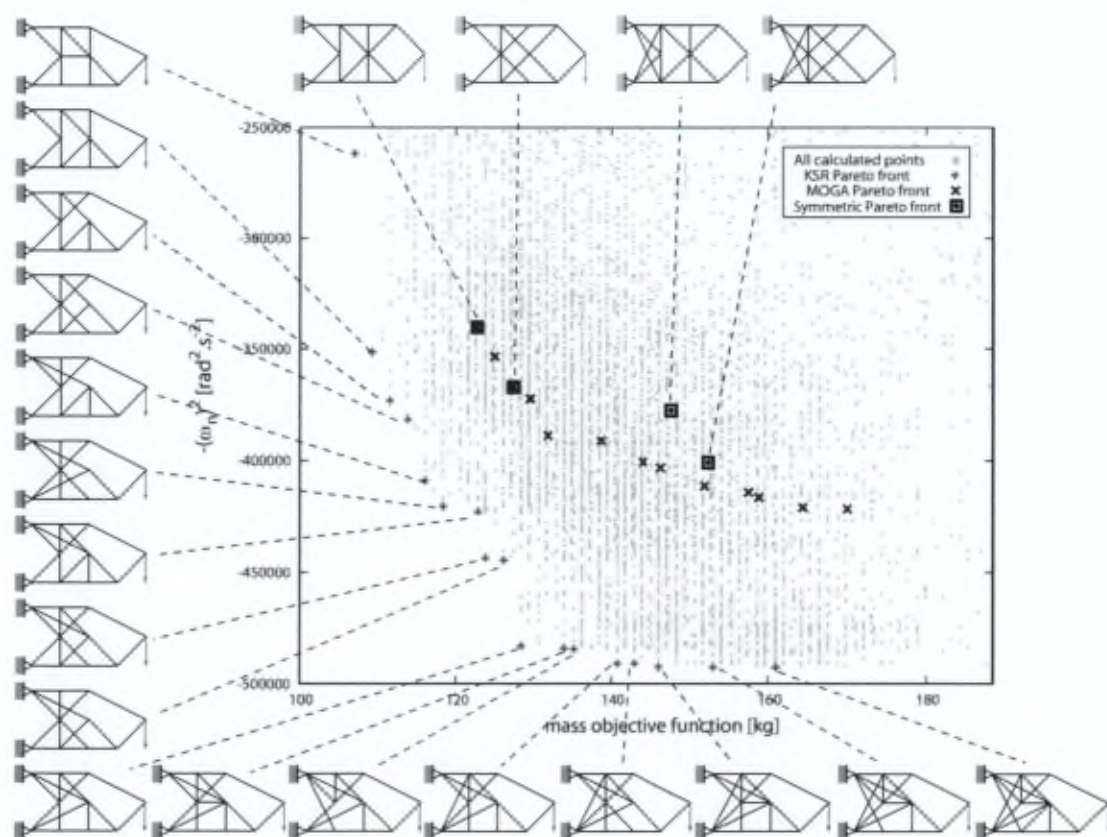


Figure 2.25: 54 bar MOGA: Pareto fronts

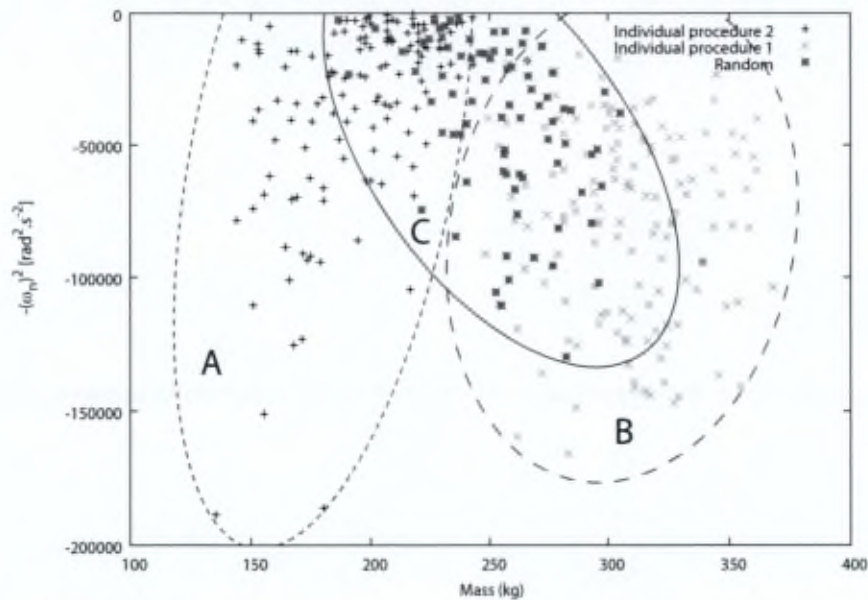


Figure 2.26: 54 bar MOGA initial population: Procedure 1, Procedure 2 and randomly seeded individuals

0.1563.

The different methods on average produce varying numbers of Pareto optimal solutions (table 2.12). The objective function values of the feasible individuals in the initial population are shown in figure 2.26. 30 % of the initial population was generated randomly (in region C), while 35% of the population was generated using procedure 1 (in region B) and the remainder using procedure 2 (in region A). Furthermore the two procedures tend to produce individuals with objective function values favoring one or the other objective function, as hypothesized. The combination of procedures allows for a greater range in the Pareto front and therefore reduced drift. Table 2.13 shows the results of trials carried out with various initial population compositions and demonstrates advantages of using both procedure 1 and 2. This strategy allows for more accurate solutions on average, and slightly faster convergence to these solutions.

The optimization algorithm with chromosome repair is shown to be highly advantageous in terms of average convergence time and finds a wider range of solutions in the Pareto optimal set. It is also clear that the multiobjective KSR algorithm finds significantly better performing solutions than the MOGA.

Table 2.12: 54 bar 2D truss: Comparison of performance of algorithms

	MOGA stable IP	KSR
Average iterations for convergence	500 +	294
Pareto optimal solutions	13.6	16.2

2.4.3 Cantilevered 3D structure: topology and sizing optimization

A cantilevered structure, consisting of a steel special truss combined with a reinforced concrete deck, is optimized using the KSR algorithm. The truss elements are connected at nodes in the deck, so that the two portions work together to ensure the strength, stiffness and stability of the structure. The algorithm was used in an initial design stage to find a 'good' configuration for the truss elements. For architectural reasons the distribution of the nodes is asymmetrical and irregular (fig. 2.27). The reinforced concrete deck is taken into account in the FEM analysis.

Parameters: The loading on the structure can be seen in figure 2.28. Nodes 1 and 2 are loaded in the y-direction with 344228 N and are unre-

Table 2.14: Material parameters and maximum deflection

Parameter	Value
E_{steel}	2.1×10^{11} Pa
E_{deck}	3×10^{10} Pa
ρ_{steel}	7.8×10^3 kg.m ⁻³
ρ_{deck}	2.5×10^3 kg.m ⁻³
$\sigma_{i,\text{steel}}^{\text{max}}$	3.55×10^8 Pa
$\sigma_{i,\text{deck}}^{\text{max}}$	5×10^7 Pa
δ_c^{max}	0.015 m
$\text{thickness}_{\text{deck}}$	0.15 m

strained. Edge A-B of the plate is loaded with a line load of 237922 N.m^{-1} in the y-direction, and 50491 N.m^{-1} vertically, and is unrestrained. The deck A-B-C-D is loaded with an evenly distributed vertical loading of 10200 N.m^{-2} . This loading is a combination of live loads and the self-weight of the deck. The self weight of the truss is neglected in the initial design stage. Edge C-D is restrained in all degrees of freedom (including rotationally), with the exception of vertical translation. Nodes 3 and 4 are translationally restrained in the three spatial directions, but are free to rotate. The nodal positions are given in table 2.15. The ground structure, with 41 topology variables (dark solid lines) is shown in figure 2.29. For the generation of the stable initial population and the KSR procedure the effect of the deck is represented by a number of (non-variable) connectivities (dashed lines) lying in the plane of the deck. An initial population consisting of 60% stable structures (using an equal number of individuals produced by the 3D variations of procedures 1 and 2) was created. The objectives and constraints considered were the same as in the previous example. The solid circular cross sections (all bar elements with the same section area) were selected from the following set: {12.5, 15.9, 19.6, 23.8, 28.3, 33.2, 38.5, 44.2, 50.3, 56.7, 63.6, 70.9, 78.5, 86.6, 95.0} $\times 10^{-4} \text{ m}^2$. The material parameters and maximum allowed deflection are found in table 2.14 and the GA parameters in table 2.16.

Results: Of the 10 runs carried out for this problem, the best performing Pareto optimal front is shown in figure 2.30. The average number of generations required for convergence was 276. The front, containing 285 solutions, is shown along with roughly every 20^{th} solution. The cross-

Table 2.15: 3D cantilevered structure: truss nodal positions (m)

Node number	x	y	z
1	0.825	0	0
2	2.475	0	0
3	0.825	4.5	0
4	2.475	4.5	0
5	1.05	1.05	0.9
6	2.55	0.75	0.9
7	2.55	2.25	0.9
8	0.75	2.85	0.9
9	0.75	4.05	0.9
10	2.55	4.05	0.9
11	0.825	1.5	0
12	0.825	3	0
13	2.475	1.5	0
14	2.475	3	0

Table 2.16: 3D Cantilevered structure: GA parameters

Parameter	Value
Population_size	400
Cross-over_rate	0.6
Mutation_rate	0.05

section increases constantly as we move from low to high mass solutions. The average generational distance was $I_{GD} = 0.0024$. In fact the Pareto front can be broken up into sub-fronts according to the cross-section size (denoted by varying shades of grey), without any overlapping. This explains the corrugated appearance of the front: each corrugation is a topology-only Pareto front for a given cross-section. In our approach all but the lowest cross-section are presented in the Pareto front. The spread of solutions along the front and for the various cross sections, is relatively uniform.

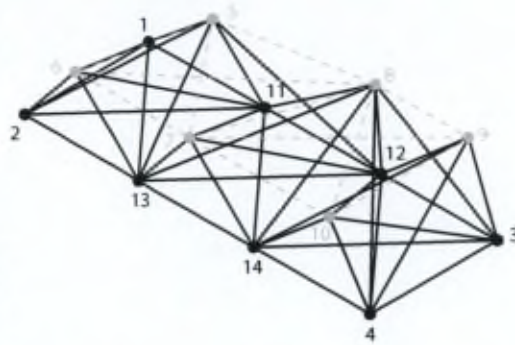


Figure 2.29: 3D cantilevered structure: ground structure

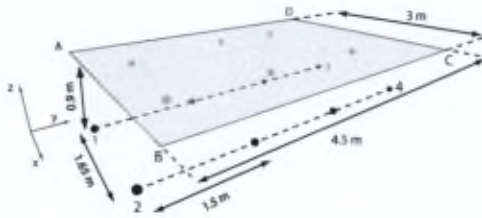


Figure 2.27: 3D cantilevered structure: nodal positions

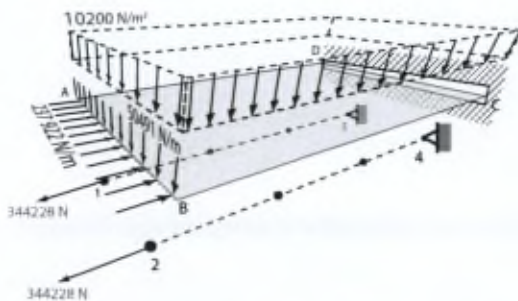


Figure 2.28: 3D cantilevered structure: loading

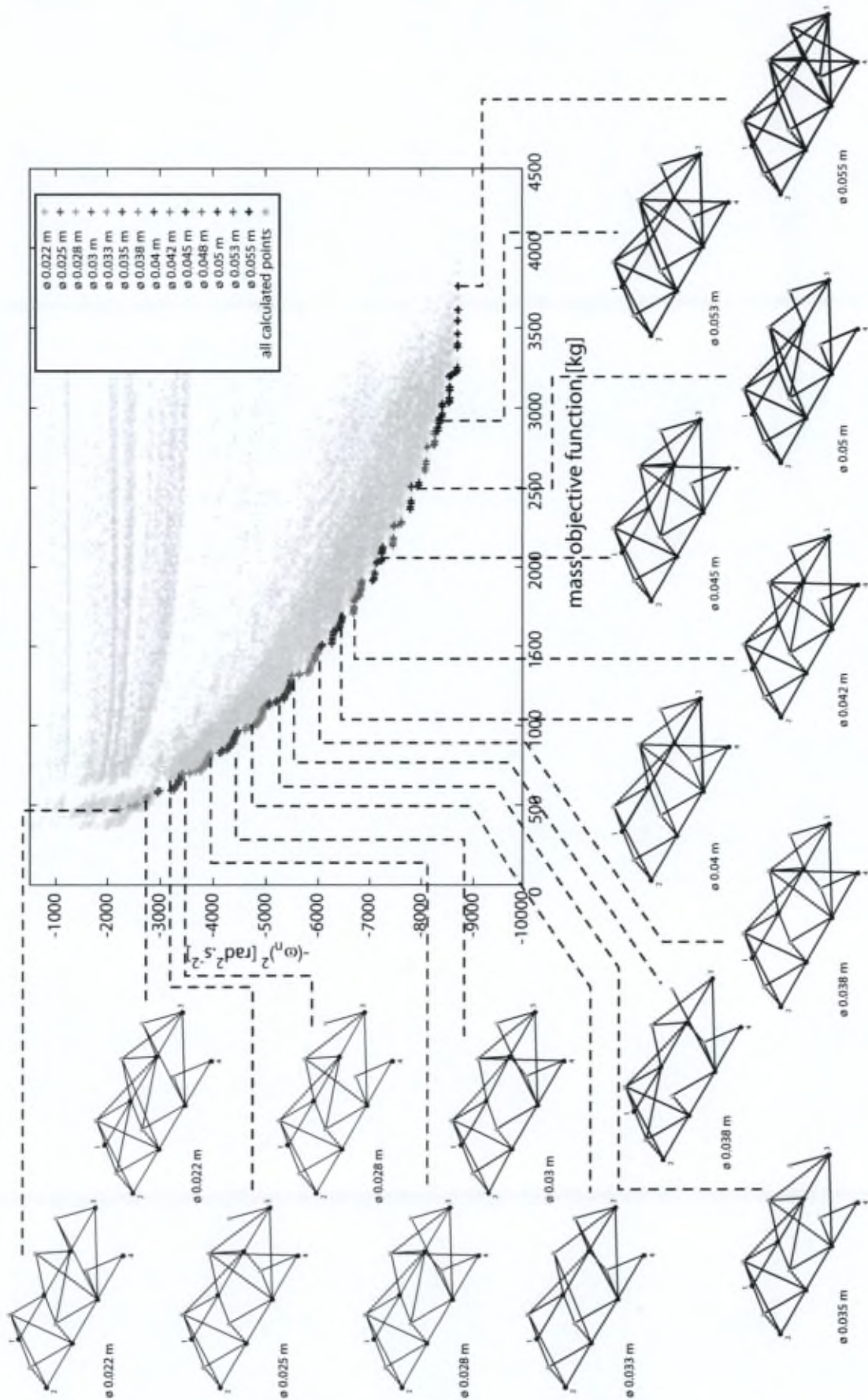


Figure 2.30: 3D cantilevered structure: Pareto front

2.5 Conclusions and future prospects

A novel approach to improve the performance of genetic algorithms in structural optimization with discrete topology variables has been proposed. The procedure makes use of multiple methods of stable initial population generation and chromosome repair of a class of kinematically unstable structures. By implementing these adaptations, knowledge of structural behavior is added to the GA. These additions allow for a compromise between the explorative character of the GA, and the reduction of the search space through addition of information. The procedure has been demonstrated on single-objective academic examples and compares well to the results in the literature. Furthermore, the method has been demonstrated on multiobjective problems and the advantages over unmodified methods shown.

Possible future prospects are listed hereafter:

- It would appear that a thorough study of the effects of the kinematic stability constraint on the feasible solution set Ω in discrete structural problems would be of great interest, given the lack of attention in the literature. The use of more advanced methods of detecting instability could be investigated, taking inspiration from graph theory and computer science, for example, are a possible future avenue of research. The method using the Singular Value Decomposition of the equilibrium matrix also appears to hold much promise for the improvement of the method since all kinematic instabilities can be detected in this way.
- Three or more objectives, and, to a lesser extent, multiple loading cases, present challenges to the approach. Adaptation of the method in this way, possibly with an automated scheme for initial population generation by criterion selection, can produce a more general method.
- The integration of shape optimization into the procedure, which could lead to a complete multiobjective layout optimization method. Layout optimization of large scale discrete structures, such as grid shells, could benefit greatly from the KSR repair procedure, since kinematic instability is frequently encountered in this type of problem.

- There is much scope for investigations into decision making and user preferences [11] as well as the handling of uncertainties [12].
- Global elastic stability of the truss structure has not been discussed here. Some research has been done in this area using nonlinear programming [3]. This is an important constraint in practice, which would make the method more relevant for practical application.
- For large scale problems, the ground structure approach may not be the most efficient. Making use of other methods of representing the design domain, for example using a variable chromosome length, may be fruitful as an adaptation of the KSR method.

Bibliography

- [1] W. Achtziger and M. Stolpe. Truss topology optimization with discrete design variables—guaranteed global optimality and benchmark examples. *Structural and Multidisciplinary Optimization*, 34:1–20, 2007.
- [2] R.J. Balling, R.R. Briggs, and K. Gillman. Multiple optimum size/shape/topology designs for skeletal structures using a genetic algorithm. *Journal of Structural Engineering*, 132:1158, 2006.
- [3] A. Ben-Tal, F. Jarre, M. Kočvara, A. Nemirovski, and J. Zowe. Optimal design of trusses under a nonconvex global buckling constraint. *Optim. Eng.*, 1(2):189–213, 2000.
- [4] F.Y. Cheng and D. Li. Multiobjective optimization design with pareto genetic algorithm. *Journal of Structural Engineering*, 123(9):1252–1261, 1997.
- [5] C.A. Coello Coello. A comprehensive survey of evolutionary-based multiobjective optimization techniques. *Knowledge and Information systems*, 1(3):129–156, 1999.
- [6] C.A. Coello Coello. A survey of constraint handling techniques used with evolutionary algorithms. *Laboratorio Nacional de Informatica Avanzada, Veracruz, Mexico, Technical report Lania-RI-99-04*, 1999.

- [7] C.A. Coello Coello, G.B. Lamont, and D.A. Van Veldhuizen. *Evolutionary algorithms for solving multi-objective problems*. Springer-Verlag New York Inc, 2002.
- [8] K. Deb and S. Gulati. Design of truss-structures for minimum weight using genetic algorithms. *Finite Elements in Analysis and Design*, 37(5):447–465, 2001.
- [9] W.S. Dorn, R.E. Gomory, and H.J. Greenberg. Automatic design of optimal structures. *Journal de Mécanique*, 3:25–52, 1964.
- [10] M.S. Eldred, B.M. Adams, K. Haskell, W.J. Bohnhoff, J.P. Eddy, D.M. Gay, J.D. Griffin, W.E. Hart, P.D. Hough, T.G. Kolda, M.L. Martinez-Canales, L.P. Swiler, J.P. Watson, and P.J. Williams. DAKOTA, a multilevel parallel object-oriented framework for design optimization, parameter estimation, uncertainty quantification, and sensitivity analysis: Version 4.1 reference manual. Technical Report SAND2006-4055, Sandia National Laboratories, Albuquerque, New Mexico, September 2007.
- [11] R. Filomeno Coelho and Ph. Bouillard. A multicriteria evolutionary algorithm for mechanical design optimization with expert rules. *International Journal of Numerical Methods in Engineering*, 62(4):516–536, 2005.
- [12] R. Filomeno Coelho, J. Lebon, and Ph. Bouillard. Hierarchical stochastic metamodels based on moving least squares and polynomial chaos expansion – Application to the multiobjective reliability-based optimization of 3D truss structures. *Structural and Multidisciplinary Optimization*, 2010. In press.
- [13] C.M. Fonseca, P.J. Fleming, et al. Genetic algorithms for multiobjective optimization: Formulation, discussion and generalization. In *Proceedings of the fifth international conference on genetic algorithms*, volume 423, pages 416–423, 1993.
- [14] L. Gil and A. Andreu. Shape and cross-section optimisation of a truss structure. *Computers & Structures*, 79(7):681–689, 2001.
- [15] D.E. Goldberg. *Genetic algorithms in search, optimization and machine learning*. Reading, MA: Addison-Wesley. XIII, 412 p. DM 104.00, 1989.
- [16] H.M. Gomes. Truss optimization with dynamic constraints using a particle swarm algorithm. *Expert Systems with Applications*, 38:957–968, January 2011.
- [17] P. Hajela and E. Lee. Genetic algorithms in truss topological optimization. *International Journal of Solids and Structures*, 32(22):3341–3357, 1995.
- [18] P. Hajela, E. Lee, and C.Y. Lin. Genetic algorithms in structural topology optimization. In M.P. Bendsøe and C.A.M. Soares, editors, *Topology design of structures*, pages 117–134. Kluwer Academic Publishers Dordrecht/Boston, 1993.
- [19] X. Huang, Z.H. Zuo, and Y.M. Xie. Evolutionary topological optimization of vibrating continuum structures for natural frequencies. *Computers & Structures*, 88(5-6):357–364, 2010.
- [20] P. Jin and W. De-yu. Topology optimization of truss structure with fundamental frequency and frequency domain dynamic response constraints. *Acta Mechanica Sinica*, 19(3):231–240, 2006.
- [21] A. Kaveh and V. Kalatjari. Topology optimization of trusses using genetic algorithm, force method and graph theory. *International Journal for Numerical Methods in Engineering*, 58(5):771–791, 2003.
- [22] H. Kawamura, H. Ohmori, and N. Kito. Truss topology optimization by a modified genetic algorithm. *Structural and Multidisciplinary Optimization*, 23(6):467–473, 2002.
- [23] J.A. Madeira, H.C. Rodrigues, and H. Pina. Multiobjective topology optimization of structures using genetic algorithms with chromosome repairing. *Structural and Multidisciplinary Optimization*, 32(1):31–39, 2006.
- [24] S. Mathakari, P. Gardoni, P. Agarwal, A. Raich, and T. Haukaas. Reliability-based optimal design of electrical transmission towers using multi-objective genetic al-

- gorithms. *Computer-Aided Civil and Infrastructure Engineering*, 22(4):282–292, 2007.
- [25] M. Ohsaki. Genetic algorithm for topology optimization of trusses. *Computers & Structures*, 57(2):219–225, 1995.
- [26] M. Papadrakakis, N. Lagaros, and V. Plevris. Multi-objective optimization of skeletal structures under static and seismic loading conditions. *Engineering Optimization*, 34(6):645–669, 2002.
- [27] N.L. Pedersen. Maximization of eigenvalues using topology optimization. *Structural and Multidisciplinary Optimization*, 20:2–11, 2000.
- [28] S. Pellegrino. Structural computations with the singular value decomposition of the equilibrium matrix. *International Journal of Solids and Structures*, 30(21):3025–3035, 1993.
- [29] J.N. Richardson, S. Adriaenssens, Ph. Bouillard, and R. Filomeno Coelho. Multiobjective topology optimization of truss structures with kinematic stability repair. *Structural and Multidisciplinary Optimization*, 46:513–532, 2012.
- [30] G.I.N. Rozvany. Difficulties in truss topology optimization with stress, local buckling and system stability constraints. *Structural and Multidisciplinary Optimization*, 11(3):213–217, 1996.
- [31] G.I.N. Rozvany. On design-dependent constraints and singular topologies. *Structural and Multidisciplinary Optimization*, 21(2):164–172, 2001.
- [32] S. Ruiyi, G. Liangjin, and F. Zijie. Truss topology optimization using genetic algorithm with individual identification technique. In S.I. Ao, L. Gelman, DD.W.L. Hukins, A. Hunter, and A.M. Korsunsky, editors, *Proceedings of the World Congress on Engineering 2009 Vol II, WCE '09, July 1 - 3, 2009, London, U.K.*, Lecture Notes in Engineering and Computer Science, pages 1089–1093. International Association of Engineers, Newswood Limited, 2009.
- [33] W.S. Ruy, Y.S. Yang, G.H. Kim, and Y.S. Yeun. Topology design of truss structures in a multicriteria environment. *Computer-Aided Civil and Infrastructure Engineering*, 16(4):246–258, 2001.
- [34] J.D. Schaffer. Multiple objective optimization with vector evaluated genetic algorithms. In *Proceedings of the 1st International Conference on Genetic Algorithms*, pages 93–100, 1985.
- [35] R. Statnikov, A. Bordetsky, J. Matusov, I. Sobol, and A. Statnikov. Definition of the feasible solution set in multicriteria optimization problems with continuous, discrete, and mixed design variables. *Nonlinear Analysis: Theory, Methods & Applications*, 71(12):e109–e117, 2009.
- [36] R. Su, X. Wang, L. Gui, and Z. Fan. Multi-objective topology and sizing optimization of truss structures based on adaptive multi-island search strategy. *Structural and Multidisciplinary Optimization*, pages 1–12, 2011.
- [37] R.L. Taylor. FEAP – A Finite Element Analysis Program, March 2008. Version 8.2 User Manual.
- [38] W.H. Tong and G.R. Liu. An optimization procedure for truss structures with discrete design variables and dynamic constraints. *Computers & Structures*, 79(2):155–162, 2001.
- [39] D. Šešok and R. Belevicius. Global optimization of trusses with a modified genetic algorithm. *Journal of Civil Engineering and Management*, 14(3):147–154, 2008.
- [40] Y. M. Xie and G. P. Steven. Evolutionary structural optimization for dynamic problems. *Computers & Structures*, 58(6):1067–1073, 1996.
- [41] E. Zitzler, L. Thiele, M. Laumanns, C.M. Fonseca, and V.G. Da Fonseca. Performance assessment of multiobjective optimizers: An analysis and review. *Evolutionary Computation, IEEE Transactions on*, 7(2):117–132, 2003.

Chapter 3

Grid shell topology optimization

Grid shells offer a solution to covering large-span areas without the need for intermediate interior supports (figure 3.1). Efficient design of grid shells is a major challenge for designers due to requirements such as optimal use of, preferably renewable, resources. In practice often a regular triangulation of a predefined global form is used, such as the welded grid shell shown in figure 3.2, without regard for the most efficient layout of material. This paper focuses on the optimization of steel grid shells in which the global shape has been determined using form-finding techniques, where the objective is to minimize the grid shell's weight. For this purpose both the location of the connections on the predetermined shape, and the connectivity (topology) of the grid shell are optimized using a Genetic Algorithm. The paper describes both the method and its application to the design of several steel grid shells, clearly showing the advantages of employing optimization techniques for this type of design.



Figure 3.1: An architectural rendering of grid shell canopy structures



Figure 3.2: Grid shell roof structure by Buro Happold at the British Museum, London, UK. Image courtesy of Travis Simon

Coupled form-finding and grid optimization approach for single layer grid shells¹

Abstract

This paper demonstrates a novel two-phase approach to the preliminary structural design of grid shell structures, with the objective of material minimization and improved structural performance. The two-phase approach consists of: (i) a form-finding technique that uses dynamic relaxation with kinetic damping to determine the global grid shell form, (ii) a genetic algorithm optimization procedure acting on the grid topology and nodal positions (together called the 'grid configuration' in this paper). The methodology is demonstrated on a case study minimizing the mass of three $24m \times 24m$ grid shells with different boundary conditions. Analysis of the three case studies clearly indicates the benefits of the coupled form-finding and grid configuration optimization approach: material mass reduction of up to 50% is achieved.

3.1 Introduction

In the last two decades new leisure and transportation facilities have experienced the emergence of free form architecture; complex curved surfaces are envisaged covering extensive unobstructed spaces. Grid shells offer a unique solution to this design challenge. In literature the wording 'reticulated', 'lattice' and 'grid' shell are largely interchangeable. In this paper, the authors refer to this type of shell as a 'grid' shell. A grid shell is essentially a shell with its structure concentrated into individual linear elements in a relatively thin grid compared to the overall dimensions of the grid shell. The grid may have more than one layer, but the overall thickness of the shell is small compared to its overall span. The structures considered in this paper are limited to single layer steel grid shells. In reviewing the design of recently re-

alized single layer steel grid shells (e.g. Nuovo Polo Fiera Milano by Massimiliano Fuksas [3, 19], Mur Island by Vito Acconci [2]) the driving design factor more often seems to have been architectural scenographic aesthetics rather than structural performance [29]. The sculptural design intent in architectural geometric processing can be appreciated for its inventiveness of plastic forms and mesh generation but thus far not for its consideration of gravity loads. The integration of structural considerations in architectural geometry processing is considered one of the most important future research topics in architectural geometry [33]. Free form shapes more often than not lead to unfavourable internal forces: under loading they do not allow membrane stresses to develop within the surface, while the grid configuration is driven by visual conventions rather than a clear structural rationale. These factors often result in structural inefficiency and higher associated construction cost. In the 20th century both architects and engineers (Gaudi [5, 22], Otto and Isler [7]) experimented with physical form-finding techniques that, for a given material, a set of boundary conditions and gravity loading, found efficient three-dimensional structural shapes. The importance of finding a funicular shape for steel grid shells lies in the fact that the evenly distributed gravity loads contributes largely to the load to be resisted. The grid elements need to be loaded axially to make most efficient use of the element cross section. Numerical form-finding techniques (force density [21], dynamic relaxation (DR) [1, 13]) have been successfully applied to weightless systems whose shape is set by the level of internal pre-stress and boundary supports. However when it comes to funicular systems whose shape is not determined by initial pre-stress but by gravity loads (such as the case for masonry, concrete or steel shells) fewer numerical methods have been developed. Kilian and Ochsendorf [25] presented a shape-finding tool for statically determinate systems based on particle-spring system solved with a Runge-Kutta solver. Block and Ochsendorf [9] published the thrust net-

¹J.N. Richardson, S. Adriaenssens, R. Filomeno Coelho, and Ph. Bouillard. Coupled form-finding and grid optimization approach for single layer grid shells. *Engineering Structures*, 52(0):230 – 239, 2013



Figure 3.3: A configuration of three grids of varying orientation with common nodes

work analysis to establish the shape of pure compression systems. Once the overall grid shell form is established the choice of the grid configuration remains an important, often neglected, question for the structural designer. Often the grid configuration generated by computer aided design software is transposed to the structural system. Triangulated grids are the most basic and intuitive means of configuring the grid on a curved surface. However, this grid is not necessarily the most structurally efficient choice for a given global form: triangulated grids tend to be more costly per square meter [33], since not all elements are necessary for structural stability. Quadrangular grid configurations with planar faces are a good alternative to triangulated grids. Adriaenssens et al. [2] used a strain energy origami approach to enforce planar face constraints in the form-finding of an irregular configured grid shell to achieve planarity of the faces. The grid shells considered in the present paper are (conservatively) modelled with negligible moment stiffness in the connections, so that a degree of triangulation is necessary to brace the shell. A very general grid can be achieved by combining quadrilateral grids with varying orientations (figure 3.3). Starting from a general grid, the configuration of the elements can be optimized to achieve improved structural behaviour of the shell and reduce unnecessary structural elements while adhering to cladding constraints. In order to not be re-

stricted to the standard grid configuration², the exact nodal positions on the global form of the grid shell surface can also be varied (referred to here as "shape optimization") to optimize the distribution of the nodes, while discrete topology optimization can explore the full search space of possible connectivities (elements between nodes) of the grid shell elements. Shape optimization of discrete structures (such as grid shells) has been carried out using techniques including linear programming (Pedersen [32]) and conjugate gradient optimization (Gil et al. [18]). Discrete truss topology optimization has also received attention including research by Beckers and Fleury [4] using a primal dual approach, Giger et al. [17] using a graph-based approach, Lamberti [27] using simulated annealing, and Rasmussen and Stolpe [34] using cut-and-branch method. Genetic algorithms (GA's) for topology optimization have been extensively applied to planar trusses [14, 20, 24, 31, 37]. However, recently researchers have turned their attention to the optimization of three-dimensional discrete systems including spatial structures [40] and grid shells [3]. Saka [38] used GA's to optimize the number of rings, element cross sections and the height of geodesic domes. Lemonge et al. [30], used GA's to solve a weight minimization problem for a dome structure, with variable element sizes. Kaveh and Talatahari [23] used Charged System Search to optimize the dome crown height, element cross section sizing and, to a lesser extent, the topology of geodesic domes. Only limited research has focused specifically on grid shell optimization, such as a multi-objective optimization scheme developed by Winslow et al. [41] for free form (not form found) grid shells, in which the element orientations are variable.

The present paper represents a novel, more general approach to preliminary design of grid shell structures by combining form-finding with grid configuration optimization techniques. The paper is organized as follows: after formulating the problem statement, the two-phase design methodology is outlined with description of the form-finding and optimization techniques. A case study of $24m \times 24m$ grid shells demonstrates the presented methodology, illustrating its usefulness as a design tool for the preliminary design of grid shells. The

²In this study 'grid configuration' refers to the grid shell topology and nodal positions. 'Configuration optimization' is achieved by variation of topology and shape variables in order to optimize the grid configuration on the global form of the grid shell.

paper concludes with a discussion of the results of the case study and suggestions for future work in the field of grid shell optimization.

3.2 Problem statement

Of all traditional structural design variables (ranging from material choice, element cross section, nodal positions, global geometry, topology, support conditions), the global geometry mostly decides whether the grid shell will be stable, safe and stiff enough [2]. The shell spans large spaces with a fine structural network of individual small elements. Shell bending needs to be avoided by finding the 'right' shape so that, under an evenly distributed gravity load, only membrane action should result. Once a 'right' global structural form is found, the search space of all nodal positions is established. The exact nodal positions and element topology can be varied to achieve specific objectives such as minimizing the material mass for a given global form.

Four structural constraints are considered in this study: (i) maximum normal stresses, (ii) local element buckling, (iii) total deflection of the grid shell, and (iv) global buckling of the structure. These constraints are chosen because they are the crucial criteria to be considered at the preliminary design stage of thin grid shell systems. Other constraints (such as dynamic constraints) are relevant at a later design stage and fall outside the scope of this paper. All values of the constraint quantities are obtained using a finite element analysis (FEA) with linear elastic isotropic truss elements, using the software package FEAP [39]. As the form-finding procedure in this paper aims at moment elimination in the surface under the loadings considered in the form-finding and optimization, only axial forces are expected in the elements and connection nodes. The intersection of the central axes of the elements at a node go through one single point, eliminating moment caused by element eccentricities. Bounds on the shape variables are set to ensure that maximum cladding dimensions are respected. The maximum element stress is constrained using the relation: $\sigma_i^{max} - |\sigma_i| \geq 0$, where σ_i^{max} is the maximum allowable (yield) stress of steel, and σ_i is the stress in element i . The local Eulerian buckling constraint is $\sigma_i^{cr} - \sigma_i \geq 0$, where $\sigma_i^{cr} = \frac{(\pi^2 E_i I_i)}{(A_i l_i^2 K^2)}$. Here E_i is the Young's modulus of steel for element i , I_i the area moment of

inertia of the cross section of element i , A_i the area of the cross section of element i , l_i the length of element i and K the effective length factor (here taken as $K = 0.9$) associated with the connections between elements. In the realized structure the steel elements will be welded to one another at the nodes offering some moment resistance. The value chosen for K is thus somewhat conservative. The total deflection of the grid shell is constrained to $\delta_z^{max} = \frac{1}{200}$ of the minimum span, as stipulated by the Eurocodes. The vertical components of the displacements calculated from the FEA are therefore limited: $\delta_z^{max} - \delta_{j,z} \geq 0$, where $\delta_{j,z}$ is the vertical displacement of the grid shell at node j under a given load. A simple method for applying the global buckling constraint is used, as suggested by Ben-Tal et al. [6]. The reader is referred to this reference work for a detailed explanation of the method. Using this method the global buckling constraint can be stated as $\mathbf{K} + \mathbf{G} \geq 0$, where \mathbf{G} is the geometric stiffness matrix, dependent on the deformed shape. Finally the nodes are constrained to a range around their initial position, for both x and y coordinates of node j : $(\Delta x_{max} - |\Delta x_j|) \geq 0$ and $(\Delta y_{max} - |\Delta y_j|) \geq 0$, where node j is not on the fixed boundary of the grid shell and $\Delta x_{max}, \Delta y_{max}$ are limit values selected by the designer, taking the maximum size of the cladding into account. All quantities of interest (objectives and constraints) are output responses that depend on the design variables. The set of all possible values of combinations of design variables forms the 'design space' or 'search space'.

3.3 Approach

A two-phase approach for grid shell design is presented that, for a set of boundary conditions and constraints, establishes a structurally efficient shell form and grid configuration. Phase 1 involves a form-finding technique to achieve a shell shape that only experiences membrane stresses under an evenly distributed gravity load, followed by Phase 2, a fine tuning of the local geometry (at nodal and connectivity level) through a topology and constrained shape optimization (figure 3.4).

An important structural design challenge lies in the determination of a three-dimensional curved surface that will hold the grid shell. For the form-finding procedure in this paper the DR method with kinetic damping usually used for pre-stressed systems, was adapted to yield 3D funicular sys-

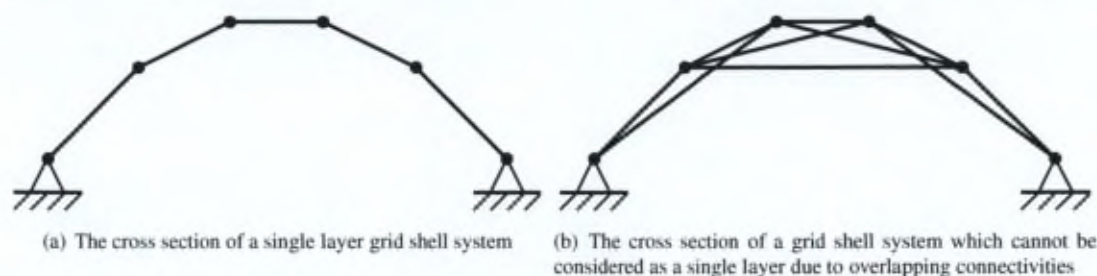


Figure 3.6: Cross sections of single layer and non-single layer grid shell systems

containing many nodes and relatively few elements between the nodes. Allowed connectivities between nodes must ensure that the grid shell remains a single layer system (as in figure 3.6(a) as opposed to figure 3.6(b)), without elements overlapping. A randomly generated initial population may lead to convergence problems; the GA struggles to find solutions which can be suitably evaluated, since they contain mechanisms. By using an initial population of predominantly kinematically stable grid shell systems this problem is alleviated. Figure 3.7 illustrates one algorithm for generating a stable initial population. Other strategies, such as grid triangulation schemes, are also possible. For a detailed description of the initial population generation schemes the reader is referred to Richardson et al. [35].

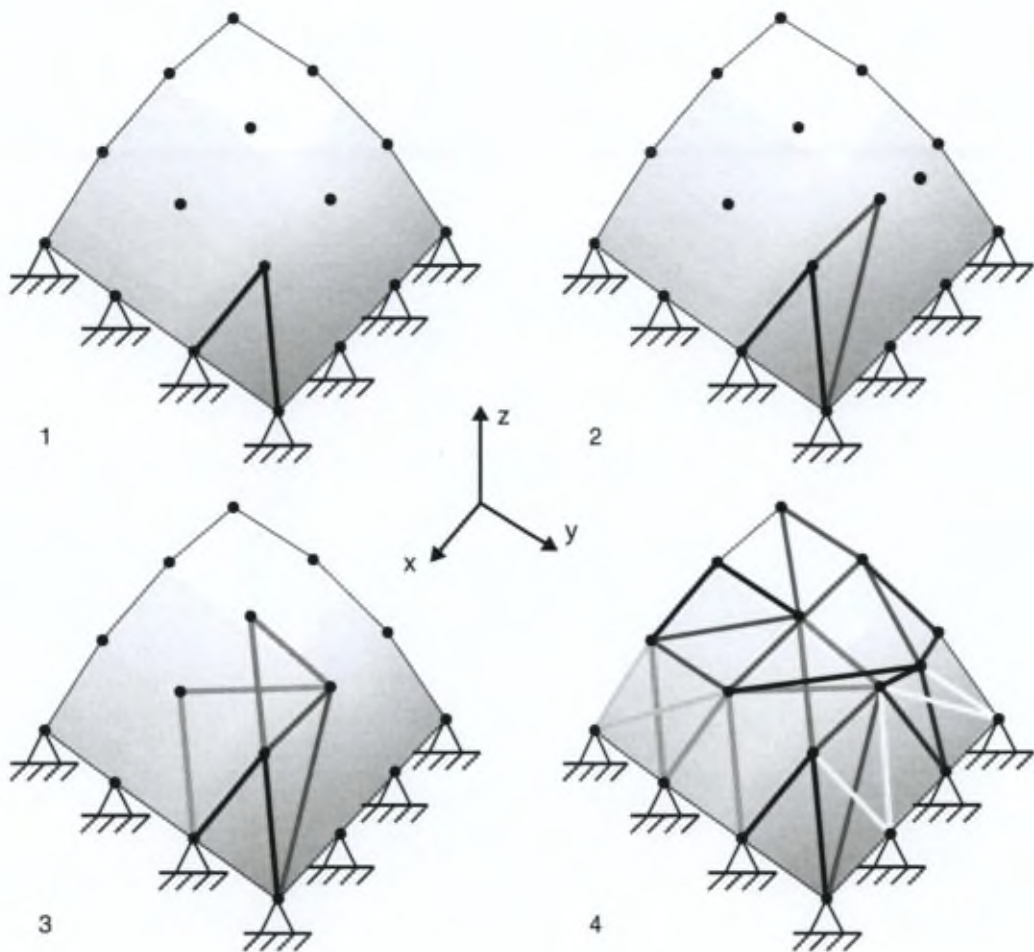


Figure 3.7: An example of how kinematically stable grid shell designs in the initial population can be generated. The figure represents a segment of a symmetric grid shell with two planes of mirror symmetry, one in the $x-z$ and one in the $y-z$ plane. (1) A stable core structure is first produced. (2, 3) Groups of elements are added onto the stable core to incorporate other nodes. (4) Once all nodes are connected the procedure is stopped. Repeating this topology according to the symmetry of the structure generally leads to a kinematically stable grid shell

3.4 Two-phase approach to the preliminary design of single layer grid shells

3.4.1 Form-finding of grid shells

The adopted form-finding method, DR with kinetic damping, is a numerical procedure that solves a set of nonlinear equations [13]. Summarized, the technique traces the motion of the structure through time under applied loading (evenly distributed gravity load in the case of grid shells). The technique is effectively the same as the Leapfrog and Verlet methods which are also used to integrate Newton's second law through time. The basis of the method is to trace step-by-step for small time increments, Δt , the motion of each interconnected node of the grid until the structure comes to rest in static equilibrium. The general DR algorithm is shown in figure 3.8. All grid elements i are assigned values for their axial stiffness $E_i A_i$. The shell edge elements are assigned higher stiffness values to model the boundary arches. The motion of the grid is caused by applying a fictitious, negative gravity load at all the grid nodes. During the form-finding process the values of all numerical quantities (EA and load) are arbitrary since it is only their ratios that effect the shape. Other initial parameters can be manipulated to steer the initial form-found global form towards an intended shape. Section 3.5.3 describes how the force-modelled shape can be controlled by varying specific parameters. This process is continued iteratively to trace the motion of the unbalanced grid shell. Kinematic damping is introduced to hinder oscillations, by setting all the nodal velocities to zero when a kinetic energy peak is detected. The process will never truly converge, but once the residual forces are below a certain tolerance, convergence has occurred for all practical purposes. At that point, a shape is achieved that is in 'static equilibrium' and the 'correct' spatial form is found. This form is the basis for the geometric constraint on the shape variables in the GA, while the element configuration used in the form-finding defines the allowed connectivities (the search space of the topology variables).

3.4.2 Grid configuration optimization of grid shells

Topology variables

In this study the 'ground structure' defines the allowable connectivities, i.e. the topological design search space. The topology variables are treated as discrete binary variables, selected from the *design set* $V = \{0, 1\}$. The cross section properties can in principle be freely chosen, however this choice should be taken into account in the formulation of the constraints.

Shape variables

The shape variables relate to two of the three Cartesian coordinates of the nodes. These shape variables can be either continuous or discrete as opposed to the topological which are binary. A geometric equality constraint is placed on the vertical coordinate of the nodes, as a function of the two horizontal coordinates $\mathbf{x} = [x, y]$:

$$h(\mathbf{x}) - z = 0 \quad (3.1)$$

where h is the expression of a smooth, continuous surface through the nodal coordinates defined by the form-finding procedure and x, y are two Cartesian coordinates on a horizontal plane. A Moving Least Squares (MLS) [28] interpolation scheme is used to approximate $h(\mathbf{x})$ (figure 3.9). Limits are placed on the shape variables to avoid overlapping of nodes or nodes switching position. MLS consists in a generalization of the least square technique. Starting from a set of reference points $\{\mathbf{x}^{(i)}, i = 1, \dots, N\}$ with the corresponding values of the scalar outputs $z^{(i)}$ (supervised learning), the moving least square approximation of the "exact" function $z(\mathbf{x})$.

Symmetry reduction

Many grid shell forms display, for example radial or mirror symmetry. This symmetry may be exploited to reduce the number of topology and shape variables, by grouping variables which are equivalent with respect to the symmetry of the grid shell. The variables in these groups are then assumed to have the same values, effectively reducing the size of the search space.

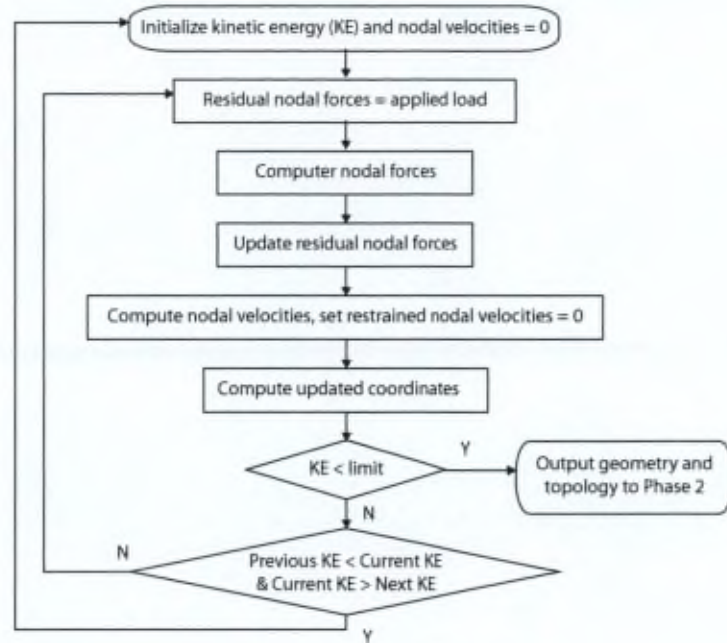


Figure 3.8: Algorithm for DR with kinetic damping used in Phase 1 of the two-phase method

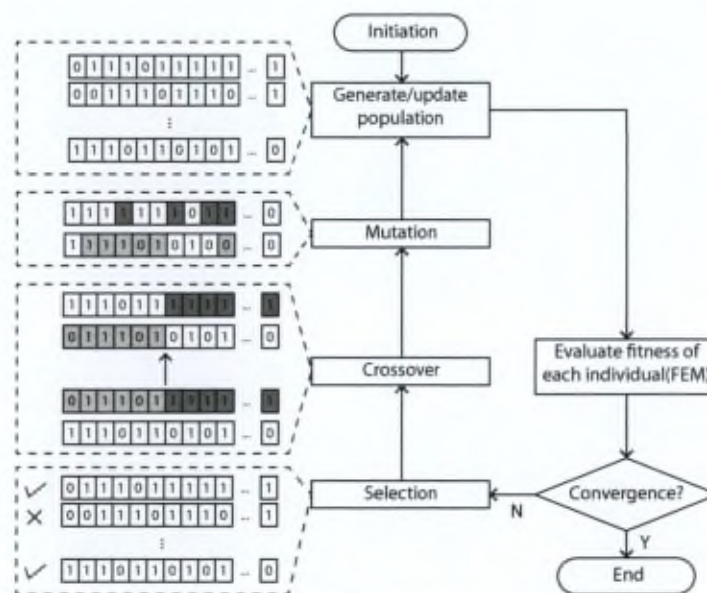


Figure 3.9: Nodal shape variable interpolation: for a given set of original nodal positions (0), an imaginary surface is defined through these points (1). For a change in nodal coordinate Δx , the z coordinate is found on the surface (2)

Nodal loading

Building codes prescribe load cases and combinations that need to be considered in the analysis of a grid shell. These include evenly distributed loading, asymmetric loading and point loads. From the point of view of the designer the choice of loading to consider in the optimization process is important. The form-finding procedure considers a single load case: an evenly distributed loading. For the sake of consistency an evenly distributed loading that would typically represent the dominant load case (in this case an evenly distributed static load such as snow and an approximation of the self-weight of the entire canopy) is used. The cladding transfers the loads to the nodes of the grid shell. This loading will be proportional to the horizontal projection of the surface area carried by the node, and is therefore a function of the geometrical positions of the nodes, which are variable. An automated scheme, such as a Voronoi decomposition of the horizontal plane projection of the grid, allows for the calculation of the loading at each point in the design space. A Voronoi diagram [26] is a spatial decomposition based on distances between a set of points (such as the grid nodes). Figure 3.10 demonstrates the relationship between the structural nodes and the nodal load calculation based on projection of Voronoi polygons. Once the Voronoi polygons corresponding to each node have been assembled, their areas are calculated and the loading transferred to an equivalent point load applied to the node in the FEA of the grid shell.

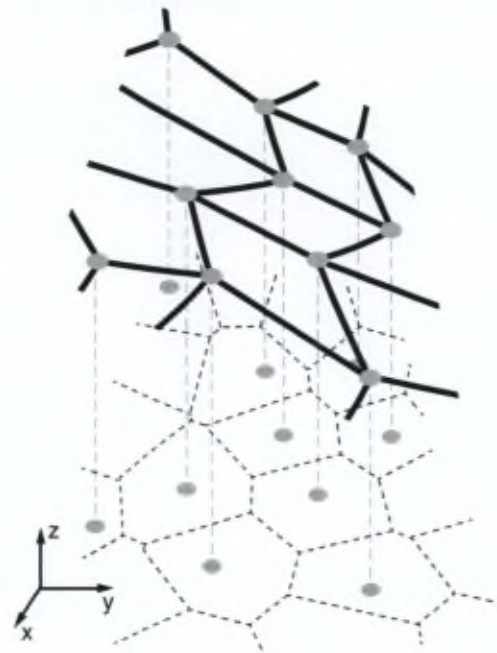


Figure 3.10: The nodes connecting structural elements (solid black lines), are projected onto a horizontal surface (grey dashed lines). The Voronoi polygons are calculated based on this projection and the relative area sizes translated to vertical point loads on the nodes

Algorithm convergence

In Phase 2 of the procedure, the GA selects a population of grid shell designs, each described by a set of shape and topology variables. After constructing a structural model (including the MLS approximation of the nodal positions and Voronoi diagram calculation of the loading), each grid shell design in the population is evaluated based on the results of an FEA. Once the GA has assessed the fitness of all grid shell designs in the population, it considers whether the stopping criterion has been met (a satisfactory convergence of the algorithm). The stopping criterion is met when the population size falls below a certain threshold, or the maximum number of iterations has been reached. If an unsatisfactory condition exists, the optimization portion of the algorithm performs another iteration. Changes are made to the population by selecting

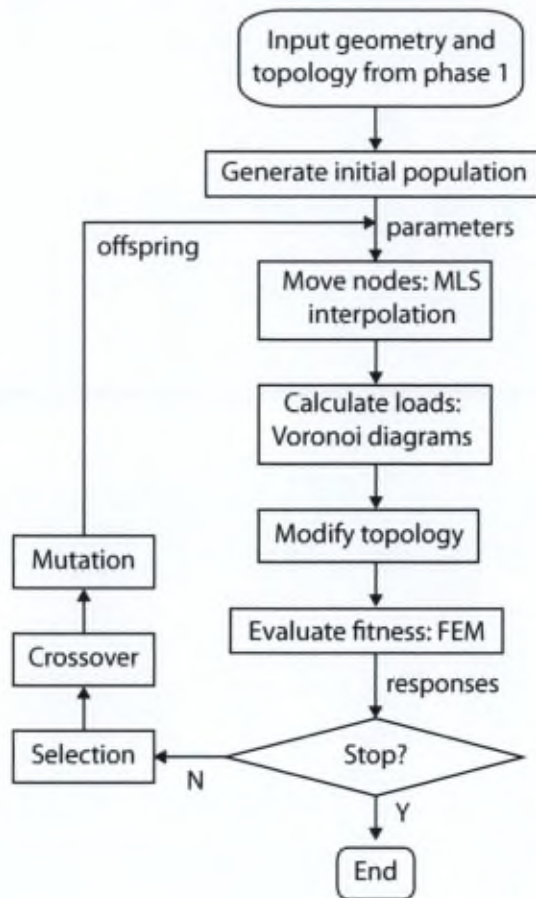


Figure 3.11: A general framework of the GA used in Phase 2 of the coupled method

grid shell designs to be retained, discarding others, introducing new individuals, mutation of chromosomes and mating of pairs to produce offspring. The exact mechanism is dependent on the method selected and the parameter values (such as the mutation rate, cross-over rate, mutation scale, etc.) chosen. Figure 3.11 shows the general framework of the algorithm in Phase 2, in the optimization of the grid shell designs.

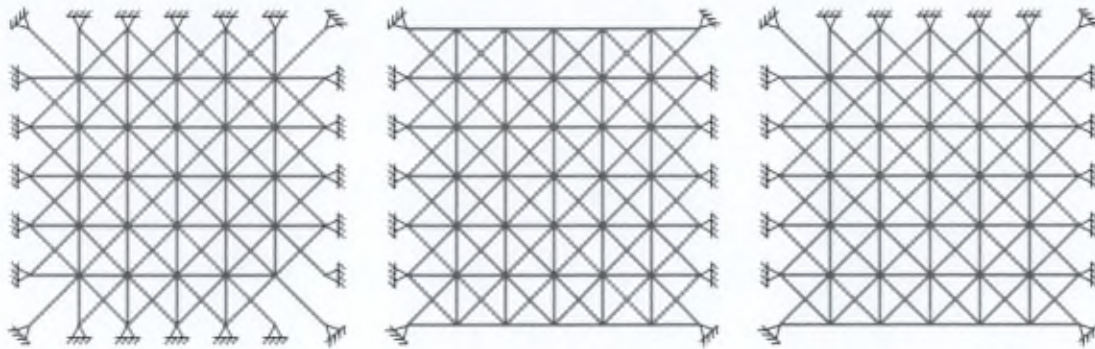
3.5 Validation of the two-phase methodology: preliminary design of $24m \times 24m$ grid shells

3.5.1 Description of the case studies

A series of three grid shell canopies, each covering a surface area of $24m \times 24m$ is to be designed. The initial geometry is a $24m \times 24m$ flat square grid of nodes with spacing of $4 \times 4m$ (figure 3.12). Three grids are overlaid on one another, one in the node grid direction and two orientated at 45 degrees to the node grid direction. This grid is relatively coarse and the initial choice of spacing depends on a number of factors including the loading on the shell and the type of cladding system. The boundary conditions for the three canopies differ: the first grid shell is linearly pin supported on all four sides, the second on two opposite sides and the third on three sides. The shape variables are discrete, with possible values taken from the set $\{-1.0m, -0.9m, \dots, 0.0m, 0.1m, 0.2m, \dots, 1.0m\}$ (Δx_{max} and Δy_{max} are both equal to $1m$). For all computations hollow, circular steel cross sections, with an outer diameter of $8.89cm$ and a wall thickness of $8mm$ were chosen based on Standard European manufactured steel sections. The density of steel is assumed to be $\rho = 7850kg.m^{-3}$. The yield stress of the steel, $\sigma^{max} = 355 \times 10^6 N.m^{-2}$, is assumed, while the Young's modulus is taken as $E = 2.0 \times 10^{11} N.m^{-2}$. The span of $24m$, is used to calculate the limit value of the deflection constraint. An evenly distributed vertical gravity loading of magnitude $3kN.m^{-2}$ is considered for the purposes of the optimization procedure. This loading represents an estimate of the grid shell self weight and a static evenly distributed load (such as snow).

3.5.2 Computation and convergence

Due to varying degrees of symmetry, the size of the three optimization problems varied, with more variables needed to describe the problems with two and three pinned sides. The GA parameters used for the three computations are summarized in table 3.1. The GA parameters are adjusted until, for 10 runs of the problem, a majority of the solutions converged to the minimum solution. The population size parameter represents the number of gen-

Figure 3.12: The $24m \times 24m$ grid shell initial connectivitiesTable 3.1: GA parameters for the $24m \times 24m$ grid shells

Parameter	4 sides pinned	2 sides pinned	3 sides pinned
Num. topology variables	19	39	70
Num. shape variables	6	14	27
Population size	500	800	1200
Stable initial population size	400	640	960
Crossover rate	0.8	0.8	0.8
Mutation rate	0.4	0.2	0.2

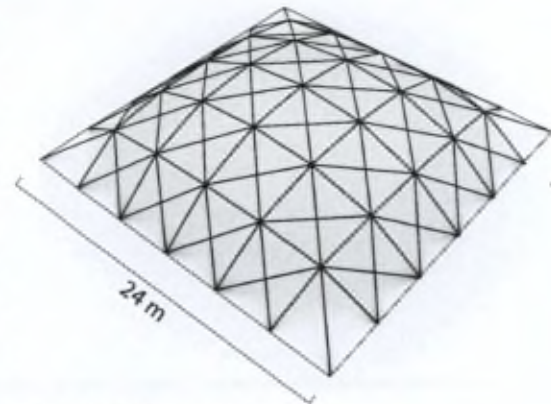
erated designs in the initial population of the GA which may become smaller after the first iteration of the GA. The stable initial population size is the number of grid shell designs in the initial population which are generated with kinematic stability (see section 3.4.2). The crossover rate and mutation rate are defined in [35]. More detailed details of the genetic algorithm used can be found in [16].

3.5.3 Designs resulting from the two-phase form-finding and optimization procedure for the $24m \times 24m$ grid shells

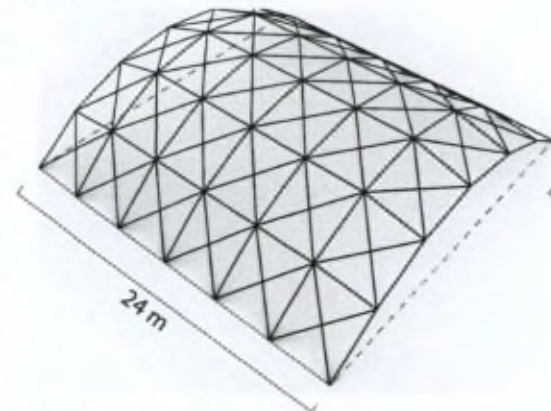
Phase 1, the form-finding, yields three initial global forms (figure 3.13) that, under evenly distributed gravity load, experience only membrane behaviour, and no bending. A height to span ratio (1 : 5), corresponding to a good arch form, is sought and achieved for all three grid shells. In the form-finding process, several input parameters can be manipulated to steer the form-found shape of the structural surface that will eventually hold the optimized grid topology. In the presented form-finding technique, one starts from an

initially two-dimensional (2D) surface that develops into a three-dimensional (3D) surface. Other form-finding techniques (e.g. particle spring system [25], thrust network analysis [9]) could be equally used to obtain this initial 3D surface. The concrete (continuous) shell builder, Isler [12] who exclusively used physical form-finding techniques, exploited (i) the initial shape and bias, (ii) the orientation of the fibres (weft and weave) and (iii) the material properties of his hanging fabrics as tools to direct the global form towards his initial intended shape. In the presented case studies (1,2, and 3) the initial 2D grid was chosen to be a $24m \times 24m$ quadrilateral grid that was further triangulated. This grid was positioned flush with the boundary edges and had identical material and geometric properties for all grid elements. The applied loads at the nodes were chosen in function of the elastic stiffness of the elements to achieve a shell target height at the free edges between 5 and 6m. This target height fulfills both functional (i.e. sufficient entrance height) and structural (i.e. sufficient arching action ratio 1/5 to 1/4 height/span ratio). Alternatively, the applied loads could have been held constant and the elastic stiffnesses of the elements adjusted to achieve the desired global form. The free boundary edges of case study 2

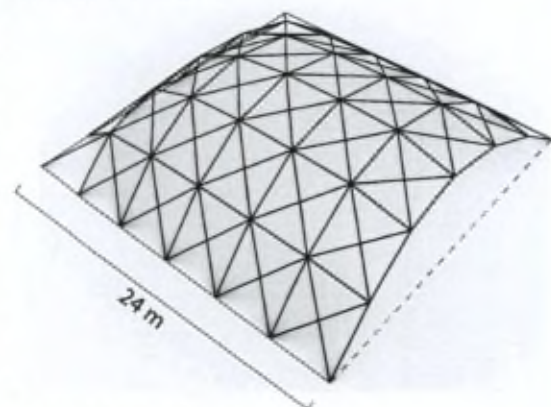
curve slightly inward in the horizontal projection. As mentioned in section 3.4.1, different parameters (tools) can be employed to steer the initial 3D shape prior to the topology optimization. To clearly demonstrate the effects of manipulating the different parameters in the form-finding process, an initial $24m \times 24m$ quadrilateral orthogonal grid without triangulation for case study 2 is considered. The initial 2D grid is a square in plan with dimensions $24m \times 24m$. Firstly, the initial orientation of the grid has an important influence on the global form in the form-finding process. By orienting the initial orthogonal grid parallel with the boundary edges, the form-finding procedure yields a singly curved parabolic cylinder as shown in figure 3.14(a). This obtained shape could be compared to the one obtained in a form-finding process for a continuous shell when neglecting the Poisson's effect. The plan projections of the two free boundary edges are straight lines that coincide with the initial 2D grid boundaries. Secondly by orienting the initial 2D square grid on the bias of the opposing end supports, the grid is deformed by shear and results in a doubly curved surface. Under these conditions, figure 3.14(b) shows a 3D surface with synclastic curvature. The horizontal projection of the free boundary edges is no longer straight but substantially curves inwards. Finally, bent-up edges at the free boundaries might be structurally desirable as they could serve as edge stiffeners. To steer the shape of case study 2 in that direction, the initial free edges in the 2D grid would have to be extended beyond the original support line. This manipulation generates an initial 3D form that has two free edges bending up normal to the 3D surface. Figure 3.14(c) shows for an initial orthogonal grid, positioned parallel with the boundary supports, this approach generates a shell form that transitions from a cylindrical central shape to an anticlastic surface with bent up edges. These bent-up edges are oriented normal to the 3D surface and can act as edge stiffeners to the shell. This parametric study shows that different form-found grid shell shapes are possible. The remainder of this study concentrates on the grid optimisation for the forms shown in figure 3.13. Figure 3.15 depicts the grid shells obtained after Phase 2 of the procedure, the grid configuration optimization. A comparative study (table 3.2) of the steel mass of the grid shells before and after Phase 2 shows that significant reductions in the mass of the grid shells can be achieved



(a) Case 1: 4 sides pinned
Total height: 5.0m
Base: $24m \times 24m$
Opening height: -

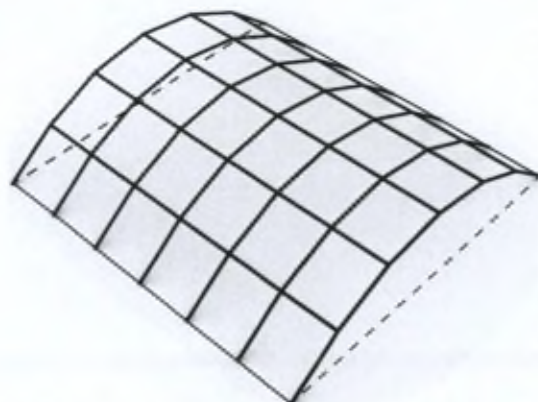


(b) Case 2: 2 sides pinned
Total height: 5.95m
Base: $24m \times 24m$
Opening height: 4.713m

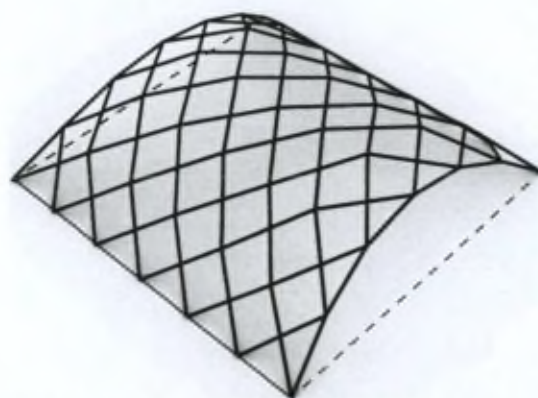


(c) Case 3: 3 sides pinned
Total height: 5.85m
Base: $24m \times 24m$
Opening height: 4.728m

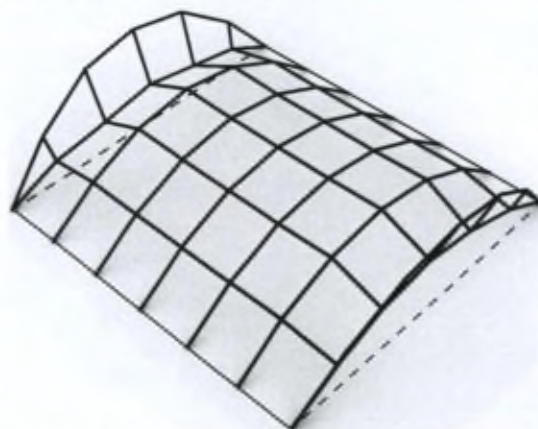
Figure 3.13: The three grid shell forms obtained after Phase 1, the form-finding. These topologies represent the ground structures for Phase 2



(a) Singly curved parabolic cylinder achieved by orienting the initial grid parallel with the boundary edges



(b) Synclastic surface achieved by orienting the initial 2D square grid on the bias of the opposing end supports



(c) Anticlastic surface with bent up edges achieved by extending initial free edges beyond the original support line

Figure 3.14: Several methods for controlling the form of the free edges used in form-finding techniques

through grid configuration optimization, while respecting the constraints³ on the deflection, local stress and buckling of the elements and buckling of the global shape. The form-found grid shell designs, achieved after Phase 1, do not violate any of the constraints. The local buckling constraint values (column 4 of table 3.2) are near the limit permitted in two of the examples. However, these designs can be vastly improved through grid configuration optimization (column 6 in table 3.2), as can be seen from the mass reduction achieved through optimization, in this case between 35 and 50%. After Phase 2 the local buckling constraints are near their limit values (column 5 in table 3.2), while the topology and nodal positions of the shell grid have changed significantly compared to the initial grid configuration.

Case 1 (figure 3.15(a)) displays a very distinctive grid configuration: the outer and inner element tiers have no diagonal bracing, except at the corners of the outer tier, while the middle tier is triangulated to brace the grid shell. Cases 2 and 3 (figures 3.15(b) and 3.15(c)) display less intuitive triangulated grid configurations, with the exception of the unsupported edges. More material is found at the top of these edges to stiffen them and prevent violation of the deflection constraint at the edges.

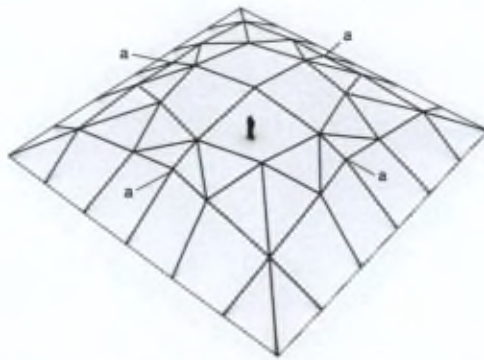
The so-called 'active constraint'⁴ plays an important role in the solutions. As a demonstration: suppose the loading is arbitrarily increased in increments from $3kN.m^{-2}$ to $8kN.m^{-2}$. For small loading (e.g. $3kN.m^{-2}$) the limits on the nodal positions are the active constraints (figure 3.16). Upon increasing the loading to $5kN.m^{-2}$ the local buckling constraint becomes active. Several of the nodes shift position relative to the previous case (from a in figure 3.16(a) to a' in figure 3.16(b)) to reduce the buckling lengths of critical elements. However, the topology remains unchanged. For a loading of $7kN.m^{-2}$ the topology changes dramatically, forming two bands of material with less material at the corners, since these represent the longest load paths. When a loading of $8kN.m^{-2}$ is applied the topology is modified so that this form is made more prominent with the addition of 4 new elements. The loads are redistributed so that the critical elements in the previous case do not buckle under this higher loading. Due to the curved shell

³The constraint values have been normalized such that their limit value is 1.

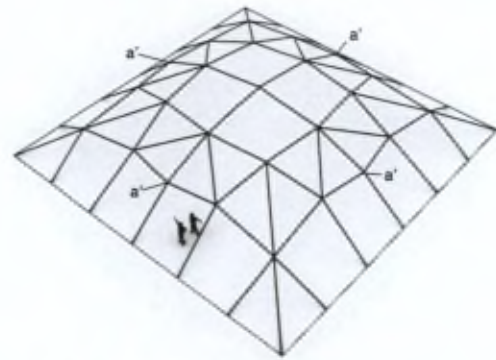
⁴An active constraint is the inequality constraint $g \leq 1$ which approaches its limit value as the optimal solution is approached ($\lim_{g \rightarrow 1} (f \rightarrow f_{min})$).

Table 3.2: Comparison of grid shells after Phase 1 and Phase 2 of the two-phase method. The values in the table represent the constraint values of the grid shells before Phase 2

Case	Mass after Phase 1	Mass after Phase 2	Local buckling constr. after Phase 1	Local buckling constr. after Phase 2	Mass reduction Phase 1 \rightarrow 2
1	9956 kg	5098kg	0.759	0.99	48.8 %
2	11260 kg	7330kg	0.8325	0.99	34.9 %
3	10484 kg	6048kg	0.96	0.99	42.3 %



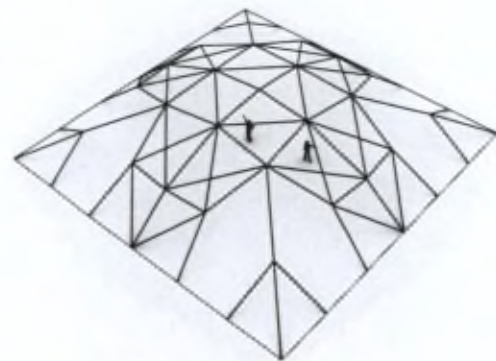
(a) $P = 3 \text{ kN.m}^{-2}$, $m = 5098 \text{ kg}$.
Active constraint: nodal position limit



(b) $P = 5 \text{ kN.m}^{-2}$, $m = 5161 \text{ kg}$.
Active constraint: local buckling

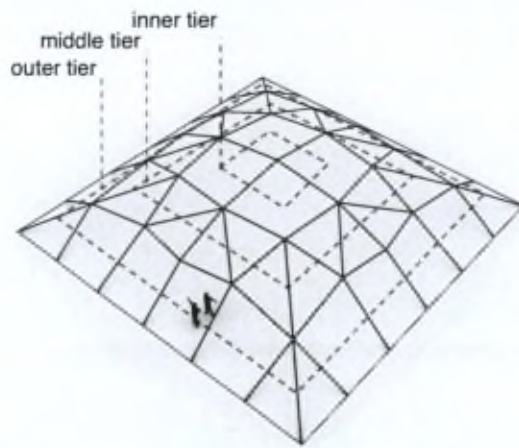


(c) $P = 7 \text{ kN.m}^{-2}$, $m = 5630 \text{ kg}$.
Active constraint: local buckling

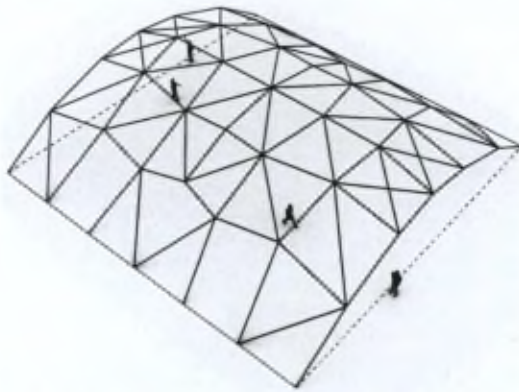


(d) $P = 8 \text{ kN.m}^{-2}$, $m = 6393 \text{ kg}$.
Active constraint: local buckling

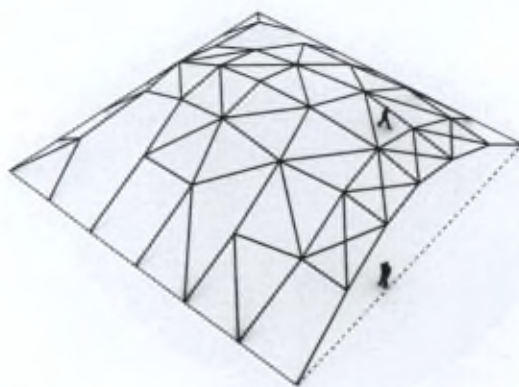
Figure 3.16: Changes in the optimal topology and nodal positions with increasing evenly distributed loading



(a) Case 1: $m = 5098\text{kg}$, Active constraint: node position limit



(b) Case 2: $m = 7330\text{kg}$, Active constraint: deflection and local buckling



(c) Case 3: $m = 6048\text{kg}$ Active constraint: local buckling

Figure 3.15: The three grid shells obtained after Phase 2, the grid configuration optimization

surface, elements crossing one another do not intersect.

Further investigation can be carried out on the structures to assess their feasibility as designs. All three resulting case study designs (shown in figure 3.15) were analysed for the serviceability and ultimate limit states according to EuroCode 3 [11] and EuroCode 1 [10]. The loading combinations included snow and wind loads. The most relevant load combinations contained asymmetric load cases due to wind and snow. For these purposes commercial finite element software was employed and several other load cases and combinations were considered, including asymmetric snow and wind loading. It was found that the most sensitive structure to global buckling under asymmetric loading was Case 2, the barrel vault.

3.6 Conclusions and Future Prospects

Grid shells have re-emerged as an important structural typology in recent years. Free form shells are structurally inefficient and costly, while grid configurations are often chosen with little consideration of structural and constructional efficiency. The approach in this paper offers solutions to these problems by suggesting a two-phase method: form-finding followed by a refinement of the grid configuration. The case study of three grid shells with the same span but different boundary conditions demonstrates the viability of this method as a preliminary design tool for grid shells. The configuration of the grid shell elements found in the case study are dissimilar to the traditional repeated pattern of regularly spaced elements for grid shells. By allowing for an optimization of the grid shell configuration, very significant reductions in mass (up to nearly 50%) were realized. As a further development of this method the sizing variables could be included in the problem formulation. As with the design of the courtyard roof for Dutch Maritime Museum [2], one cross section dimension (such as the height of an I-beam element) can be constant for all elements, while others can vary. This improves ease of connection of elements, while allowing for sizing optimization. While only one loading case was considered in this study and only the mass minimized, the designer may wish to consider a number of loading cases and/or objectives within the presented approach.

This problem can be addressed through multicriteria optimization [35]. Additional constraints (such as dynamic behavior) could be added into the problem formulation. Taking these constraints into account would also increase the applicability of the presented approach. GA's, the chosen optimization technique for this study, can easily be adapted to consider multiple objectives and constraints. Free form grid shells have been mentioned several times in the text. One fruitful avenue for further research would be to use form-finding as a technique to find structurally efficient approximate forms for free form structures. Furthermore, it may be of interest to combine the form-finding and grid configuration optimization into one, concurrent, iterative optimization process since the grid configuration effects the global form in a form-finding procedure [8], as discussed and demonstrated in section 3.5.3. This valuable extension is currently under development [15] however requires the overcoming of significant obstacles. The computational cost of GA's for discrete topology problems is relatively high, while large problems tend to experience convergence problems. One major cause of this is the kinematic stability constraint which leads to computational and convergence difficulties in larger problems. One way of dealing with this could be to integrate Kinematic Stability Repair [35]. It should be noted that many of the form-finding techniques mentioned in the literature review, could be used as a tool to generate a structural surface that exhibits only membrane action under the considered load. Finally, the grid configuration of the grid shells in the case study consist of combinations of triangulated and quadrilateral facets. To improve constructibility, future development of this method may include forced planarity of the quadrilateral grid facets.

Bibliography

- [1] S. Adriaenssens and M.R. Barnes. Tensegrity spline beam and grid shell structures. *Engineering Structures*, 23(1):29–36, 2001.
- [2] S. Adriaenssens, L. Ney, E. Bodarwe, and C.J.K. Williams. Construction constraints drive the form finding of an irregular meshed steel and glass shell. *Journal of Architectural Engineering*, 18(3):206–213, 2012.
- [3] P. Basso, A.E. Del Grosso, A. Pugnale, and M. Sassone. Computational morphogenesis in architecture : the cost optimization of free form grid-shells. *Journal of the IASS*, 50(3):143–151, 2009.
- [4] M. Beckers and C. Fleury. A primal-dual approach in truss topology optimization. *Computers & Structures*, 64(1-4):77–88, 1997.
- [5] P. Bellés, N. Ortega, M. Rosales, and O. Andrés. Shell form-finding: Physical and numerical design tools. *Engineering Structures*, 31(11):2656 – 2666, 2009.
- [6] A. Ben-Tal, F. Jarre, M. Kočvara, A. Nemirovski, and J. Zowe. Optimal design of trusses under a nonconvex global buckling constraint. *Optimization and Engineering*, 1:189–213, 2000.
- [7] D.P. Billington. *The art of structural design: a Swiss legacy*. Yale University Press, 2008.
- [8] K. Bletzinger. Form finding and morphogenesis. In Ihsan Mungan and John F. Abel, editors, *Fifty Years of Progress for Shell and Spatial Structures*, pages 459–474. 2011.
- [9] Ph. Block and J. Ochsendorf. Thrust network analysis: a new methodology for three-dimensional equilibrium. *Journal of the IASS*, 48(3):1–8, 2007.
- [10] CEN. *Eurocode 1: Actions on Structures*. European Committee for Standardisation, 2002.
- [11] CEN. *Eurocode 3: Design of Steel Structures*. European Committee for Standardisation, 2003.
- [12] J. Chilton. *Heinz Isler. The Engineer's Contribution to Contemporary Architecture*. Thomas Telford, London, 2000.
- [13] A. Day. An introduction to dynamic relaxation. *The Engineer*, 219:218–221, 1965.
- [14] K. Deb and S. Gulati. Design of truss-structures for minimum weight using genetic algorithms. *Finite Elements in Analysis and Design*, 37(5):447–465, 2001.
- [15] B. Descamps, R. Filomeno Coelho, L. Ney, and Ph. Bouillard. Multicriteria optimization of lightweight bridge structures with a constrained force density method. *Computers & structures*, 89:277–284, 2011.

- [16] M.S. Eldred, B.M. Adams, K. Haskell, W.J. Bohnhoff, J.P. Eddy, D.M. Gay, J.D. Griffin, W.E. Hart, P.D. Hough, T.G. Kolda, M.L. Martinez-Canales, L.P. Swiler, J.P. Watson, and P.J. Williams. DAKOTA, a multilevel parallel object-oriented framework for design optimization, parameter estimation, uncertainty quantification, and sensitivity analysis: Version 4.1 reference manual. Technical Report SAND2006-4055, Sandia National Laboratories, Albuquerque, New Mexico, September 2007.
- [17] M. Giger and P. Ermanni. Evolutionary truss topology optimization using a graph-based parameterization concept. *Structural and Multidisciplinary Optimization*, 32:313–326, 2006.
- [18] L. Gil and A. Andreu. Shape and cross-section optimisation of a truss structure. *Computers & Structures*, 79(7):681–689, 2001.
- [19] P. Guillaume, G. Blengini, P. Ruaut, and F. Brunetti. Nouvelle foire de milan: prouesses d’acier. *Revue du Centre Information Acier*, 8:20–27, 2005.
- [20] P. Hajela and E. Lee. Genetic algorithms in truss topological optimization. *International Journal of Solids and Structures*, 32(22):3341–3357, 1995.
- [21] H.J. and Schek. The force density method for form finding and computation of general networks. *Computer Methods in Applied Mechanics and Engineering*, 3(1):115 – 134, 1974.
- [22] S. Huerta. El cálculo de estructuras en la obra de gaudí. *Ingeniería Civil*, 130:121 –133, 2003.
- [23] A. Kaveh and S. Talatahari. Geometry and topology optimization of geodesic domes using charged system search. *Structural and Multidisciplinary Optimization*, 43:215–229, February 2011.
- [24] H. Kawamura, H. Ohmori, and N. Kito. Truss topology optimization by a modified genetic algorithm. *Structural and Multidisciplinary Optimization*, 23(6):467–473, 2002.
- [25] A. Kilian and J. Ochsendorf. Particle-spring systems for structural form-finding. *Journal of the IASS*, 46(147):77, 2005.
- [26] R. Klein. Abstract voronoi diagrams and their applications. In Hartmut Noltemeier, editor, *Computational Geometry and its Applications*, volume 333 of *Lecture Notes in Computer Science*, pages 148–157. Springer-Verlag, 1988.
- [27] L. Lamberti. An efficient simulated annealing algorithm for design optimization of truss structures. *Computers & Structures*, 86(19–20):1936–1953, 2008.
- [28] P. Lancaster and K. Salkauskas. Surfaces generated by moving least squares methods. *Mathematics of Computation*, 37(155):141–158, 1981.
- [29] N. Leach, D. Turnbull, D. Turnbull, and C. Williams. *Digital tectonics*. Wiley-Academy, 2004.
- [30] A.C.C. Lemonge, H.J.C. Barbosa, L.G. da Fonseca, and A.L.G.A. Coutinho. A genetic algorithm for topology optimization of dome structures. In H. Rodrigues, J. Herskovits, C.M. Soares, J.M. Guedes, J. Folgado, A. Araújo, F. Moleiro, J.P. Kuzhichalil, J.A. Madeira, and Z. Dimitrovová, editors, *Proceedings of the 2nd International Conference on Engineering Optimization EngOpt 2010, Lisbon, Portugal*, 2010.
- [31] M. Ohsaki. Genetic algorithm for topology optimization of trusses. *Comput. Struct.*, 57(2):219–225, 1995.
- [32] P. Pedersen. Optimal joint positions for space trusses. *Journal of the Structural Division*, 99(12):2459–2476, 1973.
- [33] H. Pottmann and D. Bentley. *Architectural geometry*. Number v. 10 in Architectural geometry. Bentley Institute Press, 2007.
- [34] M.H. Rasmussen and M. Stolpe. Global optimization of discrete truss topology design problems using a parallel cut-and-branch method. *Computers & Structures*, 86(13–14):1527–1538, 2008.
- [35] J.N. Richardson, S. Adriaenssens, Ph. Bouillard, and R. Filomeno Coelho. Multiobjective topology optimization of truss structures

- with kinematic stability repair. *Structural and Multidisciplinary Optimization*, 46:513–532, 2012.
- [36] J.N. Richardson, S. Adriaenssens, R. Filomeno Coelho, and Ph. Bouillard. Coupled form-finding and grid optimization approach for single layer grid shells. *Engineering Structures*, 52(0):230 – 239, 2013.
- [37] S. Ruiyi, G. Liangjin, and F. Zijie. Truss topology optimization using genetic algorithm with individual identification technique. In S.I. Ao, L. Gelman, D.W.L. Hukins, A. Hunter, and A.M. Korsunsky, editors, *Proceedings of the World Congress on Engineering 2009 Vol II, WCE '09, July 1 - 3, 2009, London, U.K.*, pages 1089–1093, 2009.
- [38] M.P. Saka. Optimum topological design of geometrically nonlinear single layer latticed domes using coupled genetic algorithm. *Computers & Structures*, 85:1635–1646, November 2007.
- [39] R.L. Taylor. FEAP – A Finite Element Analysis Program, March 2008. Version 8.2 User Manual.
- [40] V. Toğan and A.T. Daloğlu. Optimization of 3d trusses with adaptive approach in genetic algorithms. *Engineering Structures*, 28(7):1019 – 1027, 2006.
- [41] P. Winslow, S. Pellegrino, and S.B. Sharma. Multi-objective optimization of free-form grid structures. *Structural and Multidisciplinary Optimization*, 40(1-6):257–269, 2010.

Chapter 4

Discrete optimization applied to façade bracing

Façade bracing systems are applied all over the world in structural design to limit deflections and guarantee stability, such as the structure shown in figure 4.1. Efficient distribution of bracing over a structure is an important concern for structural design professionals and is often based on intuition and previous experience. Meanwhile the limited amount of academic research on this topic often focuses on one aspect of the design, neglecting the practical design process itself. This paper presents a topology optimization procedure for cable bracing of the hanging steel façade of a new museum in the United States (figure 4.2). In this procedure the use of a multiobjective Genetic Algorithm allows for flexibility during design modifications and accounts for uncertainty of deflection constraint values. Since the allowed position of the cables is limited, and only certain standard cable sections can be used, the design variables are discrete, and the cost function is easily defined. The presented method achieves practical solutions to a series of cost minimizing problems, giving the designer a range of optimal bracing configurations which can be selected in response to the continuously changing structural and architectural requirements throughout the design process. This research aims at stimulating discussion on optimization methods which are capable of taking the design process into account, and the possibility of using multiobjective optimization to deal with these practical design uncertainties.



Figure 4.1: Bracing of the façade of a tall building, New York NY, USA. Image courtesy of Lionel Ponce



Figure 4.2: National Museum of African American History and Culture, Washington DC, USA. The façade for the museum is braced with cable X-bracing. Image courtesy of Adjeye Associates

Flexible optimum design of a bracing system for façade design using multiobjective Genetic Algorithms¹

Abstract

X-bracing systems are widely applied in structural design to limit deflections and guarantee stability. Efficient distribution of bracing over a structure is an important concern and often based on intuition and previous experience. This paper presents a topology optimization procedure for cable bracing of the hanging steel façade of a new museum in the United States. In this procedure the use of a multi-objective Genetic Algorithm allows for flexibility during design modifications and accounts for uncertainty of deflection constraint values. The presented method achieves practical solutions to a series of cost minimizing problems, giving the designer a range of optimal bracing configurations which can be selected in response to the continuously changing structural and architectural requirements throughout the design process.

4.1 Introduction

X-bracing systems are some of the most widely applied structural systems, particularly in steel construction. Schodek [27] and Taranath [28] describe various bracing systems for frame structures including X-braced, V-braced, K-braced and Chevron-braced (inverted V) systems, of which X-bracing is the most common. One of the main difficulties when designing braced systems is the choice of the location of the bracing components. This selection is often based on intuition and previous experience. While an approach based on experience is invaluable, it does not necessarily produce the best results. The cost associated with these bracing systems lies primarily in the connections. Reducing unnecessarily large numbers

of bracings is thus of great interest to make a design cost-effective. The effective placement of the necessary amount of bracings constitutes a topology² optimization problem. This topology optimization problem is discrete rather than continuous: the possible bracing locations are limited to a set of predefined positions (such as the openings between regularly spaced columns and floors) and predefined cross-sectional profiles usually from standard catalogues of sections.

Topology optimization methods for discrete structures usually require metaheuristic approaches such as Simulated Annealing [13], Ant Colony Optimization [10] or Genetic Algorithms (GA's) [7, 11, 20]. GA's for façade design have been used to maximize thermal and lighting performance of buildings [3]. Only a few researchers have used topology optimization for braced frame structures. Mijar et al. [19] developed a continuum topology optimization formulation with hybrid Voigt-Reuss mixing rules for conceptual design of frame bracing layout. Liang et al. [15] and Liang [14] presented a performance based optimization technique with continuum topology optimization to study optimal designs of bracing systems for steel building frameworks. However, these methods can only approximate global optima of discrete problems. Academic investigations into discrete bracing topology optimization include Kaveh and Shahrrouzi [9] who combined a graph theory approach with a discrete optimization procedure to optimize braced frame systems. Kaveh and Farhoodi [8] explored an ant system for layout (sizing and topology) optimization for X-bracing of steel frames. Baldock and Shea [2] used a genetic programming method for topology optimization of bracing for steel frames. The methods mentioned above were only applied in a limited academic sense and do not address the complex, ever changing requirements during the design process.

¹J.N. Richardson, G. Nordenson, R. Laberrenne, R. Filomeno Coelho, and S. Adriaenssens. Flexible optimum design of a bracing system for façade design using multiobjective genetic algorithms. *Automation in Construction*, 32(0):80 – 87, 2013

²Topology in this context refers to the connectivity of nodes in the structural model by means of structural components such as bars and beams.

For designers it is often unclear at the initial design stage what structural components will be used in the final structural system, what their dimensions will be, and what the constraint values (such as maximal allowed deflections) will be. However, the largest gains from structural optimization are made in the initial design stages, as Luebke and Shea [16] point out, when the greatest uncertainty exists. Therefore, to be effective, the optimization process needs to account for possible design and constraint changes³. One method of taking these uncertainties into account is to simplify the problem's basic geometry and to define the uncertain constraints as additional objective functions. The resulting range of solutions allows the designer to select an appropriate solution as the design changes over time. This aim can be achieved by a so-called Multiobjective Topology Optimization (MTO) approach.

Population based stochastic methods, such as GA's, are also very well suited to multiobjective problems [21], since a number of individuals (population) is considered at any given point in the optimization procedure. This aspect is consistent with the notion of Pareto optimality in which a number of non-dominated (i.e. 'best compromise') solutions make up an optimal set (the Pareto optimal set). The combination of multiobjective optimization with GA's has been successfully applied in other fields of structural optimization (an overview can be found in [4]), while few papers [18, 23, 26] present MTO of discrete structures; MTO of bracing systems is not present in the literature.

In this paper MTO will be implemented in the design of a hanging façade system for a new museum in the United States. This work is the result of a scientific and industrial collaboration between the authors and represents a novel approach to X-bracing design for steel braced frames. Several studies have been carried out comparing the performance of various Multiobjective algorithms in structural optimization [30–32].

The remainder of the paper is structured as follows: following an explanation of the structural system for the hanging façade (section 4.2), sections 4.3 and 4.4 respectively define the problem and present the multiobjective optimization ap-

proach. Next an explanation of the computation procedure (section 4.5) and the resulting topological designs (section 4.6) are presented. The paper concludes with a discussion of the implementation and future development of the method (section 4.7).

4.2 Description of façade structural system

For the design of the museum, the façade design posed a major challenge. The structural design of the façade arose from three primary architectural objectives: to create a three-tiered sawtooth profile for the façade; to maintain a continuous atrium between the façade and the interior floors of the building; and to keep this atrium space free of structure such that the façade is independent and free-spanning between the ground and roof.

The structure is a four-sided system consisting of three levels of horizontal trusses forming the sawtooth profile which are hung by vertical cables from the fifth floor of the building (figure 4.3). The structure is supported at the base only for lateral loads. A hung system is more efficient than a bottom-supported system because it reduces dead load deflections and places the primary support members in tension rather than compression, allowing them to be slender. It also effectively pretensions the vertical members such that they are able to support compression loads due to wind and seismic effects while remaining slender.

While this system relies on pre-tensioning of the vertical hangers, it is not a cable wall in the sense that it does not rely on the tension stiffness of the cables to resist lateral loads. Instead, the horizontal trusses work in combination with the vertical and bracing cables to resist wind pressures on the façade. When wind pressure is applied to one face of the building, steel mullions transfer wind loads to the three horizontal trusses (figure 4.4). These horizontal trusses in turn span across the face of the façade to transfer the wind loads to the orthogonal walls of the façade. The vertical cables and X-bracing in the orthogonal walls act as inverted braced frames to transfer the wind shears up to the fifth floor of the building where they are taken into the concrete cores of the building. In figure 4.5 the corner detail is shown for the façade structure.

³Design changes occurring at a later stage can significantly affect the optimal solution. The optimization procedure should take this into account. This observation is particularly valuable for constraints which exclude solutions considered unfeasible outside the given bounds, yet may be feasible if these bounds change only slightly.

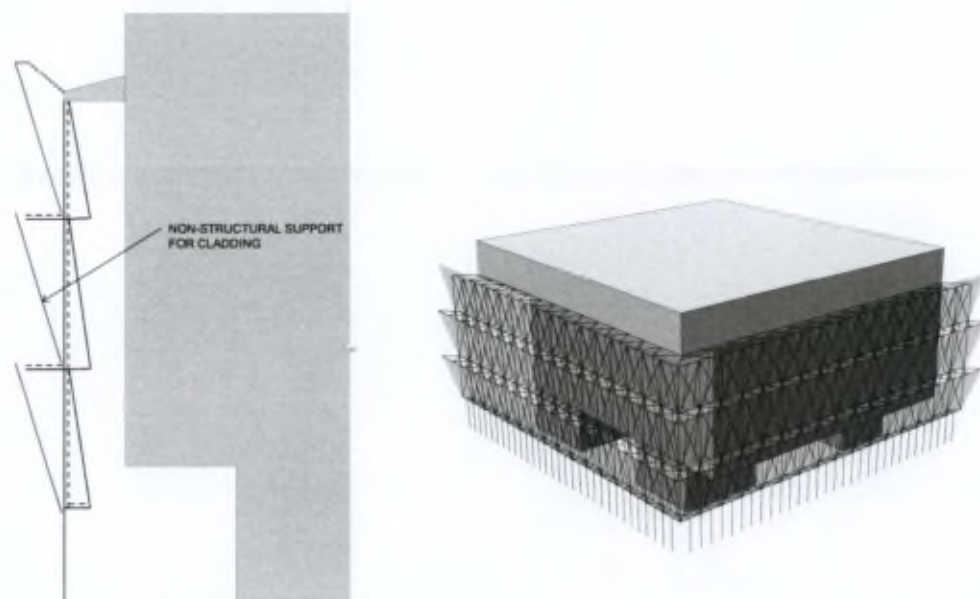


Figure 4.3: Hanging façade system

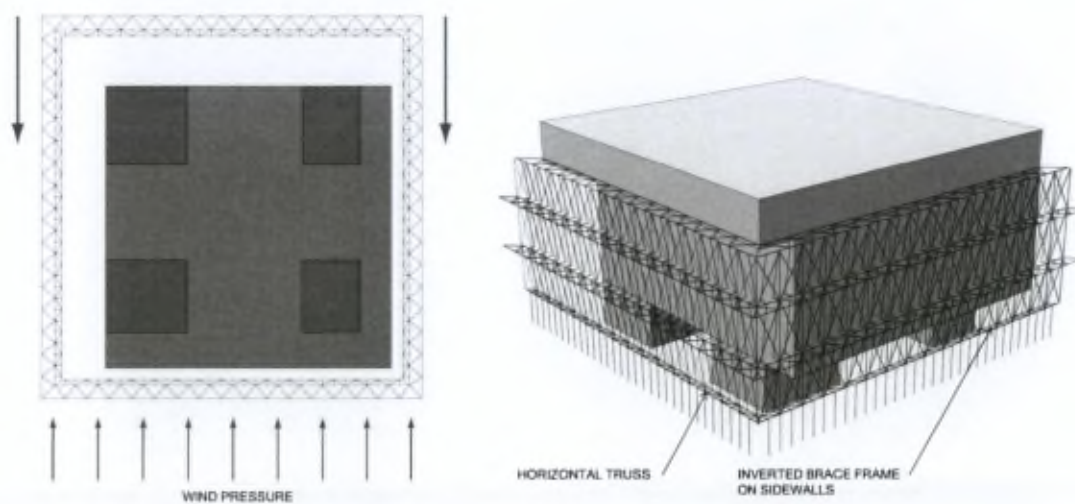


Figure 4.4: Façade structure wind loading principle

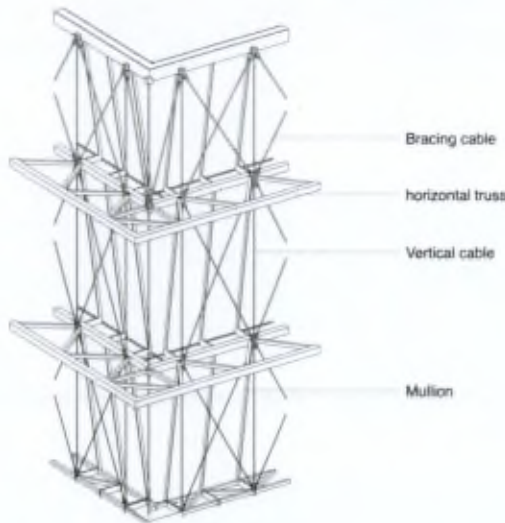


Figure 4.5: Isometry detail of corner of hanging façade system

4.3 Façade bracing problem definition

The complex 3D problem can be simplified as a series of four, independent, two dimensional problems shown in figure 4.6. The main purpose of the X-bracing is to provide in-plane stiffness under wind loading of the perpendicular façades as described in the previous section. The braced systems are supported along the top edge by pinned supports while each vertical hanger is restrained horizontally at the bottom end.

The North façade (figure 4.6(a)) layout is symmetric, as are the possible X-bracing locations. On the West façade (figure 4.6(b)) two hangers are interrupted in the middle tier resulting in an opening where no bracing can be located, and must be braced with two pairs of rigid bars under this opening. In the South and East façades (respectively figures 4.6(c) and 4.6(d)) the continuity of several of the hangers are interrupted, creating openings. The vertical hangers between the tiers are modelled as compressible (cable) truss elements, because they are assumed to be pretensioned by the dead load of the façade. The four horizontal trusses are modelled as continuous beams. The number of façade bracings is the greatest factor influencing the cost of the bracing system, the first objective function considered. The effectiveness of a given number of bracings to resist deflections

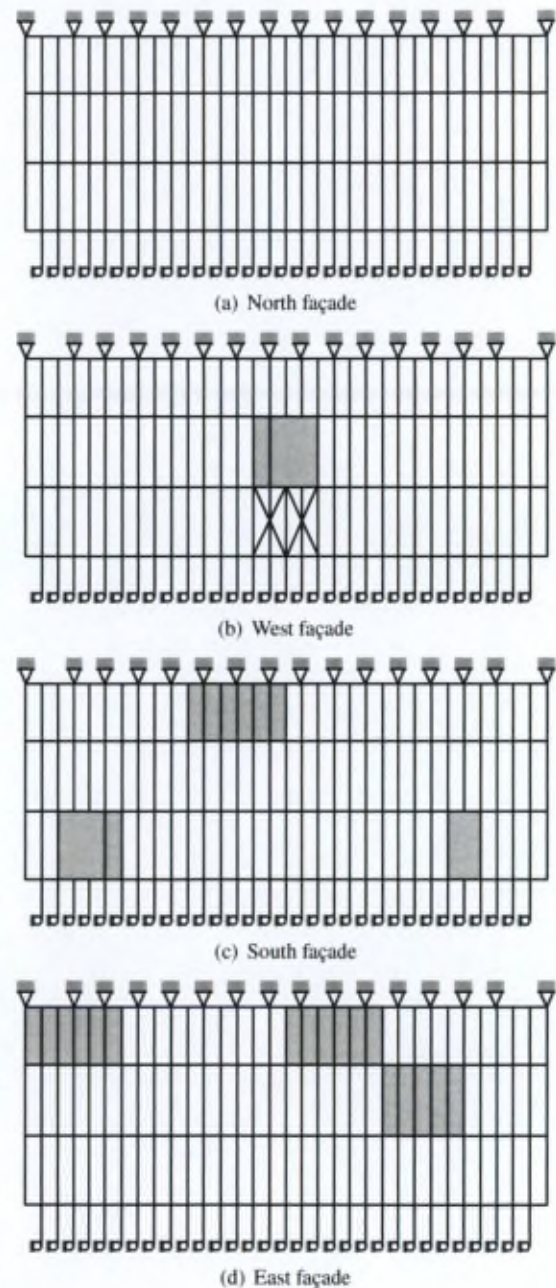


Figure 4.6: Simplified models of the four façades: the grey shaded areas represent zones where no bracing can be located. The bracing in the West façade (under the grey zone) are compulsory design elements

of each tier (the second objective function) is a function of their positions. Together, these two factors can be represented using a single type of variable: the topology variables, and both objectives set for the same problem: a multiobjective

topology optimization problem.

4.4 Approach: Multiobjective Topology Optimization using GA's

In order to obtain a range of optimal solutions, a multiobjective approach based on the multiobjective GA (MOGA) introduced by Fonseca and Fleming [6] is proposed. The MOGA optimization loop is coupled to a Finite Element Analysis program which generates the necessary responses (figure 4.7). The structural domain comprised of a set of nodes, a set of supports, a set of loads, and the non-variable structural components. In the three asymmetric problems lateral loading is applied from both directions consecutively. The worst performing of these two cases is used to evaluate the fitness of the topology design. A ground structure approach is used to define the upper bound of the topological search space.

4.4.1 Multiobjective structural optimization

The optimization problem with k objectives can be formulated as follows⁴: Given some performance criteria $f_i(\mathbf{x})$ ($i = 1, \dots, k$) which describe the performance of a structure, find the vector $\mathbf{x}^* = [x_1^*, \dots, x_n^*]$ which minimizes the vector function:

$$\mathbf{f}(\mathbf{x}) = [f_1(\mathbf{x}), \dots, f_k(\mathbf{x})]$$

subject to $g_i^l \leq g_i(\mathbf{x}) \leq g_i^u$ the constraints of the structural behaviour. \mathbf{x} is the vector of design variables, where g_i^u and g_i^l represent respectively the upper and lower bounds of the feasible solution space. In discrete topology optimization \mathbf{x} is the vector of (discrete) topology design variables. In the MTO sense optimization is most commonly described in terms of Pareto optimality.

4.4.2 Pareto optimality

In single objective optimization one solution can be defined as the 'best' solution in that it is minimal (or maximal) with respect to all other solutions. When multiple objectives are considered,

⁴for $k = 1$ the formulation describes a single objective optimization problem. For the case $k > 1$ the formulation describes a multiobjective optimization problem.

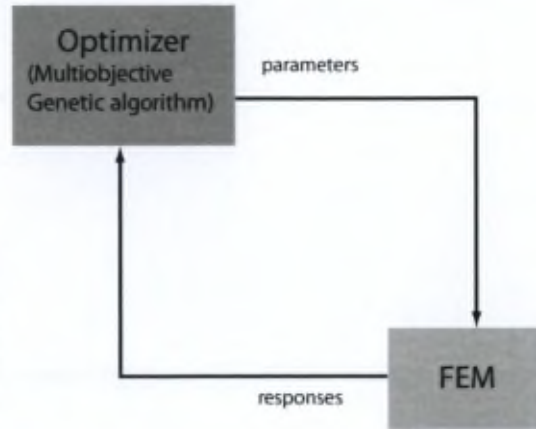


Figure 4.7: Basic algorithm scheme: a multiobjective Genetic Algorithm is coupled to a Finite Element Analysis (FEA) program

the definition of optimal solutions is less intuitive. In order to maintain the vector nature of solutions, the concepts 'Pareto optimal' and 'Pareto front' are used. Pareto optimality of a set of solutions is defined in terms of non-dominance. A design variable vector \mathbf{x}^* dominates \mathbf{x} if, for all i :

$$f_i(\mathbf{x}^*) \leq f_i(\mathbf{x}) \quad (4.1)$$

and there exists a j such that $(f_j(\mathbf{x}^*) < f_j(\mathbf{x}))$. The Pareto optimal set P_{true} is then defined as the set of vectors which are non-dominated and the Pareto front \mathcal{PF} is the set of objective function vectors corresponding to P_{true} . These notions are illustrated in figure 4.8. The concept of Pareto optimality is used to define solutions which are equivalent, depending on the importance the designer gives to each objective function.

4.4.3 Multiobjective Genetic Algorithm

The MOGA is a special class of GA, and as such use a series of biologically inspired processes applied to a population of possible solutions, as illustrated in figure 4.9. As a single objective GA, the MOGA uses a chromosome representation of the topology variables to define any given design. The chromosome is a string of concatenated entries from the design variable vector. The initial population (whose size is controlled by the population size parameter) is randomly seeded as a population of strings containing ones and zeros.

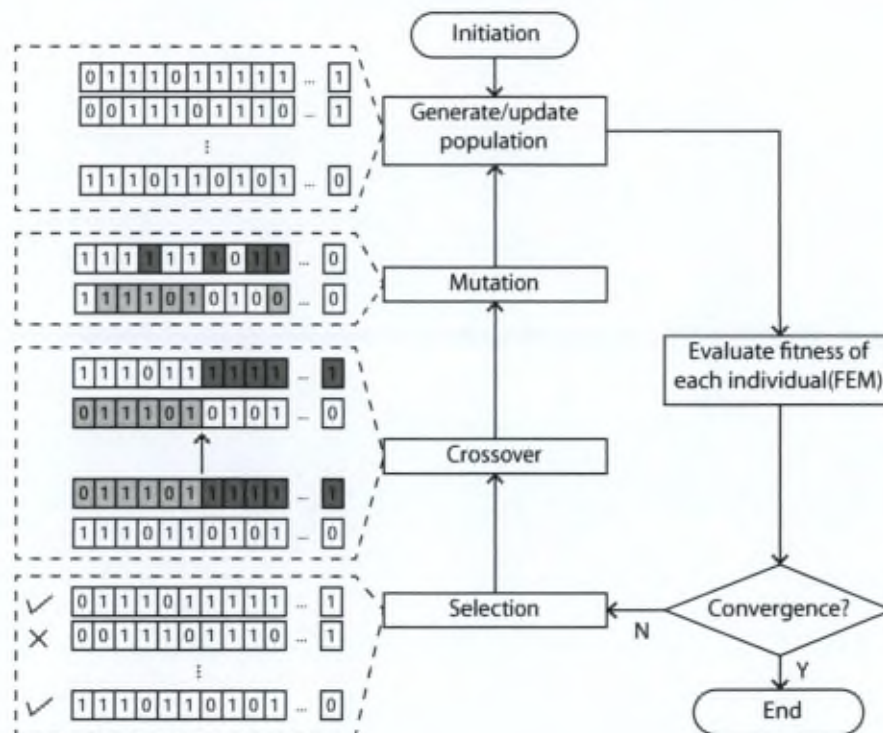


Figure 4.9: MOGA used in the façade bracing topology optimization. Several biologically inspired processes are used to optimize a population of structures. The binary string manipulation is demonstrated next to each operation

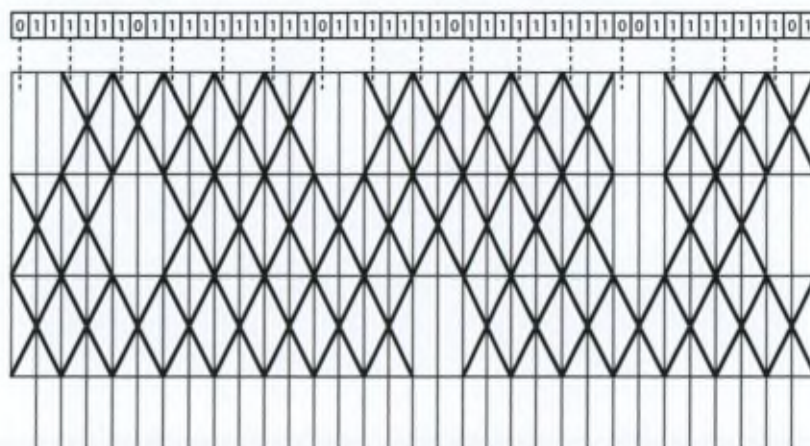


Figure 4.10: The relationship between chromosome and the bracing topology

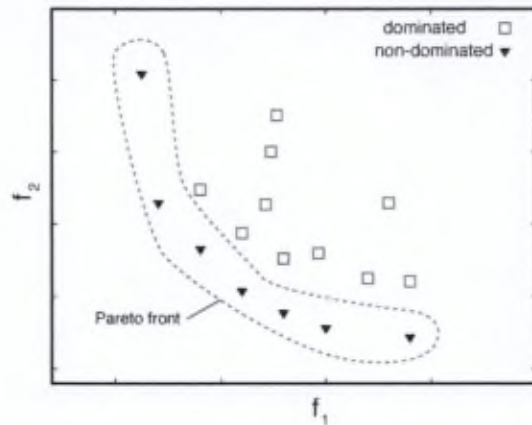


Figure 4.8: An illustration of the principals of non-dominance and Pareto front

Each '1' in the string indicates the presence of a pair of bracing cables at a particular location, shown in figure 4.10 as a vector of design variables. In this figure the number of design variables (length of the chromosome) corresponds to the number of possible positions (size of the ground structure) for pairs of bracing cables in the façade. In the design of the structures, symmetry was a desirable feature. As a result the number of design variables was reduced where symmetry could be applied. In that case each entry in the chromosome refers to the presence or absence of two pairs of cables, located symmetrically about a vertical axis. The variable values are combined with non-variable model data in the form of a finite element model. The finite element package FEAP [29] is used for a non-linear structural analysis. Upon evaluating the fitness of the systems, a ranking and selection of the current population is carried out, followed by cross-over and mutation of individuals to produce the next generation in the MOGA. The MOGA used differs from a single-objective GA in the way it evaluates the relative fitness of solutions. The algorithm involves the ranking of individuals at each iteration, with non-dominated individuals receiving the highest rank. A complete overview of the method, can be found in [4]. For these calculations the DAKOTA MOGA method [5] was used. This method performs Pareto optimization using a metric tracker to evaluate the convergence of the algorithm. This tracker evaluates three metrics associated with consecutive Pareto fronts, described in detail in the above reference.

4.5 Calculation procedure and parameters

In this particular project the designers faced the challenge of limiting the horizontal deflection relative to the height of each tier, using a bracing system. This problem can be cast as an unconstrained, bi-objective problem with the following objective functions:

$$\min_{\mathbf{x}} \mathbf{f}(\mathbf{x}) = (f_1, f_2)$$

$$\text{where } f_1 = \sum_{i=1}^n a_i x_i$$

$$f_2 = \max \left\{ \frac{|d_1|}{h_1}, \frac{|d_2 - d_1|}{h_2}, \frac{|d_3 - d_2|}{h_3} \right\} \quad (4.2)$$

where f_1 is the cost objective function, \mathbf{x} is the variable vector of length n , a_i is a weighting coefficient related to the grouping of components based on symmetry, and x_i is the topology variable associated with bracing(s) i . f_2 is the relative tier deflection objective function, h_j is the height of tier j and d_j is the measured deflection of tier j from rest position (figure 4.11). The algorithm is judged to have converged once the value of the metric tracker does not change significantly for 10 generations. The four façade systems each contain varying numbers of design variables and varying degrees of symmetry. A summary of the genetic algorithm parameters can be found in table 4.1. The MOGA parameters are adjusted until, for 10 runs of the problem, a majority of the solutions converged to the minimum solution. Due to this verification process several iterations may be necessary to achieve good results. The population size parameter represents the number of generated designs in the initial population of the MOGA and may vary after the first iteration of the MOGA.

The computational expense of the proposed approach is significant. Depending on the problem size the number of function evaluations can run into the tens or even hundreds of thousands. Large computer clusters are best suited for these computations, since parallel computing options can be exploited.

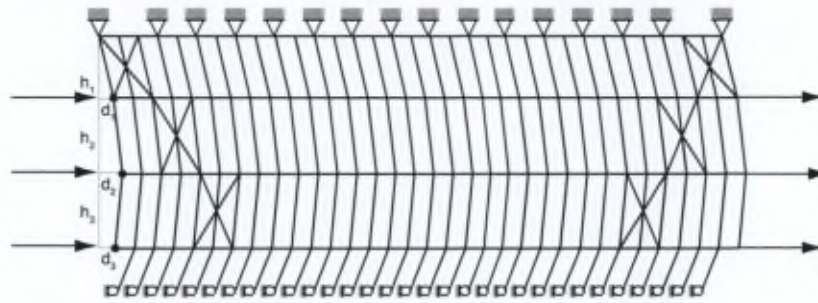


Figure 4.11: Deflected shape in plane

Parameter	N façade	W façade	S façade	E façade
Number of variables	24	22	27	26
Population size	800	800	800	800
Cross-over rate	0.9	0.9	0.9	0.9
Mutation rate	0.2	0.2	0.2	0.2
Fitness type		domination count*		
Replacement scheme		below limit* of 6		
Cross-over type		multi-point binary*		
Mutation type		offset normal*		

Table 4.1: Genetic algorithm parameters. * indicates built in DAKOTA methods

4.6 Results: a catalogue of optimal solutions

The combined Pareto fronts \mathcal{PF}_N , \mathcal{PF}_W , \mathcal{PF}_S and \mathcal{PF}_E ⁵ are shown in figure 4.12. Each front corresponds to a set of best compromise solutions for a specific façade. Since the four systems work together in the final design, it is necessary to choose solutions by grouping North, East, South and West façades to comprise one structural design. Grouping of the solutions is based on the worst performing front (façade), in this case the North façade for most of the solution space. For each solution on the worst performing front, corresponding solutions from the other three fronts can be found, as demonstrated in the insert for region IV in figure 4.12. For a given required deflection, if solution A in \mathcal{PF}_N meets this constraint value, it is selected along with B in \mathcal{PF}_W , C in \mathcal{PF}_S and D in \mathcal{PF}_E , since these are the least cost solutions with at most as little deflection as A. Similarly solutions can be grouped for any of the other regions. For regions V to XI the con-

figuration groupings are shown in table 4.2. The total cost of each solution is denoted f_1^{tot} and is simply the sum of the costs in the group. The relative deflections are scaled to allow for easy choice of solutions to meet changing constraint values. The dominant relative deflection value is denoted f_2^{tot} and have been scaled from their original values. The North and West façades where symmetry is enforced contrast the South and East façades, where the solutions display sole asymmetry. Surprisingly, the asymmetric solutions perform better than the symmetric solutions: Pareto optimal solutions for the South and East façades dominate the Pareto optimal solutions of their North and West counterparts. The reason behind this relates to the binary nature of the variables chosen, and is a remarkable result, explained in a recent paper by the authors [24].

Once the catalogue of solutions is compiled the designers are able to use it throughout the design process to achieve the most cost-effective bracing layout for a given set of circumstances. For example, consider the hypothetical design adjustments shown in figure 4.13. Assume the initial design calls for a maximal tier deflection of $\frac{h}{200}$, which, given some initial design components, can be met

⁵the subscripts refer respectively the North, West, South and East façades.

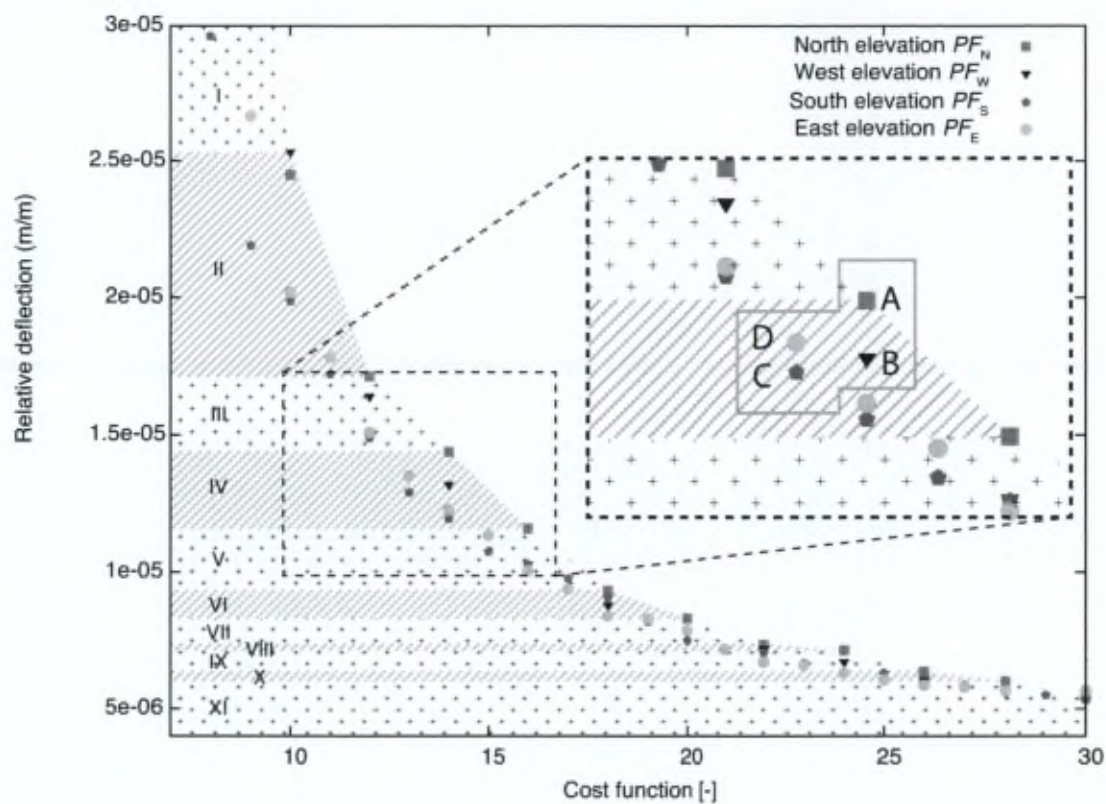


Figure 4.12: Combined Pareto fronts: configuration grouping

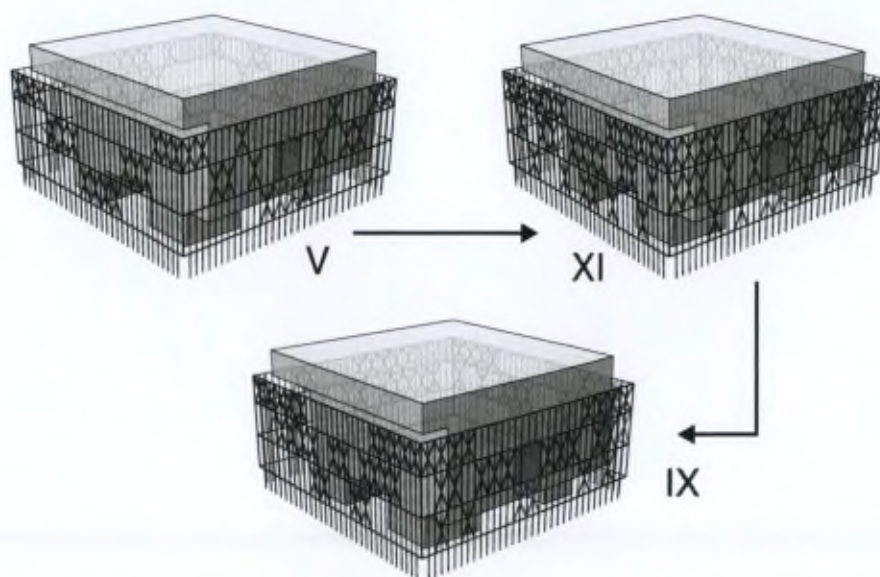


Figure 4.13: Hypothetical design evaluation based on changes in design requirements



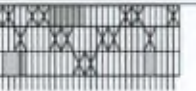



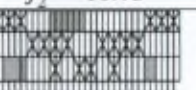
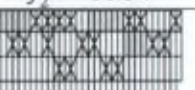

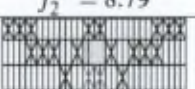

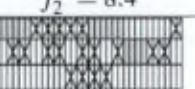




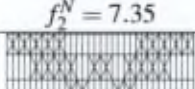
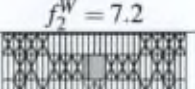
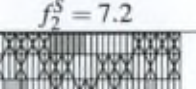
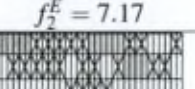
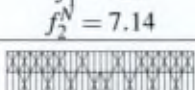
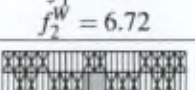
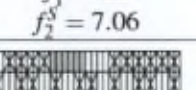
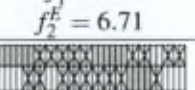
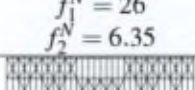
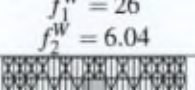
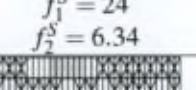
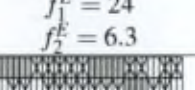
Soln.	N façade	W façade	S façade	E façade
V				
$f_1^{tot} = 62$ $f_2^{tot} = 11.59$	$f_1^N = 16$ $f_2^N = 11.59$	$f_1^W = 16$ $f_2^W = 10.3$	$f_1^S = 15$ $f_2^S = 10.75$	$f_1^E = 15$ $f_2^E = 11.34$
VI				
$f_1^{tot} = 72$ $f_2^{tot} = 9.33$	$f_1^N = 18$ $f_2^N = 9.33$	$f_1^W = 18$ $f_2^W = 8.79$	$f_1^S = 18$ $f_2^S = 9.07$	$f_1^E = 18$ $f_2^E = 8.4$
VII				
$f_1^{tot} = 78$ $f_2^{tot} = 8.31$	$f_1^N = 20$ $f_2^N = 8.31$	$f_1^W = 20$ $f_2^W = 7.76$	$f_1^S = 19$ $f_2^S = 8.18$	$f_1^E = 19$ $f_2^E = 8.28$
VIII				
$f_1^{tot} = 86$ $f_2^{tot} = 7.35$	$f_1^N = 22$ $f_2^N = 7.35$	$f_1^W = 22$ $f_2^W = 7.2$	$f_1^S = 21$ $f_2^S = 7.2$	$f_1^E = 21$ $f_2^E = 7.17$
IX				
$f_1^{tot} = 92$ $f_2^{tot} = 7.14$	$f_1^N = 24$ $f_2^N = 7.14$	$f_1^W = 24$ $f_2^W = 6.72$	$f_1^S = 22$ $f_2^S = 7.06$	$f_1^E = 22$ $f_2^E = 6.71$
X				
$f_1^{tot} = 100$ $f_2^{tot} = 6.35$	$f_1^N = 26$ $f_2^N = 6.35$	$f_1^W = 26$ $f_2^W = 6.04$	$f_1^S = 24$ $f_2^S = 6.34$	$f_1^E = 24$ $f_2^E = 6.3$
XI				
$f_1^{tot} = 108$ $f_2^{tot} = 6.0$	$f_1^N = 28$ $f_2^N = 6.0$	$f_1^W = 28$ $f_2^W = 5.58$	$f_1^S = 26$ $f_2^S = 5.89$	$f_1^E = 26$ $f_2^E = 5.87$

Table 4.2: Several solutions in the 'catalogue'

with configuration V. During the initial design solution V, with a cost of 62 units is used. However, at some point during the design process the tier deflection constraint is made more stringent so that $f_2^{tot} = \frac{h}{400}$ is required. The designers are faced with the option of adding additional bracing, or carrying out another time-consuming optimization study. With the range of solutions given above, however, solution XI ($f_{1,X}^{tot} = \frac{1}{2}f_{1,V}^{tot}$) can be chosen directly, the most cost effective (46 extra units) way possible to add additional bracing and dou-

ble the stiffness. Further in the design process the engineers decide to increase the thickness of the brass cladding panels to improve their dynamic behaviour. The increased dead-load on the hanging façade reduces lateral deflection so that the less X-bracing is required to meet the tier deflection limit value. The designers are now able to select solution IX, costing 92 units, while still meeting the deflection requirement.

4.7 Conclusions and further work

This paper presents the topology optimization method developed and used for the preliminary design of the bracing system for the hanging façade of a new museum in the United States. The approach uses multiobjective Genetic Algorithms to find a series of best compromise (Pareto optimal) solutions. The value of this method lies in its flexibility to provide solutions, allowing the designers to select optimal solutions when constraints change and modifications to the structural system occur. Since the main cost of bracing systems lies in the connections, reducing the number of bracings required results in a significant cost savings. The presented method could be extended to allow for greater freedom in the possible bracing locations. For example, bracing could span multiple tiers or across multiple columns. Other bracing typologies, such as V, K or Chevron systems could be included as design variables. These extensions would increase the number of topology variables, but not fundamentally change the problem formulation. This adaptivity is one of the strengths of MOGA's. This method could easily be extended to more than two criteria, making an even more general approach possible. Furthermore the method is general enough to be applied to a full 3D model of the structure, taking all structural components of the hanging façade into account. For example in the tall building design of the John Hancock Center (Chicago, Illinois, 1969) the diagonal bracing in one façade tends to reduce the shear lag in the perpendicular facades [12]. The solution presented in this paper decouples the structural behavior of the facades although there is interaction. Bracing in one facade may have beneficial effects on the perpendicular facades. This phenomenon has not been investigated in this paper and presents an avenue for further research. Other multiobjective methods such as multiobjective ant colony optimization [1] and multiobjective particle swarm [17] (or other classes of solution methods) may be more efficient than the MOGA to solving this problem. While these have not been investigated, a comparative study of the efficiency of various methods may lead to a more practical method for this problem.

Finally the proposed approach should be investigated within the broader context of Multidisciplinary design optimization and Multidisciplinary

collaborative design [22], both very promising instruments for structural design.

Bibliography

- [1] M. Abachizadeh and M. Tahani. An ant colony optimization approach to multi-objective optimal design of symmetric hybrid laminates for maximum fundamental frequency and minimum cost. *Structural and Multidisciplinary Optimization*, 37:367–376, 2009.
- [2] R. Baldock and K. Shea. Structural topology optimization of braced steel frameworks using genetic programming. In Ian F CEditor Smith, editor, *Intelligent Computing in Engineering and Architecture 13th EGICE Workshop*, volume 4200, pages 54–61. Springer, 2006.
- [3] L.G. Caldas and L.K. Norford. A design optimization tool based on a genetic algorithm. *Automation in Construction*, 11(2):173 – 184, 2002.
- [4] C.A. Coello Coello. A comprehensive survey of evolutionary-based multiobjective optimization techniques. *Knowledge and Information systems*, 1(3):129–156, 1999.
- [5] M.S. Eldred, B.M. Adams, K. Haskell, W.J. Bohnhoff, J.P. Eddy, D.M. Gay, J.D. Griffin, W.E. Hart, P.D. Hough, T.G. Kolda, M.L. Martinez-Canales, L.P. Swiler, J.P. Watson, and P.J. Williams. DAKOTA, a multilevel parallel object-oriented framework for design optimization, parameter estimation, uncertainty quantification, and sensitivity analysis: Version 4.1 reference manual. Technical Report SAND2006-4055, Sandia National Laboratories, Albuquerque, New Mexico, September 2007.
- [6] C.M. Fonseca, P.J. Fleming, et al. Genetic algorithms for multiobjective optimization: Formulation, discussion and generalization. In *Proceedings of the fifth international conference on genetic algorithms*, volume 423, pages 416–423, 1993.
- [7] P. Hajela and E. Lee. Genetic algorithms in truss topological optimization. *International Journal of Solids and Structures*, 32(22):3341–3357, 1995.

- [8] A. Kaveh and N. Farhoodi. Layout optimization for x-bracing of planar steel frames using ant system. *International Journal of Civil Engineering*, 8(3):256–275, 2010.
- [9] A. Kaveh and M. Shahrouzi. Graph theoretical topology control in structural optimization of frames with bracing systems. *Scientia Iranica*, 16(2):173–187, 2009.
- [10] A. Kaveh and S. Talatahari. A hybrid particle swarm and ant colony optimization for design of truss structures. *Asian Journal of Civil Engineering Building and Housing*, 9(4):329–348, 2008.
- [11] H. Kawamura, H. Ohmori, and N. Kito. Truss topology optimization by a modified genetic algorithm. *Structural and Multidisciplinary Optimization*, 23(6):467–473, 2002.
- [12] F.R. Khan. Current trends in current high rise buildings. In *Proceedings Symposium on Tall Buildings*, University of Southampton, 1966.
- [13] L. Lamberti. An efficient simulated annealing algorithm for design optimization of truss structures. *Computers & Structures*, 86(19-20):1936–1953, 2008.
- [14] Q.Q. Liang. Effects of continuum design domains on optimal bracing systems for multi-story steel building frameworks. In *Proceedings of the 5th Australasian Congress on Applied Mechanics*, volume 2, pages 794–799. Engineers Australia, 2007.
- [15] Q.Q. Liang, Y.M. Xie, and G.P. Steven. Optimal topology design of bracing systems for multi-story steel frames. *J Struct Engng ASCE*, 126(7):823–829, 2000.
- [16] C. Luebkeman and K. Shea. Cdo: Computational design + optimization in building practice. *The Arup Journal*, 3:17–21, 2005.
- [17] M. Marinaki, Y. Marinakis, and G. Stavroulakis. Fuzzy control optimized by a multi-objective particle swarm optimization algorithm for vibration suppression of smart structures. *Structural and Multidisciplinary Optimization*, 43:29–42, 2011.
- [18] S. Mathakari, P. Gardoni, P. Agarwal, A. Raich, and T. Haukaas. Reliability-based optimal design of electrical transmission towers using multi-objective genetic algorithms. *Computer-Aided Civil and Infrastructure Engineering*, 22(4):282–292, 2007.
- [19] A.R. Mijar, C.C. Swan, J.S. Arora, and I. Kosaka. Continuum topology optimization for concept design of frame bracing systems. *Journal of Structural Engineering*, 124(5):541, 1998.
- [20] M. Ohsaki. Genetic algorithm for topology optimization of trusses. *Computers & Structures*, 57(2):219–225, 1995.
- [21] M. Papadrakakis, N. Lagaros, and V. Plevris. Multi-objective optimization of skeletal structures under static and seismic loading conditions. *Engineering Optimization*, 34(6):645–669, 2002.
- [22] Z. Ren, F. Yang, N.M. Bouchlaghem, and C.J. Anumba. Multi-disciplinary collaborative building design – comparative study between multi-agent systems and multi-disciplinary optimisation approaches. *Automation in Construction*, 20(5):537 – 549, 2011.
- [23] J.N. Richardson, S. Adriaenssens, Ph. Bouillard, and R. Filomeno Coelho. Multiobjective topology optimization of truss structures with kinematic stability repair. *Structural and Multidisciplinary Optimization*, 2012. . In press.
- [24] J.N. Richardson, S. Adriaenssens, Ph. Bouillard, and R. Filomeno Coelho. Symmetry and asymmetry of solutions in discrete and continuous structural optimization. *Structural and Multidisciplinary Optimization*, 2012. . Accepted for publication.
- [25] J.N. Richardson, G. Nordenson, R. Laberene, R. Filomeno Coelho, and S. Adriaenssens. Flexible optimum design of a bracing system for façade design using multiobjective genetic algorithms. *Automation in Construction*, 32(0):80 – 87, 2013.
- [26] W.S. Ruy, Y.S. Yang, G.H. Kim, and Y.S. Yeun. Topology design of truss structures

- in a multicriteria environment. *Computer-Aided Civil and Infrastructure Engineering*, 16(4):246–258, 2001.
- [27] D.L. Schodek. *Structures*. Pearson/Prentice Hall, 5 edition, 2004.
- [28] B.S. Taranath. *Structural Analysis and Design of Tall Buildings: Steel and Composite Construction*. Taylor & Francis, 2011.
- [29] R.L. Taylor. FEAP – A Finite Element Analysis Program, March 2008. Version 8.2 User Manual.
- [30] E. Zitzler, M. Laumanns, and S. Bleuler. A Tutorial on Evolutionary Multiobjective Optimization. In X. Gandibleux, M. Sevaux, K. Sorensen, and V. T'kindt, editors, *Metaheuristics for Multiobjective Optimisation*, pages 3–37, Berlin, 2004. Springer. Lecture Notes in Economics and Mathematical Systems Vol. 535.
- [31] E. Zitzler, M. Laumanns, L. Thiele, Carlos M. Fonseca, and V. Grunert da Fonseca. Why Quality Assessment of Multiobjective Optimizers Is Difficult. In W.B. Langdon, E. Cant'u-Paz, K. Mathias, R. Roy, D. Davis, R. Poli, K. Balakrishnan, V. Honavar, G. Rudolph, J. Wegener, L. Bull, M.A. Potter, A.C. Schultz, J.F. Miller, E. Burke, and N. Jonoska, editors, *Proceedings of the Genetic and Evolutionary Computation Conference (GECCO'2002)*, pages 666–673, San Francisco, California, July 2002. Morgan Kaufmann Publishers.
- [32] E. Zitzler, L. Thiele, M. Laumanns, C.M. Fonseca, and V. Grunert da Fonseca. Performance Assessment of Multiobjective Optimizers: An Analysis and Review. *IEEE Transactions on Evolutionary Computation*, 7(2):117–132, April 2003.

Chapter 5

Symmetry considerations in discrete optimization

Symmetry as a concept is very broad and intuitive, invoking notions of simplicity, purity (for example in religious and utopian buildings such as in figure 5.1) and efficiency. Figure 5.2 shows a tiling pattern with five-fold rotational geometric symmetry. In optimization problems geometric symmetry in the problem formulation is often considered to be an opportunity to intelligently reduce the problem size, by recognizing that the solution will necessarily be symmetric. Investigation of solutions found in chapters 3 and 4, seemed to contradict this. For example, in the façade bracing problem, when no symmetry constraint was applied, asymmetric solutions were found which consistently outperformed the solutions found when the symmetry of the façade was enforced. This despite the fact that the latter problem reduced the cardinality of the search space and was a computationally much less expensive problem to solve. It became evident that the presence of the discrete design variables was responsible for this counter-intuitive behaviour.

The following paper presents a more rigorous explanation of the mathematical underpinning of this finding. While this theory is applied to structural topology optimization of trusses, it has direct application to all forms of optimization involving geometric symmetry and discrete design variables. For this reason, this chapter can be considered the most fundamental portion of the thesis.

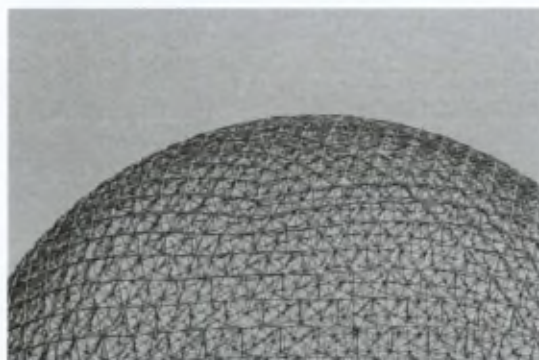


Figure 5.1: Various types of symmetry are present in the design of the Biosphere by Buckminster Fuller, Montreal, Canada. Image courtesy of Simon Bonaventure

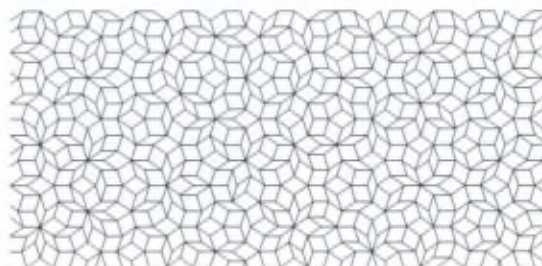


Figure 5.2: A tiling pattern with five-fold rotational symmetry

Symmetry and asymmetry of solutions in discrete variable structural optimization¹

Abstract

In this paper symmetry and asymmetry of optimal solutions in symmetric structural optimization problems is investigated, based on the choice of variables. A group theory approach is used to define the symmetry of the structural problems in a general way. This approach allows the set of symmetric structures to be described and related to the entire search space of the problem. A relationship between the design variables and the likelihood of finding symmetric or asymmetric solutions to problems is established. It is shown that an optimal symmetric solution (if any) does not necessarily exist in the case of discrete variable problems, regardless of the size of the discrete, countable set from which variables can be chosen. Finally a number of examples illustrate these principles on simple truss structures with discrete topology and sizing variables.

5.1 Introduction

In structural engineering discrete variable optimization is of great interest, given the discrete nature of building components. Symmetry reduction of structural problems is a well established technique for structural analysis. In the past several decades the mathematical rigour of group theory has been applied to symmetric structural problems [26], leading to the development of structural analysis techniques for discrete structures. Bifurcation problems [19] of framework and latticed domes [10, 11] are amongst the most widely studied of these problems. In static analysis, symmetric frame structures [27, 29] have been studied using group theoretic symmetry reduction techniques. Group theoretic methods combined with graph products have been developed by [14] and [13] in order to analyse symmetric-regular struc-

tures such as space trusses. [12] and [26] provide more complete reviews of the applications of symmetry tools and group theory in structural mechanics problems.

In numerous studies of symmetric discrete topology optimization the approach has been to enforce symmetry, leading to significant simplification of the problem by reducing the number of design variables [2, 6]. The consequent reduction in the problem size and hence the computational costs, are strong motivating factors for this approach. However, as will be seen, in discrete topology optimization this simplification often leads to suboptimal solutions. The authors were motivated to undertake this research on the basis of observed asymmetric results to (both constrained and unconstrained) symmetric discrete topology optimization problems [20]. However, a recent paper by [24] illustrates the attention this subject is now receiving. Asymmetry in discrete topology optimization was also noted by [1]. In topology optimization with continuous design variables [22] shows the existence of a symmetric solution, and possible non-uniqueness of the optimal solution, while [16] attributed asymmetric material layout in continuum problems to numerical roundoff and local asymmetric solutions. [5] demonstrated asymmetric solutions in frame topology optimization with non-convex constraints. In a recent paper, [8] showed the role of convexity in the ensuring the existence of symmetric solutions in continuous problems. However, it is shown that the validity of symmetry reduction in symmetric optimization problems is also largely dependent on the nature of the design variables.

Starting from these observations the remainder of the paper is ordered as follows: After an explanation of the scope and several important definitions (section 5.2), the relation between the search space and its symmetric subset is discussed (section 5.3). Next objective functions (section 5.4) as well as the existence of optimal solutions, with discrete variables are investigated (section 5.5). Finally several examples are presented (section 5.6).

¹J.N. Richardson, S. Adriaenssens, Ph. Bouillard, and R. Filomeno Coelho. Symmetry and asymmetry of solutions in discrete variable structural optimization. *Structural and Multidisciplinary Optimization*, 47(5):631–643, 2013

5.2 Scope and definitions

The investigation focuses on truss-like structures with discrete variable bar cross section areas. It is conceivable that the principles developed in this paper apply to topology optimization problems other than the structural kind. Such problems may include thermal, optical and other optimization problems. Furthermore the principles may also apply to discrete sizing and shape variables. However, the authors are primarily interested in structural topology optimization problems and only single objective optimization problems are considered.

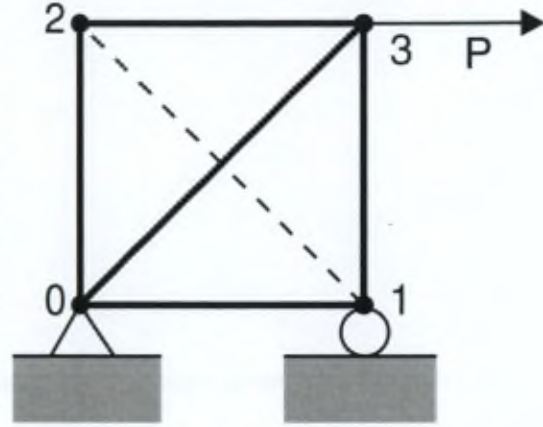


Figure 5.3: A 6 bar 2D truss design. The dashed line indicates a possible connection between nodes 1 and 2. This connection forms part of the problem ground structure, but is absent in this specific design

5.2.1 General definitions

The structural topology optimization problem consists of: (i) A set of nodes with fixed spatial coordinates; (ii) a set of boundary conditions corresponding to selected nodes; (iii) a set of loads applied to selected nodes; and (iv) a set of allowed structural connectivities between the nodes, called a *ground structure*. The nodal connectivity of the ground structure can be represented by an *adjacency matrix* A_{GS} . The structure in figure 5.3 has a ground structure with

$$A_{GS} = \begin{pmatrix} 0 & 1 & 1 & 1 \\ & 0 & 1 & 1 \\ & \text{sym.} & 0 & 1 \\ & & & 0 \end{pmatrix}.$$

A *design* is a particular structure represented by the problem definition and a specific set of values for the design variables \mathbf{x} . For example, in topology optimization, the values of \mathbf{x} may represent the binary existence or non-existence of elements, and as such correspond directly to A_{GS} . The set of allowable values for the terms in \mathbf{x} is referred to as the *design set* V . The particular design in figure 5.3 is described by adjacency matrix

$$A = \begin{pmatrix} 0 & 1 & 1 & 1 \\ & 0 & 0 & 1 \\ & \text{sym.} & 0 & 1 \\ & & & 0 \end{pmatrix}$$

and variable vector

$$\mathbf{x} = [1, 1, 1, 0, 1, 1]^T.$$

Each design corresponds to a value of the *objective function* $f(\mathbf{x})$, used to evaluate the structural

performance. The optimization problem is subject to inequality and equality constraints, respectively denoted $\mathbf{g}(\mathbf{x}) \leq 0$ and $\mathbf{h}(\mathbf{x}) = 0$. Each design is a *member* of a set of all possible designs, the *problem search space* \mathcal{S} . The search space is defined by the bounds of the design variables. The *feasible subset* $\Omega_f \subseteq \mathcal{S}$ is the set of values of the variables for which no constraint on the problem is violated, i.e. Ω_f is bounded by the constraints on the problem. The *symmetric subset* $\Omega_{sym} \subseteq \mathcal{S}$ is the set of all possible geometrically and mechanically symmetric structures in \mathcal{S} . The *feasible symmetric subset* $\Omega_{f,sym} \subseteq \mathcal{S}$ of the search space is the intersection of the symmetric and feasible subsets $\Omega_{f,sym} = \Omega_f \cap \Omega_{sym}$. The optimal subset $\Omega_{opt} \subseteq \Omega_f \subseteq \mathcal{S}$ is the set of designs corresponding to the values of \mathbf{x} such that the objective function $f(\mathbf{x})$ is minimized (or maximized) in the global sense. A schematic representation of the various sets is summarized in figure 5.4.

5.2.2 Group theory and group representation

Geometric symmetry is intuitive and easy to visualize, however it can be described more rigorously using mathematical operations. Structures are said to be symmetric with respect to an operation if that operation maps the structure into coincidence with itself while preserving the distance

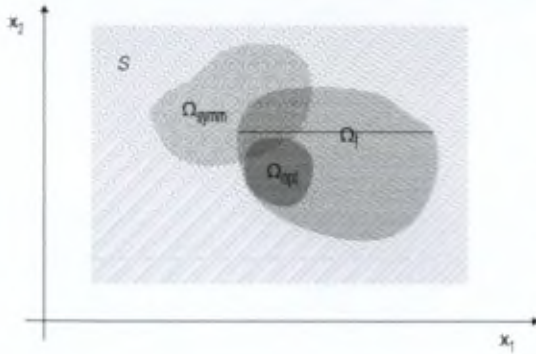


Figure 5.4: Sets and subsets of the variable space

5.3 Search space and symmetric subset

Using the concepts from section 5.2, Ω_{sym} can be constructed and related to \mathcal{S} in a symmetric topology optimization problem. If the structure represented by a vector \mathbf{x} is symmetric with group \mathcal{G} , it can be reduced to a non-unique vector \mathbf{x}' such that:

$$\mathbf{x} = \bigcup_{l \in \mathcal{G}} l(\mathbf{x}').$$

An equivalent algebraic form can be stated as follows:

$$\mathbf{x} = \frac{\sum_{l=1}^n \sum_{\kappa=1}^n (l(\mathbf{x}_{l\kappa}) + \kappa(\mathbf{x}_{l\kappa}))}{2} \quad (5.1)$$

where $\mathbf{x}_{l\kappa}$ is such that²:

$$l(\mathbf{x}_{l\kappa}) = \kappa(\mathbf{x}_{l\kappa}), \quad l \neq \kappa \quad (5.2)$$

and

$$l(\mathbf{x}_{ll}) \bigcap_{l, \kappa \in \mathcal{G}} \kappa(\mathbf{x}_{l\kappa}) = \mathbf{0}_l \quad (5.3)$$

where $\mathbf{0}_l$ is the null vector of length l . Figure 5.5 illustrates this concept for symmetry operation l on a structure with 6-fold symmetry. Since only symmetry operations κ and ν have an impact on the vectors relating to l (for this choice of \mathbf{x}') the other 4 symmetry operations are not shown. The symmetric subset can be mapped to the search space by means of the reduced permutation matrix \mathbf{P}' , constructed as follows:

$$\mathbf{P}' = \bigcup_{l \in \mathcal{G}} \mathbf{P}_l.$$

All identical rows of \mathbf{P}' can be collapsed, rendering \mathbf{P}'' with dimension $n \times l$, where $n \leq l$. In this way all symmetric members of \mathcal{S} , the m -dimensional $\mathbf{x}'' \in \Omega_{sym}$ can be constructed as n -dimensional $\mathbf{x} \in \mathcal{S}$:

$$\mathbf{x} = \mathbf{P}''^T \mathbf{x}'' \quad (5.4)$$

In the above example, $\mathbf{x}' = [1, 1, 1, 0, 0, 0, 0, 0, 0, 0, 0]^T$, and $\mathbf{x}'' = [1, 1, 1]^T$. Noting that both \mathbf{x} and \mathbf{x}'' can be represented by binary strings (by concatenating the entries), both \mathcal{S} and Ω_{sym} are countable sets which can be mapped to real positive integers.

between all points in the structure. Symmetry is studied through algebraic structures called *symmetry groups*. Simply stated: a symmetry group \mathcal{G} is formed by the set of possible symmetry operations that do not result in a change in the structure. The number of symmetry groups is finite [12] and can be reduced depending on the type of structures under consideration. In this study we consider only finite structures which are not symmetric under dilatation or translation, the so-called *point symmetry groups*. Point groups leave at least one point fixed under all operations in the group [17]. Thirty two unique point groups exist. In the topology optimization problems considered here, the symmetry group of the structure is defined by the non-variable aspects of the problem: the boundary conditions (supports) and non-variable structural components (such as truss elements, etc.). The loading need not necessarily be symmetric [28], however for the sake of simplicity symmetric loading is considered in the examples. Any operation in the point group \mathcal{G} , acting on a vector $\mathbf{x} \in \Omega_{sym}$, can be represented by the *permutation matrix* \mathbf{P} such that $\mathbf{P}^T \mathbf{x} = \mathbf{x}$ [3]. We denote the permutation of \mathbf{x} , under symmetry operation $l \in \mathcal{G}$, $l(\mathbf{x}) = \mathbf{P}_l^T \mathbf{x}$. The set of permutation matrices \mathbf{P} is a *representation* of \mathcal{G} . Representation theory is used to exploit symmetry in linear problems allowing for the separation of solutions into subsets corresponding to the subspaces of the problem. The reader is referred to Hamermesh's excellent book [9] for an overview of group theoretic concepts.

²The notation $\mathbf{x}_{l\kappa}$ refers to the characteristics of the vector under the symmetry transformations l and κ .

5.4 Objective functions and constraints

In this paper we consider only mass minimization and compliance minimization. No explicit constraints (such as maximum stress in elements, buckling of elements, deflection, ...) are considered, with the exception of the kinematic stability of the structures and a constraint on the volume of the minimum compliance problem.

5.4.1 Mass objective function

Mass minimization is an important objective in structural optimization. In the context of truss structures, the mass objective function is expressed as follows:

$$f_m(\mathbf{x}) = \sum_{k=1}^l m_k = \sum_{k=1}^l \rho_k A_k L_k x_k$$

where $x_k \in \mathbf{x}$, m_k , A_k , L_k and ρ_k are respectively the mass, cross-section area, length and density of element k . Since the function $f_m(\mathbf{x})$ is linear in $\mathbf{x} \in \mathbb{R}^n$, it is a convex function, bounded only by the kinematic stability of the structure.

5.4.2 Compliance objective function

The compliance energy

$$f_c(\mathbf{x}) = \mathbf{f}^\top \mathbf{u} = \mathbf{f}^\top \mathbf{K}^{-1} \mathbf{f}$$

is one of the most widely studied objective functions in structural topology optimization [4]. Here \mathbf{f} is a vector of external loads, \mathbf{u} is the vector of nodal displacements and \mathbf{K} is the stiffness matrix of the structure. It has been shown that, if a structural optimization problem is expressed in terms of variable bar areas, the compliance objective function is convex [25]. As mentioned an inequality constraint is placed on the volume of the structure, usually a maximum volume fraction V_f , the quotient of the volume of the specific design to the volume of the ground structure.

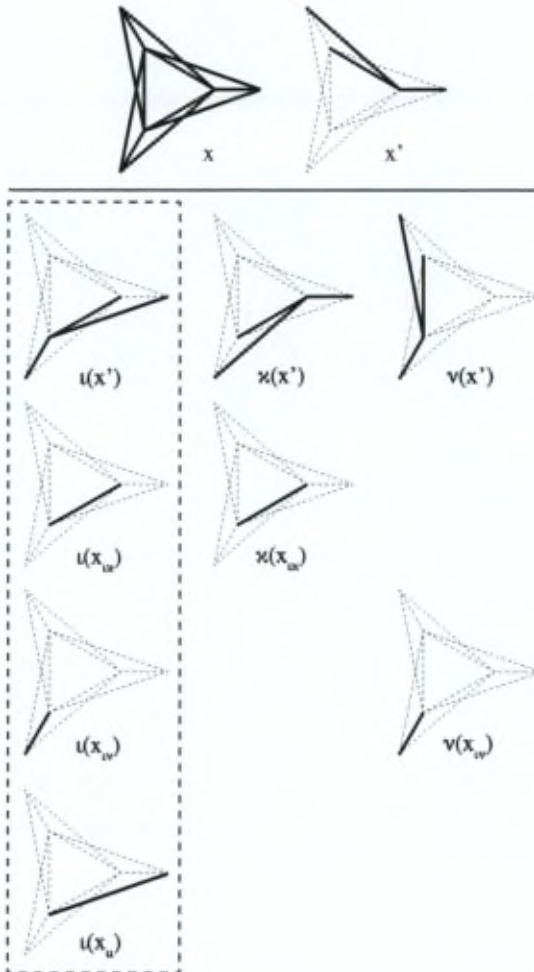


Figure 5.5: Symmetric structure variable vector reduction: an illustration

5.5 Convex combination: existence of solutions

Existence of solutions in topology optimization problems has been addressed widely in the literature, of which [15], [23], [7], and references

therein are only a few. The convex combination of designs i represented by variable vectors \mathbf{x}_i is a design \mathbf{x} , such that:

$$\mathbf{x} = \sum_i \lambda_i \mathbf{x}_i. \quad (5.5)$$

where $\lambda_i \in [0, 1]$, $\sum_i \lambda_i = 1$, Ω is some set of designs and

$$\mathbf{x}_i = [x_{i,1}, x_{i,2}, \dots, x_{i,l}]^T.$$

[22] and [8] have recently demonstrated the necessary existence of symmetric solutions to a class of problems with continuous design variables. In what follows we investigate the case where the design variable vectors have discrete entries.

5.5.1 Convex combination and variable mapping

Given a function $f: \mathcal{S} \rightarrow \mathbb{R}$, any convex combination of the variables will have a corresponding value to which the function f can map it. If, in addition, the function is an affine mapping, the map of the convex combination of the variables will be the convex combinations of the mappings

$$f\left(\sum_{i=1}^n \lambda_i \mathbf{x}_i\right) = \sum_{i=1}^n \lambda_i f(\mathbf{x}_i). \quad (5.6)$$

Therefore any convex combination of variables will also be a convex combination in the function space. Therefore if convex combinations of both \mathbf{x} and $f(\mathbf{x})$ are possible, any convex combination of optimal solutions is also optimal, and the convex combination of the variables maps to this optimal function value. Jensen's inequality states that, for a convex function

$$f\left(\sum_{i=1}^n \lambda_i \mathbf{x}_i\right) \leq \sum_{i=1}^n \lambda_i f(\mathbf{x}_i). \quad (5.7)$$

In one variable this can be interpreted as saying that the secant line of a convex function lies "above" the graph. However, since $f(\mathbf{x}_i) = f(\mathbf{x}_j)$ for all $\mathbf{x}_i, \mathbf{x}_j \in \Omega_{opt}$, on the optimal set, equation (5.7) becomes equation (5.6). If an asymmetric optimal solution can be found, the symmetry group permutations of this design are also optimal, since the structures are equivalent according to the problem statement. The convex combination of the variables can be mapped to the convex combination of the objective functions via an affine mapping. This combination is therefore also optimal.

5.5.2 Convex combination with discrete variables

Binary variables

In this section, the bar sizing variables are considered to be discrete, binary variables $x_j \in \{0, 1\}$. The convex combinations of n vectors lead to a system of equations, where the following holds:

$$x_j \in \{0, 1\} \quad \text{iff} \quad \left(\sum_{i=1}^n \lambda_i x_{i,j}\right) \in \{0, 1\}.$$

Two scenarios are possible for any x_j :

1. $x_{i,j} = x_{l,j}, \forall i, l$
2. $\exists i, l: x_{i,j} \neq x_{l,j}$

In the former case the convex combination can be constructed, but this is a trivial case where the vectors are identical. In the latter the linear combination of the vectors, having elements in $\{0, 1\}$, can only be constructed if

$$\sum_{i=1}^n x_{i,j} = \begin{cases} \sum_{i=1}^n x_{i,j} \\ 0 \end{cases} \quad \forall j$$

However this construction would violate the condition that $\sum_{i=1}^n \lambda_i = 1$.

Theorem 1. *For any set of (non-trivial) binary variable vectors, no convex combination of these vectors is possible, unless they are identical.*

Proof. If at least n entries in \mathbf{x} are non-zero, a system of n equations $\sum_{i=1}^n \lambda_i x_{i,j} = 1$ can be set up. In

the non-trivial case, for some j : $\sum_{i=1}^n x_{i,j} = r$, where $r \in \{1 \dots (n-1)\}$ and none of the vectors \mathbf{x}_i is the trivial null vector, so that $0 < \lambda_i \leq 1$. Assume that the i 's for which $x_{i,j} = 0$ are in a set A of size $n-r$. Then $\sum_{i=1}^n \lambda_i x_{i,j} = \sum_{i \notin A} \lambda_i = 1$. Therefore: $\sum_{i \notin A} \lambda_i + \sum_{k \in A} \lambda_k > 1$ and the linear combination is not convex. \square

This automatically leads to the following result:

Corollary 2. *In symmetric binary topology optimization problems, if an asymmetric optimal solution exists, no corresponding symmetric solution can necessarily be constructed.*

Proof. As in section 5.5 the symmetric solution can be expressed as the convex combination the permuted asymmetric solution. However it has been shown that the convex combination of any binary adjacency matrices cannot be constructed. Therefore, no corresponding symmetric solution necessarily exists, and if a symmetric solution does exist it is unique. \square \square

Since no convex mapping is possible between symmetric and asymmetric solutions, and at most one optimal symmetric solution exists, the relative sizes of the symmetric and asymmetric feasible solution sets plays a role in the probability of the existence of a symmetric solution. Conversely, in the convex case, since all asymmetric solutions have corresponding symmetric solutions through convex combination, this does not effect the probability.

Discrete variables from finite sets

Let us now consider non-binary discrete sets. Here variables are taken from sets of the following form:

$$V = \{0, 1, 2, \dots, m\}$$

Consider the simple case with the convex combination of n vectors such that:

$$\mathbf{x} = \sum_{i=1}^n \lambda_i \mathbf{x}_i. \quad (5.8)$$

Then for any n , $\lambda = \frac{1}{n}$, and $n\mathbf{x} = \sum_{i=1}^n \mathbf{x}_i$. The entries of $n\mathbf{x}$ can be seen as a series of linear Diophantine equations, with coefficients in the n -tuple $(1, 1, 1, \dots, 1)$. For any entry x_j in \mathbf{x} all entries $x_{i,j}$ in \mathbf{x}_i , satisfying the equation

$$n \cdot x_j = \sum_{i=1}^n x_{i,j}. \quad (5.9)$$

will be a valid convex combination. This amounts to the partition of $n \cdot x_j$ into parts $(1, 1, 1, \dots, 1)$ and the number of such solutions in $x_{j,1}, \dots, x_{j,n}$ is called the *restricted denumerant* [18], denoted $D_V(n \cdot x_j; 1, 1, \dots, 1)$. If $m \rightarrow \infty$, $V \equiv \mathbb{N}$, the number of such tuples satisfying equation (5.9) is $\binom{n(a+1)-1}{n-1}$. However, for a restricted design set V , this does not hold and the number of possible solutions is reduced for $V \subset \mathbb{N}$. In this case the relation is more complex, however the proportion of combinations to all perturbations is reliant on

the number of terms in the combination and tends asymptotically to $\frac{1}{n}$. The total probability of forming convex combinations $P(\mathbf{x})$ of the form in (5.8) can be calculated as follows:

$$P(\mathbf{x}) = \sum_{h=1}^p P(\mathbf{x}^{(h)}) = \sum_{h=1}^p \prod_{j=1}^k P(x_j^{(h)}) \quad (5.10)$$

where $\mathbf{x}^{(h)}$ is the h^{th} permutation of possible vectors \mathbf{x} and $p = k^m$ the total number of permutations. The total number of permutations is simply n^{m+1} and so the total probability of combination is $\frac{D_V(n \cdot \mathbf{x}; 1, 1, \dots, 1)}{n^{m+1}}$.

Returning to the binary case, it is clear that $D_{0,1}(n \cdot 1; 1, \dots, 1) = 1$, since $n \cdot 1 = 1 + 1 + \dots + 1$ n times. Similarly $D_{0,1}(n \cdot 0; 1, \dots, 1) = 1$. Therefore only convex combinations of identical, symmetric structures can be combined. The total probability of finding symmetric solutions to discrete variable problems is then:

$$P_{\text{tot}}(\mathbf{x}) = \frac{1}{(m+1)^{l-l'}} + P(\mathbf{x})$$

where l' is the length of the vector \mathbf{x}' in equation (5.4). Intuitively this probability can be expected to be low for most discrete problems. In structural optimization we are interested in comparing discrete sets with the same upper and lower bounds, for example $V_a = \{0, 0.5, 1\}$ and $V_b = \{0, 0.2, 0.4, 0.6, 0.8, 1\}$. In the combinatoric context described above, these sets are equivalent to those of the form $\{0, 1, \dots, m\}$ which can, for example, be scaled to within the bounds 0 and 1 by multiplying each element by a factor $\frac{1}{m}$. In our case:

$$V_a = \left\{ \frac{1}{a} \cdot 0, \frac{1}{a} \cdot 1, \frac{1}{a} \cdot 2 \right\}$$

$$V_b = \left\{ \frac{1}{b} \cdot 0, \frac{1}{b} \cdot 1, \dots, \frac{1}{b} \cdot 5 \right\}$$

where $a = 2$ and $b = 5$. It can easily be seen that this in no way affects the probabilities discussed above. To avoid confusion, in the examples we will refer to design sets using the following notation:

$$V_m = \left\{ \frac{1}{m} \cdot 0, \frac{1}{m} \cdot 1, \dots, \frac{1}{m} \cdot m \right\}$$

in the knowledge that they are equivalent (in the combinatoric sense) to a set $V'_m = \{0, 1, \dots, m\}$.

5.6 Examples

Several examples illustrate the principles discussed above. The first is a 2D truss, with point

group S_2 , consisting only of the identity operation and a line of 'mirror symmetry' through the middle of the structure. In this example the design variables are chosen from the binary $\{0, 1\}$ set. Next, a 9 bar truss with 3-fold rotational symmetry is investigated. The design variables can take on values from a larger design set, consisting of 6 discrete values. The final example is a 3D pylon structure, with three-fold rotational symmetry about a central, vertical axis, and three planes of 'mirror symmetry', as well as the identity operation. This structure therefore has dihedral symmetry group D_3 . In the first and third examples two possible objective functions, namely the mass of the structure and the compliance energy under a given loading, are investigated. All possible topologies (the entire search space) are evaluated and the symmetric subset of the search space constructed as described above. The optimal asymmetric solutions can then be compared with the best performing symmetric solutions. Finally, we investigate the effects of increasing the design set size on the 3D pylon example.

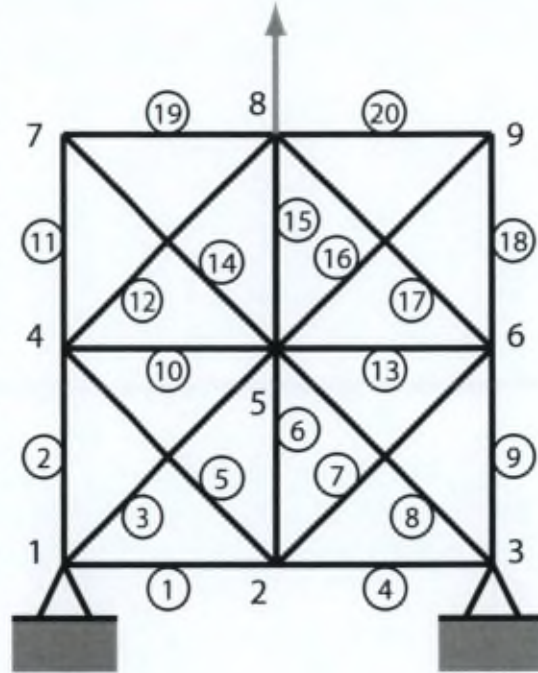


Figure 5.6: 20 bar 2D problem ground structure. Nodes are labelled with numbers, while the bar numbering is circled

5.6.1 20 bar 2D truss

Problem

The ground structure of the 20 bar topology optimization problem is shown in figure 5.6. For this problem the nodes are distributed regularly on a grid with spacing one unit in the two (Euclidean) dimensions of the problem. The nodal coordinates, supports and loading are as follows:

$$\mathbf{c} = \begin{pmatrix} 0,0 \\ 1,0 \\ 2,0 \\ 0,1 \\ 1,1 \\ 2,1 \\ 0,2 \\ 1,2 \\ 2,2 \end{pmatrix} \quad \mathbf{b}_c = \begin{pmatrix} 1,1 \\ 0,0 \\ 0,0 \\ 1,1 \\ 0,0 \\ 0,0 \\ 0,0 \\ 0,0 \\ 0,0 \end{pmatrix} \quad \mathbf{p} = \begin{pmatrix} 0,0 \\ 0,0 \\ 0,0 \\ 0,0 \\ 0,0 \\ 0,0 \\ 0,0 \\ 0,1 \\ 0,0 \end{pmatrix}.$$

The symmetry of the structure is expressed by the automorphism group \mathcal{G} of the graph with adjacency matrix \mathbf{A} , representing the topology of the structure. The structure has symmetry point group $S_2 = \{E, \sigma\}$, where E is the identity operation and σ a reflection about a vertical line through nodes 2, 5 and 8. The adjacency matrix and variable vector

for the ground structure are as follows:

$$\mathbf{A}_{GS} = \begin{pmatrix} 0 & 1 & 0 & 1 & 1 & 0 & 0 & 0 & 0 \\ & 0 & 1 & 1 & 1 & 1 & 0 & 0 & 0 \\ & & 0 & 0 & 1 & 1 & 0 & 0 & 0 \\ & & & 0 & 1 & 0 & 1 & 1 & 0 \\ & & & & 0 & 1 & 1 & 1 & 1 \\ & & & & & 0 & 0 & 1 & 1 \\ \text{sym.} & & & & & & 0 & 1 & 0 \\ & & & & & & & 0 & 1 \\ & & & & & & & & 0 \end{pmatrix}$$

$$\mathbf{x}_{GS} = \mathbf{e}_{20}$$

where \mathbf{e}_{20} is a 20 dimensional vector of ones. Keeping the nodal connectivity in mind, it is relatively simple to construct the topological permutation matrix P_σ :

$$\mathbf{P}_\sigma = \begin{pmatrix} 0 & 0 & 0 & 1 & 0 & 0 & 0 & 0 & 0 & 0 & 0 & 0 & 0 & 0 & 0 & 0 & 0 & 0 & 0 \\ 0 & 0 & 0 & 0 & 0 & 0 & 0 & 0 & 1 & 0 & 0 & 0 & 0 & 0 & 0 & 0 & 0 & 0 & 0 \\ 0 & 0 & 0 & 0 & 0 & 0 & 0 & 1 & 0 & 0 & 0 & 0 & 0 & 0 & 0 & 0 & 0 & 0 & 0 \\ 1 & 0 & 0 & 0 & 0 & 0 & 0 & 0 & 0 & 0 & 0 & 0 & 0 & 0 & 0 & 0 & 0 & 0 & 0 \\ 0 & 0 & 0 & 0 & 0 & 0 & 1 & 0 & 0 & 0 & 0 & 0 & 0 & 0 & 0 & 0 & 0 & 0 & 0 \\ 0 & 0 & 0 & 0 & 0 & 1 & 0 & 0 & 0 & 0 & 0 & 0 & 0 & 0 & 0 & 0 & 0 & 0 & 0 \\ 0 & 0 & 0 & 0 & 1 & 0 & 0 & 0 & 0 & 0 & 0 & 0 & 0 & 0 & 0 & 0 & 0 & 0 & 0 \\ 0 & 0 & 1 & 0 & 0 & 0 & 0 & 0 & 0 & 0 & 0 & 0 & 0 & 0 & 0 & 0 & 0 & 0 & 0 \\ 0 & 1 & 0 & 0 & 0 & 0 & 0 & 0 & 0 & 0 & 0 & 0 & 0 & 0 & 0 & 0 & 0 & 0 & 0 \\ 0 & 0 & 0 & 0 & 0 & 0 & 0 & 0 & 0 & 0 & 1 & 0 & 0 & 0 & 0 & 0 & 0 & 0 & 0 \\ 0 & 0 & 0 & 0 & 0 & 0 & 0 & 0 & 0 & 0 & 0 & 0 & 0 & 0 & 0 & 1 & 0 & 0 & 0 \\ 0 & 0 & 0 & 0 & 0 & 0 & 0 & 0 & 0 & 0 & 0 & 0 & 0 & 0 & 0 & 0 & 1 & 0 & 0 \\ 0 & 0 & 0 & 0 & 0 & 0 & 0 & 0 & 0 & 1 & 0 & 0 & 0 & 0 & 0 & 0 & 0 & 0 & 0 \\ 0 & 0 & 0 & 0 & 0 & 0 & 0 & 0 & 0 & 0 & 0 & 0 & 0 & 0 & 1 & 0 & 0 & 0 & 0 \\ 0 & 0 & 0 & 0 & 0 & 0 & 0 & 0 & 0 & 0 & 0 & 0 & 0 & 1 & 0 & 0 & 0 & 0 & 0 \\ 0 & 0 & 0 & 0 & 0 & 0 & 0 & 0 & 0 & 0 & 0 & 0 & 1 & 0 & 0 & 0 & 0 & 0 & 0 \\ 0 & 0 & 0 & 0 & 0 & 0 & 0 & 0 & 0 & 0 & 1 & 0 & 0 & 0 & 0 & 0 & 0 & 0 & 0 \\ 0 & 0 & 0 & 0 & 0 & 0 & 0 & 0 & 0 & 0 & 0 & 1 & 0 & 0 & 0 & 0 & 0 & 0 & 0 \\ 0 & 0 & 0 & 0 & 0 & 0 & 0 & 0 & 0 & 0 & 0 & 0 & 0 & 1 & 0 & 0 & 0 & 0 & 0 \\ 0 & 0 & 0 & 0 & 0 & 0 & 0 & 0 & 0 & 0 & 0 & 0 & 0 & 0 & 0 & 1 & 0 & 0 & 0 \\ 0 & 0 & 0 & 0 & 0 & 0 & 0 & 0 & 0 & 0 & 0 & 0 & 0 & 0 & 0 & 0 & 0 & 1 & 0 \\ 0 & 0 & 0 & 0 & 0 & 0 & 0 & 0 & 0 & 0 & 0 & 0 & 0 & 0 & 0 & 0 & 0 & 0 & 1 \end{pmatrix}.$$

Furthermore, a decomposition of the vector \mathbf{x}_{GS} can be made

$$\mathbf{x}_{\sigma\sigma} = \mathbf{x}_{EE} = [1, 1, 1, 0, 1, 0, 0, 0, 0, 1, 1, 1, 0, 1, 0, 0, 0, 0, 1, 0]^\top$$

and

$$\mathbf{x}_{E\sigma} = \mathbf{x}_{\sigma E} = [0, 0, 0, 0, 0, 1, 0, 0, 0, 0, 0, 0, 0, 0, 0, 1, 0, 0, 0, 0]^\top.$$

It can be easily confirmed that, as in equation (5.1)

$$\frac{2E(\mathbf{x}_{EE}) + E(\mathbf{x}_{E\sigma}) + \sigma(\mathbf{x}_{E\sigma}) + 2\sigma(\mathbf{x}_{\sigma\sigma})}{2} = \mathbf{x}.$$

Ω_{sym} has $2^{11} = 2048$ members, while the topological search space \mathcal{S} has 2^{20} members. Since no mapping through convex combination of asymmetric solutions is possible, the probability of finding a symmetric optimal solution is will not be increased by convex mapping.

Results

For simplicity sake the variables of each design have been mapped to natural numbers $\mathbf{x} \rightarrow \mathbb{N}$, since a one-to-one mapping is possible and this allows for plotting of the results. To do this the topology variables are taken to be the digits of a binary number, and its equivalent base 10 number plotted to a position on the horizontal axis. All feasible masses of the structures in \mathcal{S} and in Ω_{sym} are

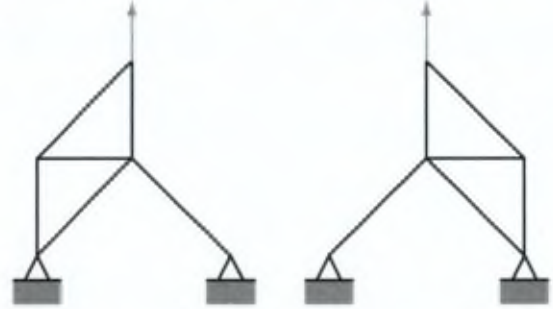


Figure 5.8: 20 bar 2D truss problem: minimum objective function values, both mass and compliance ($V \leq 0.4$)

shown³ in figure 5.7. Note that the minimum feasible mass is not symmetric. The two (feasible) minimum mass structures are shown in figure 5.8. As expected the two solutions are asymmetric, mirror images of one another about a vertical line. For the compliance objective function, taking the volume fraction $V \leq 0.4$, the same topology is found as in figure 5.8. The minimum symmetric mass (solution shown in figure 5.9) is 1.33 times greater than the asymmetric minimum mass solution.

³The vertical gaps in the graph are a result of groups of binary numbers whose equivalent structures share common mechanical instabilities. These instabilities are considered non-feasible and therefore not plotted.

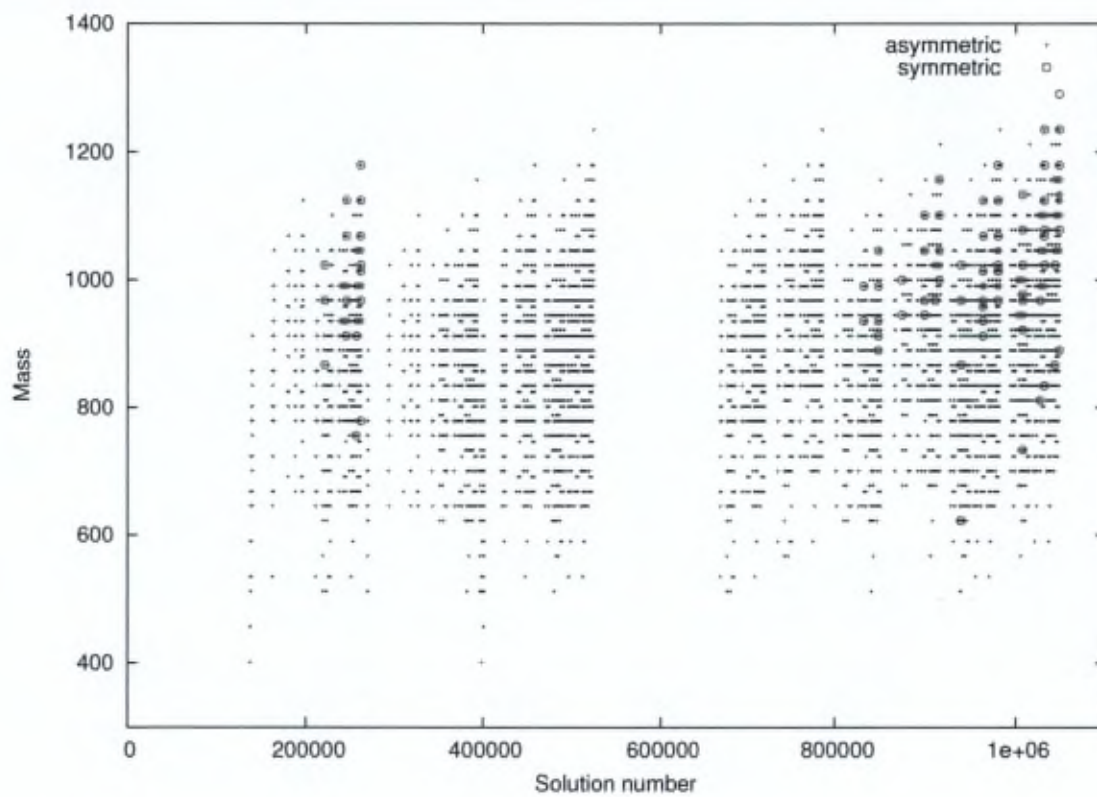


Figure 5.7: 20 bar 2D truss problem: symmetric and asymmetric structure mass objective functions

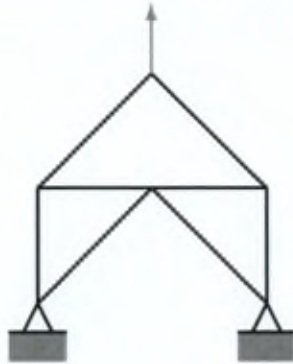


Figure 5.9: 20 bar 2D truss problem: minimum mass stable, symmetric structure

5.6.2 9 bar truss

In this example a 9 bar truss (seen in figures 5.10 and 5.11) is considered with the sizing variables taken from the design set V_5 . The truss has 3-fold rotational symmetry about a central point:

$$C_3 = \{E, C_3, C_3^2\}. \quad (5.11)$$

C_3 results in a one third rotation, while C_3^2 results in two thirds of a complete rotation. E is simply the identity operation. The reduced permutation matrix is a 3×6 matrix:

$$P'' = \begin{pmatrix} 1 & 0 & 0 & 1 & 0 & 0 & 1 & 0 & 0 \\ 0 & 1 & 0 & 0 & 1 & 0 & 0 & 1 & 0 \\ 0 & 0 & 1 & 0 & 0 & 1 & 0 & 0 & 1 \end{pmatrix}$$

In addition to the probability of finding some symmetric solution directly, convex mapping between asymmetric and equivalent symmetric solutions also exists. If an asymmetric optimal solution can be found, a symmetric solution can only be constructed of the form:



Figure 5.10: 9 bar 3D structure

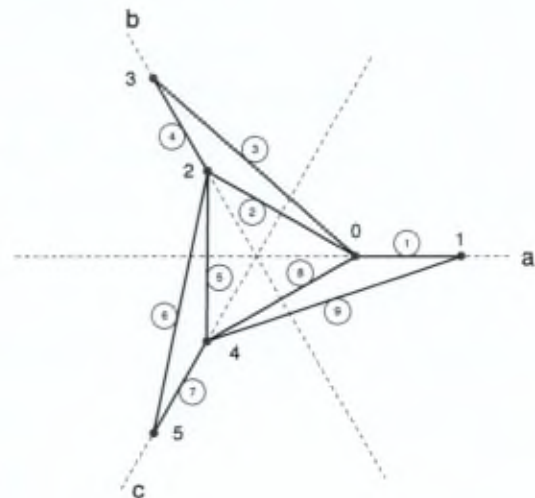


Figure 5.11: 9 bar 3D structure plan view and numbering

$$\begin{pmatrix} x_1 \\ x_2 \\ x_3 \\ x_4 \\ x_5 \\ x_6 \\ x_7 \\ x_8 \\ x_9 \end{pmatrix} = \frac{1}{3} \mathbf{P}_E \begin{pmatrix} x_{1,1} \\ x_{1,2} \\ x_{1,3} \\ x_{1,4} \\ x_{1,5} \\ x_{1,6} \\ x_{1,7} \\ x_{1,8} \\ x_{1,9} \end{pmatrix} + \frac{1}{3} \mathbf{P}_{C_3} \begin{pmatrix} x_{1,1} \\ x_{1,2} \\ x_{1,3} \\ x_{1,4} \\ x_{1,5} \\ x_{1,6} \\ x_{1,7} \\ x_{1,8} \\ x_{1,9} \end{pmatrix} + \frac{1}{3} \mathbf{P}_{C_3^2} \begin{pmatrix} x_{1,1} \\ x_{1,2} \\ x_{1,3} \\ x_{1,4} \\ x_{1,5} \\ x_{1,6} \\ x_{1,7} \\ x_{1,8} \\ x_{1,9} \end{pmatrix}$$

$$= \frac{1}{3} \begin{pmatrix} x_{1,1} \\ x_{1,2} \\ x_{1,3} \\ x_{1,4} \\ x_{1,5} \\ x_{1,6} \\ x_{1,7} \\ x_{1,8} \\ x_{1,9} \end{pmatrix} + \frac{1}{3} \begin{pmatrix} x_{1,4} \\ x_{1,5} \\ x_{1,6} \\ x_{1,7} \\ x_{1,8} \\ x_{1,9} \\ x_{1,1} \\ x_{1,2} \\ x_{1,3} \end{pmatrix} + \frac{1}{3} \begin{pmatrix} x_{1,7} \\ x_{1,8} \\ x_{1,9} \\ x_{1,1} \\ x_{1,2} \\ x_{1,3} \\ x_{1,4} \\ x_{1,5} \\ x_{1,6} \end{pmatrix} \quad (5.12)$$

Equation (5.12) can be reduced and the problem restated as finding values $x_{i,1} \dots x_{i,9}$ in V such that $x_i \in V$:

$$3x'_1 = x_{1,1} + x_{1,4} + x_{1,7} \quad (5.13)$$

$$3x'_2 = x_{1,2} + x_{1,5} + x_{1,8} \quad (5.14)$$

$$3x'_3 = x_{1,3} + x_{1,6} + x_{1,9} \quad (5.15)$$

which is equivalent to $3\mathbf{x}' = \mathbf{P}'\mathbf{x}_1$. Using equation (5.10), the probability that \mathbf{x}_1 can be combined in such a way that an equivalent symmetric solution exists is $(0.329)^3 \approx 0.0355$. In fact, as m increases (taking design sets V_m), so this probability asymptotically converges to $\frac{1}{3^3}$. The asymptotic behaviour can clearly be seen in figure 5.12 showing the proportion of combinable structures as the size of V increases from 3 to 21 values. As m increases beyond 10, this proportion remains relatively constant. More generally the proportion is asymptotic to $\frac{1}{n^3}$.

5.6.3 24 bar 3D truss

Problem

In this example a 24 bar 3D truss (figure 5.13) is investigated. The structure has dihedral symmetry group

$$D_3 = \{E, C_3, C_3^2, C_2^a, C_2^b, C_2^c\}$$

These operations are identical to those in the C_3 group in (5.11), with 3 additional mirror symmetry operations around vertical planes through lines

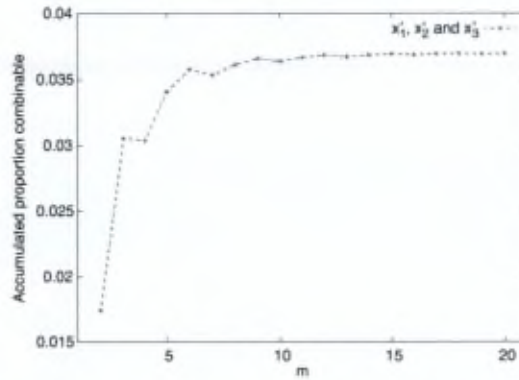


Figure 5.12: Probability of symmetry resulting through convex combination of asymmetric optimal solutions for the 9 bar truss

a, b and c in the plan view of the ground structure in figure 5.14. Three vertical, unitary point forces act on the three highest nodes on the structure. Only binary topology variables are used and a unit bar section area taken for simplicity sake. All three supports are pinned, restraining displacements translationally in all three dimensions.

Results

All 2^{24} designs in the search space were calculated. Only 64 structures in the search space are D_3 group symmetric. The 8 least mass solutions are shown in figure 5.15. Two distinct solutions can be seen. Taking structure 1 as one of these, the following mappings are present:

$$\mathbf{x}_2 = \sigma_a(\mathbf{x}_1)$$

$$\mathbf{x}_4 = C_3^2(\mathbf{x}_1)$$

$$\mathbf{x}_5 = C_2^b(\mathbf{x}_1)$$

$$\mathbf{x}_7 = C_3(\mathbf{x}_1)$$

$$\mathbf{x}_8 = C_2^b(\mathbf{x}_1).$$

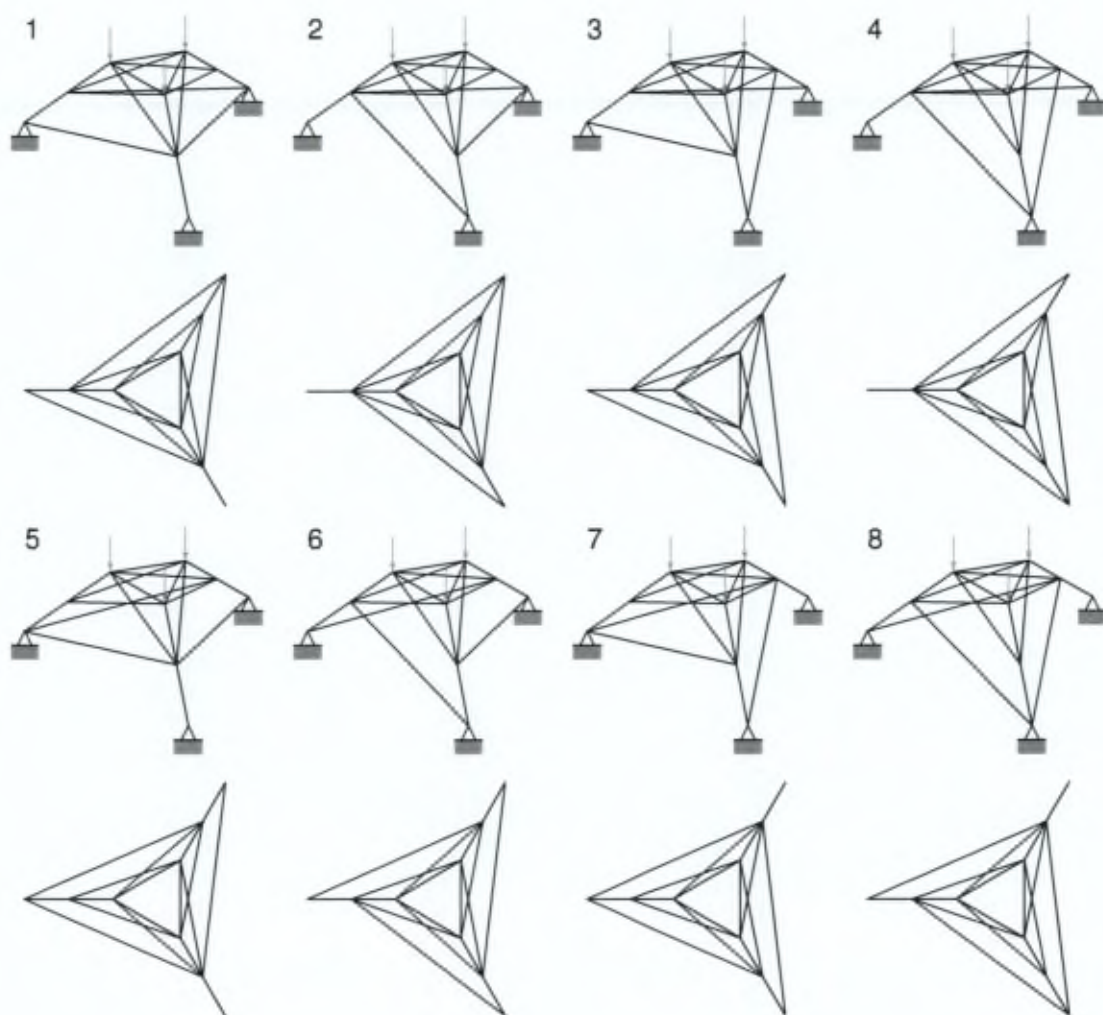


Figure 5.15: 24 bar 3D structure: least mass solutions

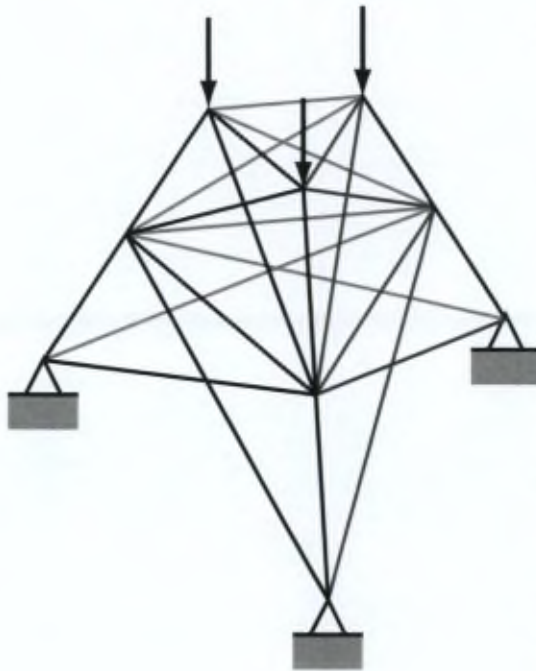


Figure 5.13: 24 bar 3D structure ground structure

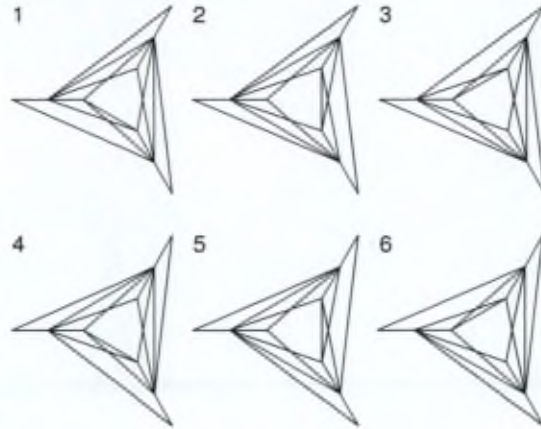


Figure 5.16: 24 bar 3D structure: lowest compliance energy solutions

The second type is structures number 3 and 6. For this structure the following holds:

$$\begin{aligned} \mathbf{x}_7 &= C_2^a(\mathbf{x}_3) = C_2^b(\mathbf{x}_3) = C_2^c(\mathbf{x}_3) \\ \mathbf{x}_3 &= C_3(\mathbf{x}_3) = C_3^2(\mathbf{x}_3) \\ \mathbf{x}_7 &= C_3(\mathbf{x}_7) = C_3^2(\mathbf{x}_7). \end{aligned}$$

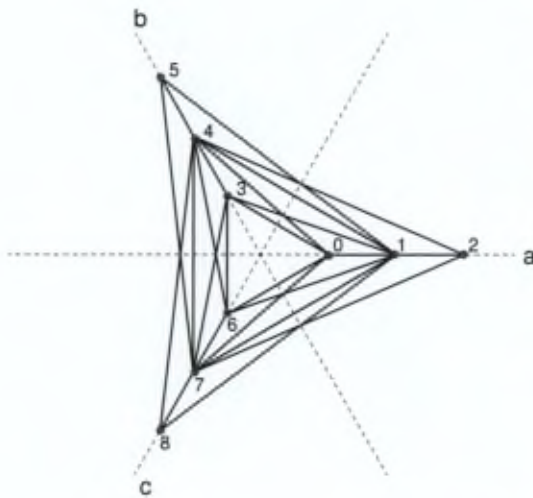


Figure 5.14: 24 bar 3D structure ground structure plan view

In figure 5.16 the minimum compliance results are shown, with volume fraction constraint $V \leq 0.7$. These results demonstrate one single, asymmetric solution, and the 5 other permutations corresponding to the D_3 group. None of the optimal structures are symmetric with respect to the symmetry group D_3 . In the case of the compliance minimization problem, the structures do not possess any of the non-trivial symmetries in this group. The symmetric minimum mass solution was approximately 1.2 times the mass of the asymmetric solution, while for the compliance solutions, this ratio was approximately 1:1.14.

Larger design sets

Suppose now the size of the design set is increased from 2 to $m+1$ possible values. Following the method in example 2, the following equations re-

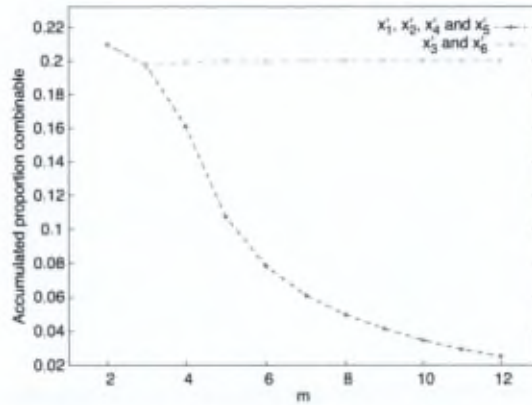


Figure 5.17: 24 bar 3D truss: contribution of terms to probability of symmetry resulting through convex combination of asymmetric optimal solutions

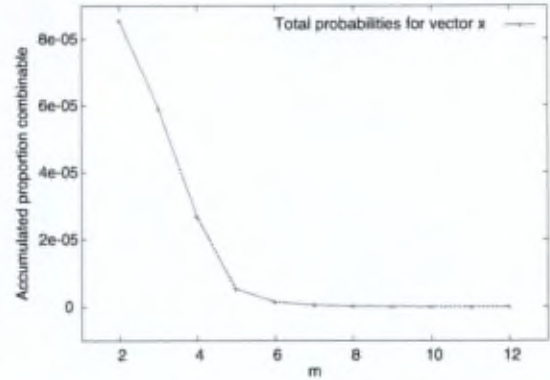


Figure 5.18: 24 bar 3D truss: probability of symmetry resulting through convex combination of asymmetric optimal solutions

sult:

$$5x'_1 = x_{1,1} + 2x_{1,23} + 2x_{1,15} \quad (5.16)$$

$$5x'_2 = 2x_{2,4} + 2x_{2,16} + x_{2,2} \quad (5.17)$$

$$5x'_3 = x_{3,5} + x_{3,19} + x_{3,7} + x_{3,17} + x_{3,10} \quad (5.18)$$

$$5x'_4 = x_{6,6} + 2x_{6,24} + 2x_{6,18} \quad (5.19)$$

$$5x'_5 = 2x_{8,11} + 2x_{8,20} + x_{8,8} \quad (5.20)$$

$$5x'_6 = x_{9,12} + x_{9,22} + x_{9,13} + x_{9,21} + x_{9,14} \quad (5.21)$$

For equations (5.16), (5.17), (5.19) and (5.20), the number of possible solutions is now found as the denominator $D_V(5x'_i; 1, 2, 2)$. As seen for $m = 1$ ($V_m = \{0, 1\}$), only the number of symmetric solutions contributes to the probability of finding a symmetric solution to the problem. Taking $m = 2$, a significant proportion of the possible solutions can be mapped to equivalent symmetric solutions. However, as m increases $D_V(5x'_i; 1, 2, 2)$ decreases proportionally to the total number of solutions, decreasing the probability of finding an asymmetric solution which can be mapped to an equivalent symmetric solution. This probability can be seen in figures 5.17 and 5.18. The first of these figures shows the combination probability for equations (5.16), (5.17), (5.19) and (5.20), against the same probability for equations (5.18), (5.21). The second shows the total probability for all vectors x_i . Note that the asymptotic convergence to $\frac{1}{n^2}$ no longer occurs.

A surprising result follows: given this type of symmetry, the larger the discrete group from which variables can be taken, the smaller the probability of being able to find a symmetric solution which is optimal, however this probability is non-zero.

5.7 Conclusions and discussion

In this paper we have proven and demonstrated in the examples, that, given a binary topology problem of the type discussed above, no symmetric solution necessarily exists. The number of design variables and degree of symmetry play important parts in the probability of finding symmetric solutions in discrete problems. We have shown that as the size of the discrete design set increases, this probability does not tend to 1, but instead to values related to the group symmetry itself. For certain types of symmetry the size of the discrete set is only important for small values of m near to 1. However, the probability will decrease significantly with increasing design set size for certain types of symmetry. The examples demonstrate that the probability of achieving symmetric results to discrete symmetric problems remains very low, even when the design set is very large.

These conclusions emphasize an important fact: it is not reasonable to assume that symmetric problems will lead to symmetric results when the variables are discrete. This calls into question the practice of reducing the problem size in discrete optimization by taking symmetry into account. In the examples, the asymmetric solutions performed significantly better compared to the best symmetric solutions. The authors believe that the evidence suggests that there is some room for discussion on this front. It is the hope that a relaxing of this assumption may lead to more efficient and elegant designs in practice. The investigation has focussed on topology optimization, however, it is easily extendible to other kinds of discrete optimization.

Bibliography

- [1] W. Achtziger and M. Stolpe. Truss topology optimization with discrete design variables—guaranteed global optimality and benchmark examples. *Structural and Multidisciplinary Optimization*, 34(1):1–20, 2007.
- [2] Y. Bai, E. Klerk, D. Pasechnik, and R. Sotirov. Exploiting group symmetry in truss topology optimization. *Optimization and Engineering*, 10(3):331–349, 2008.
- [3] K. Balasubramanian. Graph theoretical perception of molecular symmetry. *Chemical Physics Letters*, 232(56):415 – 423, 1995.
- [4] M.P. Bendsøe and O. Sigmund. *Topology optimization: theory, methods, and applications*. Springer, 2003.
- [5] G. Cheng and X. Liu. Discussion on symmetry of optimum topology design. *Structural and Multidisciplinary Optimization*, pages 1–5, 2011.
- [6] K. Deb and S. Gulati. Design of truss-structures for minimum weight using genetic algorithms. *Finite Elements in Analysis and Design*, 37(5):447–465, 2001.
- [7] A. Evgrafov. On globally stable singular truss topologies. *Structural and Multidisciplinary Optimization*, 29:170–177, 2005.
- [8] X. Guo, C. Ni, G. Cheng, and Z. Du. Some symmetry results for optimal solutions in structural optimization. *Structural and Multidisciplinary Optimization*, pages 1–15, 2012.
- [9] M. Hamermesh. *Group theory and its application to physical problems*. Dover books on physics and chemistry, Dover Publications, 1989.
- [10] T.J. Healey. A group-theoretic approach to computational bifurcation problems with symmetry. *Computer Methods in Applied Mechanics and Engineering*, 67(3):257 – 295, 1988.
- [11] K. Ikeda and K. Murota. Bifurcation analysis of symmetric structures using block-diagonalization. *Computer Methods in Applied Mechanics and Engineering*, 86:215–243, March 1991.
- [12] R.D. Kangwai, S.D. Guest, and S. Pellegrino. An introduction to the analysis of symmetric structures. *Computers & Structures*, 71(6):671–688, 1999.
- [13] A. Kaveh and M. Nikbakht. Analysis of space truss towers using combined symmetry groups and product graphs. *Acta Mechanica*, 218:133–160, 2011.
- [14] A. Kaveh, M. Nikbakht, and H. Rahami. Improved group theoretic method using graph products for the analysis of symmetric-regular structures. *Acta Mechanica*, 210:265–289, 2010.
- [15] U. Kirsch. On singular topologies in optimum structural design. *Structural and Multidisciplinary Optimization*, 2(3):133–142, 1990.
- [16] I. Kosaka and C.C. Swan. A symmetry reduction method for continuum structural topology optimization. *Computers & Structures*, 70(1):47 – 61, 1999.
- [17] J.W. Leech. How to use groups. *American Journal of Physics*, 38:273–273, 1970.
- [18] J. Øystein and J.A. Sellers. Partitions with parts in a finite set. *International Journal of Number Theory*, 2(3):455–468, 2006.
- [19] J.D. Renton. On the stability analysis of symmetrical frameworks. *Quarterly Journal of Mechanics and Applied Mathematics*, 17:175–197, 1964.
- [20] J.N. Richardson, S. Adriaenssens, Ph. Bouillard, and R. Filomeno Coelho. Multiobjective topology optimization of truss structures with kinematic stability repair. *Structural and Multidisciplinary Optimization*, 2012. In press.
- [21] J.N. Richardson, S. Adriaenssens, Ph. Bouillard, and R. Filomeno Coelho. Symmetry and asymmetry of solutions in discrete variable structural optimization. *Structural and Multidisciplinary Optimization*, 47(5):631–643, 2013.
- [22] G.I.N. Rozvany. On symmetry and non-uniqueness in exact topology optimization. *Structural and Multidisciplinary Optimization*, pages 1–21, 2010.

- [23] G.I.N. Rozvany and T. Birker. On singular topologies in exact layout optimization. *Structural and Multidisciplinary Optimization*, 8:228–235, 1994.
- [24] M. Stolpe. On some fundamental properties of structural topology optimization problems. *Structural and Multidisciplinary Optimization*, 41(5):661–670, 2010.
- [25] K. Svanberg. On local and global minima in structural optimization. In E. Atrek, R. H. Gallagher, K. M. Ragsdell, and O. C. Zienkiewicz, editors, *New directions in optimal structural design*. John Wiley and Sons, 1984.
- [26] A. Zingoni. Group-theoretic exploitations of symmetry in computational solid and structural mechanics. *International Journal for Numerical Methods in Engineering*, 79(February):253–289, 2009.
- [27] A. Zingoni, M.N. Pavlovic, and G.M. Zlokovic. Application of group theory to the analysis of space frames. In GAR Parke and CM Howard, editors, *Space Structures*, pages 1334–1347. Thomas Telford: London, 1993.
- [28] A. Zingoni, M.N. Pavlovic, and G.M. Zlokovic. A symmetry-adapted flexibility approach for multi-storey space frames: eneral outline and symmetry-adapted redundants. *Structural Engineering Review*, 7(2):107–119, 1995.
- [29] Đ. Zloković. *Group theory and G-vector spaces in structures: vibrations, stability, and status*. Ellis Horwood series in civil engineering. E. Horwood, 1989.

Chapter 6

Structural optimization under uncertainty

Uncertainties play a vital role in engineering practice and are often accounted for using concepts such as safety factors. While these coefficients provide a reliable margin, they are generally overly conservative and do not meet the needs of optimization procedures, which are also interested in the sensitivity of optimal solutions to perturbation, the robustness of solutions. Deterministic structural optimization is a well established academic field, however, uncertainties on structural optimization problems are a relatively new branch of research. In real-world structures uncertainty exists on material properties, manufacturing tolerances and loading of structures and these can have significant impact on the performance of the structures designed using an optimization procedure. Consider the truss structure in figure 6.1(a) with deterministic loading and accompanying topology optimization solution in figure 6.1(b). From the point of view of the deterministic loading this structure may be the optimal solution, however it is completely unacceptable from a real-world perspective, since any lateral loading on the node will result in unacceptably large displacements. If some uncertainty on the direction of the loading is introduced (figure 6.1(c)), a completely different solution will be found, such as that shown in figures 6.1(d) or in the bridge structure in figure 6.2. The goal of the paper in this chapter is to address robust topology optimization of both continuum and truss-like structures, in a common framework, taking material uncertainties into account. Derivation of the gradients of the objective function are given in appendix A.

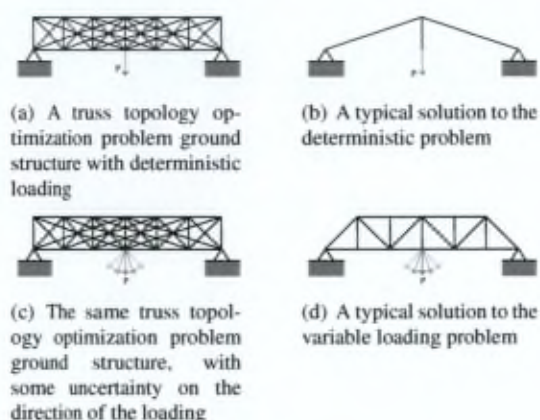


Figure 6.1: Truss topology optimization problems with deterministic and variable loading



Figure 6.2: The Millennium Bridge over the River Liffey, Dublin, Ireland. Image courtesy of William Murphy

A unified stochastic framework for robust topology optimization of continuum and truss-like structures¹

Abstract

In this paper a framework is introduced for robust structural topology optimization for 2D and 3D continuum and truss problems. The uncertain material parameters are modelled using a spatially correlated random field which is discretized using the Karhunen-Loève expansion. Spectral stochastic finite element method is used, with a polynomial chaos expansion to propagate uncertainties on the material characteristics to the response quantities. In continuum structures either 2D or 3D random fields are modelled across the structural domain, while representation of the material uncertainties in linear truss elements is achieved by expanding 1D random fields along the length of the elements. Several examples demonstrate the method on both 2D and 3D continuum and truss structures, showing that this common framework provides an interesting insight on robustness vs. optimality for the test problems considered.

6.1 Introduction

This research focusses on a novel robust structural topology optimization method for 2D and 3D continuum and truss problems. Structural optimization taking uncertainties into account is of significant importance to designers, since real-world structures require both efficient use of material and accurate modelling of material properties, manufacturing tolerances and loading of structures. When considering candidate designs, engineers are concerned with the sensitivity of the designs to small variations which can be quantified as uncertainties. Uncertainties play an important role in engineering practice and are often accounted for using coefficients such as safety factors. While these coefficients provide a reliable margin, they do not

meet the needs of optimization procedures, which should also account for the sensitivity of optimal solutions to perturbation, measured via the concept of robustness. Robust design optimization offers an approach for taking these uncertainties into account, and expressing the sensitivity of the structural responses to variations along with the mean response.

The limited number of approaches to take these uncertainties into account in structural optimization are summarized in overviews by Tsompanakis et al. [23] and Schueller and Jensen [16]. To the authors' knowledge, no common frameworks exist for robust optimization of both continuum and truss structures. The majority of the structural optimization studies accounting for uncertainty are concerned with shape optimization, while only a few studies deal with uncertainties in topology optimization.

The limited number of works on the subject have been completed in the last decade or so, mostly focussing on random loading in continuum structural optimization. De Gournay et al. [5] used a level set (LS) approach to shape and topology optimization minimizing the 'worst case' compliance under perturbation of the loading. Kogiso et al. [11] used the homogenization approach for a sensitivity-based robust topology optimization (RTO) for compliant mechanisms, considering random variation on the loading direction. Conti et al. [4] formulated a LS-based shape optimization method under stochastic loading, making use of a two-stage stochastic programming approach. Lógó et al. [12] developed a new loading criterion for compliance minimization for probabilistic loading, and extended this to uncertainties on the loading location [13].

Several works on taking geometric uncertainty into account in continuum structures have recently been completed. Seepersad et al. [17] focus on designing mesoscopic material topology, where imperfections due to the manufacturing process are of great importance. Guest and Igusa [8] used a mean compliance formulation under uncertainties

¹J.N. Richardson, R. Filomeno Coelho, and S. Adriaenssens. A unified stochastic framework for robust topology optimization of continuum and truss-like structure. *Computers & Structures*, 2013. Submitted for publication

on the nodal locations. Wang et al. [24] demonstrated a method for robust topology optimization applied to photonic waveguides using SIMP, with manufacturing uncertainties, by approximation by the threshold projection method.

The integration of material uncertainties in continuum robust structural optimization has also been addressed very recently in several publications. Chen et al. [3] proposed a LS based robust shape and topology optimization (RSTO) method, taking material uncertainties into account. Important work has very recently been done on robust shape and topology optimization of two dimensional structures [22] for mass minimization, using a polynomial chaos approach. 3D structures appear to have not been dealt with broadly, with the exception of [3].

The representation of uncertainties in robust optimization of truss structures has also been relatively neglected and investigations thus far have failed to take some key features of trusses, such as element length, into account. Yonekura and Kanno [25] used semidefinite programming to solve truss robust topology problems with uncertainties on loading, while Kang and Bai [10] recently considered bounded uncertainties in truss structures. Asadpoure et al. [1] developed a robust formulation for mass minimization of truss structures with uncertainties on the material properties.

All of these methods use an adaptation of a deterministic optimization algorithm to incorporate uncertainties, either choosing to deal with only continuum or only truss-like structures.

Starting from these considerations the remainder of the paper is ordered as follows: modelling of uncertainties is introduced in section 6.2, with the adaptation specifically for topology optimization considered in section 6.3. Computational examples of this method follow (section 6.4) and a discussion and suggestions for further work is then given (section 6.5).

6.2 Modelling of uncertainties for continuum and truss-like structures

In this investigation the material uncertainties are expressed in terms of a spatially varying random field, which is discretized using a Karhunen-Loève (KL) expansion. Random fields allow for expression of spatially correlated random quantities,

while being general enough to model uncorrelated quantities too. Spectral Stochastic Finite Element Method (SSFEM) [20] is used to derive the statistical measures of the response, allowing for a quantification of the terms of the objective function (a linear combination of the mean and standard deviation of the compliance), for a given volume fraction. Material models are generally expressed in terms of Gaussian or lognormal probability distributions, both of which can be taken into account in the SSFEM framework. In continuum structures the random field may be correlated over the entire domain, while in truss structures this is not the case; therefore, a novel analysis method for modelling the variation of material properties along the length of individual truss elements is developed, based on the SSFEM framework, and used for topology optimization of truss structures. Derivations of the objective function and the sensitivities necessary for the optimization procedure are demonstrated, making use of the response quantities. SSFEM discretization consists of series expansion of realizations of the original random field $H(\mathbf{x}, \theta)$ over a complete set of deterministic functions [20], where θ is a vector of random variables. The obtained series are then truncated after finite number of terms. Various discretization methods are available of which the Karhunen-Loève expansion (KL) is the most efficient in terms of the number of random variables required for a given accuracy [20], making it a good candidate for the computationally expensive task of design optimization. A Gaussian random field $H(\mathbf{x}, \theta)$ can be expanded as follows:

$$H(\mathbf{x}, \theta) = \mu(\mathbf{x}) + \sum_{i=1}^{\infty} \sqrt{\lambda_i} \xi_i(\theta) \phi_i(\mathbf{x}) \quad (6.1)$$

where $\mu(\mathbf{x})$ is the mean value of the random phenomenon, λ_i 's and ϕ_i 's respectively the eigenvalues and eigenfunctions of the covariance kernel, and ξ_i 's the random variables. The approximated field \hat{H} can be found by truncating terms above some value M , defined for example through a so-called energy criterion (viz. a minimum percentage of the L2-norm of the approximated field should be preserved):

$$\hat{H} = \mu(\mathbf{x}) + \sum_{i=1}^M \sqrt{\lambda_i} \xi_i(\theta) \phi_i(\mathbf{x}) \quad (6.2)$$

Truss analysis accounting for material property uncertainty is often achieved by associating a random

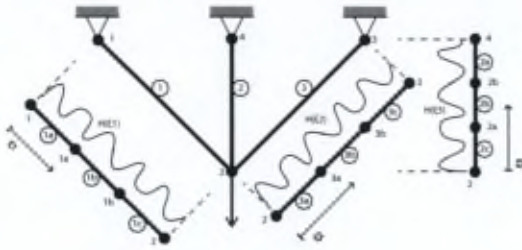


Figure 6.3: Truss element-level 1D random fields

variable with a the cross section area of each bar element [1, 15]. This approach has two fundamental shortcomings:

1. The approach presupposes a small scale for the problem, while trusses and individual truss elements are typically large in scale, and
2. the relative lengths of the elements are neglected in the probabilistic model.

At the scale of truss elements, often several meters in length, the variability of material properties along the length of the element can be very significant, spatially correlated quantities. Global 2D and 3D correlated random fields are not appropriate for modelling this variability, since no correlation exists between the material properties of separate elements. The proposed approach constructs individual 1D random fields across the individual truss elements, subdividing elements into segments. The compliance analysis and topology variables apply to the truss scale elements and nodes (figure 6.3). If each element is substructured as shown in figure 6.3, a simple expression can be found to approximate the relative stiffness of the element as a whole, based on sampling the element-level field:

$$\hat{H}_e = \frac{1}{\sum_{j=1}^{N_{se}} \left(\mu_j(\mathbf{x}_j) + \sum_{i=1}^M \sqrt{\lambda_i} \xi_i(\theta) \phi_i(\mathbf{x}_j) \right)} \quad (6.3)$$

where \hat{H}_e is the element-level random field, μ_j is the mean value of the random field for sub-element j , and N_{se} is the total number of sub-elements. Since $\mu_j(\mathbf{x}_j)$ is constant for the element e , the following expression results:

$$\hat{H}_e = \mu(\mathbf{x}) + \sum_{i=1}^M \frac{\sqrt{\lambda_i} \xi_i(\theta)}{\sum_{j=1}^{N_{se}} \frac{1}{\phi_j(\mathbf{x}_j)}} \quad (6.4)$$

The remainder of the method is analogous to the continuum case.

6.3 Introducing uncertainties for robust topology optimization

6.3.1 Deterministic continuum topology optimization with the SIMP method

An important aspect of robust optimization consists in the modelling of the uncertainties to be included in the analysis portion of the optimization process. For this purpose a good understanding of the deterministic method (in this case SIMP) to be adapted to account for uncertainties is imperative. A classical way to state the (single objective) optimization problem is the minimization of some function f (the objective function) of the design variables \mathbf{x} , subject to some constraints g and h :

$$\begin{aligned} \min_{\mathbf{x}} f(\mathbf{x}) \\ \text{subject to: } \begin{cases} g(\mathbf{x}) \leq 0 \\ h(\mathbf{x}) = 0 \end{cases} \end{aligned} \quad (6.5)$$

In the case of compliance minimization the objective function can be written as follows:

$$f(\mathbf{x}) = C = \mathbf{f}^T \mathbf{u} \quad (6.6)$$

where \mathbf{f} is the external loading on the structure and \mathbf{u} the nodal displacements. Typically the volume of the structure is constrained:

$$\frac{V(\mathbf{x})}{V_0} - c = 0 \quad (6.7)$$

where $V(\mathbf{x})$ and V_0 are respectively the volume of a design and the reference volume (the fraction of these quantities is called the volume fraction), and c is some constant chosen by the designer. The design variables $\mathbf{x} = [x_1 \ x_2 \ \dots \ x_e \ \dots \ x_N]$ are scalars associated with element e where $e = 1 \dots N$ and N is the number of elements in the finite element mesh. For continuum problems x_e is a coefficient of the density of the element such that $x_{e,min} \leq x_e \leq 1$. SIMP has been exceedingly successful and implemented in numerous papers [2, 6, 19]. Using the SIMP formulation, the element stiffness matrix can be written as $\mathbf{K}_e = x_e^p \mathbf{K}_e^*$, where \mathbf{K}_e^* is the

stiffness matrix with density equal to the standard material density, and p is a penalty value chosen by the user (often taken as 3 for continuum structures) [19]. When truss structures are considered this type of penalization can be neglected by setting $p = 1$. The SIMP compliance objective function (6.6) and sensitivities are then calculated as follows:

$$C(\mathbf{x}) = \sum_{e=1}^N (x_e)^p \mathbf{u}_e^T \mathbf{K}_e \mathbf{u}_e. \quad (6.8)$$

$$\frac{\partial C}{\partial x_e} = -p(x_e)^{p-1} \mathbf{u}_e^T \mathbf{K}_e \mathbf{u}_e. \quad (6.9)$$

Restrictions on the design space for continuum structures are essential for dealing with questions of existence of solutions [19]. Sigmund [18] introduced a mesh independency filtering technique which modifies the element sensitivities. Another method for ensuring existence of solutions was introduced by Guest et al. [9] using a minimum length scale.

6.3.2 Principle of the spectral stochastic finite element method

In the SIMP approach the element stiffness matrix \mathbf{K}_e can then be written as:

$$\mathbf{K}_e(\theta) = \mathbf{K}_{e,0} + \sum_{i=1}^M \xi_i(\theta) \sqrt{\lambda_i} \int_{\Omega_e} \boldsymbol{\varphi}_i(\mathbf{x}) \mathbf{B}^T \mathbf{D}_0 \mathbf{B} d\Omega_e \quad (6.10)$$

where $\mathbf{K}_{e,0}$ is the deterministic element stiffness matrix, \mathbf{B} is the matrix that relates the components of strain to the element nodal displacements, and \mathbf{D}_0 the deterministic elasticity matrix. Assembling matrices $\mathbf{K}_{e,i} = \sqrt{\lambda_i} \int_{\Omega_e} \boldsymbol{\varphi}_i(\mathbf{x}) \mathbf{B}^T \mathbf{D}_0 \mathbf{B} d\Omega_e$ to their global form \mathbf{K}_i over the structural domain Ω_e , the equilibrium equation becomes:

$$\left(\mathbf{K}_0 + \sum_{i=1}^M \mathbf{K}_i \xi_i(\theta) \right) \mathbf{u}(\theta) = \mathbf{f} \quad (6.11)$$

Modelling of the response to a random process requires an expansion in which the covariance function need not be explicitly known [7]. The PCE assumes the random displacements $u(\theta)$ can be expanded as follows:

$$u(\theta) = \sum_{j=0}^{P-1} u_j \Psi_j(\theta) \quad (6.12)$$

where the set $\{\Psi_j\}$, $j = 0 \dots \infty$, is a set of orthogonal polynomials in ξ_k , and $k = 0 \dots \infty$. Truncating terms in equation (6.11) and substituting equation (6.12):

$$\left(\sum_{i=0}^M \mathbf{K}_i \xi_i(\theta) \right) \left(\sum_{j=0}^{P-1} \mathbf{u}_j \Psi_j(\theta) \right) = \mathbf{f} \quad (6.13)$$

A more convenient form of equation (6.13) can be found by minimizing the residual due to truncation, arriving at the following form:

$$\begin{bmatrix} \mathbf{K}_{0,0} & \dots & \mathbf{K}_{0,P-1} \\ \vdots & \ddots & \vdots \\ \mathbf{K}_{P-1,0} & \dots & \mathbf{K}_{P-1,P-1} \end{bmatrix} \begin{bmatrix} \mathbf{u}_0 \\ \vdots \\ \mathbf{u}_{P-1} \end{bmatrix} = \begin{bmatrix} \mathbf{f}_0 \\ \vdots \\ \mathbf{f}_{P-1} \end{bmatrix} \quad (6.14)$$

where $\mathbf{K}_{i,j}$ is an $N \times N$ matrix, \mathbf{u}_i are $N \times 1$ vectors associated with the polynomial expansion of the response, and \mathbf{f}_i are $N \times 1$ vectors of loading. Note that the system to be inverted is $NP \times NP$ in size, so that the size of the PCE expansion will have a significant impact on the computational cost of the solution. The details of this and other derivations can be found in [20].

6.3.3 Stochastic finite element method for uncertainty propagation in topology optimization

The robust form of the compliance objective function is commonly expressed as the weighted sum of the two statistical measures, namely the mean and standard deviation:

$$\min_{\mathbf{x}} \hat{C} = E[C] + \alpha \sqrt{\text{Var}[C]} \quad (6.15)$$

where $E[C]$ is the expected value of the compliance, $\text{Var}[C]$ the variance of the compliance and α is a weighting coefficient chosen by the user. If the loading is deterministic the mean value (expectancy) of the compliance is given by:

$$E[C] = E[\mathbf{f}^T \mathbf{u}] = \mathbf{f}_0^T E[\mathbf{u}] \quad (6.16)$$

In the case of a PCE of the response $E[\mathbf{u}] = \mathbf{u}_0$, where \mathbf{u}_0 corresponds to the nodal displacements for polynomial Ψ_0 . Finally:

$$E[C] = \mathbf{f}_0^T \mathbf{u}_0 \quad (6.17)$$

Once again considering deterministic loading, the variance of the compliance can be found:

$$\text{Var}[C] = \text{Var}[\mathbf{f}^T \mathbf{u}] = \mathbf{f}_0^T \text{Cov}[\mathbf{u}] \mathbf{f}_0 \quad (6.18)$$

where $Cov[\mathbf{u}]$ is the covariance matrix of \mathbf{u} , and is found by the expression [20]:

$$Cov[\mathbf{u}] = \sum_{j=1}^{P-1} E[\Psi_j^2] \mathbf{u}_j \mathbf{u}_j^T \quad (6.19)$$

where Ψ_j are the components of the polynomial basis of the displacement field corresponding to displacement vectors \mathbf{u}_j . The objective function can then be expressed simply as:

$$\hat{C} = \mathbf{f}_0^T \mathbf{u}_0 + \alpha \mathbf{f}_0^T \left(\sum_{j=1}^{P-1} E[\Psi_j^2] \mathbf{u}_j \mathbf{u}_j^T \right) \mathbf{f}_0 \quad (6.20)$$

The sensitivities of the objective function with respect to the design variables \mathbf{x} are found making use of the adjoint method, starting from equation (6.15) and taking the derivative with respect to the design variables (6.15) as in [1]:

$$\frac{\partial \hat{C}}{\partial \mathbf{x}} = \frac{\partial E[C]}{\partial \mathbf{x}} + \alpha \frac{\partial (\sqrt{Var[C]})}{\partial \mathbf{x}} \quad (6.21)$$

The sensitivities at the element level, as prescribed by the SIMP method, can then be found as follows:

$$\begin{aligned} \frac{\partial \hat{C}_e}{\partial x_e} = & -p x_e^{p-1} \left(\sum_{k=0}^{P-1} \sum_{l=0}^{P-1} \sum_{i=0}^M E[\xi_i \Psi_k \Psi_l] \mathbf{u}_{e,k}^T \mathbf{K}_e^* \mathbf{u}_{e,l} \right) \\ & - \frac{\alpha p x_e^{p-1}}{\sqrt{Var[C]}} \sum_{j=1}^{P-1} \left(\sum_{k=0}^{P-1} \sum_{l=0}^{P-1} \sum_{i=0}^M E[\xi_i \Psi_j \Psi_k \Psi_l] \mathbf{u}_{e,k}^T \right. \\ & \left. \mathbf{K}_e^* \mathbf{u}_{e,l} \right) \mathbf{u}_j^T \mathbf{f}_0 \end{aligned} \quad (6.22)$$

The above expression is very similar to the expression for the displacement constraints as found by [22].

6.4 Computational examples

The proposed method is demonstrated on a number of test problems: a 2D cantilever, a 3D bridge structure and a 2D truss problem. It should be noted that a 3D truss example would be almost equivalent to the 2D case and is therefore omitted for the sake of brevity.

Recalling the parameters associated with the uncertainty quantification, results are shown for varying values of the standard deviation σ and correlation lengths l_i of the random field in dimension i , as well as the additive coefficient in the objective function α . For all computational examples

the order of the polynomial chaos expansion of the responses is taken to be $P = 2$. The method of moving asymptotes [21] was used to solve the optimization problem in the computational examples.

6.4.1 2D Continuum cantilever

Problem

In this problem a 2D cantilever structure is considered. The domain is discretized using 100×30 2D quad elements, $r_{min} = 1.5$, the penalization constant $p = 3$, and the volume fraction $V_0 = 0.5$. The problem domain, supports and loading are shown in figure 6.4(a). A fourth-order ($M = 4$) KL expansion was used to discretize the lognormal random field representing the uncertain Young's modulus of the material, with unit mean value. The correlation length of this field was taken to be $l_x = 20$ spatial units in the x-direction and $l_y = 10$ in the y-direction. A vertical unit load was applied at the tip of the cantilever, and a clamped boundary condition applied at the other edge of the domain.

Results

The deterministic solution to this problem is shown in figure 6.4(b). In table 6.1 an overview of the solutions to the problem are given, for values of σ between 0.2 and 0.4, and α between 3 and 9. The plot showing the objective function values is given in figure 6.5. Linear regression analysis shows a perfect linear relation, with $R^2 = 1$, in all of the optimal solutions α for constant values of σ . Clear differences in topology can be seen, particularly for lower values of α . When α increases above 5, the topology remains similar, although the shape changes between the various solutions.

The lognormal material uncertainties have introduced an asymmetry in the solutions which is not observed if the same problem is run with Gaussian random field properties. Similarly, for a small value of the field expansion ($M = 2$), this asymmetry is not observed. Sufficiently high order truncation of the field is necessary to capture the true behaviour of the randomness. The analysis results were confirmed using Monte Carlo simulations to approximate first and second order responses of the system. The compliance statistics for one of the problems were calculated, and normalized relative to the SSFEM results and the results are shown in table 6.2. The results show good agreement,

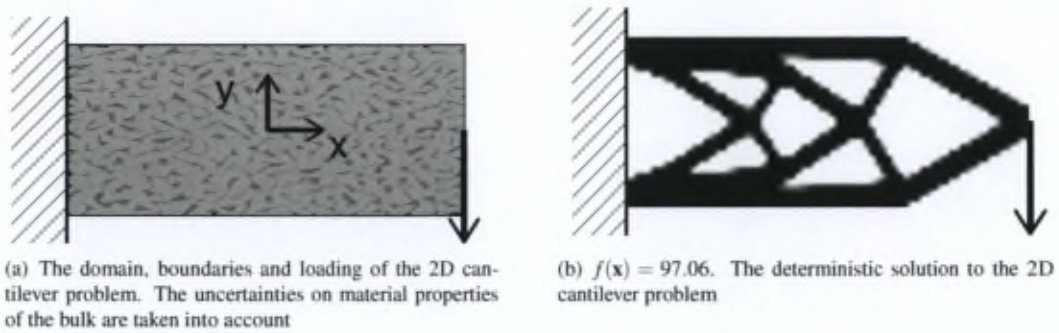


Figure 6.4: 2D cantilever problem. Problem set up and deterministic solution













α	$\sigma = 0.2$	$\sigma = 0.3$	$\sigma = 0.4$
3	 $f(\mathbf{x}) = 123.28$	 $f(\mathbf{x}) = 138.41$	 $f(\mathbf{x}) = 154.81$
5	 $f(\mathbf{x}) = 139.34$	 $f(\mathbf{x}) = 162.54$	 $f(\mathbf{x}) = 187.72$
7	 $f(\mathbf{x}) = 155.22$	 $f(\mathbf{x}) = 186.86$	 $f(\mathbf{x}) = 220.6$
9	 $f(\mathbf{x}) = 171.12$	 $f(\mathbf{x}) = 211.38$	 $f(\mathbf{x}) = 253.82$

Table 6.1: 2D cantilever problem. Resulting topologies for various values of the standard deviation σ and the factor α

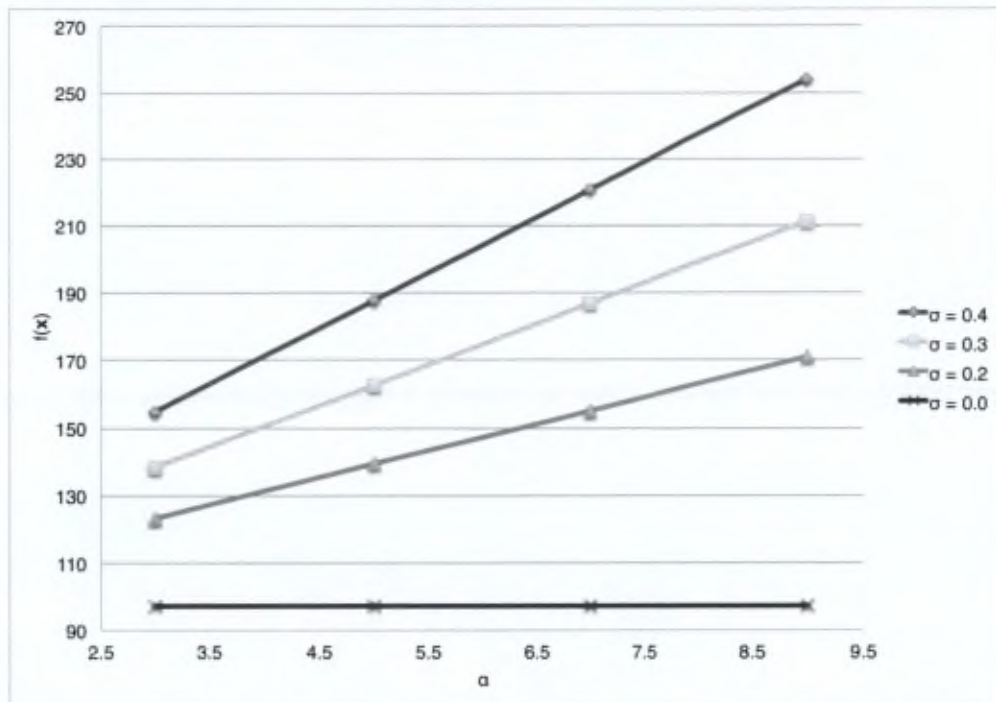


Figure 6.5: 2D cantilever problem. Plot of the objective function values for various values of α and $f(\mathbf{x})$

even for the small number of Monte Carlo simulations considered.

6.4.2 3D Continuum bridge

Problem

In this example the 3D domain is defined as shown in figure 6.6(a). The structural domain is discretized using $80 \times 10 \times 20$ 8-node brick elements, loaded by a single unit point load in the center of the top face, and is simply supported at the 4 lower corners. Symmetry is used to reduce the problem size. For all of the solutions that follow, the volume fraction is $V_0 = 0.2$, $r_{min} = 2.5$, $\alpha = 7$, $\mu = 1$, and $p = 3$ penalization is used. The standard deviation and correlation lengths are varied.

Results

The deterministic solution is shown in figure 6.6(b), while the resulting topologies for various values of the parameters σ and l are shown in figure 6.7. For small values of σ only minor variation is visible. Note that for all the non-deterministic solutions the main arch of the structure is split in

Simulations	μ	σ
SSFEM	1	1
100 MC	0.9991	1.0094
1000 MC	1.0004	1.0038

Table 6.2: Comparison of SSFEM and Monte Carlo results for compliance statistics for the 2D cantilever problem



Figure 6.7: 3D bridge problem. Resulting topologies for various values of the standard deviation σ and the correlation length l

two, meeting only at the loading point, while a single arch characterizes the deterministic solution. Another prominent difference is the topology of the middle struts in the truss-like continua resulting from the optimization process. In several of the structures these struts are separate on either side of the bridge deck, however, with higher values of σ the two struts merge into one, splitting apart near the bottom. In profile it can be seen that the general shape of the arch is more rounded for higher values of l .

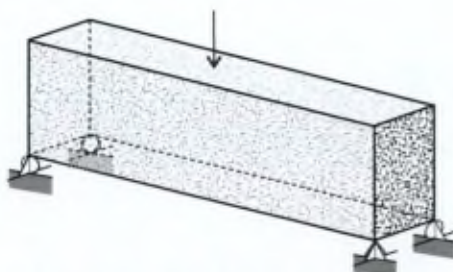
6.4.3 2D truss problem

Problem

A 2D truss problem, similar to that found in [8] is used to demonstrate the method. This problem consists of 25 nodes, each connected to every other node by a bar element, 300 elements in total. The nodes are spaced one unit apart in the x -direction and $\frac{4}{3}$ units apart in the y -direction. The structure is simply supported at two bottom corner nodes and loaded along the bottom edge of the structure by unit vertical loads (figure 6.8(a)). The elements are subdivided into 5 segments and a volume fraction of $V_0 = 0.05$ is taken as a constraint on the problem. No filtering or penalization ($p = 1$) is applied to truss problems. A 3rd-order KL expansion is used to discretize the random field.

Results

The deterministic solution to the problem is shown in figure 6.8(b). The solutions for various values of the standard deviation and α -coefficient are given in figure 6.9. The values of the objective functions are plotted for various values of the α and σ , for $l = 0.5$ in figure 6.10(a). A linear relation can be seen between the various solutions, as expected. If these solutions are compared to the same plot for $l = 0.1$ (figure 6.10(b)), it can clearly be seen that the value of the correlation length has an effect on the dispersion of the solutions in the function space. This demonstrates the importance of considering this property in truss problems, something that can only be achieved by including the random field variations along the length of the elements.



(a) The domain, boundaries and loading of the 3D bridge problem. The uncertainties on material properties of the bulk are taken into account



(b) Deterministic solution to the 3D bridge problem

Figure 6.6: 3D bridge problem. Problem set up and deterministic solution

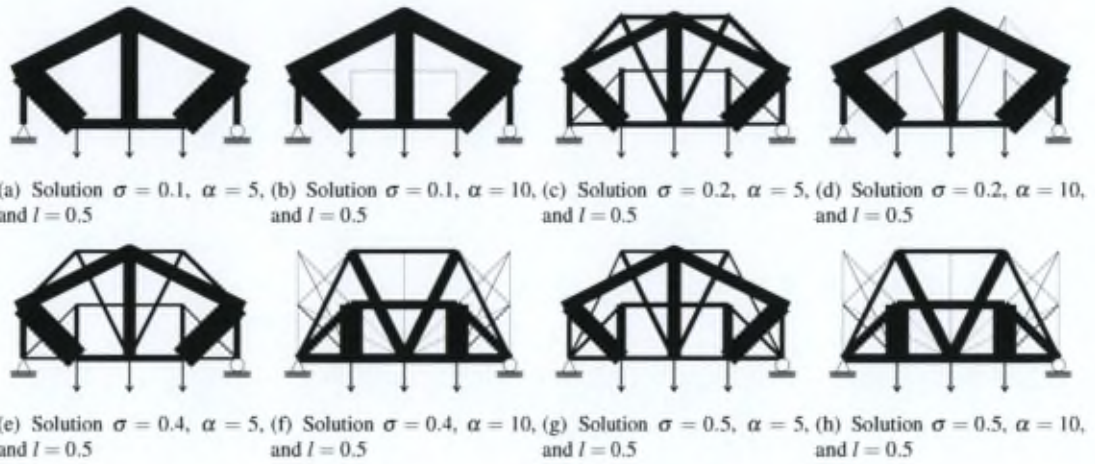
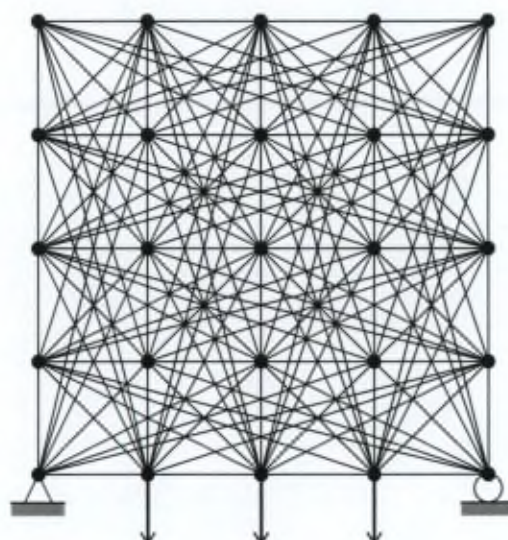


Figure 6.9: 2D truss problem probabilistic solutions

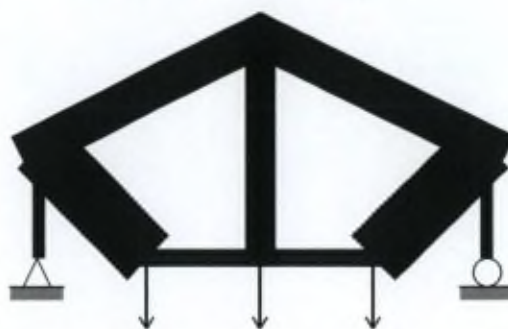
6.5 Conclusions

This research presents a framework for topology optimization of both continuum and truss structures using spectral stochastic finite element method. The analysis method is used to quantify both the material uncertainties, and the variations of the responses required for the compliance objective function. Using these quantities, expressions for both the objective function and the sensitivities of the objective function with regard to the design variables are found. A novel approach to truss analysis is introduced to model material uncertainties across elements of varying lengths. The method is demonstrated on both 2D and 3D continuum examples and on a truss example. The examples clearly show that varying the material parameters has a significant effect on the shape and topology of solutions. Even relatively small values of the standard deviation of the material parameters can have a significant effect on the optimal topologies. Robust topologies tend to be topologically more complex than deterministic ones. Additionally, asymmetries in the robust optimal solutions may be observed when the material stiffness follows a lognormal distribution.

The truss example demonstrates the importance of the correlation length to the solution of the truss optimization problem. This parameter is indicative of the effect of modelling the random field across the entire length of the element. It has been seen that significantly different results are achieved by varying this parameter.



(a) 2D truss problem ground structure



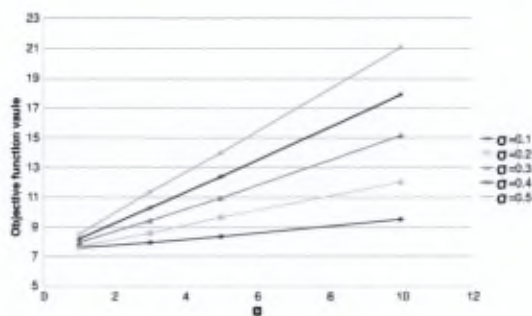
(b) 2D truss problem probabilistic solutions

Figure 6.8: 2D truss problem: Problem set up and deterministic solution

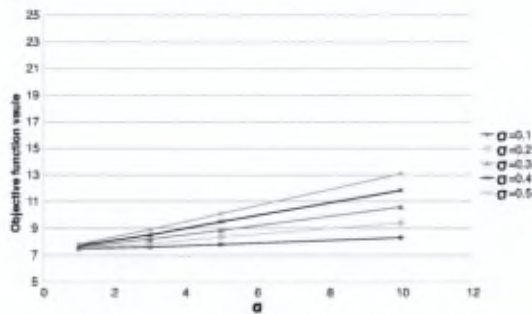
Observing the form of the equilibrium equation, it is clear that the introduction of loading uncertainties can be achieved relatively easily, and without significantly increased computational expense for the analysis.

Bibliography

- [1] A. Asadpoure, M. Tootkaboni, and J.K. Guest. Robust topology optimization of structures with uncertainties in stiffness - application to truss structures. *Computers & Structures*, 89:1131–1141, June 2011.
- [2] M.P. Bendsøe and N. Kikuchi. Generating optimal topologies in structural design using a homogenization method. *Computer Methods in Applied Mechanics and Engineering*, 71(2):197–224, 1988.
- [3] S. Chen, W. Chen, and S. Lee. Level set based robust shape and topology optimization under random field uncertainties. *Structural and Multidisciplinary Optimization*, 41(4):507–524, 2010.
- [4] S. Conti, H. Held, M. Pach, M. Rumpf, and R. Schultz. Shape optimization under uncertainty: A stochastic programming perspective. *SIAM J. on Optimization*, 19:1610–1632, January 2009.
- [5] F. de Gournay, G. Allaire, and F. Jouve. Shape and topology optimization of the robust compliance via the level set method. *Control, Optimisation and Calculus of Variations*, 14(1):43–70, 2007.
- [6] P. Duysinx and M.P. Bendsøe. Topology optimization of continuum structures with local stress constraints. *International Journal for Numerical Methods in Engineering*, 43(8):1453–1478, 1998.
- [7] R. Ghanem and P.D. Spanos. Polynomial chaos in stochastic finite elements. *Journal of Applied Mechanics*, 57(1):197–202, 1990.
- [8] J. Guest and T. Igusa. Structural optimization under uncertain loads and nodal locations. *Computer Methods in Applied Mechanics and Engineering*, 198(1):116–124, 2008.



(a) results for correlation length $l = 0.5$, for various values of σ and α



(b) results for correlation length $l = 0.1$, for various values of σ and α

Figure 6.10: Values of the objective function for various parameters

- [9] J.K. Guest, J.H. Prévost, and T. Belytschko. Achieving minimum length scale in topology optimization using nodal design variables and projection functions. *International Journal for Numerical Methods in Engineering*, 61(2):238–254, 2004.
- [10] Z. Kang and S. Bai. On robust design optimization of truss structures with bounded uncertainties. *Structural and Multidisciplinary Optimization*, 47(5):699–714, 2013.
- [11] N. Kogiso, W. Ahn, S. Nishiwaki, K. Izui, and M. Yoshimura. Robust topology optimization for compliant mechanisms considering uncertainty of applied loads. *Journal of Advanced Mechanical Design, Systems, and Manufacturing*, 2(1):96–107, 2008.
- [12] J. Lógó, M. Ghaemi, and M.M. Rad. Optimal topologies in case of probabilistic loading: The influence of load correlation. *Mechanics Based Design of Structures and Machines*, 37(3):327–348, 2009.
- [13] J. Lógó, D.B. Merczel, and L. Nagy. On optimal topologies for the case of uncertain load positions. *Environmental Engineering*, pages 1–12, 2011.
- [14] J.N. Richardson, R. Filomeno Coelho, and S. Adriaenssens. A unified stochastic framework for robust topology optimization of continuum and truss-like structure. *Computers & Structures*, 2013. Submitted for publication.
- [15] E. Sandgren and T.M. Cameron. Robust design optimization of structures through consideration of variation. *Computers & Structures*, 80(20-21):1605 – 1613, 2002.
- [16] G. Schueller and H. Jensen. Computational methods in optimization considering uncertainties - an overview. *Computer Methods in Applied Mechanics and Engineering*, 198(1):2–13, 2008.
- [17] C.C. Seepersad, J.K. Allen, D.L. McDowell, and F. Mistree. Robust design of cellular materials with topological and dimensional imperfections. *Journal of Mechanical Design*, 128:1285, 2006.
- [18] O. Sigmund. On the design of compliant mechanisms using topology optimization. *Mechanics Based Design of Structures and Machines*, 25(4):493–524, 1997.
- [19] O. Sigmund. A 99 line topology optimization code written in Matlab. *Structural and Multidisciplinary Optimization*, 21(2):120–127, 2001.
- [20] B. Sudret and A. Der Kiureghian. *Stochastic finite element methods and reliability: a state-of-the-art report*. Dept. of Civil and Environmental Engineering, University of California, 2000.
- [21] K. Svanberg. The method of moving asymptotes – a new method for structural optimization. *International Journal for Numerical Methods in Engineering*, 24(2):359–373, 1987.
- [22] M. Tootkaboni, A. Asadpoure, and J.K. Guest. Topology optimization of continuum structures under uncertainty - a polynomial chaos approach. *Computer Methods in Applied Mechanics and Engineering*, 2011.
- [23] Y. Tsompanakis, N.D. Lagaros, and M. Papadrakakis. *Structural Design Optimization Considering Uncertainties*. Structures and Infrastructures Series. Taylor & Francis, 2008.
- [24] F. Wang, J.S. Jensen, O. Sigmund, and N.K. All. Robust topology optimization of photonic crystal waveguides with tailored dispersion properties. *Building*, 17(3):1–33, 2011.
- [25] Kazuo Y. and Yoshihiro K. Global optimization of robust truss topology via mixed integer semidefinite programming. *Optimization and Engineering*, 11(3):355–379, 2010.

Chapter 7

Truss optimization with discrete design variables under uncertainty

In the previous chapter, the concept of robust topology optimization (RTO) was explained. RTO was applied to structural topology optimization on structures with continuous design variables and material stiffness uncertainties. Figure 7.1 shows a series of test samples used to determine the characteristics of a material. As seen in chapters 2, 3, 4 and 5, discrete design variables are of major importance to designers of civil engineering truss-like structures, such as this show in figure 7.2. In this chapter the RTO approach from chapter 6 is extended to uncertainties on both the material stiffness (as discussed in chapter 6) and loading uncertainties, for structures with discrete design variables. Chapter 2 discusses the necessity of multiobjective optimization algorithms, applying genetic algorithms to discrete variable optimization problems of truss-like structures. In this chapter a multiobjective perspective to RTO is introduced in order to address several challenges facing optimizers of civil engineering structures. This chapter can be seen as a synthesis of the various methods discussed in the thesis, containing elements of each of the previous chapters to a greater or lesser extent.

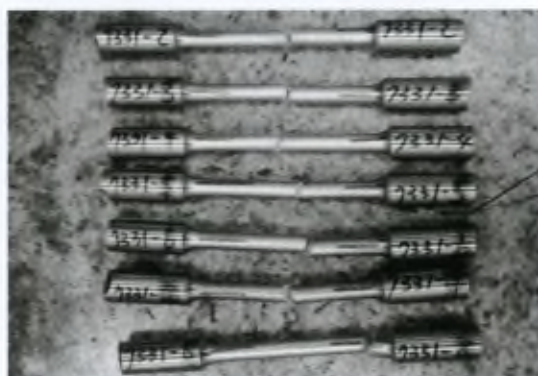


Figure 7.1: Test samples from a series of tension tests to determine the characteristics of the yield stress of a material



Figure 7.2: A truss pedestrian bridge at the Devos Hospital in Grand Rapids, MI, USA, undergoing construction. The loading of the bridge throughout its lifetime is subject to a large amount of random variation. Image courtesy of John Eisenschenk

Robust topology optimization of truss-like structures with random loading and material properties: a multi-objective perspective¹

Abstract

In this paper an approach to robust topology optimization for truss-like structures with material and loading uncertainties, and discrete design variables, is investigated. Uncertainties on the loading direction and magnitude, as well as spatially correlated material stiffness, are included in the problem formulation using spectral stochastic finite element analysis, taking truss element length into account in the uncertainties on the material properties. In this way a more realistic random field representation of the material uncertainties can be achieved, compared to classical scalar random variable approaches. Additionally, a multiobjective approach is used to generate Pareto optimal solutions to the truss optimization problems. In an example it is shown how the mean and standard deviation of the compliance can be considered as separate objectives, avoiding the need for a combination factor which may be difficult to choose correctly in the classical single-objective approach. Further examples considering the mass and deflection of the structure are solved, showing the effects of the novel truss-like structure material modelling on the robust optimal designs.

7.1 Introduction

Structural optimization taking uncertainties into account is of importance to designers, since real-world structures require both efficient use of material and accurate modelling of material properties, manufacturing tolerances and loading of structures. When considering candidate topological designs, engineers are concerned with the sensitivity of the designs to small variations which

can be quantified as uncertainties. In order to address this the concept of robust topology optimization (RTO) has become increasingly important in recent years, incorporating the variability of candidate solutions when considering the efficiency of that solution for dealing with a specific structural problem. In the last decade several important papers focussing on RTO have appeared. Kogiso et al. [13] used a sensitivity-based RTO for compliant mechanisms, with random variation on the loading direction. De Gournay et al. [3] investigated shape and topology optimization for minimal compliance, minimizing the 'worst case' compliance under perturbation of the loading. Guest and Igusa [8] used a mean compliance formulation under uncertainties on the nodal locations, while Lógó et al. [15] developed a new loading criterion for compliance minimization for probabilistic loading, and extended this to uncertainties on the loading location [16]. Chen et al. [2] proposed a robust shape and topology optimization (RSTO) method, taking material uncertainties into account. Tootkaboni et al. [28] developed a robust formulation for mass minimization with uncertainties on the material properties, using a polynomial chaos approach. Wang et al. [29] demonstrated a method for robust topology optimization applied to photonic waveguides, with manufacturing uncertainties. However, in spite of this recent research interest, several issues have been neglected:

1. The representation of random uncertainties in the literature is not always accurate, leading to incorrect quantification of the robustness of solutions.
2. Generally more than one type of uncertainty needs to be considered: material properties, loading, nodal positions, etc. The derivatives required for gradient-based methods become difficult or extremely complicated to define analytically in these circumstances.
3. Robust formulations of the topology opti-

¹J.N. Richardson, R. Filomeno Coelho, and S. Adriaenssens. Robust topology optimization of truss-like structures with random loading and material properties: a multi-objective perspective. *Structural and Multidisciplinary Optimization*, 2013. Submitted for publication

mization problem require a combination of two distinct quantities: mean and standard deviation. Often this is done through a virtually arbitrary linear combination of these response quantities.

4. Truss structures contain bar elements in which the material properties vary along the length of a single element, and therefore cannot be dealt with in the same way as continuum structures.
5. Truss topology optimization problems often require discrete variable formulations [20]. Gradient-based algorithms are often poorly suited for addressing this class of problems.
6. Increasingly designers wish to take more than one objective into account in the optimization of real-world structures.
7. Designers are often concerned with objective functions which are broader than the classical compliance or mass functions. Such objectives generally do not lend themselves to classical gradient-based solutions and multi-objective methods of this kind have not been properly developed.

Starting from these considerations the paper is arranged as follows: the approach to the uncertainty modelling and the optimization approach is given in section 7.2, followed by an explanation of the multiobjective approach in section 7.3. Finally, several examples are given in section 7.4 and conclusions discussed in section 7.5.

7.2 Uncertainty quantification and optimization approach

The representation of uncertainties in robust optimization of truss structures has been relatively neglected and investigations thus far have failed to take some key features of trusses, such as element length, into account. Asadpoure et al. [1] developed a method for RTO of truss structures taking material stiffness uncertainties into account, assigning scalar uncertainties to each cross-section. Yonekura and Kanno [30] used semidefinite programming to solve truss robust topology problems with uncertainties on loading, while Kang and Bai [11] recently considered bounded uncertainties in truss structures.

On the other hand random fields allow for the expression of spatially varying material properties to be taken into consideration, and the stochastic finite element framework allows for integration of these fields into the structural analysis. The mean and standard deviations of the resulting structural responses can be extracted from this analysis and used in the definition of the objective function(s). Within the robust formulation, it is required to take both first order (mean) and second (variance or standard deviation) order statistical moments of the structural response h into account. Generally a single-objective approach is adopted, considering the weighted sum of these two quantities:

$$\min_{\mathbf{x}} f(\mathbf{x}) = E[h(\mathbf{x})] + \alpha \text{Std}[h(\mathbf{x})] \quad (7.1)$$

However, particularly in the case of discrete variable problems, the choice of α may not be evident. For this purpose, it is of interest to consider the statistical moments of the response as separate objectives within a multiobjective framework, as done by Padovan et al. [18] for example.

In this investigation the uncertainties on the Young's modulus are expressed in terms of a spatially varying random field, which is discretized using a Karhunen-Loève (KL) expansion. Random fields allow for expression of spatially correlated random quantities, while being general enough to model uncorrelated quantities too. A novel application of Spectral Stochastic Finite Element Method (SSFEM) [27] is used for truss structures to derive the statistical measures of the response, allowing for a quantification of the terms of the objective functions and constraints. This method was developed by Richardson et al. [22], in which it was discussed how the framework could be extended to allow for introduction of loading uncertainties.

7.2.1 Material uncertainties

Material uncertainties are quantified in terms of probability distributions on values such as the Young's modulus. Material models are generally expressed in terms of Gaussian or lognormal probability distributions, both of which can be taken into account within the SSFEM framework. SSFEM discretization generally consists of series expansion methods, expanding any realization of the original random field $H(\mathbf{x}, \theta)$ over a complete set of deterministic functions [27], where θ is a vector of random variables. The obtained series are then

truncated after a finite number of terms. Various discretization methods are available of which the KL expansion is the most efficient in terms of the number of random variables required for a given accuracy [27]. A Gaussian random field $H(\mathbf{x}, \theta)$ can be expanded as follows:

$$H(\mathbf{x}, \theta) = \mu(\mathbf{x}) + \sum_{i=1}^{\infty} \sqrt{\lambda_i} \xi_i(\theta) \phi_i(\mathbf{x}) \quad (7.2)$$

where $\mu(\mathbf{x})$ is the mean value of the random phenomenon, λ_i 's and ϕ_i 's respectively the eigenvalues and eigenfunctions of the covariance kernel, and ξ_i 's the random variables. The approximated field \hat{H} can be found by truncating terms above some value M :

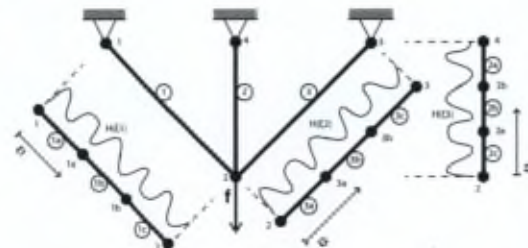
$$\hat{H} = \mu(\mathbf{x}) + \sum_{i=1}^M \sqrt{\lambda_i} \xi_i(\theta) \phi_i(\mathbf{x}) \quad (7.3)$$

In continuum structures the random field may be correlated over the entire domain, however in truss-like structures this is not the case. Truss analysis accounting for material property uncertainty is often achieved by associating a random variable with the cross section area of each bar element. This approach has two fundamental shortcomings:

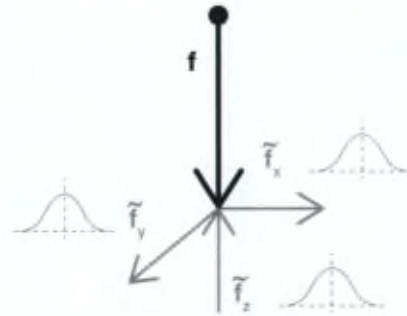
1. The approach presupposes a small scale for the problem, while trusses and individual truss elements are typically large in scale, and
2. the relative lengths of the elements are neglected in the probabilistic model.

At the scale of truss elements, often several meters in length, the variability of material properties along the length of the element can be very significant, spatially correlated quantities. Global 2D and 3D correlated random fields are not appropriate for modelling this variability, since no correlation exists between the material properties of separate elements. The proposed approach constructs individual 1D random fields across the individual truss elements, discretizing elements into sub-divisions. The analysis and topology variables apply to the truss scale elements and nodes (figure 7.3(a)). If each element is subdivided as shown in figure 6.3, a simple expression can be found to approximate the relative stiffness of the element as a whole, based on sampling the element-level field:

$$\hat{H}_e = \frac{1}{\sum_{j=1}^{N_{el}} \left(\mu_j(\mathbf{x}_j) + \sum_{i=1}^M \sqrt{\lambda_i} \xi_i(\theta) \phi_i(\mathbf{x}_j) \right)} \quad (7.4)$$



(a) Truss element-level 1D random fields



(b) Modelling of random loading with deterministic load \mathbf{f} and random components $\tilde{\mathbf{f}}_i$

Figure 7.3: Schematic representation of the uncertainties on the material stiffness and loading magnitude and direction

where \hat{H}_e is the element-level random field, μ_j is the mean value of the random field for sub-division j , and N_{se} is the number of sub-divisions. Since $\mu_j(\mathbf{x}_j)$ is constant for the element e , the following expression results:

$$\hat{H}_e = \mu(\mathbf{x}) + \sum_{i=1}^M \frac{\sqrt{\lambda_i} \xi_i(\theta)}{\sum_{j=1}^{N_{se}} \frac{1}{\varphi_i(\mathbf{x}_j)}} \quad (7.5)$$

The remainder of the analysis method is analogous to the continuum case and was introduced in [22]. The reader is referred to this publication for further details.

7.2.2 Loading uncertainties

It is desirable to quantify the uncertainty on the magnitude and direction of the load applied to the structure. The framework described here allows for loading uncertainties to be introduced directly. The loading uncertainty can be expanded in the polynomial basis as follows, as described in [26]:

$$\mathbf{f} = \sum_{j=0}^{\infty} \mathbf{f}_j \Psi_j \quad (7.6)$$

Practically the uncertainties on the load magnitude and direction can be modelled as additional vectors with random magnitude and fixed direction parallel to the global coordinate system (figure 7.3(b)).

7.2.3 Spectral Stochastic Finite Element Method

The above uncertainties can be combined for the purposes of the analysis, using SSFEM. The element stiffness matrix \mathbf{K}_e can then be written as:

$$\mathbf{K}_e(\theta) = \mathbf{K}_{e,0} + \sum_{i=1}^M \xi_i(\theta) \sqrt{\lambda_i} \int_{\Omega_e} \varphi_i(\mathbf{x}) \mathbf{B}^\top \mathbf{D}_0 \mathbf{B} d\Omega_e \quad (7.7)$$

where $\mathbf{K}_{e,0}$ is the deterministic element stiffness matrix, \mathbf{B} is the matrix that relates the components of strain to the element nodal displacements, and \mathbf{D}_0 the deterministic elasticity matrix.

Assembling matrices $\mathbf{K}_{e,i} = \sqrt{\lambda_i} \int_{\Omega_e} \varphi_i(\mathbf{x}) \mathbf{B}^\top \mathbf{D}_0 \mathbf{B} d\Omega_e$ to their global form \mathbf{K}_i , the equilibrium equation becomes:

$$\left(\mathbf{K}_0 + \sum_{i=1}^M \mathbf{K}_i \xi_i(\theta) \right) \mathbf{u}(\theta) = \mathbf{f} \quad (7.8)$$

Modelling of the response to a random process requires an expansion in which the covariance function need not be explicitly known [7]. The PCE assumes the random displacements $\mathbf{u}(\theta)$ can be expanded as follows:

$$\mathbf{u}(\theta) = \sum_{j=0}^{P-1} \mathbf{u}_j \Psi_j(\theta) \quad (7.9)$$

where the set $\{\Psi_j\}$, $j = 0 \dots \infty$, is a set of orthogonal polynomials in ξ_k , and $k = 0 \dots \infty$. Truncating terms in equation (7.8) and substituting equation (7.9):

$$\left(\sum_{i=0}^M \mathbf{K}_i \xi_i(\theta) \right) \left(\sum_{j=0}^{P-1} \mathbf{u}_j \Psi_j(\theta) \right) = \sum_{j=0}^{P-1} \mathbf{f}_j \Psi_j \quad (7.10)$$

A more convenient form of equation (7.10) can be found by minimizing the residual due to truncation, arriving at the following form:

$$\begin{bmatrix} \mathbf{K}_{0,0} & \dots & \mathbf{K}_{0,P-1} \\ \vdots & \ddots & \vdots \\ \mathbf{K}_{P-1,0} & \dots & \mathbf{K}_{P-1,P-1} \end{bmatrix} \begin{bmatrix} \mathbf{u}_0 \\ \vdots \\ \mathbf{u}_{P-1} \end{bmatrix} = \begin{bmatrix} \mathbf{f}_0 \\ \vdots \\ \mathbf{f}_{P-1} \end{bmatrix} \quad (7.11)$$

where $\mathbf{K}_{i,j}$ is an $N \times N$ matrix, \mathbf{u}_i are $N \times 1$ vectors associated with the polynomial expansion of the response, and \mathbf{f}_i are $N \times 1$ vectors of loading. Note that the system to be inverted is $NP \times NP$ in size, so that the size of the PCE expansion will have a significant impact on the computational cost of the solution. The details of this and other derivations can be found in [27] and [26].

7.2.4 Objectives and constraints

Innumerable objective functions can be defined and implemented in this framework. Here we have chosen to demonstrate the method using three such functions, defined in this section.

Compliance

The compliance objective function is the subject of a large portion of the structural optimization literature. For the case of deterministic loading the expression for the expectancy (mean value) of the compliance can be stated as follows:

$$E[C] = E[\mathbf{f}^\top \mathbf{u}] = \mathbf{f}_0^\top E[\mathbf{u}] = \mathbf{f}_0^\top \mathbf{u}_0, \quad (7.12)$$

and the variance as:

$$\text{Var}[C] = \text{Var}[\mathbf{f}^\top \mathbf{u}] = \mathbf{f}_0^\top \text{Cov}[\mathbf{u}] \mathbf{f}_0 \quad (7.13)$$

where $Cov[\mathbf{u}]$ is the covariance matrix of \mathbf{u} , and is found by the expression [27]:

$$Cov[\mathbf{u}] = \sum_{j=1}^{P-1} E[\Psi_j^2] \mathbf{u}_j \mathbf{u}_j^T \quad (7.14)$$

where Ψ_j are the components of the polynomial basis of the displacement field corresponding to displacement vectors \mathbf{u}_j . Equation (7.12) relies on the fact that the PCE of the response is of the form that $E[\mathbf{u}] = \mathbf{u}_0$, where \mathbf{u}_0 corresponds to the nodal displacements for polynomial Ψ_0 . The details of the derivation can be found in [22].

Mass

Perhaps equally as prevalent in the literature is the mass objective function. This function can be very simply stated as:

$$M = \rho \sum_{e=1}^{N_e} x_e V_e \quad (7.15)$$

where ρ is the material volumetric mass factor.

Volume fraction constraint

The compliance problem or a deflection minimization problem typically requires an upper limit on the volume (often in the form of a simple constraint referred to as the *volume fraction* in the literature). The volume fraction constraint can be written as:

$$\frac{\sum_{e=1}^{N_e} x_e V_e}{V_0} - 1 \leq 0 \quad (7.16)$$

7.3 Multiobjective approach

Metaheuristic algorithms pose solutions to several of the problems stated in section 7.1. They are generally gradient free, capable of handling multiple objectives and well suited to discrete and mixed variable problems. Due to these characteristics, they also deal well with the many types of objective functions and constraints typically arising in structural optimization applications. While the use of non-gradient algorithms has been criticised in the literature [25], these algorithms are very useful in situations where the lack of gradient information is present (due to the non-differentiability of the objective function, a function of the stochastic

variables in both material and loading uncertainties). Truss problems also do not suffer from issues of mesh coarseness, since each element represents a truss bar.

Of the metaheuristic algorithms, genetic algorithms (GAs) (and their multiobjective counterparts) are perhaps the most widely applied in structural optimization [10, 12, 17]. A simple robust optimization procedure for truss structures using GA's has been introduced by [24], only considering mass minimization. Deb and Gupta [4] investigated robust Pareto-optimal solutions in multiobjective optimization, while Gunawan and Azarm [9] researched multiobjective robust optimization using a sensitivity region concept. Quiang et al. [19] used a GA combined with a degree of robustness concept to develop a multiobjective robust optimization method. A very recent study by Lee and Kwong [14], considered tolerances of design variables and variation in the problem parameters for multiobjective problems.

The general multiobjective optimization problem can be stated as follows: given some structural performance criteria

$f_i(\mathbf{x})$ ($i = 1, \dots, k$), find the vector $\mathbf{x}^* = [x_1^*, \dots, x_n^*]$ which minimizes the vector function: $\mathbf{f}(\mathbf{x}) = [f_1(\mathbf{x}), \dots, f_k(\mathbf{x})]$, subject to $g(\mathbf{x}) \leq 0$ and $h(\mathbf{x}) = 0$, the constraints of the structural problem. In the case of structural optimization problems \mathbf{x} is the vector of design variables, where $g(\mathbf{x})$ and $h(\mathbf{x})$ represent respectively the inequality and equality constraints on the problem. Various multiobjective genetic algorithms are available in the literature. Among them the Non-dominated Sorting GA - II (NSGA-II) was introduced by Deb et al. [5] employs an elitist sorting process, generating new populations by sorting solutions according to their rank.

The multiobjective formulation allows for freedom in the definition of separate objectives. It is possible to define multiple, separate robust objectives of the form in equation (7.1) and use these in the optimization. It is also possible to decouple each objective of the form equation (7.1) into two separate objectives, each consisting of the mean or standard deviation of the original objective. In this way two times the number of objectives are considered by the optimization procedure.

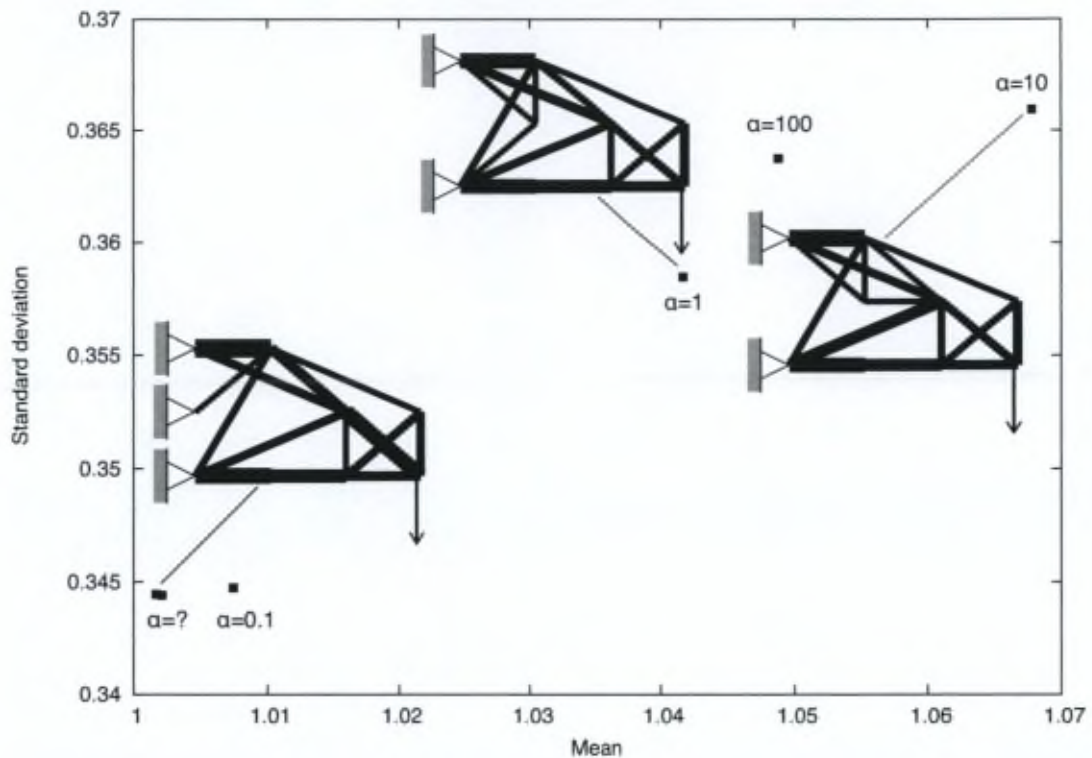


Figure 7.5: Solutions to the robust compliance problem in mean and standard deviation space

7.4 Examples

7.4.1 Robustness topology optimization for compliance minimization as a multiobjective problem

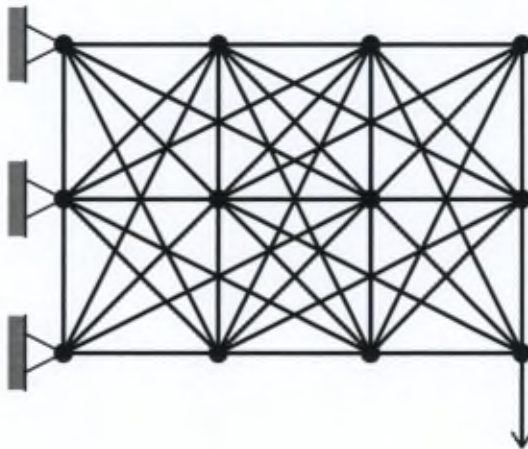


Figure 7.4: 2D cantilever truss-like ground structure

In equation 7.1, a factor α is used to linearly combine the mean and standard deviation into a single objective function. The choice of the α -factor is a point of some discussion in the literature. If one considers the mean and standard deviation as objective functions within their own right, the single objective problem becomes a bi-objective problem, where α reflects the preference of the designer. In this problem the 43-bar truss-like structure shown in figure 7.4 is considered. The spacing of the grid is one unit in both the x -direction and y -direction. The variation on the material properties is quantified using a Gaussian, 1D random field with standard deviation of $\sigma_E = 0.35$ times the mean value of the Young's modulus and a correlation length of 1 unit, with 5 subdivisions per truss bar element. Both KL and PC expansions of order 2 were used. The allowed bar cross section

area sizes are 0 and a range from 4 to 12 in steps of 0.8 square units. A volume fraction of $\frac{1}{6}$ was used to constrain the problem. The GA parameters chosen are: *crossover* = 0.9, *mutation* = 0.5, and *population size* = 400. In this problem, robust minimization of the compliance was considered. Using the multiobjective approach, two structures with very close mean and standard deviations were found. These two structures are Pareto dominant with respect to the other possibilities and have the same topology, shown in figure 7.5, with the label " $\alpha = ?$ ". The solutions to the single-objective problems for $\alpha = 0.1$, $\alpha = 1$, $\alpha = 10$ and $\alpha = 100$ are also shown in the figure. The topologies for $\alpha = 1$ and $\alpha = 10$ are also given. Note that the optimal solution for $\alpha = 100$ is dominated by $\alpha = 0.1$, but dominates $\alpha = 10$. The multiobjective approach dominates all of the tested single-objective solutions. The solutions found using the multiobjective approach have a topology which is distinct from the tested single-objective solutions.

7.4.2 Optimization of a truss-like structure for minimum mass and deflection

Many practical optimization problems require the consideration of objective functions such as mass and deflection. In this example the same truss-like cantilever structure (the ground structure is shown in figure 7.4) consisting of 43 bar elements is considered. The allowed bar cross section area sizes are 0 and a range between 8 and 12 in steps of 0.8 square units. The value of the α -factor was 5. All GA and geometric parameters are the same as in the previous example. Two scenarios are considered: i) the deterministic case, ii) and variation of both the loading and material properties ($\sigma_P = 0.35$ and $\sigma_E = 0.35$). The Pareto fronts of the deterministic and probabilistic solutions are shown in figure 7.6, along with some of the topologies present in the fronts. In this figure the mean values of the mass and compliance functions are shown for the deterministic and probabilistic cases. Clear differences can be seen in the topologies of the respective fronts, resulting in greater mean mass and compliance function values for the probabilistic case. Note that in the probabilistic front, some of the solutions are in fact not Pareto dominant (they are dominated by other solutions). This is due to the fact that the optimization routine was optimizing a combination of mean

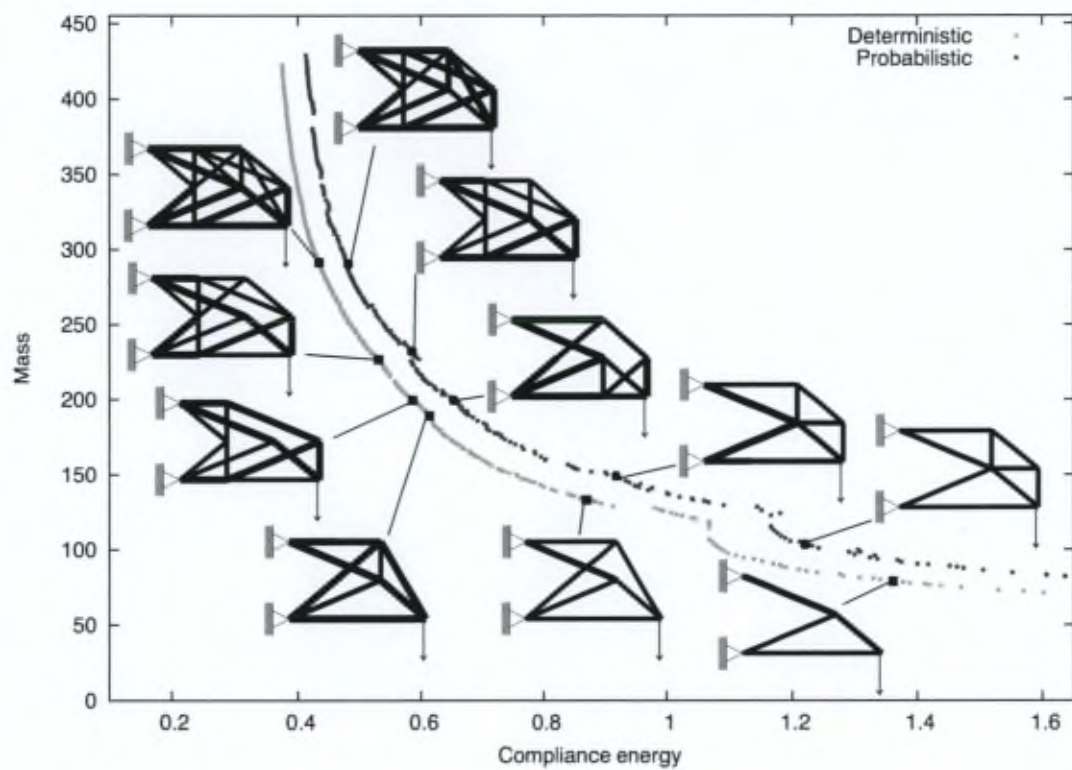


Figure 7.6: Pareto front of the solutions to the mass and compliance minimization multiobjective problems

7.5 Conclusions and further work

A method was demonstrated for robust topology optimization of discrete variable truss-like structures with material and loading uncertainties. Random fields were used to model the variation of the material stiffness along the bar elements of the structures. Loading uncertainties were introduced through a simple adaptation of the spectral stochastic finite element analysis method. A multi-objective approach was used, taking both the mean and standard deviation as objectives. In the example, this approach eliminates the need to choose the combinatoric factor which casts the problem as a single-objective one. The multiobjective approach outperformed all of the tested single-objective solutions, in which various values of the combinatoric factor α were used. A slightly surprising result of the example is the existence of two very similar optimal solutions. The existence of multiple solutions may be attributable to the presence of discrete design variables. This phenomenon may be similar to the discussion on the non-existence of symmetric optimal solutions in discrete design variable problems, as discussed in [21].

In the case of the mass and compliance minimization problem, both material stiffness uncertainties and loading uncertainties were considered. The results demonstrated a number of best trade-off robust solutions to the problem. As expected the robust solutions were dominated by the deterministic Pareto front. In the mean objective value space, not all solutions to the robust problem were Pareto optimal.

As Sigmund points out [25], graph theoretical approaches such as those used in [6] may be more useful to solve truss-like problems than non-gradient approaches. This should be further investigated.

Including uncertainties on the geometry could be a final step in the development of a complete method for robust truss topology optimization. It should be investigated how this effects the SSFEM approach proposed in this paper.

Bibliography

- [1] A. Asadpoure, M. Tootkaboni, and J.K. Guest. Robust topology optimization of structures with uncertainties in stiffness - application to truss structures. *Computers & Structures*, 89:1131–1141, June 2011.
- [2] S. Chen, W. Chen, and S. Lee. Level set based robust shape and topology optimization under random field uncertainties. *Structural and Multidisciplinary Optimization*, 41(4):507–524, 2010.
- [3] F. de Gournay, G. Allaire, and F. Jouve. Shape and topology optimization of the robust compliance via the level set method. *Control, Optimisation and Calculus of Variations*, 14(1):43–70, 2007.
- [4] K. Deb and H. Gupta. Searching for robust pareto-optimal solutions in multi-objective optimization. In Carlos A. Coello Coello, Arturo Hernández Aguirre, and Eckart Zitzler, editors, *Evolutionary Multi-Criterion Optimization*, volume 3410 of *Lecture Notes in Computer Science*, pages 150–164. Springer Berlin Heidelberg, 2005.
- [5] K. Deb, A. Pratap, S. Agarwal, and T. Meyarivan. A fast and elitist multiobjective genetic algorithm: Nsga-ii. *Evolutionary Computation, IEEE Transactions on*, 6(2):182–197, 2002.
- [6] B. Descamps and R. Filomeno Coelho. Graph Theory in Evolutionary Truss Design Optimization. In A H Gandomi, X-S Yang, S Talatahari, and A H Alavi, editors, *Metaheuristic Applications in Structures and Infrastructures*, pages 241–268. Elsevier B.V., 2013.
- [7] R. Ghanem and P.D. Spanos. Polynomial chaos in stochastic finite elements. *Journal of Applied Mechanics*, 57(1):197–202, 1990.
- [8] J. Guest and T. Igusa. Structural optimization under uncertain loads and nodal locations. *Computer Methods in Applied Mechanics and Engineering*, 198(1):116–124, 2008.
- [9] S. Gunawan and S. Azarm. Multi-objective robust optimization using a sensitivity region concept. *Structural and Multidisciplinary Optimization*, 29(1):50–60, 2005.
- [10] P. Hajela and E. Lee. Genetic algorithms in truss topological optimization. *International Journal of Solids and Structures*, 32(22):3341–3357, 1995.

- [11] Z. Kang and S. Bai. On robust design optimization of truss structures with bounded uncertainties. *Structural and Multidisciplinary Optimization*, 47(5):699–714, 2013.
- [12] H. Kawamura, H. Ohmori, and N. Kito. Truss topology optimization by a modified genetic algorithm. *Structural and Multidisciplinary Optimization*, 23(6):467–473, 2002.
- [13] N. Kogiso, W. Ahn, S. Nishiwaki, K. Izui, and M. Yoshimura. Robust topology optimization for compliant mechanisms considering uncertainty of applied loads. *Journal of Advanced Mechanical Design, Systems, and Manufacturing*, 2(1):96–107, 2008.
- [14] J. Lee and Y. Kwon. Conservative multi-objective optimization considering design robustness and tolerance: a quality engineering design approach. *Structural and Multidisciplinary Optimization*, 47(2):259–272, 2013.
- [15] J. Lógó, M. Ghaemi, and M.M. Rad. Optimal topologies in case of probabilistic loading: The influence of load correlation. *Mechanics Based Design of Structures and Machines*, 37(3):327–348, 2009.
- [16] J. Lógó, D.B. Merczel, and L. Nagy. On optimal topologies for the case of uncertain load positions. *Environmental Engineering*, pages 1–12, 2011.
- [17] M. Ohsaki. Genetic algorithm for topology optimization of trusses. *Computers & Structures*, 57(2):219–225, 1995.
- [18] L. Padovan, V. Pediroda, and C. Poloni. Multi objective robust design optimization of airfoils in transonic field. In V. Capasso and J. Périaux, editors, *Multidisciplinary Methods for Analysis Optimization and Control of Complex Systems*, volume 6 of *Mathematics in Industry*, pages 283–295. Springer Berlin Heidelberg, 2005.
- [19] J. Qiang, R. Qi, and F. Qian. Multi-objective robust optimization based on nsga-ii and degree of robustness. In *Intelligent Control and Automation (WCICA), 2010 8th World Congress on*, pages 4859–4864, 2010.
- [20] J.N. Richardson, S. Adriaenssens, Ph. Bouillard, and R. Filomeno Coelho. Multiobjective topology optimization of truss structures with kinematic stability repair. *Structural and Multidisciplinary Optimization*, 46:513–532, 2012.
- [21] J.N. Richardson, S. Adriaenssens, Ph. Bouillard, and R. Filomeno Coelho. Symmetry and asymmetry of solutions in discrete variable structural optimization. *Structural and Multidisciplinary Optimization*, 47(5):631–643, May 2013.
- [22] J.N. Richardson, S. Adriaenssens, and R. Filomeno Coelho. Robust topology optimization of 2d and 3d continuum and truss structures using a spectral stochastic finite element method. In *10th World Congress on Structural and Multidisciplinary Optimization (WCSMO 10), Orlando, Florida, USA, May 19–24, 2013*.
- [23] J.N. Richardson, R. Filomeno Coelho, and S. Adriaenssens. Robust topology optimization of truss-like structures with random loading and material properties: a multi-objective perspective. *Structural and Multidisciplinary Optimization*, 2013. Submitted for publication.
- [24] E. Sandgren and T.M. Cameron. Robust design optimization of structures through consideration of variation. *Computers & Structures*, 80(20–21):1605–1613, 2002.
- [25] O. Sigmund. On the usefulness of non-gradient approaches in topology optimization. *Structural and Multidisciplinary Optimization*, 43(5):589–596, 2011.
- [26] B. Sudret, M. Berveiller, and M. Lemaire. A stochastic finite element procedure for moment and reliability analysis. *European Journal of Computational Mechanics*, 15(7–8):825–866, 2006.
- [27] B. Sudret and A. Der Kiureghian. *Stochastic finite element methods and reliability: a state-of-the-art report*. Dept. of Civil and Environmental Engineering, University of California, 2000.
- [28] M. Tootkaboni, A. Asadpoure, and J.K. Guest. Topology optimization of continuum structures under uncertainty - a polynomial chaos approach. *Computer Methods in Applied Mechanics and Engineering*, 2011.

- [29] F. Wang, J.S. Jensen, O. Sigmund, and N.K. All. Robust topology optimization of photonic crystal waveguides with tailored dispersion properties. *Building*, 17(3):1–33, 2011.
- [30] K. Yonekura and Y. Kanno. Global optimization of robust truss topology via mixed integer semidefinite programming. *Optimization and Engineering*, 11:355–379, 2010.

Chapter 8

Conclusions and further work

8.1 Main findings of the research

The main focus of the thesis has been on developing topology optimization methods to be applied to truss-like structures. A method for improving performance in discrete variable topology optimization of these structures has been proposed. Topology optimization of a number of important structural systems, such as grid shells and bracing systems, has been addressed in detail. A very specific issue relating to geometric symmetry in discrete variable optimization, which became evident from the optimization of these special structures, was also investigated. Methods were developed to allow for robust optimization of both continuum and truss-like structures within a common framework, for both single and multiple objectives. Advancing topology optimization from theory to practice in civil engineering structures is a challenge with many facets. While many challenges remain, in this thesis, several important aspects have been addressed. The following three subsections summarize these answers to the challenges expressed in section 1.2.

8.1.1 Improving genetic-based topology optimization by incorporating kinematic stability considerations

The presence of discrete topological design variables in the class of problems addressed, leads to algorithm performance problems. In order to address this a novel approach has been proposed. The procedure makes use of a stable initial population and chromosome repair of kinematically unstable structures. By implementing these adaptations, knowledge of structural behaviour is added to the optimization algorithm. These additions allow for a compromise with the explorative character of the heuristic algorithm, reducing the search space through addition of information. The procedure was demonstrated on single-objective academic examples and compares well to the results in the literature, demonstrated on multiobjective problems showing advantages over unmodified methods. Large scale problems appear to benefit most from the proposed method, making this method of practical relevance to designers of civil engineering structures.

8.1.2 Optimization methods applied to grid shell and façade bracing design

Free form shells are structurally inefficient and costly, while grid configurations are often chosen with little consideration of structural and constructional efficiency. The approach in chapter 3 offers solutions to these problems by suggesting a two-phase method: form-finding followed by a refinement of the grid configuration. The case study of three grid shells with the same span but different boundary conditions demonstrates the viability of this method as a preliminary design tool for grid shells. The configuration of the grid shell elements found in the case study are dissimilar to the traditional repeated pattern of regularly spaced elements for grid shells. By allowing for an optimization of the grid shell configuration, very significant reductions in mass were realized.

Similarly, a topology optimization method was developed for the preliminary design of bracing systems. The approach uses multiobjective Genetic Algorithms to find a series of best compromise (Pareto optimal) solutions. The value of this method lies in its flexibility to provide solutions, allowing the designers to select optimal solutions when constraints change and modifications to the structural system occur. Since the main cost of bracing systems lies in the connections, reducing the number of bracings required results in a significant cost savings.

Through a detailed investigation of symmetry and asymmetry in discrete variable optimization it has been demonstrated that, given a binary topology problem of the type discussed, no symmetric solution necessarily exists. The number of design variables and degree of symmetry play important parts in the probability of finding symmetric solutions in discrete problems. It was shown that as the size of the discrete design set increases, this probability does not tend to 1, but instead to values related to the group symmetry itself. However, the probability will decrease significantly with increasing design set size for certain types of symmetry. The examples demonstrate that the probability of achieving symmetric results to discrete symmetric problems remains very low, even when the design set is very large. This investigation may have wide-ranging implications to any form of optimization with geometric symmetry and discrete design variables.

8.1.3 Accounting for random uncertainty in structural optimization

The research on uncertainties in structural optimization presents a framework for topology optimization of both continuum and truss structures using spectral stochastic finite element method. The analysis method was used to quantify material uncertainties, loading uncertainties, and the variations of the responses required for the objective functions. A novel approach to truss analysis was introduced to model material uncertainties across elements of varying lengths. An investigation of robust topology optimization of discrete variable truss-like structures was undertaken, using a multiobjective approach. The methods were demonstrated on both 2D and 3D continuum and on truss examples. The examples clearly show that varying the material parameters has a significant effect on the shape and topology of solutions. Even relatively small values of the standard deviation of the material parameters can have a significant effect on the optimal topologies. Robust topologies tend to be topologically more complex than deterministic ones. Additionally, asymmetries in the robust optimal solutions may be observed when the material stiffness follows a lognormal distribution.

The truss examples demonstrate the importance of the correlation length to the solution of the truss optimization problems. This parameter is indicative of the effect of modelling the random field across the entire length of the element. It has been seen that significantly different results are achieved by varying this parameter.

8.2 Suggested further work

The research carried out in this thesis has helped to highlight a number of challenges yet to be addressed in the theoretical development of methods for topology optimization in structural applications. Broadly speaking these challenges relate to at least one of the following aspects: the nature of the variables, the problem formulation, the nature of the objectives, and, finally computational cost.

A number of challenges relating to the **variables** used in the optimization procedure are very pertinent to future research:

- In the above investigation material and loading random uncertainties were included in the RTO formulation. As an extension, random

uncertainties on the geometry should also be included [14]. Additionally, knowledge from experiments could be introduced to more accurately characterize the random uncertainties. For this purpose a Bayesian approach could be used [10, 11].

- Discrete variable optimization has been a major thread throughout this thesis. This type of optimization is quite distinct from continuous variable optimization. A review of the literature shows that this fact has been somewhat under appreciated. Further investigation into the specific difficulties and perhaps opportunities of this type of optimization is necessary to be truly rigorous in the understanding of structural optimization. Furthermore categorical variables play a major role for the implementation of optimization methods in structural engineering. The representation and handling of these variables in optimization algorithms is still an open question [8].

Besides the impact of the choice of variables, the **problem formulation** itself also presents several challenges to optimization research:

- In this manuscript, amongst other things, a common framework was presented for RTO of both continuum and truss-like structures. For the purposes of general structural optimization problems, a more general framework is necessary, able to deal with various types of structures, different types of design variables, multiple objectives, different types of uncertainties, topology, shape and sizing optimization, both robustness and reliability, etc. For instance, combining robust and reliable optimization would be of major importance, since both of these aspects are incredibly important to real-world design problems. The method used in chapters 6 and 7 to investigate RTO, were originally applied to reliability analysis [17]. The SSFEM method is therefore a very promising candidate for a possible robust and reliable topology optimization framework.
- Multi-objective problems are becoming more and more relevant to designers. For this purpose novel methods have been proposed to integrate multi-objective optimization and reliability in a common framework, account-

ing for the specific nature of Pareto optimization [3, 7, 15]. The same could be achieved for RTO and a combined robust and reliable topology optimization formulation.

- Large scale structural optimization problems (especially those with discrete design variables) offer numerous challenges to current optimization procedures. Not least of these challenges is the complex nature of large scale structures such as bridges, in which many partners work together on integrated design models. An example of this multidisciplinary design approach is the use of Building Information Models in which various partners have access to the same design virtual model, containing information on all aspects of the design. Combining various optimization routines in a single model will be one of the major challenges facing optimizers in the future. Multidisciplinary design optimization (MDO) may offer a way to deal with this problem in an efficient way. MDO can be applied to complex problems, decomposing them and optimizing the parts concurrently. This method allows for specializations to work together on one structure, achieving a more efficient optimization process as demonstrated by Balling et al. [2]. MDO incorporating uncertainty is in its relative infancy, with only some research has been done on reliability quantification in MDO [9]. Robust and reliable MDO could be a very fruitful area of research indeed, although presumably extremely complex and computationally expensive. Metamodels could potentially serve as a way to facilitate this complexity by reducing the computational cost requirements.

The complexities of the problem formulation are compounded by the nature of the **objectives**, which are becoming more and more sophisticated with the ever changing requirements of designers. This raises several important challenges:

- Minimization of objectives such as mass and compliance energy have been studied extensively in the literature and are primarily relevant to the aerospace and automotive industries. In this context they are synonymous with the concept of sustainability since they reduce fuel consumption and cost. In the civil engineering context, sustainability is instead

associated with concepts such as embodied energy or maintenance costs [1]. Maximizing sustainability may require the definition of complex metrics which are not simply composed. It has been discussed in chapter 7 that metaheuristic algorithms offer the opportunity to take complex objectives into account [4, 16].

- Accounting for aspects such as non-linear behaviour [12], damage and other physics (heat exchange for façades, etc.) is important to designers. This avenue of research may be very useful and important to optimizers of civil engineering structures, in order to establish the relevance of the discipline both academically and to industry.

Large, complex simulations to evaluate the objectives require extensive computational resources. As one of the main barriers to acceptance of structural optimization in practice is the feasibility of optimization methods to the industry.

Computational cost in terms of time and resources remains a serious challenge for developments in the field of structural optimization. At this point two prominent avenues exist for possible improvement:

1. Parallel computing (with the modification in the algorithms it requires) [1], and
2. model reduction, by Proper Orthogonal Decomposition [5], Proper Generalized Decomposition [13], Krylov decomposition [5], etc.

Both of these aspects are important for the further reduction of the computational cost of structural optimization methods. An interesting application that could benefit from improved computational performance is the simultaneous coupling of form-finding with structural optimization (as alluded to in chapter 4). Form-finding methods have been developed somewhat independently of structural optimization methods, while they are both of great interest to designers. Combining form-finding and optimization methods [6] poses a number of challenges for researchers, not least of which is the computational cost of truly simultaneous form-finding and structural optimization. Intelligent methods, for example refining the convergence criterion of both form finding and optimization algorithms at consecutive iterations, could be relevant in this regard.

Bibliography

- [1] H. Adeli and K.C. Sarma. *Cost Optimization of Structures: Fuzzy Logic, Genetic Algorithms, and Parallel Computing*. Wiley, 2006.
- [2] R. Balling and M.R. Rawlings. Collaborative optimization with disciplinary conceptual design. *Structural and Multidisciplinary Optimization*, 20(3):232–241, 2000.
- [3] M. Basseur and E. Zitzler. Handling uncertainty in indicator-based multiobjective optimization. *International Journal of Computational Intelligence Research*, 2(3):255–272, 2006.
- [4] L. G. Caldas and L. K. Norford. A design optimization tool based on a genetic algorithm. *Automation in Construction*, 11(2):173 – 184, 2002.
- [5] K. Carlberg and C. Farhat. An adaptive pod-krylov reduced-order model for structural optimization. In *Proceedings of the eighth World Congress on Structural and Multidisciplinary Optimization*, June 2009.
- [6] B. Descamps and R. Filomeno Coelho. A lower-bound formulation for the geometry and topology optimization of truss structures under multiple loading. *Structural and Multidisciplinary Optimization*, 48(1):49–58, 2013.
- [7] R. Filomeno Coelho. Co-evolutionary optimization for multi-objective design under uncertainty. *ASME Journal of Mechanical Design*, 135(2):021006, 2013.
- [8] R. Filomeno Coelho. Metamodels for mixed variables based on moving least squares. *Optimization and Engineering*, pages 1–19, 2013.
- [9] F. Hui and L. Weiji. An efficient method for reliability-based multidisciplinary design optimization. *Chinese Journal of Aeronautics*, 21(4):335 – 340, 2008.
- [10] T. Igusa, S.G. Buonopane, and B.R. Ellingwood. Bayesian analysis of uncertainty for structural engineering applications. *Structural Safety*, 24(2-4):165–186, 2002.
- [11] A. Kumar, P.B. Nair, A.J. Keane, and S. Shahpar. Robust design using Bayesian Monte Carlo. *International Journal for Numerical Methods in Engineering*, 73:1497–1517, 2008.
- [12] A.C.C. Lemonge, M.M. Silva, and H.J.C. Barbosa. Design optimization of geometrically nonlinear truss structures considering cardinality constraints. In *Evolutionary Computation (CEC), 2011 IEEE Congress on*, pages 29–36, 2011.
- [13] A. Leygue and E. Verron. A first step towards the use of proper general decomposition method for structural optimization. *Archives of Computational Methods in Engineering*, 17(4):465–472, 2010.
- [14] A. Nouy, A. Clément, F. Schoefs, and N. Moës. An extended stochastic finite element method for solving stochastic partial differential equations on random domains. *Computer Methods in Applied Mechanics and Engineering*, 197:4663–4682, 2008.
- [15] S. Rangavajhala and S. Mahadevan. Joint probability formulation for multiobjective optimization under uncertainty. *Journal of Mechanical Design*, 133:051007, May 2011.
- [16] Z. Ren, F. Yang, N.M. Bouchlaghem, and C.J. Anumba. Multi-disciplinary collaborative building design – comparative study between multi-agent systems and multi-disciplinary optimisation approaches. *Automation in Construction*, 20(5):537 – 549, 2011.
- [17] B. Sudret and A. Der Kiureghian. *Stochastic finite element methods and reliability: a state-of-the-art report*. Dept. of Civil and Environmental Engineering, University of California, 2000.

Appendices



Appendix A

Derivation of robust compliance objective sensitivities

The SSFEM approach is based on the form of the equilibrium equations in equation (6.13). The error \mathbf{r} in this form can be minimized by requiring it to be orthogonal to the Hilbert space spanned by the polynomials Ψ_l in the PCE [1]:

$$E[\mathbf{r}, \Psi_l] = E\left[\sum_{k=0}^{P-1} \sum_{i=0}^M \mathbf{K}_i \mathbf{u}_k \xi_i \Psi_k \Psi_l - \mathbf{f} \Psi_l\right] = 0 \quad (\text{A.1})$$

It can also be shown that:

$$\mathbf{u}_j = \frac{E[\mathbf{u} \Psi_j]}{E[\Psi_j^2]} \quad (\text{A.2})$$

Using the adjoint method we can rewrite equation (6.16) as:

$$E[C] = \mathbf{f}_0^\top E[\mathbf{u}] - \sum_{l=0}^{P-1} \lambda_l E[\mathbf{r}, \Psi_l] \quad (\text{A.3})$$

Differentiating with respect to the design variables \mathbf{x} :

$$\frac{\partial E[C]}{\partial \mathbf{x}} = \mathbf{f}_0^\top \frac{\partial E[\mathbf{u}]}{\partial \mathbf{x}} - \sum_{l=0}^{P-1} \lambda_l \sum_{k=0}^{P-1} \sum_{i=0}^M E\left[\xi_i \Psi_k \Psi_l \frac{\partial \mathbf{K}_i}{\partial \mathbf{x}} \mathbf{u}_k + \xi_i \Psi_k \Psi_l \mathbf{K}_i \frac{\partial \mathbf{u}_k}{\partial \mathbf{x}}\right] \quad (\text{A.4})$$

We now choose $\lambda_l = \mathbf{u}_l^\top$, and recall that $\Psi_0 = 1$:

$$\frac{\partial E[C]}{\partial \mathbf{x}} = \mathbf{f}_0^\top \frac{\partial E[\mathbf{u}]}{\partial \mathbf{x}} - \sum_{l=0}^{P-1} \sum_{k=0}^{P-1} \sum_{i=0}^M E\left[\xi_i \Psi_k \Psi_l \mathbf{u}_l^\top \frac{\partial \mathbf{K}_i}{\partial \mathbf{x}} \mathbf{u}_k + \xi_i \Psi_k \Psi_l \mathbf{u}_l^\top \mathbf{K}_i \frac{\partial \mathbf{u}_k}{\partial \mathbf{x}}\right] \quad (\text{A.5})$$

$$= \mathbf{f}_0^\top \frac{\partial E[\mathbf{u}]}{\partial \mathbf{x}} - \sum_{l=0}^{P-1} \sum_{k=0}^{P-1} \sum_{i=0}^M E\left[\xi_i \Psi_k \Psi_l \mathbf{u}_l^\top \frac{\partial \mathbf{K}_i}{\partial \mathbf{x}} \mathbf{u}_k + \xi_i \Psi_0 \Psi_l \mathbf{u}_l^\top \mathbf{K}_i \frac{\partial \mathbf{u}_k}{\partial \mathbf{x}} \Psi_k\right] \quad (\text{A.6})$$

$$= \mathbf{f}_0^\top \frac{\partial E[\mathbf{u}]}{\partial \mathbf{x}} - \sum_{l=0}^{P-1} \sum_{k=0}^{P-1} \sum_{i=0}^M E\left[\xi_i \Psi_k \Psi_l \mathbf{u}_l^\top \frac{\partial \mathbf{K}_i}{\partial \mathbf{x}} \mathbf{u}_k\right] - \mathbf{f}_0^\top \frac{\partial E[\mathbf{u}]}{\partial \mathbf{x}} \quad (\text{A.7})$$

$$= - \sum_{l=0}^{P-1} \sum_{k=0}^{P-1} \sum_{i=0}^M E\left[\xi_i \Psi_k \Psi_l \mathbf{u}_l^\top \frac{\partial \mathbf{K}_i}{\partial \mathbf{x}} \mathbf{u}_k\right] \quad (\text{A.8})$$

At the element level this simplifies to:

$$\frac{\partial E[C]}{\partial x_e} = - \sum_{l=0}^{P-1} \sum_{k=0}^{P-1} \sum_{i=0}^M E\left[\xi_i \Psi_k \Psi_l \mathbf{u}_{e,l}^\top \frac{\partial \mathbf{K}_{e,i}}{\partial x_e} \mathbf{u}_{e,k}\right] \quad (\text{A.9})$$

$$= - p(x_e)^{p-1} \sum_{l=0}^{P-1} \sum_{k=0}^{P-1} \sum_{i=0}^M E\left[\xi_i \Psi_k \Psi_l \mathbf{u}_{e,l}^\top \mathbf{K}_e^* \mathbf{u}_{e,k}\right] \quad (\text{A.10})$$

where \mathbf{K}_e^* is the deterministic element stiffness matrix. The derivative of the standard deviation can be found in a similar manner.

$$\text{Var}[C] = \mathbf{f}_0^\top \text{Cov}[\mathbf{u}] \mathbf{f}_0 - \text{term} \quad (\text{A.11})$$

$$\frac{\partial \sqrt{\text{Var}[C]}}{\partial \mathbf{x}} = \frac{1}{2\sqrt{\text{Var}[C]}} \frac{\partial}{\partial \mathbf{x}} \left(\mathbf{f}_0^\top \left(\sum_{j=1}^{P-1} E[\Psi_j^2] \mathbf{u}_j \mathbf{u}_j^\top \right) \mathbf{f}_0 \right) \quad (\text{A.12})$$

It can be shown that $\mathbf{u}_j^\top \frac{\partial \mathbf{u}_j}{\partial \mathbf{x}}$ is symmetric, and therefore:

$$\frac{\partial \sqrt{\text{Var}[C]}}{\partial \mathbf{x}} = \frac{1}{\sqrt{\text{Var}[C]}} \mathbf{f}_0^\top \left(\sum_{j=1}^{p-1} E[\Psi_j^2] \frac{\partial \mathbf{u}_j}{\partial \mathbf{x}} \mathbf{u}_j^\top \right) \mathbf{f}_0 \quad (\text{A.13})$$

$$= \frac{1}{\sqrt{\text{Var}[C]}} \mathbf{f}_0^\top \left(\sum_{j=1}^{p-1} E \left[\frac{\partial \mathbf{u}_j}{\partial \mathbf{x}} \right] \mathbf{u}_j^\top \right) \mathbf{f}_0 \quad (\text{A.14})$$

$$= - \frac{1}{\sqrt{\text{Var}[C]}} \left(\sum_{j=1}^{p-1} \sum_{l=0}^{p-1} \sum_{k=0}^{p-1} \sum_{i=0}^M E[\xi_i \Psi_k \Psi_l \Psi_j] \mathbf{u}_l^\top \frac{\partial \mathbf{K}_i}{\partial \mathbf{x}} \mathbf{u}_k \mathbf{u}_j^\top \right) \mathbf{f}_0 \quad (\text{A.15})$$

The last equation follows since we have seen that:

$$\mathbf{f}_0^\top \frac{\partial E[\mathbf{u}]}{\partial \mathbf{x}} = - \sum_{l=0}^{p-1} \sum_{k=0}^{p-1} \sum_{i=0}^M E[\xi_i \Psi_k \Psi_l] \mathbf{u}_l^\top \frac{\partial \mathbf{K}_i}{\partial \mathbf{x}} \mathbf{u}_k \quad (\text{A.16})$$

At the element level, this reduces to:

$$\frac{\partial \sqrt{\text{Var}[C_e]}}{\partial x_e} = - \frac{\alpha p x_e^{p-1}}{\sqrt{\text{Var}[C]}} \sum_{j=1}^{p-1} \left(\sum_{k=0}^{p-1} \sum_{l=0}^{p-1} \sum_{i=0}^M E[\xi_i \Psi_j \Psi_k \Psi_l] \mathbf{u}_{e,k}^\top \mathbf{K}_e^* \mathbf{u}_{e,l} \right) \mathbf{u}_j^\top \mathbf{f}_0 \quad (\text{A.17})$$

Bibliography

- [1] B. Sudret and A. Der Kiureghian. *Stochastic finite element methods and reliability: a state-of-the-art report*. Dept. of Civil and Environmental Engineering, University of California, 2000.

Appendix B

Overview of solution algorithms in structural optimization

In structural optimization, generally no analytical solution to the above mentioned problems are possible. Therefore the search space is navigated in search of the optimal solution, by means of a numerical optimization algorithm. These numerical procedures fall into two broad categories: gradient-based and gradient-free algorithms. Hybrid algorithms making use of both gradient and non-gradient based algorithms are also used. What follows is a very short overview of the prominent algorithms used in the field.

B.1 Overview of gradient-based optimization algorithms in topology optimization

Gradient-based optimization methods have a long and rich history, arising from the development of differential calculus by Leibniz and Newton. Gauss and Newton developed the earliest iterative optimization methods. This class of optimization method makes use of the first and second order derivatives of the objective functions and constraints, or some approximation of these gradients. The popularity of these approaches lies in the mathematical rigour and relative efficiency of the computations. Several methods have successfully been applied in the topology optimization literature. In simple terms gradient-based optimization algorithms assess the gradient of the constrained objective function at a given point in the function space and use this information to advance the search in the next iteration(s). Some of the most popular gradient-based algorithms used in structural optimization are:

Sequential linear programming (SLP) [8] starts from an estimate of the optimal solution, and solves a sequence of linearisation of the model. This is equivalent to solving a series of linear programming problems, which is relatively computationally inexpensive. Due to these advantages, SLP is used quite widely in structural optimization [26, 30].

Sequential quadratic programming (SQP) [21, 27] requires twice continuous differentiability of both the objective function and the constraints. The basis of the SQP method is the solution of a sequence of optimization subproblems. Each of the subproblems is in itself an optimization of a quadratic

model of the objective function, subject to linearised constraints.

Optimality criteria (OC) methods [24] consist of a combination of a statement governing the state of the design (the optimality criteria definition) and an algorithm used to resize the structure to satisfy the optimality criterion. An example of an optimality criterion is the so-called fully stressed design state. OC has been applied in some of the fundamental works on topology optimization [4, 24]. *The method of moving asymptotes (MMA)* [5, 25] uses a strictly convex approximating subproblem for each step of the iterative procedure. The generation of the subproblems is dictated by the moving asymptotes. MMA in particular has become widely applied in topology optimization literature [1, 22, 28].

B.2 Overview of gradient-free optimization algorithms in topology optimization

Gradient-free algorithms are widely applied in structural optimization problems where gradient-based methods cannot be applied¹. In simple terms, gradient-free algorithms make use of a sampling of the search space to make inferences about the optimality of solutions. Broadly speaking the following categories can be defined [11]:

1. Physical Algorithms
2. Swarm Algorithms
3. Direct Search Algorithms
4. Evolutionary Algorithms (EA)

Physical Algorithms include Harmony Search [9, 16], inspired by sound wave interaction, Simulated Annealing [15, 18, 29], based on the annealing process of cooling metal, Ray optimization [12, 13], inspired by the transition of light between mediums, and Tabu [10] search which attempts to escape local minima by combining with other algorithms, improving local searches by using memory structures that describe the visited solutions or user-provided sets of rules. *Swarm Algorithms* include Ant Colony optimization [2, 6, 17], which is inspired by the search process employed by ants looking for

¹This section owes much to the work of Hare et al. [11].

food, Particle Swarm optimization [7, 14, 17, 20], an algorithm using moving 'particles' which are influenced by their neighbours in how they move throughout the search space, and Artificial bee colony [19], optimization which mimics the behaviour of a swarm of bees foraging for food.

Direct search algorithms include directional direct search [3], simplicial direct search [23], which evaluates the objective function at a set of points forming a simplex to determine the next iteration, simplex gradient methods, which uses a simplex gradient as a substitute for the gradient, and trust region methods.

Evolutionary Algorithms are perhaps the most prominent of the gradient-free optimization algorithms, of which Genetic Algorithms (GA's) are the most widely applied. These algorithms use principles inspired by biological evolution in populations. In general the algorithm relies on three main operators: selection, mutation and cross-over. Successive iterations (generations) are found by assessing the fitness of individual designs in the previous population and applying these three operators based on this fitness. GA's are used in some of the papers in this text.

While many optimization algorithms are available, it is important to be able to match the particulars of the problem to be optimized and the strengths of chosen algorithm. A thorough understanding of the search space is of primal importance for this. The parametrization and type of information available to the optimization algorithm will play an important roll in this regard.

Bibliography

- [1] A. Asadpoure, M. Tootkaboni, and J.K. Guest. Robust topology optimization of structures with uncertainties in stiffness - application to truss structures. *Comput. Struct.*, 89:1131–1141, June 2011.
- [2] I. Aydoğdu and M.P. Saka. Ant colony optimization of irregular steel frames including elemental warping effect. *Advances in Engineering Software*, 44(1):150 – 169, 2012.
- [3] R.D. Baldock, K. Shea, and D. Eley. Evolving optimized braced steel frameworks for tall buildings using modified pattern search. In *Proceedings of the International Conference on Computing in Civil Engineering, Cancun, Mexico*. ASCE, July 2005.
- [4] M.P. Bendsøe and O. Sigmund. *Topology Optimization: Theory, Methods, and Applications*. Engineering Online Library. Springer, 2003.
- [5] M. Bruyneel, P. Duysinx, and C. Fleury. A family of mma approximations for structural optimization. *Structural and Multidisciplinary Optimization*, 24(4):263–276, 2002.
- [6] M. Dorigo, V. Maniezzo, and A. Coloni. Ant system: optimization by a colony of cooperating agents. *Trans. Sys. Man Cyber. Part B*, 26(1):29–41, 1996.
- [7] P.C. Fourie and A.A. Groenwold. The particle swarm optimization algorithm in size and shape optimization. *Structural and Multidisciplinary Optimization*, 23(4):259–267, 2002.
- [8] D. Fujii and N. Kikuchi. Improvement of numerical instabilities in topology optimization using the slp method. *Structural and Multidisciplinary Optimization*, 19(2):113–121, 2000.
- [9] Z.W. Geem, J.H. Kim, and G.V. Loganathan. A new heuristic optimization algorithm: Harmony search. *SIMULATION*, 76(2):60–68, 2001.
- [10] F. Glover. Tabu search - part i. *ORSA Journal on Computing*, 1(3):190–206, 1989.
- [11] W. Hare, J. Nutini, and S. Tesfamariam. A survey of non-gradient optimization methods in structural engineering. *Advances in Engineering Software*, 59(0):19 – 28, 2013.
- [12] A. Kaveh and M. Khayatazad. A new meta-heuristic method: Ray optimization. *Computers & Structures*, 112(0):283 – 294, 2012.
- [13] A. Kaveh and M. Khayatazad. Ray optimization for size and shape optimization of truss structures. *Computers & Structures*, 117(0):82 – 94, 2013.
- [14] A. Kaveh and S. Talatahari. Particle swarm optimizer, ant colony strategy and harmony search scheme hybridized for optimization of truss structures. *Computers & Structures*, 87(5):267 – 283, 2009.

- [15] S. Kirkpatrick, C. D. Gelatt, and M. P. Vecchi. Optimization by simulated annealing. *Science*, 220(4598):671–680, 1983.
- [16] K.S. Lee and Z.W. Geem. A new meta-heuristic algorithm for continuous engineering optimization: harmony search theory and practice. *Computer Methods in Applied Mechanics and Engineering*, 194(36):3902 – 3933, 2005.
- [17] G.C. Luh and C.Y. Lin. Structural topology optimization using ant colony optimization algorithm. *Applied Soft Computing*, 9(4):1343–1353, 2009.
- [18] S. Manoharan and S. Shanmuganathan. A comparison of search mechanisms for structural optimization. *Computers & Structures*, 73(1):363 – 372, 1999.
- [19] R. Parpinelli, C. Benitez, and H. Lopes. Parallel approaches for the artificial bee colony algorithm. In B. Panigrahi, Y. Shi, and M. Lim, editors, *Handbook of Swarm Intelligence*, volume 8 of *Adaptation, Learning, and Optimization*, pages 329–345. Springer Berlin Heidelberg, 2010.
- [20] R.E. Perez and K. Behdinan. Particle swarm approach for structural design optimization. *Computers & Structures*, 85(19):1579 – 1588, 2007.
- [21] L.X. Qian, W.X. Zhong, K.T. Cheng, and Y.K. Sui. An approach to structural optimization –sequential quadratic programming, sqp. *Engineering Optimization*, 8(1):83–100, 1984.
- [22] D. Qin and Q. Zhu. Structural topology optimization of box girder based on method of moving asymptotes (mma). In *Proceedings of the 2010 International Conference on Intelligent Computation Technology and Automation - Volume 03*, ICICTA '10, pages 402–405. IEEE Computer Society, 2010.
- [23] H. Rahami, A. Kaveh, M. Aslani, and R. Najian Asl. A hybrid modified genetic-nelder mead simplex algorithm for large-scale truss optimization. *Iran University of Science & Technology*, 1, 2011.
- [24] O. Sigmund. A 99 line topology optimization code written in Matlab. *Structural and Multidisciplinary Optimization*, 21(2):120–127, 2001.
- [25] K. Svanberg. The method of moving asymptotes - a new method for structural optimization. *International Journal for Numerical Methods in Engineering*, 24(2):359–373, 1987.
- [26] K. Svanberg and M. Werme. Topology optimization by sequential integer linear programming. In M.P. Bendsøe, N. Olhoff, and O. Sigmund, editors, *IUTAM Symposium on Topological Design Optimization of Structures, Machines and Materials*, volume 137 of *Solid Mechanics and Its Applications*, pages 425–436. Springer Netherlands, 2006.
- [27] C.C. Swan and J.S. Arora. Topology design of material layout in structured composites of high stiffness and strength. *Structural optimization*, 13(1):45–59, 1997.
- [28] M. Tootkaboni, A. Asadpoure, and J.K. Guest. Topology optimization of continuum structures under uncertainty - a polynomial chaos approach. *Computer Methods in Applied Mechanics and Engineering*, 2011.
- [29] V. Černý. Thermodynamical approach to the traveling salesman problem: An efficient simulation algorithm. *Journal of Optimization Theory and Applications*, 45(1):41–51, January 1985.
- [30] R.J. Yang and C.H. Chuang. Optimal topology design using linear programming. *Computers & Structures*, 52(2):265 – 275, 1994.

Complete bibliography

- [1] *Topics in Applied Mechanics*, chapter Structural Optimization History and State-of-the-art, pages 339–345. Kluwer Academic Publishers, 1993.
- [2] The american heritage dictionary of the english language, fourth edition, 2003.
- [3] I.A. Azid, A.S.K. Kwan, and K.N. Seetharamu. An evolutionary approach for layout optimization of a three-dimensional truss. *Structural and Multidisciplinary Optimization*, 24(4):333–337, 2002.
- [4] Y. Bai, E. Klerk, D. Pasechnik, and R. Sotirov. Exploiting group symmetry in truss topology optimization. *Optimization and Engineering*, 10(3):331–349, 2008.
- [5] M. Beckers and C. Fleury. A primal-dual approach in truss topology optimization. *Computers & Structures*, 64(1-4):77–88, 1997.
- [6] L. Gil and A. Andreu. Shape and cross-section optimisation of a truss structure. *Computers & Structures*, 79(7):681–689, 2001.
- [7] P. Hajela and E. Lee. Genetic algorithms in truss topological optimization. *International Journal of Solids and Structures*, 32(22):3341–3357, 1995.
- [8] A.C.C. Lemonge, H. J.C. Barbosa, L.G. da Fonseca, and A.L.G.A. Coutinho. A genetic algorithm for topology optimization of dome structures. In H. Rodrigues, J. Herskovits, C.M. Soares, J.M. Guedes, J. Folgado, A. Araújo, F. Moleiro, J.P. Kuzhichalil, J.A. Madeira, and Z. Dimitrovová, editors, *Proceedings of the 2nd International Conference on Engineering Optimization EngOpt 2010, Lisbon, Portugal*, 2010.
- [9] C. Luebke and K. Shea. Cdo: Computational design + optimization in building practice. *The Arup Journal*, 3:17–21, 2005.
- [10] P. Pedersen. Optimal joint positions for space trusses. *Journal of the Structural Division*, 99(12):2459–2476, 1973.
- [11] J.N. Richardson, S. Adriaenssens, Ph. Bouillard, and R. Filomeno Coelho. Multiobjective topology optimization of truss structures with kinematic stability repair. *Structural and Multidisciplinary Optimization*, 46:513–532, 2012.
- [12] J.N. Richardson, S. Adriaenssens, Ph. Bouillard, and R. Filomeno Coelho. Symmetry and asymmetry of solutions in discrete variable structural optimization. *Struct. Multidisc. Optim.*, 47(5):631–643, May 2013.
- [13] J.N. Richardson, S. Adriaenssens, R. Filomeno Coelho, and Ph. Bouillard. Coupled form-finding and grid optimization approach for single layer grid shells. *Engineering Structures*, 52(0):230 – 239, 2013.
- [14] J.N. Richardson, G. Nordenson, R. Laberrenne, R. Filomeno Coelho, and S. Adriaenssens. Flexible optimum design of a bracing system for façade design using multiobjective genetic algorithms. *Automation in Construction*, 32(0):80 – 87, 2013.
- [15] G.I.N. Rozvany. On symmetry and non-uniqueness in exact topology optimization. *Structural and Multidisciplinary Optimization*, pages 1–21, 2010.
- [16] C.C. Swan and S.F. Rahmatalla. Strategies for Computational Efficiency in Continuum Structural Topology Optimization. *Advances in Engineering Structures, Mechanics & Construction*, pages 673–683, 2006.
- [17] D. Šešok and R. Belevicius. Global optimization of trusses with a modified genetic algorithm. *Journal of Civil Engineering and Management*, 14(3):147–154, 2008.
- [18] W. Achtziger and M. Stolpe. Truss topology optimization with discrete design variables—guaranteed global optimality and benchmark examples. *Structural and Multidisciplinary Optimization*, 34:1–20, 2007.
- [19] R.J. Balling, R.R. Briggs, and K. Gillman. Multiple optimum size/shape/topology designs for skeletal structures using a genetic algorithm. *Journal of Structural Engineering*, 132:1158, 2006.

- [20] A. Ben-Tal, F. Jarre, M. Kočvara, A. Nemirovski, and J. Zowe. Optimal design of trusses under a nonconvex global buckling constraint. *Optim. Eng.*, 1(2):189–213, 2000.
- [21] F.Y. Cheng and D. Li. Multiobjective optimization design with pareto genetic algorithm. *Journal of Structural Engineering*, 123(9):1252–1261, 1997.
- [22] C.A. Coello Coello. A comprehensive survey of evolutionary-based multiobjective optimization techniques. *Knowledge and Information systems*, 1(3):129–156, 1999.
- [23] C.A. Coello Coello. A survey of constraint handling techniques used with evolutionary algorithms. *Laboratorio Nacional de Informatica Avanzada, Veracruz, Mexico, Technical report Lania-RI-99-04*, 1999.
- [24] C.A. Coello Coello, G.B. Lamont, and D.A. Van Veldhuizen. *Evolutionary algorithms for solving multi-objective problems*. Springer-Verlag New York Inc, 2002.
- [25] K. Deb and S. Gulati. Design of truss-structures for minimum weight using genetic algorithms. *Finite Elements in Analysis and Design*, 37(5):447–465, 2001.
- [26] W.S. Dorn, R.E. Gomory, and H.J. Greenberg. Automatic design of optimal structures. *Journal de Mécanique*, 3:25–52, 1964.
- [27] M.S. Eldred, B.M. Adams, K. Haskell, W.J. Bohnhoff, J.P. Eddy, D.M. Gay, J.D. Griffin, W.E. Hart, P.D. Hough, T.G. Kolda, M.L. Martinez-Canales, L.P. Swiler, J.P. Watson, and P.J. Williams. DAKOTA, a multilevel parallel object-oriented framework for design optimization, parameter estimation, uncertainty quantification, and sensitivity analysis: Version 4.1 reference manual. Technical Report SAND2006-4055, Sandia National Laboratories, Albuquerque, New Mexico, September 2007.
- [28] R. Filomeno Coelho and Ph. Bouillard. A multicriteria evolutionary algorithm for mechanical design optimization with expert rules. *International Journal of Numerical Methods in Engineering*, 62(4):516–536, 2005.
- [29] R. Filomeno Coelho, J. Lebon, and Ph. Bouillard. Hierarchical stochastic metamodels based on moving least squares and polynomial chaos expansion – Application to the multiobjective reliability-based optimization of 3D truss structures. *Structural and Multidisciplinary Optimization*, 2010. In press.
- [30] C.M. Fonseca, P.J. Fleming, et al. Genetic algorithms for multiobjective optimization: Formulation, discussion and generalization. In *Proceedings of the fifth international conference on genetic algorithms*, volume 423, pages 416–423, 1993.
- [31] D.E. Goldberg. *Genetic algorithms in search, optimization and machine learning*. Reading, MA: Addison-Wesley. XIII, 412 p. DM 104.00, 1989.
- [32] H.M. Gomes. Truss optimization with dynamic constraints using a particle swarm algorithm. *Expert Systems with Applications*, 38:957–968, January 2011.
- [33] P. Hajela, E. Lee, and C.Y. Lin. Genetic algorithms in structural topology optimization. In M.P. Bendsøe and C.A.M. Soares, editors, *Topology design of structures*, pages 117–134. Kluwer Academic Publishers Dordrecht/Boston, 1993.
- [34] X. Huang, Z.H. Zuo, and Y.M. Xie. Evolutionary topological optimization of vibrating continuum structures for natural frequencies. *Computers & Structures*, 88(5-6):357–364, 2010.
- [35] P. Jin and W. De-yu. Topology optimization of truss structure with fundamental frequency and frequency domain dynamic response constraints. *Acta Mechanica Solida Sinica*, 19(3):231–240, 2006.
- [36] A. Kaveh and V. Kalatjari. Topology optimization of trusses using genetic algorithm, force method and graph theory. *International Journal for Numerical Methods in Engineering*, 58(5):771–791, 2003.
- [37] H. Kawamura, H. Ohmori, and N. Kito. Truss topology optimization by a modified genetic algorithm. *Structural and Multidisciplinary Optimization*, 23(6):467–473, 2002.

- [38] J.A. Madeira, H.C. Rodrigues, and H. Pina. Multiobjective topology optimization of structures using genetic algorithms with chromosome repairing. *Structural and Multidisciplinary Optimization*, 32(1):31–39, 2006.
- [39] S. Mathakari, P. Gardoni, P. Agarwal, A. Raich, and T. Haukaas. Reliability-based optimal design of electrical transmission towers using multi-objective genetic algorithms. *Computer-Aided Civil and Infrastructure Engineering*, 22(4):282–292, 2007.
- [40] M. Ohsaki. Genetic algorithm for topology optimization of trusses. *Computers & Structures*, 57(2):219–225, 1995.
- [41] M. Papadrakakis, N. Lagaros, and V. Plevris. Multi-objective optimization of skeletal structures under static and seismic loading conditions. *Engineering Optimization*, 34(6):645–669, 2002.
- [42] N.L. Pedersen. Maximization of eigenvalues using topology optimization. *Structural and Multidisciplinary Optimization*, 20:2–11, 2000.
- [43] S. Pellegrino. Structural computations with the singular value decomposition of the equilibrium matrix. *International Journal of Solids and Structures*, 30(21):3025–3035, 1993.
- [44] G.I.N. Rozvany. Difficulties in truss topology optimization with stress, local buckling and system stability constraints. *Structural and Multidisciplinary Optimization*, 11(3):213–217, 1996.
- [45] G.I.N. Rozvany. On design-dependent constraints and singular topologies. *Structural and Multidisciplinary Optimization*, 21(2):164–172, 2001.
- [46] S. Ruiyi, G. Liangjin, and F. Zijie. Truss topology optimization using genetic algorithm with individual identification technique. In S.I. Ao, L. Gelman, DD.W.L. Hukins, A. Hunter, and A.M. Korsunsky, editors, *Proceedings of the World Congress on Engineering 2009 Vol II, WCE '09, July 1 - 3, 2009, London, U.K.*, Lecture Notes in Engineering and Computer Science, pages 1089–1093. International Association of Engineers, Newswood Limited, 2009.
- [47] W.S. Ruy, Y.S. Yang, G.H. Kim, and Y.S. Yeun. Topology design of truss structures in a multicriteria environment. *Computer-Aided Civil and Infrastructure Engineering*, 16(4):246–258, 2001.
- [48] J.D. Schaffer. Multiple objective optimization with vector evaluated genetic algorithms. In *Proceedings of the 1st International Conference on Genetic Algorithms*, pages 93–100, 1985.
- [49] R. Statnikov, A. Bordetsky, J. Matusov, I. Sobol, and A. Statnikov. Definition of the feasible solution set in multicriteria optimization problems with continuous, discrete, and mixed design variables. *Nonlinear Analysis: Theory, Methods & Applications*, 71(12):e109–e117, 2009.
- [50] R. Su, X. Wang, L. Gui, and Z. Fan. Multi-objective topology and sizing optimization of truss structures based on adaptive multi-island search strategy. *Structural and Multidisciplinary Optimization*, pages 1–12, 2011.
- [51] R.L. Taylor. FEAP – A Finite Element Analysis Program, March 2008. Version 8.2 User Manual.
- [52] W.H. Tong and G.R. Liu. An optimization procedure for truss structures with discrete design variables and dynamic constraints. *Computers & Structures*, 79(2):155–162, 2001.
- [53] Y. M. Xie and G. P. Steven. Evolutionary structural optimization for dynamic problems. *Computers & Structures*, 58(6):1067–1073, 1996.
- [54] E. Zitzler, L. Thiele, M. Laumanns, C.M. Fonseca, and V.G. Da Fonseca. Performance assessment of multiobjective optimizers: An analysis and review. *Evolutionary Computation, IEEE Transactions on*, 7(2):117–132, 2003.
- [55] S. Adriaenssens and M.R. Barnes. Tensegrity spline beam and grid shell structures. *Engineering Structures*, 23(1):29–36, 2001.

- [56] S. Adriaenssens, L. Ney, E. Bodarwe, and C.J.K. Williams. Construction constraints drive the form finding of an irregular meshed steel and glass shell. *Journal of Architectural Engineering*, 18(3):206–213, 2012.
- [57] P. Basso, A.E. Del Grosso, A. Pugnale, and M. Sassone. Computational morphogenesis in architecture : the cost optimization of free form grid-shells. *Journal of the IASS*, 50(3):143–151, 2009.
- [58] M. Beckers and C. Fleury. A primal-dual approach in truss topology optimization. *Computers & Structures*, 64(1-4):77–88, 1997.
- [59] P. Bellés, N. Ortega, M. Rosales, and O. Andrés. Shell form-finding: Physical and numerical design tools. *Engineering Structures*, 31(11):2656 – 2666, 2009.
- [60] D.P. Billington. *The art of structural design: a Swiss legacy*. Yale University Press, 2008.
- [61] K. Bletzinger. Form finding and morphogenesis. In Ihsan Mungan and John F. Abel, editors, *Fifty Years of Progress for Shell and Spatial Structures*, pages 459–474. 2011.
- [62] Ph. Block and J. Ochsendorf. Thrust network analysis: a new methodology for three-dimensional equilibrium. *Journal of the IASS*, 48(3):1–8, 2007.
- [63] CEN. *Eurocode 1: Actions on Structures*. European Committee for Standardisation, 2002.
- [64] CEN. *Eurocode 3: Design of Steel Structures*. European Committee for Standardisation, 2003.
- [65] J. Chilton. *Heinz Isler. The Engineer's Contribution to Contemporary Architecture*. Thomas Telford, London, 2000.
- [66] A. Day. An introduction to dynamic relaxation. *The Engineer*, 219:218–221, 1965.
- [67] B. Descamps, R. Filomeno Coelho, L. Ney, and Ph. Bouillard. Multicriteria optimization of lightweight bridge structures with a constrained force density method. *Computers & structures*, 89:277–284, 2011.
- [68] M. Giger and P. Ermanni. Evolutionary truss topology optimization using a graph-based parameterization concept. *Structural and Multidisciplinary Optimization*, 32:313–326, 2006.
- [69] P. Guillaume, G. Blengini, P. Ruaut, and F. Brunetti. Nouvelle foire de milan: prouesses d'acier. *Revue du Centre Information Acier*, 8:20–27, 2005.
- [70] H.J. and Schek. The force density method for form finding and computation of general networks. *Computer Methods in Applied Mechanics and Engineering*, 3(1):115 – 134, 1974.
- [71] S. Huerta. El cálculo de estructuras en la obra de gaudí. *Ingeniería Civil*, 130:121 –133, 2003.
- [72] A. Kaveh and S. Talatahari. Geometry and topology optimization of geodesic domes using charged system search. *Structural and Multidisciplinary Optimization*, 43:215–229, February 2011.
- [73] A Kilian and J. Ochsendorf. Particle-spring systems for structural form-finding. *Journal of the IASS*, 46(147):77, 2005.
- [74] R. Klein. Abstract voronoi diagrams and their applications. In Hartmut Noltemeier, editor, *Computational Geometry and its Applications*, volume 333 of *Lecture Notes in Computer Science*, pages 148–157. Springer-Verlag, 1988.
- [75] L. Lamberti. An efficient simulated annealing algorithm for design optimization of truss structures. *Computers & Structures*, 86(19-20):1936–1953, 2008.
- [76] P. Lancaster and K. Salkauskas. Surfaces generated by moving least squares methods. *Mathematics of Computation*, 37(155):141–158, 1981.
- [77] N. Leach, D. Turnbull, D. Turnbull, and C. Williams. *Digital tectonics*. Wiley-Academy, 2004.
- [78] H. Pottmann and D. Bentley. *Architectural geometry*. Number v. 10 in Architectural geometry. Bentley Institute Press, 2007.

- [79] M.H. Rasmussen and M. Stolpe. Global optimization of discrete truss topology design problems using a parallel cut-and-branch method. *Computers & Structures*, 86(13-14):1527–1538, 2008.
- [80] M.P. Saka. Optimum topological design of geometrically nonlinear single layer latticed domes using coupled genetic algorithm. *Computers & Structures*, 85:1635–1646, November 2007.
- [81] V. Toğan and A.T. Daloglu. Optimization of 3d trusses with adaptive approach in genetic algorithms. *Engineering Structures*, 28(7):1019 – 1027, 2006.
- [82] P. Winslow, S. Pellegrino, and S.B. Sharma. Multi-objective optimization of free-form grid structures. *Structural and Multidisciplinary Optimization*, 40(1-6):257–269, 2010.
- [83] M. Abachizadeh and M. Tahani. An ant colony optimization approach to multi-objective optimal design of symmetric hybrid laminates for maximum fundamental frequency and minimum cost. *Structural and Multidisciplinary Optimization*, 37:367–376, 2009.
- [84] L.G. Caldas and L.K. Norford. A design optimization tool based on a genetic algorithm. *Automation in Construction*, 11(2):173 – 184, 2002.
- [85] A. Kaveh and N. Farhoodi. Layout optimization for x-bracing of planar steel frames using ant system. *International Journal of Civil Engineering*, 8(3):256–275, 2010.
- [86] A. Kaveh and M. Shahrouzi. Graph theoretical topology control in structural optimization of frames with bracing systems. *Scientia Iranica*, 16(2):173–187, 2009.
- [87] A. Kaveh and S. Talatahari. A hybrid particle swarm and ant colony optimization for design of truss structures. *Asian Journal of Civil Engineering Building and Housing*, 9(4):329–348, 2008.
- [88] F.R. Khan. Current trends in current high rise buildings. In *Proceedings Symposium on Tall Buildings*, University of Southampton, 1966.
- [89] Q.Q. Liang. Effects of continuum design domains on optimal bracing systems for multi-story steel building frameworks. In *Proceedings of the 5th Australasian Congress on Applied Mechanics*, volume 2, pages 794–799. Engineers Australia, 2007.
- [90] Q.Q. Liang, Y.M. Xie, and G.P. Steven. Optimal topology design of bracing systems for multi-story steel frames. *J Struct Engng ASCE*, 126(7):823–829, 2000.
- [91] M. Marinaki, Y. Marinakis, and G. Stavroulakis. Fuzzy control optimized by a multi-objective particle swarm optimization algorithm for vibration suppression of smart structures. *Structural and Multidisciplinary Optimization*, 43:29–42, 2011.
- [92] A.R. Mijar, C.C. Swan, J.S. Arora, and I. Kosaka. Continuum topology optimization for concept design of frame bracing systems. *Journal of Structural Engineering*, 124(5):541, 1998.
- [93] Z. Ren, F. Yang, N.M. Bouchlaghem, and C.J. Anumba. Multi-disciplinary collaborative building design – comparative study between multi-agent systems and multi-disciplinary optimisation approaches. *Automation in Construction*, 20(5):537 – 549, 2011.
- [94] D.L. Schodek. *Structures*. Pearson/Prentice Hall, 5 edition, 2004.
- [95] B.S. Taranath. *Structural Analysis and Design of Tall Buildings: Steel and Composite Construction*. Taylor & Francis, 2011.
- [96] E. Zitzler, M. Laumanns, and S. Bleuler. A Tutorial on Evolutionary Multiobjective Optimization. In X. Gandibleux, M. Sevaux, K. Sorensen, and V. T'kindt, editors, *Metaheuristics for Multiobjective Optimisation*, pages 3–37, Berlin, 2004. Springer. Lecture Notes in Economics and Mathematical Systems Vol. 535.
- [97] E. Zitzler, M. Laumanns, L. Thiele, Carlos M. Fonseca, and V. Grunert da Fonseca. Why Quality Assessment of Multiobjective Optimizers Is Difficult. In W.B. Langdon, E. Cant'u-Paz, K. Mathias, R. Roy, D. Davis,

- R. Poli, K. Balakrishnan, V. Honavar, G. Rudolph, J. Wegener, L. Bull, M.A. Potter, A.C. Schultz, J.F. Miller, E. Burke, and N. Jonoska, editors, *Proceedings of the Genetic and Evolutionary Computation Conference (GECCO'2002)*, pages 666–673, San Francisco, California, July 2002. Morgan Kaufmann Publishers.
- [98] K. Balasubramanian. Graph theoretical perception of molecular symmetry. *Chemical Physics Letters*, 232(56):415–423, 1995.
- [99] M.P. Bendsøe and O. Sigmund. *Topology optimization: theory, methods, and applications*. Springer, 2003.
- [100] G. Cheng and X. Liu. Discussion on symmetry of optimum topology design. *Structural and Multidisciplinary Optimization*, pages 1–5, 2011.
- [101] A. Evgrafov. On globally stable singular truss topologies. *Structural and Multidisciplinary Optimization*, 29:170–177, 2005.
- [102] X. Guo, C. Ni, G. Cheng, and Z. Du. Some symmetry results for optimal solutions in structural optimization. *Structural and Multidisciplinary Optimization*, pages 1–15, 2012.
- [103] M. Hamermesh. *Group theory and its application to physical problems*. Dover books on physics and chemistry. Dover Publications, 1989.
- [104] T.J. Healey. A group-theoretic approach to computational bifurcation problems with symmetry. *Computer Methods in Applied Mechanics and Engineering*, 67(3):257–295, 1988.
- [105] K. Ikeda and K. Murota. Bifurcation analysis of symmetric structures using block-diagonalization. *Computer Methods in Applied Mechanics and Engineering*, 86:215–243, March 1991.
- [106] R.D. Kangwai, S.D. Guest, and S. Pellegrino. An introduction to the analysis of symmetric structures. *Computers & Structures*, 71(6):671–688, 1999.
- [107] A. Kaveh and M. Nikbakht. Analysis of space truss towers using combined symmetry groups and product graphs. *Acta Mechanica*, 218:133–160, 2011.
- [108] A. Kaveh, M. Nikbakht, and H. Rahami. Improved group theoretic method using graph products for the analysis of symmetric-regular structures. *Acta Mechanica*, 210:265–289, 2010.
- [109] U. Kirsch. On singular topologies in optimum structural design. *Structural and Multidisciplinary Optimization*, 2(3):133–142, 1990.
- [110] I. Kosaka and C.C. Swan. A symmetry reduction method for continuum structural topology optimization. *Computers & Structures*, 70(1):47–61, 1999.
- [111] J.W. Leech. How to use groups. *American Journal of Physics*, 38:273–273, 1970.
- [112] J. Øystein and J.A. Sellers. Partitions with parts in a finite set. *International Journal of Number Theory*, 2(3):455–468, 2006.
- [113] J.D. Renton. On the stability analysis of symmetrical frameworks. *Quarterly Journal of Mechanics and Applied Mathematics*, 17:175–197, 1964.
- [114] G.I.N. Rozvany and T. Birker. On singular topologies in exact layout optimization. *Structural and Multidisciplinary Optimization*, 8:228–235, 1994.
- [115] M. Stolpe. On some fundamental properties of structural topology optimization problems. *Structural and Multidisciplinary Optimization*, 41(5):661–670, 2010.
- [116] K. Svanberg. On local and global minima in structural optimization. In E. Atrek, R. H. Gallagher, K. M. Ragsdell, and O. C. Zienkiewicz, editors, *New directions in optimal structural design*. John Wiley and Sons, 1984.
- [117] A. Zingoni. Group-theoretic exploitations of symmetry in computational solid and structural mechanics. *International Journal for Numerical Methods in Engineering*, 79(February):253–289, 2009.
- [118] A. Zingoni, M.N. Pavlovic, and G.M. Zlokovic. Application of group theory to the analysis of space frames. In GAR Parke and CM Howard, editors, *Space Structures*, pages 1334–1347. Thomas Telford: London, 1993.

- [119] A. Zingoni, M.N. Pavlovic, and G.M. Zlokovic. A symmetry-adapted flexibility approach for multi-storey space frames: eneral outline and symmetry-adapted redundants. *Structural Engineering Review*, 7(2):107–119, 1995.
- [120] Đ. Zloković. *Group theory and G-vector spaces in structures: vibrations, stability, and status*. Ellis Horwood series in civil engineering. E. Horwood, 1989.
- [121] A. Asadpoure, M. Tootkaboni, and J.K. Guest. Robust topology optimization of structures with uncertainties in stiffness - application to truss structures. *Computers & Structures*, 89:1131–1141, June 2011.
- [122] M.P. Bendsøe and N. Kikuchi. Generating optimal topologies in structural design using a homogenization method. *Computer Methods in Applied Mechanics and Engineering*, 71(2):197–224, 1988.
- [123] S. Chen, W. Chen, and S. Lee. Level set based robust shape and topology optimization under random field uncertainties. *Structural and Multidisciplinary Optimization*, 41(4):507–524, 2010.
- [124] S. Conti, H. Held, M. Pach, M. Rumpf, and R. Schultz. Shape optimization under uncertainty: A stochastic programming perspective. *SIAM J. on Optimization*, 19:1610–1632, January 2009.
- [125] F. de Gournay, G. Allaire, and F. Jouve. Shape and topology optimization of the robust compliance via the level set method. *Control, Optimisation and Calculus of Variations*, 14(1):43–70, 2007.
- [126] P. Duysinx and M.P. Bendsøe. Topology optimization of continuum structures with local stress constraints. *International Journal for Numerical Methods in Engineering*, 43(8):1453–1478, 1998.
- [127] R. Ghanem and P.D. Spanos. Polynomial chaos in stochastic finite elements. *Journal of Applied Mechanics*, 57(1):197–202, 1990.
- [128] J. Guest and T. Igusa. Structural optimization under uncertain loads and nodal locations. *Computer Methods in Applied Mechanics and Engineering*, 198(1):116–124, 2008.
- [129] J.K. Guest, J.H. Prévost, and T. Belytschko. Achieving minimum length scale in topology optimization using nodal design variables and projection functions. *International Journal for Numerical Methods in Engineering*, 61(2):238–254, 2004.
- [130] Z. Kang and S. Bai. On robust design optimization of truss structures with bounded uncertainties. *Structural and Multidisciplinary Optimization*, 47(5):699–714, 2013.
- [131] N. Kogiso, W. Ahn, S. Nishiwaki, K. Izui, and M. Yoshimura. Robust topology optimization for compliant mechanisms considering uncertainty of applied loads. *Journal of Advanced Mechanical Design, Systems, and Manufacturing*, 2(1):96–107, 2008.
- [132] J. Lógó, M. Ghaemi, and M.M. Rad. Optimal topologies in case of probabilistic loading: The influence of load correlation. *Mechanics Based Design of Structures and Machines*, 37(3):327–348, 2009.
- [133] J. Lógó, D.B. Merczel, and L. Nagy. On optimal topologies for the case of uncertain load positions. *Environmental Engineering*, pages 1–12, 2011.
- [134] J.N. Richardson, R. Filomeno Coelho, and S. Adriaenssens. A unified stochastic framework for robust topology optimization of continuum and truss-like structure. *Computers & Structures*, 2013. Submitted for publication.
- [135] E. Sandgren and T.M. Cameron. Robust design optimization of structures through consideration of variation. *Computers & Structures*, 80(20-21):1605 – 1613, 2002.
- [136] G. Schueller and H. Jensen. Computational methods in optimization considering uncertainties - an overview. *Computer Methods in Applied Mechanics and Engineering*, 198(1):2–13, 2008.
- [137] C.C. Seepersad, J.K. Allen, D.L. McDowell, and F. Mistree. Robust design of cellular materials with topological and dimensional imperfections. *Journal of Mechanical Design*, 128:1285, 2006.
- [138] O. Sigmund. On the design of compliant mechanisms using topology optimization.

- Mechanics Based Design of Structures and Machines*, 25(4):493–524, 1997.
- [139] O. Sigmund. A 99 line topology optimization code written in Matlab. *Structural and Multidisciplinary Optimization*, 21(2):120–127, 2001.
- [140] B. Sudret and A. Der Kiureghian. *Stochastic finite element methods and reliability: a state-of-the-art report*. Dept. of Civil and Environmental Engineering, University of California, 2000.
- [141] K. Svanberg. The method of moving asymptotes – a new method for structural optimization. *International Journal for Numerical Methods in Engineering*, 24(2):359–373, 1987.
- [142] M. Tootkaboni, A. Asadpoure, and J.K. Guest. Topology optimization of continuum structures under uncertainty - a polynomial chaos approach. *Computer Methods in Applied Mechanics and Engineering*, 2011.
- [143] Y. Tsompanakis, N.D. Lagaros, and M. Papadrakakis. *Structural Design Optimization Considering Uncertainties*. Structures and Infrastructures Series. Taylor & Francis, 2008.
- [144] F. Wang, J.S. Jensen, O. Sigmund, and N.K. All. Robust topology optimization of photonic crystal waveguides with tailored dispersion properties. *Building*, 17(3):1–33, 2011.
- [145] Kazuo Y. and Yoshihiro K. Global optimization of robust truss topology via mixed integer semidefinite programming. *Optimization and Engineering*, 11(3):355–379, 2010.
- [146] K. Deb and H. Gupta. Searching for robust pareto-optimal solutions in multi-objective optimization. In Carlos A. Coello Coello, Arturo Hernández Aguirre, and Eckart Zitzler, editors, *Evolutionary Multi-Criterion Optimization*, volume 3410 of *Lecture Notes in Computer Science*, pages 150–164. Springer Berlin Heidelberg, 2005.
- [147] K. Deb, A. Pratap, S. Agarwal, and T. Meyarivan. A fast and elitist multiobjective genetic algorithm: Nsga-ii. *Evolutionary Computation, IEEE Transactions on*, 6(2):182–197, 2002.
- [148] B. Descamps and R. Filomeno Coelho. Graph Theory in Evolutionary Truss Design Optimization. In A H Gandomi, X-S Yang, S Talatahari, and A H Alavi, editors, *Metaheuristic Applications in Structures and Infrastructures*, pages 241–268. Elsevier B.V., 2013.
- [149] S. Gunawan and S. Azarm. Multi-objective robust optimization using a sensitivity region concept. *Structural and Multidisciplinary Optimization*, 29(1):50–60, 2005.
- [150] J. Lee and Y. Kwon. Conservative multi-objective optimization considering design robustness and tolerance: a quality engineering design approach. *Structural and Multidisciplinary Optimization*, 47(2):259–272, 2013.
- [151] L. Padovan, V. Pediroda, and C. Poloni. Multi objective robust design optimization of airfoils in transonic field. In V. Capasso and J. Périaux, editors, *Multidisciplinary Methods for Analysis Optimization and Control of Complex Systems*, volume 6 of *Mathematics in Industry*, pages 283–295. Springer Berlin Heidelberg, 2005.
- [152] J. Qiang, R. Qi, and F. Qian. Multi-objective robust optimization based on nsga-ii and degree of robustness. In *Intelligent Control and Automation (WCICA), 2010 8th World Congress on*, pages 4859–4864, 2010.
- [153] J.N. Richardson, S. Adriaenssens, and R. Filomeno Coelho. Robust topology optimization of 2d and 3d continuum and truss structures using a spectral stochastic finite element method. In *10th World Congress on Structural and Multidisciplinary Optimization (WCSMO 10), Orlando, Florida, USA, May 19–24, 2013*.
- [154] J.N. Richardson, R. Filomeno Coelho, and S. Adriaenssens. Robust topology optimization of truss-like structures with random loading and material properties: a multi-objective perspective. *Structural and Multidisciplinary Optimization*, 2013. Submitted for publication.
- [155] O. Sigmund. On the usefulness of non-gradient approaches in topology optimization. *Structural and Multidisciplinary Optimization*, 43(5):589–596, 2011.

- [156] B. Sudret, M. Berveiller, and M. Lemaire. A stochastic finite element procedure for moment and reliability analysis. *European Journal of Computational Mechanics*, 15(7–8):825–866, 2006.
- [157] H. Adeli and K.C. Sarma. *Cost Optimization of Structures: Fuzzy Logic, Genetic Algorithms, and Parallel Computing*. Wiley, 2006.
- [158] R. Balling and M.R. Rawlings. Collaborative optimization with disciplinary conceptual design. *Structural and Multidisciplinary Optimization*, 20(3):232–241, 2000.
- [159] M. Basseur and E. Zitzler. Handling uncertainty in indicator-based multiobjective optimization. *International Journal of Computational Intelligence Research*, 2(3):255–272, 2006.
- [160] K. Carlberg and C. Farhat. An adaptive pod-krylov reduced-order model for structural optimization. In *Proceedings of the eighth World Congress on Structural and Multidisciplinary Optimization*, June 2009.
- [161] B. Descamps and R. Filomeno Coelho. A lower-bound formulation for the geometry and topology optimization of truss structures under multiple loading. *Structural and Multidisciplinary Optimization*, 48(1):49–58, 2013.
- [162] R. Filomeno Coelho. Co-evolutionary optimization for multi-objective design under uncertainty. *ASME Journal of Mechanical Design*, 135(2):021006, 2013.
- [163] R. Filomeno Coelho. Metamodels for mixed variables based on moving least squares. *Optimization and Engineering*, pages 1–19, 2013.
- [164] F. Hui and L. Weiji. An efficient method for reliability-based multidisciplinary design optimization. *Chinese Journal of Aeronautics*, 21(4):335–340, 2008.
- [165] T. Igusa, S.G. Buonopane, and B.R. Ellingwood. Bayesian analysis of uncertainty for structural engineering applications. *Structural Safety*, 24(2–4):165–186, 2002.
- [166] A. Kumar, P.B. Nair, A.J. Keane, and S. Shahpar. Robust design using Bayesian Monte Carlo. *International Journal for Numerical Methods in Engineering*, 73:1497–1517, 2008.
- [167] A.C.C. Lemonge, M.M. Silva, and H.J.C. Barbosa. Design optimization of geometrically nonlinear truss structures considering cardinality constraints. In *Evolutionary Computation (CEC), 2011 IEEE Congress on*, pages 29–36, 2011.
- [168] A. Leygue and E. Verron. A first step towards the use of proper general decomposition method for structural optimization. *Archives of Computational Methods in Engineering*, 17(4):465–472, 2010.
- [169] A. Nouy, A. Clément, F. Schoefs, and N. Moës. An extended stochastic finite element method for solving stochastic partial differential equations on random domains. *Computer Methods in Applied Mechanics and Engineering*, 197:4663–4682, 2008.
- [170] S. Rangavajhala and S. Mahadevan. Joint probability formulation for multiobjective optimization under uncertainty. *Journal of Mechanical Design*, 133:051007, May 2011.
- [171] I. Aydoğdu and M.P. Saka. Ant colony optimization of irregular steel frames including elemental warping effect. *Advances in Engineering Software*, 44(1):150–169, 2012.
- [172] R.D. Baldock, K. Shea, and D. Eley. Evolving optimized braced steel frameworks for tall buildings using modified pattern search. In *Proceedings of the International Conference on Computing in Civil Engineering, Cancun, Mexico*. ASCE, July 2005.
- [173] M. Bruyneel, P. Duysinx, and C. Fleury. A family of mma approximations for structural optimization. *Structural and Multidisciplinary Optimization*, 24(4):263–276, 2002.
- [174] M. Dorigo, V. Maniezzo, and A. Colnori. Ant system: optimization by a colony of cooperating agents. *Trans. Sys. Man Cyber. Part B*, 26(1):29–41, 1996.
- [175] P.C. Fourie and A.A. Groenwold. The particle swarm optimization algorithm in size

- and shape optimization. *Structural and Multidisciplinary Optimization*, 23(4):259–267, 2002.
- [176] D. Fujii and N. Kikuchi. Improvement of numerical instabilities in topology optimization using the slp method. *Structural and Multidisciplinary Optimization*, 19(2):113–121, 2000.
- [177] Z.W. Geem, J.H. Kim, and G.V. Loganathan. A new heuristic optimization algorithm: Harmony search. *SIMULATION*, 76(2):60–68, 2001.
- [178] F. Glover. Tabu search - part i. *ORSA Journal on Computing*, 1(3):190–206, 1989.
- [179] W. Hare, J. Nutini, and S. Tesfamariam. A survey of non-gradient optimization methods in structural engineering. *Advances in Engineering Software*, 59(0):19 – 28, 2013.
- [180] A. Kaveh and M. Khayatazad. A new meta-heuristic method: Ray optimization. *Computers & Structures*, 112(0):283 – 294, 2012.
- [181] A. Kaveh and M. Khayatazad. Ray optimization for size and shape optimization of truss structures. *Computers & Structures*, 117(0):82 – 94, 2013.
- [182] A. Kaveh and S. Talatahari. Particle swarm optimizer, ant colony strategy and harmony search scheme hybridized for optimization of truss structures. *Computers & Structures*, 87(5):267 – 283, 2009.
- [183] S. Kirkpatrick, C. D. Gelatt, and M. P. Vecchi. Optimization by simulated annealing. *Science*, 220(4598):671–680, 1983.
- [184] K.S. Lee and Z.W. Geem. A new meta-heuristic algorithm for continuous engineering optimization: harmony search theory and practice. *Computer Methods in Applied Mechanics and Engineering*, 194(36):3902 – 3933, 2005.
- [185] G.C. Luh and C.Y. Lin. Structural topology optimization using ant colony optimization algorithm. *Applied Soft Computing*, 9(4):1343–1353, 2009.
- [186] S. Manoharan and S. Shanmuganathan. A comparison of search mechanisms for structural optimization. *Computers & Structures*, 73(1):363 – 372, 1999.
- [187] R. Parpinelli, C. Benitez, and H. Lopes. Parallel approaches for the artificial bee colony algorithm. In B. Panigrahi, Y. Shi, and M. Lim, editors, *Handbook of Swarm Intelligence*, volume 8 of *Adaptation, Learning, and Optimization*, pages 329–345. Springer Berlin Heidelberg, 2010.
- [188] R.E. Perez and K. Behdinan. Particle swarm approach for structural design optimization. *Computers & Structures*, 85(19):1579 – 1588, 2007.
- [189] L.X. Qian, W.X. Zhong, K.T. Cheng, and Y.K. Sui. An approach to structural optimization –sequential quadratic programming, sqp. *Engineering Optimization*, 8(1):83–100, 1984.
- [190] D. Qin and Q. Zhu. Structural topology optimization of box girder based on method of moving asymptotes (mma). In *Proceedings of the 2010 International Conference on Intelligent Computation Technology and Automation - Volume 03*, ICICTA '10, pages 402–405. IEEE Computer Society, 2010.
- [191] H. Rahami, A. Kaveh, M. Aslani, and R. Najian Asl. A hybrid modified genetic-nelder mead simplex algorithm for large-scale truss optimization. *Iran University of Science & Technology*, 1, 2011.
- [192] K. Svanberg and M. Werme. Topology optimization by sequential integer linear programming. In M.P. Bendsøe, N. Olhoff, and O. Sigmund, editors, *IUTAM Symposium on Topological Design Optimization of Structures, Machines and Materials*, volume 137 of *Solid Mechanics and Its Applications*, pages 425–436. Springer Netherlands, 2006.
- [193] C.C. Swan and J.S. Arora. Topology design of material layout in structured composites of high stiffness and strength. *Structural optimization*, 13(1):45–59, 1997.
- [194] V. Černý. Thermodynamical approach to the traveling salesman problem: An efficient simulation algorithm. *Journal of Optimization Theory and Applications*, 45(1):41–51, January 1985.
- [195] R.J. Yang and C.H. Chuang. Optimal topology design using linear programming. *Computers & Structures*, 52(2):265 – 275, 1994.

List of Publications

Book chapters

- [1] J. N. Richardson, R. Filomeno Coelho, Ph. Bouillard, and S. Adriaenssens. Discrete topology optimization – Connectivity for gridshells. In S. Adriaenssens, Ph. Block, D. Veenendaal, and C. Williams, editors, *Shells for Architecture – Form finding and structural optimization*. Routledge Architecture/Taylor & Francis, 2013. In press.

Journal articles

- [2] J.N. Richardson, R. Filomeno Coelho, and S. Adriaenssens. Robust topology optimization of truss-like structures with random loading and material properties: a multi-objective perspective. *Structural and Multidisciplinary Optimization*, 2013. Submitted for publication.
- [3] J.N. Richardson, R. Filomeno Coelho, and S. Adriaenssens. A unified stochastic framework for robust topology optimization of continuum and truss-like structure. *Computers & Structures*, 2013. Submitted for publication.
- [4] J.N. Richardson, G. Nordenson, R. Laberrenne, R. Filomeno Coelho, and S. Adriaenssens. Flexible optimum design of a bracing system for façade design using multiobjective genetic algorithms. *Automation in Construction*, 32(0):80 – 87, 2013.
- [5] J.N. Richardson, S. Adriaenssens, Ph. Bouillard, and R. Filomeno Coelho. Symmetry and asymmetry of solutions in discrete variable structural optimization. *Struct. Multidiscip. Optim.*, 47(5):631–643, May 2013.
- [6] J.N. Richardson, S. Adriaenssens, R. Filomeno Coelho, and Ph. Bouillard. Coupled form-finding and grid optimization approach for single layer grid shells. *Engineering Structures*, 52(0):230 – 239, 2013.

- [7] J.N. Richardson, S. Adriaenssens, Ph. Bouillard, and R. Filomeno Coelho. Multiobjective topology optimization of truss structures with kinematic stability repair. *Structural and Multidisciplinary Optimization*, 46:513–532, 2012.

Conference proceedings

- [8] J. N. Richardson, S. Adriaenssens, G. Nordenson, R. Filomeno Coelho, and R. Laberrenne. Design of a museum façade bracing system for changing performance requirements using multiobjective optimization. In *ASCE/SEI Structures Congress, Boston, Massachusetts, April 3–5, 2014*. Accepted.
- [9] J.N. Richardson, S. Adriaenssens, and R. Filomeno Coelho. Robust topology optimization of 2d and 3d continuum and truss structures using a spectral stochastic finite element method. In *10th World Congress on Structural and Multidisciplinary Optimization (WCSMO 10), Orlando, Florida, USA, May 19–24, 2013*.
- [10] J. N. Richardson, S. Adriaenssens, Ph. Bouillard, and R. Filomeno Coelho. Symmetry of solutions in discrete and continuous structural topology optimization. In B. H. V. Topping, editor, *Eleventh International Conference on Computational Structures Technology (CST 2012), Dubrovnik, Croatia, September 4–7, 2012*.
- [11] J. N. Richardson, S. Adriaenssens, Ph. Bouillard, and R. Filomeno Coelho. Optimization of truss structures with kinematic stability repair. In A. G. Malan, P. Nithiarasu, and B. D. Reddy, editors, *Second African Conference on Computational Mechanics – AfriCOMP11, Cape Town, South Africa, January 5–8, 2011*.

Summary

The goal of this thesis is the development of theoretical methods targeting the implementation of topology optimization in structural engineering applications. In civil engineering applications, structures are typically assemblies of many standardized components, such as bars, where the largest gains in efficiency can be made during the preliminary design of the overall structure. The work is aimed mainly at truss-like structures in civil engineering applications, however several of the developments are general enough to encompass continuum structures and other areas of engineering research too. The research aims to address the following challenges:

- Discrete variable optimization, generally necessary for truss problems in civil engineering, tends to be *computationally very expensive*,
- the gap between *industrial applications* in civil engineering and *optimization research* is quite large, meaning that the developed methods are currently not fully embraced in practice, and
- industrial applications demand *robust and reliable solutions* to the real-world problems faced by the civil engineering profession.

In order to face these challenges, the research is divided into several research papers, included as chapters in the thesis.

Discrete binary variables in structural topology optimization often lead to very large computational cost and sometimes even failure of algorithm convergence. A novel method was developed for improving the performance of topology optimization problems in truss-like structures with discrete design variables, using so-called Kinematic Stability Repair (KSR).

Two typical examples of topology optimization problems with binary variables are bracing systems and steel grid shell structures. These important industrial applications of topology optimization are investigated in the thesis. A novel method is developed for topology optimization of grid shells whose global shape has been determined by form-finding. Furthermore a novel technique for façade bracing optimization is developed. In this application a multiobjective approach was used to give the designers freedom to make changes, as the design advanced at

various stages of the design process.

The application of the two methods to practical engineering problems, inspired a theoretical development which has wide-reaching implications for discrete optimization: the pitfalls of symmetry reduction. A seemingly self-evident method of cardinality reduction makes use of geometric symmetry reduction in structures in order to reduce the problem size. It is shown in the research that this assumption is not valid for discrete variable problems. Despite intuition to the contrary, for symmetric problems, asymmetric solutions may be *more* optimal than their symmetric counterparts.

In reality many uncertainties exist on geometry, loading and material properties in structural systems. This has an effect on the performance (robustness) of the non-ideal, realized structure. To address this, a general robust topology optimization framework for both continuum and truss-like structures, developing a novel analysis technique for truss structures under material uncertainties, is introduced. Next, this framework is extended to discrete variable, multiobjective optimization problems of truss structures, taking uncertainties on the material stiffness and the loading into account. Two papers corresponding to the two chapters were submitted to the journal *Computers and Structures and Structural and Multidisciplinary Optimization*.

Finally, a concluding chapter summarizes the main findings of the research. A number of appendices are included at the end of the manuscript, clarifying several pertinent issues.

